Vibratory screening of drilling fluids

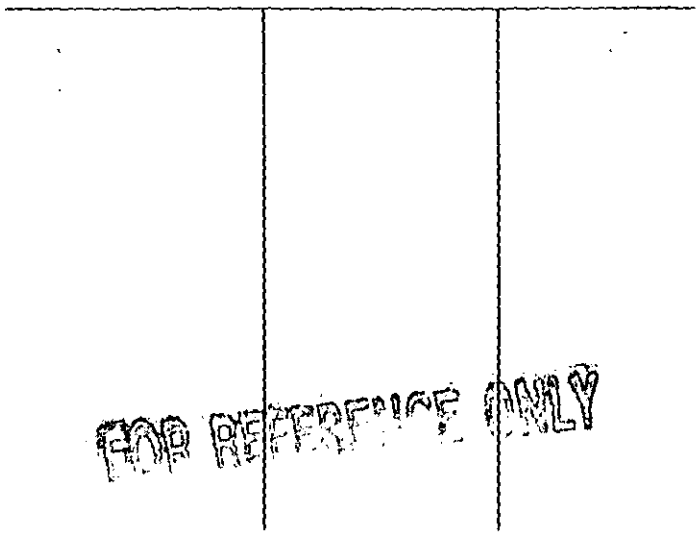

VIBRATORY SCREENING OF DRILLING FLUIDS

by

Martin John Pitt

A Doctoral Thesis

Submitted in partial fulfilment of the requirements for the award of

Doctor of Philosophy

of the Loughborough University of Technology

ABSTRACT

A study has been made at full scale of the use of vibrating near-horizontal screens for the removal of particles from drilling muds, which are shear-thinning fluids. A mass balance analysis was used to establish criteria for effective operation of such devices.

A previous study of these devices by Hoberock was critically examined. It was extended experimentally, and its hypotheses tested. As a result, Hoberock's proposals have been modified.

A model has been developed to predict flow through the screens, which has been validated with laboratory and field data. Observations upon solids transport on wet screens have been compared with the much earlier work of Kluge on dry screening.

It was shown that vertical acceleration was the principal factor in both cases. For fine screens, a minimum acceleration is required to overcome the apparent yield stress of the fluid. However, the advantage gained by further increasing the peak acceleration was found to diminish with higher accelerations. This is believed to be due to flow back through the screen during the part of the cycle when the screen is accelerated downwards through the fluid. It further appears that with sufficient screen acceleration air can be forced upward through the mesh, so that a point is reached beyond which the flow capacity of the screen deteriorates with increasing acceleration.

Solids transport behaviour was shown to agree with a physical model in which the moving bed lifts off the screen then lands at a time so as to coincide with a particular point in the cyclic motion of the screen. Thus a minimum acceleration was required for levitation, and a relatively sharp optimum was observed where the landing position was at the most favourable part of the cycle. At lower accelerations the bed moved in a creeping manner with little relative motion of particles. At higher accelerations the bed became vibrationally fluidized.

ACKNOWLEDGMENTS

Thanks are due to the following:

The Science and Engineering Research Council for the provision of the primary funds. British Petroleum plc (Petroleum Engineering) for the provision of additional funds, materials and practical assistance. Thule United of Aberdeen for the loan of a prototype vibratory screening unit plus screens and for practical assistance. Mr R. Buxton of Powder Products Ltd for the provision of materials and other help.

Credit must be given in respect of supervision to Prof D. C. Freshwater (LUT), Prof B. S. Scarlett (then LUT, now of the University of Delft), Dr A. C. Todd (Heriot-Watt University), Dr A. S. Ward (LUT), and especially Dr R. J. Akers (LUT).

I am grateful to the following for their help and useful advice during the experimental programme: M. G. Bailey, W. S. Galloway and N. Wright (Thule United); T. Bailey and N. R. Booth (BP); G. Boyden, L. Moore, I. Sinclair (LUT).

For constructive comments on the text of this thesis I would like to thank Prof G. G. Haselden (Leeds University), P. J. Lloyd (LUT) and Dr P. R. Lundie.

CONTENTS

LIST OF FIGURES

LIST OF TABLES

1 INTRODUCTION

This thesis is a study of factors that determine the performance of a vibrating screen being used for the removal of rock cuttings from drilling muds. These screens are the main items of equipment in most mud solids control systems, and therefore have a profound effect on the efficiency of the overall drilling operation. (The performance of the drill-bit itself is greatly impaired by rock cuttings returned to the hole by the circulating fluid.) A short account of drilling and the part played by in it by drilling muds is followed by a more detailed description of the nature of the fluids themselves, the need for solids control, and how it is generally achieved. This chapter represents the necessary background for the basis of the research, which is given in detail in chapter 2.

1.1 Drilling for Oil and Gas - a brief description

To appreciate the role of solids control in drilling fluids, it is necessary to understand something of drilling practice. Above all, it must be emphasized that oil drilling is an extremely expensive operation, where the onus is on the operator to get a good hole in the minimum time.

The ease and rate of drilling rock in the exploration and production of oil is to a considerable extent dependent on the existence of an effective drilling mud system. The mud has a complex range of functions which are further considered in section 1.2.2. An essential feature of the mud system is the provision of means for the removal of rock cuttings from the circulating flow. Solids removal is the subject of this thesis and will be discussed in more detail in chapter 2. The purpose of this introduction is to briefly discuss drilling in general and show how mud solids control is an important topic.

The drill bit is the heart of the operation and the start of the solids control problem. There are a number of designs available, the exact one being chosen according to the expected geology and the experienced judgment of the drilling contractor. The traditional toothed wheel bit operates by a chipping mechanism in suitable formations to produce relatively coarse cuttings. By contrast, the diamond bit works by a grinding mechanism producing much smaller particles from similar rocks. In

recent years, some bit designs have been produced which act by a chisel operation, sometimes producing obvious 'shavings' of the rock. The speed of rotation and penetration rate also affect the size of particles which will be produced. In practice, drilling is usually carried out at the fastest penetration rate which does not give a serious risk of problems such as the bit jamming.

The drill bit is attached to a pipe of substantially smaller diameter than the cutting diameter of the bit. A fluid is pumped down this pipe, passing through jets in the bit, and returns to the surface through the annulus between the pipe and the hole. The fluid carries the drill cuttings to the surface where they are separated, so that the fluid can be re-used. This is the solids control process.

In the great majority of drill-sites, the bit is rotated by turning the pipe from the surface (using a turntable and a square section). Down-hole turbine motors powered by the flow of drilling fluid are sometimes used, particularly for deviated drilling and very often in the Soviet Union.

It is possible to use gases or foam as the drilling fluid, but this is extremely rare. The most common fluids are water/clay or oil/clay, though polymer solutions have some use. For this reason, they are commonly known as 'muds'. The properties and composition of muds will be discussed in section 1.2.

Drilling is carried out in stages. After drilling to a certain depth, the drill is withdrawn, the hole is cased with steel pipe, and a slightly smaller bit is used for the next section. Several bits may be required for a single stage, and changing a bit also requires withdrawal of the entire drill-string, a lengthy and hence costly process.

The drilling mud may be modified or replaced with a totally different formulation several times during drilling. For example, it is common in North Sea drilling to use a water-base mud for the top section and an oil-base mud for deeper drilling. In addition, the mud flow rate is varied, being reduced with subsequent stages as the hole becomes narrower. The physical properties and flow rate of the mud have a considerable effect on the performance and hence penetration rate of the bit.

1.2 Drilling Fluids

1.2.1 Literature

The classical book on this topic is 'Composition and Properties of Oil Well Drilling Fluids', edited by W.F.Rogers up to the 3rd edition (1963). The 4th edition (1980) is by G.R.Gray, H.C.H.Darley and W.F.Rogers, and represents a total revision in the light of major changes in practice since 1963.

The other major book is 'Drilling and Drilling Fluids' by G.V.Chilingarian and P.Vorabutr, published in 1981 and reprinted in 1983 with some updating. Together, these two books provide a fairly complete survey of the literature and practice up to about 1979. Both are descriptive in nature, though that of Chilingarian and Vorabutr is more academic in style. In addition, it consists of chapters by individual authors (or groups) whereas Gray, Darley and Rogers appear to be sole authors.

The Noyes Data Corporation has published a book (edited by M.W.Ranney, 1979) entitled 'Crude Oil Drilling Fluids', which is a review of U.S. patents on this topic since 1974. It would be very much in character for this publisher to produce further reviews of this and similar subjects.

The Royal Society of Chemistry have published the proceedings of a conference entitled 'Chemicals in the Oil Industry' (edited by P.Ogden, 1983) which gives some information on recent mud practice around Great Britain.

The American Petroleum Institute has designated section 13 of its publications for recommended practices and information bulletins on drilling for oil and gas. These include: **Spec 13A** (1981) "Specification for Oil Well Drilling Fluids"; **RP 13B** (1982) "Recommended Practice for Standard Procedure for Testing Drilling Fluids"; **Bull 13C** (1974) "Bulletin on Drilling Fluids Processing Equipment"; **Bull 13D** (Bulletin on the Rheology of Oil-Well Drilling Fluids"; **Bull 13F** (1978) "Bulletin on Oil and Gas Well Drilling Fluid Chemicals".

A French publication (available in English) is the 'Drilling Mud and Cement Slurry Rheology Manual' (1982) by the Chambre Syndicale de la Recherche et de la Production du Petrole et du Gaz Naturel, which is essentially an engineer's deskbook. Unlike the American publications, it is in S.I. units.

Finally, the companies which supply or use drilling fluids have their own manuals, some of which may be available to customers. For example, NL Baroid Petroleum Services have a 'Manual of Drilling Fluids Technology'. Not unreasonably, these are oriented to making good use of the company's products.

Individual papers appear quite often in the oil industry journals, and are referred to where appropriate in this thesis. A recent general review of muds was given by Simpson (1985).

1.2.2 **Functions and Properties**

A practical drilling mud is a compromise between a variety of needs, and the mud engineer has to adjust its chemical and physical properties to allow for a number of functions. A typical mud is highly shear-thinning. It travels at moderately high shear rates [~1000 s^{-1}] under turbulent flow down the drill pipe (giving lower viscosity and hence lower power loss), experiences extremely high shear rates [~10^5 s^{-1}] around the drill bit (giving minimum viscosity and maximum penetration between particles), then travels up the annulus at a low shear rate [5 to 170 s^{-1}] in laminar flow (giving high viscosity so that cuttings can be suspended and carried to the surface).

Control of rheology and flow rate are the major factors in mud management: excessive viscosity gives power losses, while excessive flow gives hole erosion, but the flow in the annulus must be maintained faster than the slip velocity of the cuttings.

In fact, it is advantageous if the cuttings remain suspended when the flow is stopped, which regularly occurs. Many clay formulations are thixotropic - i.e. they gel upon standing - but sufficiently slow settling rates can also be achieved by polymer mixtures with an apparent yield point - i.e. very high viscosity at very low shear rates. The accumulation of degraded drilled solids has a major (usually unwelcome) effect on mud rheology, which is an important reason to minimize such a build-up by adequate solids control.

The mud also acts as a lubricant in two ways. Firstly, it reduces friction between the rotating drill pipe and the wall or casing, particularly where the hole is curved. Secondly, it cools and lubricates the bearings present in many drill bits, which can fail in a few hours if overheated. King (1959) reported that recirculated drilled solids cause a drastic reduction in bit-bearing life.

Along with the rheology, the density and chemical condition of the mud must be controlled to stabilize the walls of the hole. The density of the mud is often increased by the addition of a powdered heavy mineral, barite (occasionally by other minerals or by dissolved salts) so that the hydraulic pressure can resist the force exerted on the hole by the surrounding geological formations. Such weighted muds are more expensive, but commonly required during deeper drilling.

The mud must also be prevented from having an adverse chemical reaction with the walls. For example, water can dissolve away rock salt (unless it is saturated with salt) and it can cause shales to expand causing extensive break-up of the formation with large sections sloughing off into the hole. Such effects can be limited by the use of additives or by changing the base fluid to oil. It is perhaps not widely appreciated that even a small amount of destabilization can affect solids control both by causing the walls to crumble and thus increasing the amount of unwelcome solids, but also by making particles degrade in transit to the surface.

Since many geological formations are porous, there can be a loss of base fluid or whole mud into the strata. This can be reduced by restricting the excess pressure on the mud and by using a mud which tends to clog the pores and form a filter cake on the walls. This is most commonly achieved with clay-based muds, but may be effected by special additives in other fluids.

1.2.3 Composition

Essentially, a drilling mud must contain a base fluid and a viscosifier. To this may be added a weighting agent if necessary. Some chemical conditioning is required, even if only to raise the pH to be fully alkaline. If the viscosifier does not itself seal off the hole wall, then a separate filtration control agent may be added. If the viscosifier gives too high a gel strength, then chemicals called thinners may be used. The rheology of the mud may be adjusted by chemicals affecting the degree of flocculation of particles. Salts are used to reduce damage to the formation by ionic imbalance. In addition, the mud may contain some kind of preservative (against biodegradation), emulsifiers and anti-corrosion agents. Chemicals are also used to reduce the adverse effects of certain drilled solids, or the residues from cementing operations.

A typical mud supply company has a range of 50 to 100 products. Furthermore, a computer search of literature from 1970 to 1980 revealed an average of 73 patents per year for novel drilling mud components or formulations. In fact, a substantial book has been written which simply reviews such patents since 1974 (Ranney 1979). However, the majority of muds in use can be basically described as in Table 1.1, though the details and some additives will differ considerably. All may be weighted.

Table 1.1 Basic Mud Formulations

FRESH WATER MUD:
water + bentonite + NaOH

LIME MUD
water + bentonite + lime + deflocculant + polymer

SALT WATER MUD
brine + attapulgite + starch + NaOH

LOW SOLIDS MUD
water **or** brine + polymers + NaOH

OIL MUD
oil + asphalt + soaps + water + NaOH

INVERT MUD
oil + water + treated clay + emulsifiers

The most widely used (and cheapest) viscosifier is bentonite, a clay mineral. The highest quality (i.e. the highest viscosity per weight used) is Wyoming bentonite, which is almost entirely sodium montmorillonite. It works well in fresh water, and can with suitable additives be used in brackish water, but is less effective in the presence of high concentrations of salt. Where brine is the base fluid, then so-called 'salt-water clay', the mineral attapulgite, is used. This normally requires starch as a filtration loss control agent.

Synthetic polymers can be used as viscosifiers in water. Some are used as 'extenders' for the clays or to restore the rheology of a used mud. However, it is possible to prepare a 'low solids' drilling fluid in which the rheology is entirely due to polymers, and it has been claimed that such fluids reduce overall drilling costs (Hall 1968). Darley (1976) discusses the advantages of such fluids, and Lauzon (1982) reviews practice in the use of polymers as viscosifiers and stabilizers. Apparently there is considerable usage of polymers in North Sea drilling (Moore 1977). Chilingarian & Vorabutr (1983) devote a chapter to polymer fluids.

The use of oil instead of water as a base fluid removes many of the problems of interaction with the geological formation, though it is of course much more expensive. For reasons of availability, diesel oil or crude oil was generally used. However, the disposal of oil-contaminated cuttings posed a risk to the environment, so oil-based muds virtually went out of use in the mid-1970's (Caenn & Chilingarian: Appendix F in the 1983 edition of Chilingarian & Vorabutr). The industry proceeded to develop clean oils which were relatively non-harmful to the environment, so that oil muds now occupy more than 10% of mud usage (Ibid.) and about 50% in the North Sea (Stevenson 1983).

Oil can be viscosified by the addition of soaps and high-molecular weight organics such as asphalt. A 'straight' oil mud usually contains a little water and calcium chloride to balance the chemical potential of the rocks being drilled. Asphalt provides good filtration loss control,but oil muds have decidedly inferior rheology compared with water/clay muds.

A system which combines much of the advantages of both base fluids is the 'invert' mud, where up to 40% by volume of water is emulsified into oil with suitable surfactants. To give good rheology, a chemically modified bentonite ('bentone') is used: this is colloidally stable in the presence of oil. A secondary surfactant may well be used to keep barite (weighting agent) dispersed. Calcium chloride is again used to balance the chemical activity relative to the formation. These are evidently the oil muds most commonly used in the North Sea (Stevenson 1983, and private communications).

1.2.4 Economics

Drilling fluids affect the cost of a well through the cost of materials, the cost of waste disposal, the cost of solids control, and the major influence they have on the efficiency of drilling.

The average cost of drilling fluid for a single well in Western Europe is estimated at £ 100,000 for water-based and £ 150,000 for oil-based mud (Parker 1983). U.S.A. costs range from £ 15,000 at some sites to £ 300,000 for really deep wells. The latter number about 1000 per annum (Ibid.). In all cases the component which contributes the biggest cost is the weighting agent, usually barite. There is thus some incentive to be especially careful with weighted muds, and to adapt the solids control so as to minimize barite losses (Kennedy 1974). A batch of oil-based mud can cost 2 to 3 times as much as the equivalent water system, so contractors try to salvage as much as possible (Moore 1977).

Changes to the solids control procedure can have a great impact on these costs. For example, the same contractor drilled two wells less than half a mile apart with different solids control. The mud costs in one case were $ 35,000, in the other $ 13,000 (Anon 1983). At one well-site, the contractor calculated the cost of chemical additives in the reserve mud pit to be one million dollars. A change to a more closed solids control system with barite recovery reduced daily mud costs to a quarter (Ibid.).

In general, a typical mud costs $ 50 to $ 200 per barrel to make up fresh, and about $ 1 per barrel per day to maintain (Adams & Frederick 1982). Failure of the solids control system to the extent of adding one

barrel of solids to the mud will typically cost $ 250 in mud replacement, though an extreme case could be imagined in which the cost was 10 times greater (Wells 1975). The same author has criticized the most common method of controlling mud properties (dilution) as being uneconomic (Wells 1976a).

An extreme example of the savings to be made is quoted by Pierce & Alexander (1984) for very difficult down-hole conditions. A mud programme of brines then oil muds had a total cost of $ 1.63 million, whereas a programme using polymer viscosifiers achieved a similar well for $ 0.33 million, and in a shorter time.

Important though mud costs are, it can be argued that the greatest economic benefits of a good mud system come from improved efficiency of drilling. In general, more effective mud choice and more effective solids control will allow drilling in a shorter time period, with fewer drill-bits and with less risk of a stuck pipe, which are all major cost benefits (Chilingarian & Vorabutr 1983; Gray, Darley & Rogers 1980; Moore 1977; Anon 1983; Kennedy 1974; LeBlanc 1978; Wilson, Callendar & Mosher 1977; Ormsby 1981; Kalil, Speers & Robinson 1982). This is illustrated in Figure 1.1. However Simpson (1985) has been critical of oil companies for seeking to minimize mud and solids control costs rather than appreciating the reduction in overall costs which can be achieved by optimum mud condition.

Figure 1.1 Effect of Solids in Mud on Drilling
(Lott, 1973)

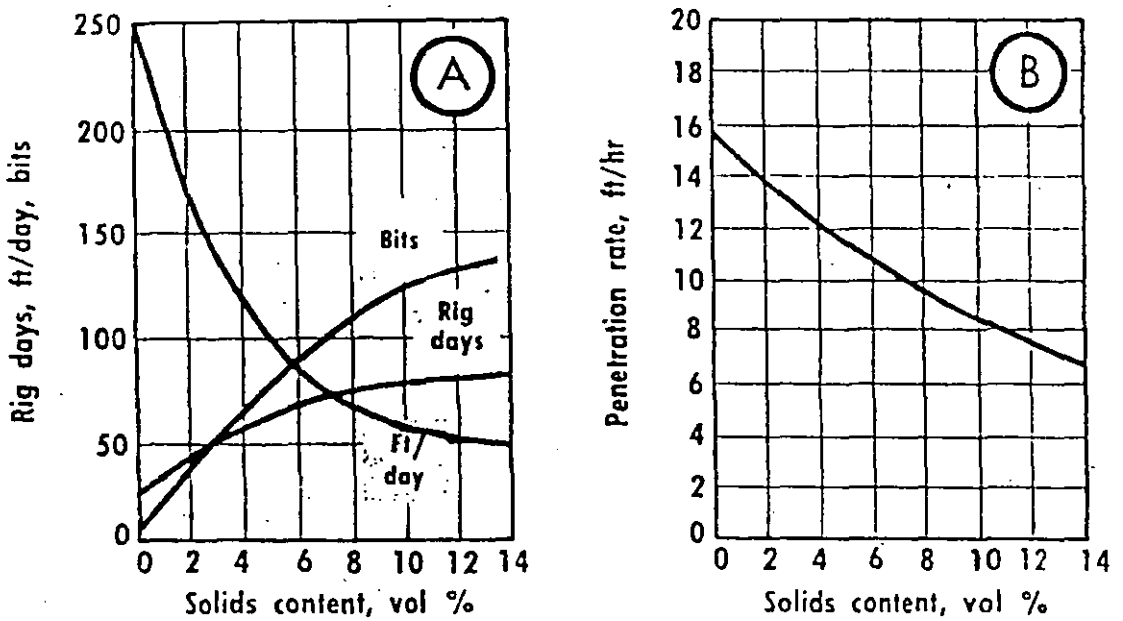

1.3 The Effect of Drilled Solids on the Drilling Fluid

1.3.1 General Comments

Drilled solids have an effect depending upon (a) their chemical nature (b) their particle size (c) their ease of degradation (d) their concentration (e) the mud formulation. The mud engineer essentially controls the last two conditions, which can however affect the others. For example the degree of flocculation affects the effective particle size, and is affected by the chemical composition. Similarly, the chemical content can affect the surface stability of particles and thus their tendency to break up.

A special set of terms are in use in the industry for particle size. For example, any particles which have been passed by the shale shaker (say below 420 μm) but which do not pass a standard 74 μm screen are referred to as sands, irrespective of their mineral composition. Particles smaller than this, but greater than about 2 μm are called silts, whereas smaller particles are commonly called clays, whatever their origin. A different system of naming was suggested by Field & Anderson in 1972, and adopted by the American Petroleum Institute in 1974, but appears to have made little impact.

It is also common practice to refer to 'low gravity solids' to distinguish between drilled solids and weighting material in the same size range. Barite is mostly in the size range 10 to 80 μm, but may be partially separated from low gravity solids in the silt range by a density-dependent process rather than screening.

It is essentially impractical to remove particles below 2 μm (i.e. colloids) from the base fluid, so it is clearly best to separate any larger drilled solids before they degrade to this level. (To deal with an excess of colloidal material, it is usual practice to discard and replace some of the base fluid.) Shales are particularly prone to degrade to colloidal size. Conversely, a sandstone will often break down quite quickly to its component grains, which are then resistant to further size reduction.

1.3.2 Density

Minerals are more dense than drilling base fluids, so the universal effect of solids accumulation is an increase in density. Generally the mud engineer will wish to maintain the minimum density which does not cause formation problems, as this gives quicker drilling (Gray, Darley & Rogers 1980; Chilingarian & Vorabutr 1983). According to Chambers (1966) an increase of 1% by volume of solids gives 5% slower penetration rate. Increased density also increases the risk of a drill-pipe getting stuck (Adams 1977; Love 1983).

The usual method of limiting density is by diluting or partially replacing the mud. For weighted fluids this means the loss of expensive barite, so density increases are undesirable in both weighted and unweighted systems. For all fluids a greater turnover increases disposal costs and requires larger reserve storage.

1.3.3 Filter Cake

A good drilling mud will deposit a thin cake on the hole walls, which limits the loss of fluid to formation. As the solids content of the mud increases, the thickness of filter cake increases even more rapidly (Wells 1975). A thick filter cake can cause pressure surges, casing problems and of course the risk of drill-pipe sticking (Ibid.; Robinson & Heilhecker 1975; Gray Darley & Rogers 1980; Chilingarian & Vorabutr 1983). Obviously, certain types of solids will increase the coefficient of friction of the filter cake.

The effect of drilled solids on mud rheology will be discussed in the following section.

1.4 Rheology and Drilling Fluids

1.4.1 Time-Independent Properties

Drilling muds are non-Newtonian: i.e. they cannot have their flow properties defined by a single viscosity. Most commonly, they are shear-thinning, that is to say, the apparent viscosity decreases as the applied shear rate increases.

In order to cause fluid to flow a shearing stress must be applied, and this results in a rate of change of velocity of the fluid with distance, known as the shear rate. For measurement of non-Newtonian fluids it is normal to utilize devices which can either apply a known shear stress and measure the resulting shear rate, or alternatively apply a fixed shear rate and measure the shear stress from the force needed. These instruments are called rheometers. A plot of shear rate versus shear stress from such measurements is called a rheogram, and serves to characterize the flow properties of a (time-independent) non-Newtonian fluid.

By definition, viscosity is the shear stress divided by the shear rate, so a rheogram permits the calculation of effective viscosity at any shear rate. For a Newtonian fluid, the viscosity is constant, so the rheogram consists of a straight line through the origin. This may be expressed in an equation relating shear stress τ to shear rate $\dot{\gamma}$ and viscosity μ, thus:

$$\tau = \mu \dot{\gamma} \qquad (1)$$

Typical drilling muds give rheograms which are curved. For the purpose of calculation, these curves are usually approximated by one of two hypothetical fluids, the **Bingham Plastic** and the **Power Law Fluid.** These are illustrated on Figure 1.2.

Figure 1.2 Newtonian, Bingham and Power Law Fluids

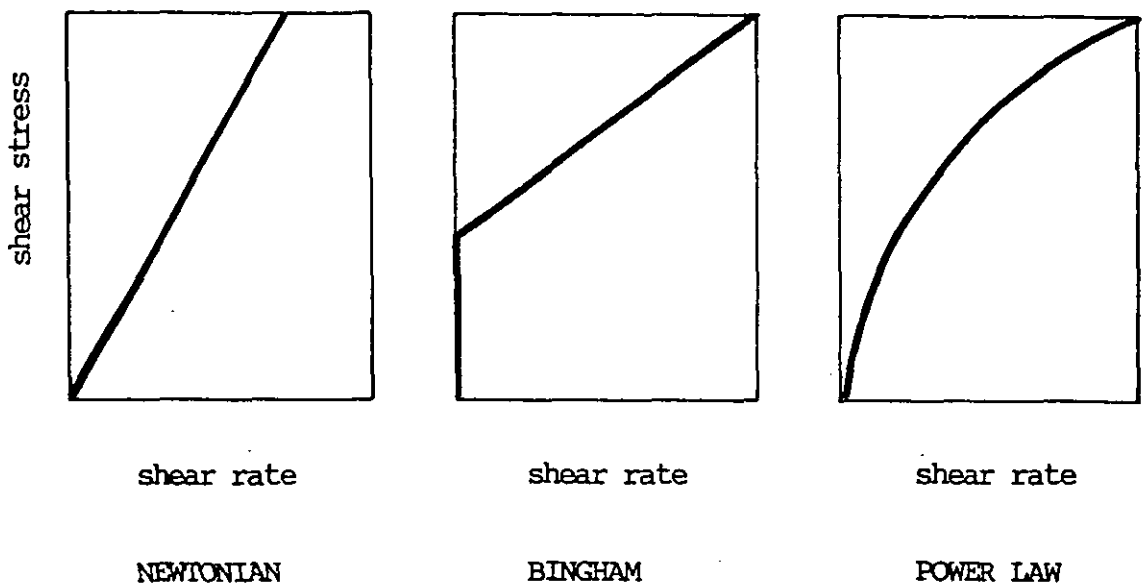

The **Bingham Plastic** has a straight-line rheogram, but does not go through the origin. Instead, there is no flow at all until a certain minimum shear stress (called the yield stress, or yield point) is exceeded. Higher stresses give a response proportional to the excess above the yield point. A Bingham Plastic can therefore be uniquely defined by two parameters, its **yield point**, and the slope of its line, which is called its **plastic viscosity.** This can be expressed in an equation relating shear stress τ to shear rate $\dot{\gamma}$ via the yield stress τ_y, and the plastic viscosity μ_p thus:

$$\tau = \tau_y + \mu_p \dot{\gamma} \qquad (2)$$

In reality, no fluid is truly plastic, because this implies infinite viscosity at very small shear rates. However, if low shear rates are not important, then the upper portion of the rheogram is often sufficiently flat for a straight-line approximation to suffice. If this gives a significant intercept on the stress axis (i.e an apparent yield stress), then the fluid is said to be **pseudoplastic.**

In drilling it is normal practice to measure the mud viscosity at two shear rates, 511 s^{-1} and 1022 s^{-1} by means of a two-speed rheometer, and thereby calculate the Bingham Plastic parameters. Figure 1.3 shows a full rheogram, and the Bingham Plastic approximation as usually applied.

Figure 1.3 Rheogram of Rig Fluid [XC of Marsh Funnel 38 s] by Weissenberg Rheogoniometer, with the Bingham Plastic Approximation

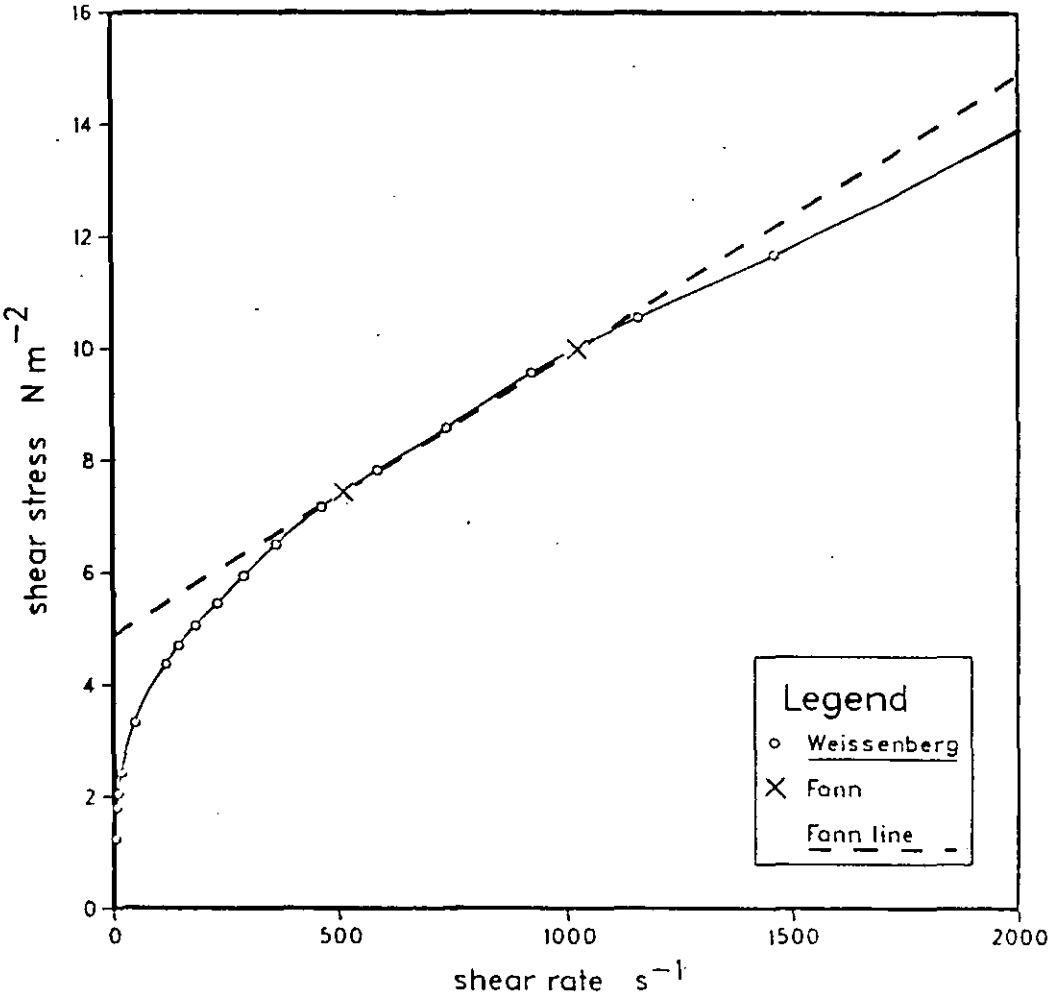

The **Power Law Fluid** can be defined by a similar equation:

$$\tau = k \dot{\gamma}^{n} \qquad (3)$$

where **k** is the **Power Law Constant** or **consistency** and where **n** is the **Power Law Index.** In logarithmic form this is:

$$\log \tau = \log k + n \log \dot{\gamma} \qquad (4)$$

In practice this means that measurements are made at several shear rates (usually 5 points in oil-well drilling). The results are plotted on log-log graph paper and a straight line put through them to give **k** and **n** (intercept and slope). Actually there are theoretical objections and the data usually shows perceptible curvature, but it is convenient to have a curve defined by only two parameters, so this approximation is widely accepted for situations where the Bingham Plastic is insufficient.

Both of these equations can be reduced to the Newtonian one. A Bingham Plastic where $\tau_y = 0$ is Newtonian, as is a Power Law fluid where $n = 1$. In the latter case, **k** is equal in both value and dimensions to μ, but more usually **k** is of non-integer dimensions. For shear-thinning fluids (which drilling muds are) then $n < 1$. Values greater than unity correspond to the shear-thickening situation, which applies in some other industries.

1.4.2 Time-Dependent Properties

The above discussion relates to fluids where the time of shearing does not affect the resulting shear rate. Two principal exceptions are fluids which are **viscoelastic** or **thixotropic.**

Viscoelastic fluids do not respond to rapid changes in shear stress by immediately changing to a new equilibrium shear rate. Instead they deform in a manner analogous to an elastic solid: the equilibrium shear rate is then reached over a measurable time as the stored energy is dissipated via viscous damping. In addition, the application of a shearing stress causes stress in a direction normal to the plane of shear. Such behaviour can be measured by rapidly varying a stress field and analysing the phased response, and by normal stress measurements. However, it is a non-equilibrium phenomenon and thus cannot be deduced from a standard rheogram which is generally at or near equilibrium. Viscoelasticity generally involves decay processes with time constants of the order of a second or less: it is thus (in common practice though not intrinsically) a phenomenon of significance over short time periods.

Polymer solutions commonly have elastic properties, and this is certainly the case for XC (Thurston & Pope, 1981; Elson et al.,1982). However, viscoelasticity only becomes apparent with higher concentrations of bentonite (Cheng, Ray & Valentin, 1965) and is not normally needed to explain its flow properties (Cheng & Evans, 1965; Weymann, Chuang & Ross, 1973).

It was therefore considered that viscoelasticity was probably not the principal reason for the fact that drilling muds will more easily pass through a vibrating than a stationary mesh. Moreover, it did not prove necessary to invoke the phenomenon in order to explain the results found in this thesis, though it is possible that a more complete theory could include it as a factor. For the present work, any such attempt would have made both practical and theoretical studies vastly more complex.

Thixotropy arises when a fluid takes a relatively long time (seconds to hours) to come to equilibrium under shear. it may be explained in terms of a fluid structure which is restored in the absence of shear and slowly broken down by prolonged shearing to a dynamic state when breakdown and restoration are equal. Thus, for example, a bentonite suspension allowed to stand overnight acquires a so-called 'gel' state of high viscosity which takes some time to be broken down by shearing to a more fluid state. This can be demonstrated by rheometer measurements in which the shear rate is increased and then decreased: different values of shear stress result for the same shear rate with a different history. The resulting hysteresis loops (for example in Figure 1.4) are indicative of (but not a measurement of) thixotropy. Similarly, Figure 1.5 shows how the apparent viscosity decreases under steady shear.

Thixotropy is a general feature of bentonite suspensions, and therefore applicable to drilling muds. However, limited practical experiments indicated that a bentonite mud was not noticeably altered by the shear experienced on passing through a vibrating screen on the Main Rig. (The residence time and shear rate are insufficient to cause significant breakdown of structure.) Thus thixotropy was not of importance in the theoretical analysis. Unfortunately, it would have been a practical obstacle, because the bentonite mud rheology <u>did</u> change (due to breakdown by pumping) during the course of a day, and even during experimental runs, depending on the flow-rates used. therefore it was not possible to present an identical liquid (in terms of flow properties) to screens at different angles and at different flow-rates. Moreover, even if such had been achieved, it would have been difficult (and probably impossible) to make measurements which could unambiguously define the rheogram that truly represented the fluid under those conditions.

It was therefore decided to use liquids where thixotropy was not noticeable. These could be unambiguously characterized, and their behaviour explained on the basis of their rheograms.

Figure 1.4 Rheograms of Bentonite Dispersions showing hysteresis

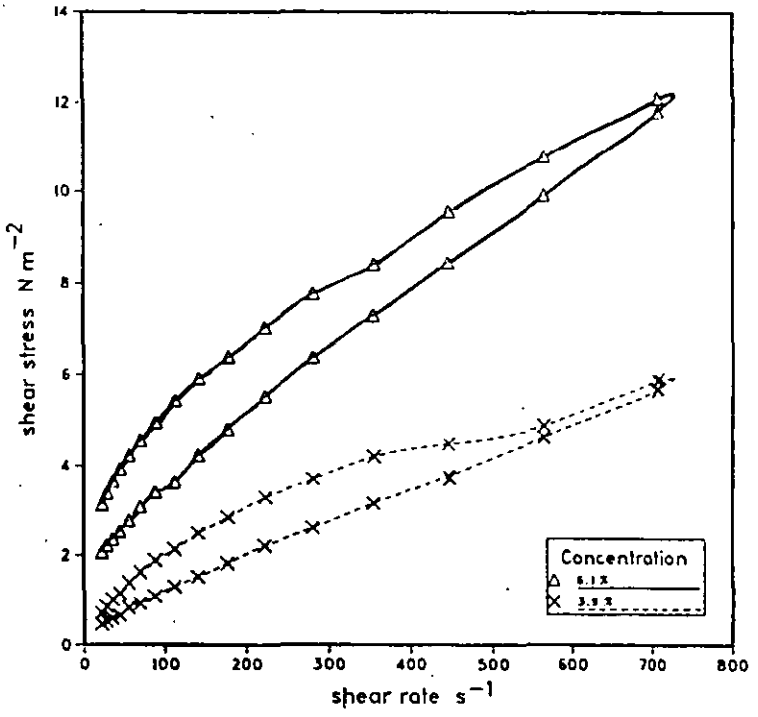

Figure 1.5 Thixotropy of 8.4% Bentonite in Water: viscosity change under constant shear rate

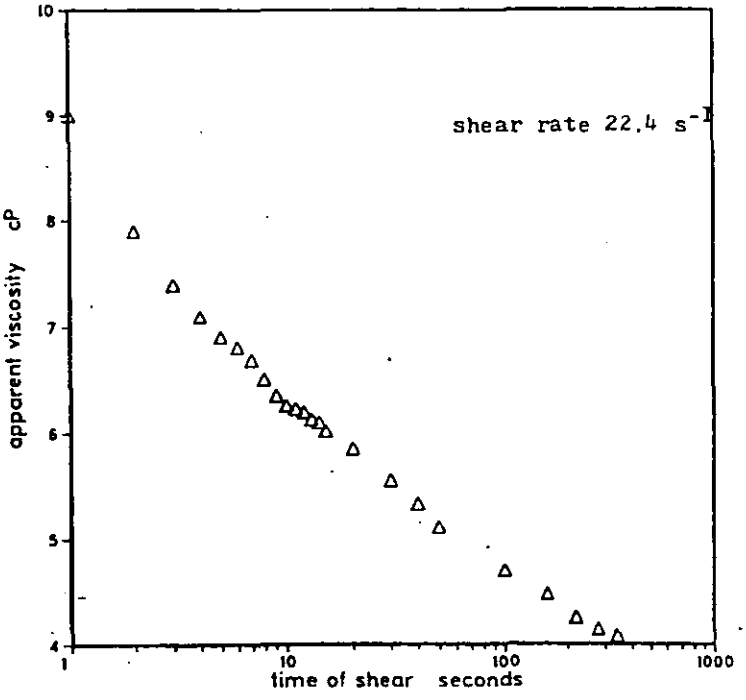

1.4.3 Desirable Mud Conditions

The rheological state of the drilling mud is a major concern of the mud engineer, though it is often compromised by other considerations. As a primary requirement, the rheology must be recoverable: that is, it must not be irreversibly changed to an important degree by down-hole conditions. These include a region of extreme shear rates (of the order of 10^5 s^{-1}) at the bit and possibly temperatures in excess of 100°C in some locations.

As a general rule, the minimum specification for a mud is set by the annulus condition. For the prevailing flow-rate and geometry (hence shear rate) the mud viscosity must be sufficient so that the mud velocity is greater than the slip velocity of the solid particles generated by drilling. This could of course be accomplished with a Newtonian fluid, but the high viscosity required would cause considerable pressure losses (hence energy needs) for the fluid being pumped down from the surface to the bit. A shear-thinning fluid shows a lower effective viscosity at the higher shear rates within the drill-pipe. Therefore, the lower viscosity under these conditions the better, favouring fluids which are highly shear-thinning. (In addition, the flow of mud actually contributes to the cutting action of the bit: an important hydraulic criterion is that as much of the pump energy as possible should be delivered as kinetic energy at the bit, and not dissipated en route.)

An excessive viscosity in the annulus will cause power losses. However, it is convenient if the mud holds particles in suspension when flow is stopped for any period. This can be accomplished with a mud which is thixotropic and has sufficient gel strength. If the mud does not gel, then some delay in settling will be given by a high viscosity at the low shear rates provided by settling particles.

Overall, it is necessary to maintain a balance between mud properties and mud flow-rate which keeps the drill bit clear, but does not cause hole enlargement or wall erosion, and minimizes the power required to pump. In addition, the mud must be stable (and preferably stabilizing) to down-hole conditions, must be capable of recycling, and should not be drastically affected by accumulated drilled solids, as will now be discussed.

1.4.4 Effect of Drilled Solids

So far as their effect on viscosity is concerned, drilled solids may be classed as 'active' or 'inert', the latter having effects on density and viscosity which are almost entirely due to their size and concentration. For example, small particles of sand will increase the viscosity of a liquid according to the volume fraction they occupy (Einstein's Law). However, clay minerals in water exert a much greater effect than this accounts for, and are thus 'active'. In addition, chemicals such as calcium ions can dissolve out of solids and affect some sensitive muds.

It is possible for particles to react chemically with the mud system and cause it to lose viscosity, but in most cases drilled solids increase the viscosity of the system. A high concentration of solids of any size will cause interference with flow if the particles interact attractively. This is generally recognized as a high 'Plastic Viscosity' or PV, with an associated energy penalty and other effects. For muds which already contain a high level of non-clay solids (barite or impurities in the bentonite) then further additions can increase the volume fraction so as to cause a disproportionate increase in viscosity.

For example, take a mud containing 20% by volume of inert solids, which is a volume fraction ϕ of 0.25. According to the equation of Mooney (1951):

$$\frac{\text{viscosity of suspension}}{\text{viscosity of base fluid}} = \exp\left(\frac{2.5\,\phi}{1 - \phi/0.65}\right) \quad (5)$$

then the overall viscosity is 2.75 times that of the base fluid (e.g. water plus polymer or colloidal clay).

Increasing the inert solids to 25% increases the volume fraction to 0.33, and the viscosity ratio to 5.5, i.e. the effective viscosity of the mud is doubled. A further 1% solids (say barite to adjust the density) increases the ration to 6.76.

Conversely, it will be seen that under these circumstances a little dilution will have a large effect, which accounts for the traditional reliance on this method of mud maintenance. However, the effect of a dilution programme is to steadily increase the ratio of drilled solids to viscosifier. This is particularly important where accumulated drilled solids come into the colloid size range due to attrition or spontaneous breakdown.

Virtually by definition, materials used as commercial viscosifiers are colloidal, and hence drilled solids which are of colloidal size can have similar effect. This is detected in practice by an increase in the 'Yield Point' (YP) or the ratio YP/PV. Dilution may restore the Marsh Funnel viscosity or the YP but is unlikely to restore the rheology to that of the original mud. In this respect, drilled solids give less shear-thinning character (i.e. the Power Law Index closer to unity). Thus the annulus conditions may be acceptable, but the effective viscosity at the drill-bit is much higher, giving reduced efficiency (e.g. Block 1982).

Particles of near colloid size have a very high specific surface area. This can attract surface active chemicals, making them less available for maintaining the correct chemical state of the mud. In fact, the volume of water adsorbed can significantly reduce the amount of free water and hence affect some formulations. A general review of colloid aspects of drilling fluid rheology is by Browning, 1976.

Some drilled solids can flocculate to give an unacceptably high gel strength. This has been a major problem, now generally controlled by deflocculating chemicals, or 'thinners'. However, the use of additives is expensive, particularly where there are changes in formations being drilled, so that both flocculants and deflocculants may be required at different times.

In all cases it is clear that efficient removal of drilled solids soon after their generation is the most effective way of maintaining the desired mud properties.

1.5 Solids Control Equipment

1.5.1 General Description

The aim of solids control is to remove undesirable solids from the mud whilst retaining valuable liquid and desirable solids (weighting agent) as far as possible. Figure 1.6 (below) is taken from page 480 of Chilingarian & Vorabutr (1983) and illustrates the main items of equipment commonly used in a typical layout. The surface stock of mud is kept in a series of steel tanks of which all but the first are stirred. Additions of dilution fluid or chemicals can be made at suitable points in the system, and there is a general movement of mud from one end to another via pumps, separating devices, overflows and inter-tank connections.

Figure 1.6 Layout of a Simple Solids Control System

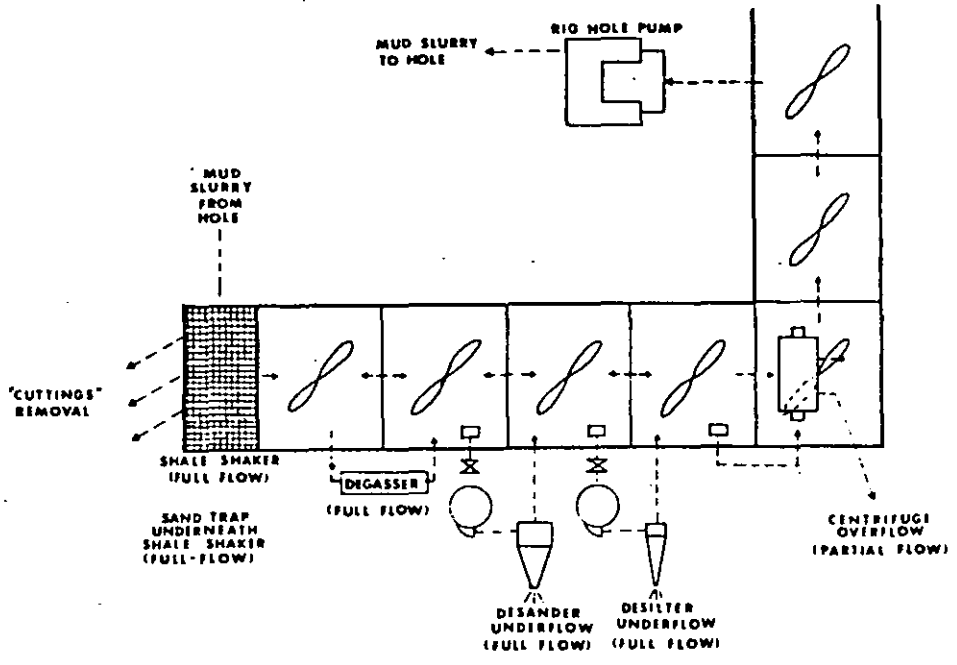

The entire flow of mud from the hole is passed through a vibrating screen unit called a 'shale shaker'. (It is increasingly common to have two or three units in parallel.) This discards the coarsest solids and discharges mud into an unstirred tank called a 'sand trap'. Some settling occurs in this tank, but the amount of solids removal is usually small, due to the short residence time. Its principal function is to catch very large particles if the shale shaker screen should become holed, or if it is temporarily bypassed.

The mud overflows from the sand trap into a stirred tank. This is often fitted with a device to remove gas bubbles, or (as is shown here) there is a degasser placed in the flow between this and the next tank. The entry of gas into the drilling mud in neither routine nor uncommon, but when it does occur it will severely impair the performance of centrifugal pumps and hydrocyclones.

The mud is drawn by centrifugal pump (to give sufficient pressure) from a stirred tank and passed through a 'desander' to the next tank. The desander is a bank of 150 mm hydrocyclones, sufficient in number for the flow rate. As its name implies, it is expected to remove the majority of particles down to 74 μm. A similar bank of 100 mm hydrocyclones is then used to remove particles down to about 40 μm, this being called a 'desilter'.

Finally, a portion of the flow is treated by a continuous centrifuge. This typically separates particles larger than 3 μm. Whether the solid or liquid is discarded will depend on the mud system used, as will be discussed in section 1.5.5

1.5.2 Shale Shaker

Many designs have been tried with more or less commercial success, but according to Brandt & Love (1982) the majority use a downward-sloping mesh screen. Linear vibration is used, but the most common motion is approximately circular from an eccentrically mounted horizontal shaft. The mud is fed into a tank (called the 'possum tank') and overflows via an adjustable weir onto the high end of the screen. In this configuration, the solids travel down and off the screen by gravity. The screen motion

serves to lift particles and prevent a filter cake forming. It is also presumed to shear the mud and aid its flow through the screen by reducing the effective viscosity.

However, designs are now in use with very little slope, with horizontal screens and even adverse tilts. It is clear that for such units the vibration must actively convey screened solid. For this reason, linear vibration is usually along a line tilted forward of that normal to the screen. Circular motion has the upper portion of the locus moving in the desired direction of solids travel. (For downward tilted units the reverse of this motion may be used.)

One manufacturer (Swaco) produces a circular slightly domed screen which is fed at the centre and rotated so that the solids spiral to the outer edge. A review of commercial designs is given by Hoberock (1981a).

A significant feature of shale shakers is the universal presence of a bypass valve. If the screen became blocked then whole mud would be discharged off the end, so the operator can instead divert the flow around the screens. This facility is also used to keep the mud flowing (and hence drilling continuing) when a screen is being replaced or other maintenance is required. The use and misuse of the bypass will be discussed in section 1.6.

In 1976, Wells reported that shale shaker screens in common use were 10 to 14 mesh (1.9 to 1.3 mm aperture). In 1978, several authors reported that 'fine screens' of 40 to 80 mesh (381 to 178 μm) had become accepted, the latter being a practical limit (Cagle & Wilder 1978a, 1978b, Leblanc 1978). Screens finer than 80 mesh generally have a coarser mesh to provide mechanical support. This also has the bonus of providing some coarse screening if the fine screen should develop holes (Brandt & Love 1982).

Some manufacturers offer screen sizes down to 200 mesh (74 μm). However these (and even finer meshes) are more likely to be used in combination devices for barite recovery (see section 1.5.4). Fine meshes are desirable to remove smaller particles, but they are limited in fluid capacity: put simply, it is hard to pass viscous mud through small holes

It is possible to use two shaking screens in series, with the second having a finer mesh. Thus several models have been produced with two 'decks' - i.e. one screen below another, both fixed to a frame

('basket') and therefore being moved by a single vibrator. The use of finer screens is usually in double deck units where the upper screen provides a reduction in the solids loading and some mechanical protection for the lower one. Fine meshes are also associated with near horizontal decks.

A variety of mesh weaves are available, with square weaves being the most common. Rectangular holes are said to give less tendency to blockage with near-size particles (Brandt & Love 1982). Patent layered screens have had similar claims along with improved life and fluid capacity (Cagle & Wilder 1978a, 1978b).

1.5.3 Hydrocyclones

Hydrocyclones are centrifugal separating devices where the energy is provided by the pressure drop of the liquid passing through. They are used for a variety of process engineering purposes, as described by Bradley (1965) and Trawinski (1978, 1985). Svarovsky (1981) gives general design criteria. White (1982a, 1982b, 1982c) reported actual tests to predict performance with drilling muds, and gave an extensive trouble-shooting guide (1982c). Young & Robinson (1982b, 1982c) discussed the sizing and arrangement of hydrocyclones on drill-sites. Ormsby (1982) edited the IADC manual on hydrocyclones for drilling muds.

General practice in oil-well drilling is to use hydrocyclones of 150 to 300 mm diameter as 'desanders' followed by 100 mm cones as 'desilters'. Cones as small as 50 mm may be used if the drilling process gives a preponderance of particles below 100 μm. Desanders give a D_{50} cut point in the region of 40 to 100 μm, and desilters in the region of 25 to 50 μm for typical cuttings

Clearly, the desander reduces the solids load on the desilter, and likewise the shale shaker reduces the solids load on the desander. Large particles or an excessive load may plug the bottom (solids discharge) of a hydrocyclone, which means that no separation occurs and the pumping energy is wasted (and in fact contributes to wear). Conversely, the plugging of the inlet to the hydrocyclone will cause clean mud (from other hydrocyclones) to be sucked back from the outlet manifold and vented via

the bottom discharge, thereby wasting whole mud in addition to loss of separation (Ormsby 1982; White 1982c).

The effect of higher solids concentration is to reduce the efficiency (elevate the cut point) of hydrocyclones. It is therefore considered best practice to run them on a flow rate of about 125% of the mud rate - i.e. 25% of the cleaned mud is circulated back to dilute the incoming mud (Ormsby 1982; White 1982c; Young & Robinson 1982c). Greater dilutions can be used, but there is a cost penalty in the extra pumping required. Furthermore, too great a demand on the pump (or insufficient pump power for any reason) results in an incorrect flow pattern developing inside the cone, giving less separation and loss of quantities of mud from the bottom discharge (most authors cited).

Two principal variations of design are the 'balanced' and the 'choke-bottom'. The balanced design creates a slight suction at the base, drawing in air. It can discharge relatively dry solids and will release little or no liquid from the bottom outlet when fed with solids-free feed. Conversely, the choke-bottom design operates under a positive internal pressure, and discharges much the same volume of bottom outflow with solids-free or solids-loaded feed. As the name implies, it can be choked so that the outflow is a relatively concentrated slurry.

Balanced hydrocyclones can be adjusted to give a drier product, but this poses the risk of material adhering inside the cone and ultimately blocking the outlet. Choke-bottom units are less prone to this problem, but if the solids discharge is restricted too much then some solid will be re-entrained and carried into the cleaned mud. Thus for both types, the best solids removal results from a wet discharge (Ormsby 1982; White 1982a, 1982c; Young & Robinson 1982c).

There is no doubt that hydrocyclones are of major importance: on one well it was estimated that the desanders provided 80% of the solids removal (Dawson & Annis 1977). However, being forced settling devices they are favoured by lower viscosity fluids and their performance is affected by variations in density and solids loading. There are some genuine practical difficulties in keeping them well-tuned (Young & Robinson 1982b). Ormsby (1973b) noted that an incorrectly matched pump is a cause of cyclone inefficiency.

The same author (in Chilingarian & Vorabutr 1983) observed "If a hydrocyclone is operating properly it is saving money, whereas if it is not functioning properly, it is costing a great deal of money".

1.5.4 Hydrocyclone / Screen Combinations

Combination units of hydrocyclones above fine-mesh vibrating screens were introduced in the early 1970's for salvaging barite from weighted muds (Kennedy 1974; Robinson & Heilhecker 1975; Anon 1976; Dawson & Annis 1977; Robinson 1982). They are commonly known as 'mud cleaners' and exploit the different separating principles of the two devices. They are used in place of desilter hydrocyclones.

The hydrocyclones on such units produce a solids slurry discharge in roughly the silt range. However, since the operating principle is one of forced settling, barite particles separate out alongside drilled solids roughly 50% larger. Thus the undersize from a suitable screen will be richer in the barite particles than the oversize, since it separates on the basis of size. The barite-rich product is returned to the system to add weight, thereby reducing the need for make-up barite. The screen oversize is waste. Clearly there is a balance between salvaging maximum barite and discarding maximum drilled solids.

These devices have near horizontal screens and much of the present work is applicable to them.

1.5.5 Centrifuges

The practical use of centrifuges in solids control commenced in the 1950's (Bobo & Hoch 1954). The IADC have announced (Brandt & Love 1982) that 'Handbook 8' in their 'Mud Equipment Manual' series is about centrifuges, but this was not yet available at the time of writing. A good recent description is by Ormsby (chapter 12 in Chilingarian & Vorabutr 1983).

The term centrifuge in this application is commonly applied to two sorts of device, the usual one being a scroll decanting continuous-conveying unit. The less common unit is referred to by Ormsby (Ibid.) as a 'holey rotor', and effectively is a centrifugal concentrator with a slurry discharge, in contrast to the much drier product of the true centrifuge. Both can achieve a similar effect in the commonest usage (barite saving in weighted water muds) but the decanting centrifuge is more versatile, and the following comments refer to this type of device.

A centrifuge can separate all normal drilled solids greater than 3 um (and 2 um barite), though the speed actually used may give a higher cut point. It produces a very clean fluid and a very dry solid, though which is discarded depends on the mud system. For example, in an expensive oil or polymer fluid without weighting material the solid will be waste and the liquid will be retained. Conversely, for a water-based clay mud weighted with barite, the solid will contain 70% or more of the barite, whereas the liquid will contain fine solids which increase the viscosity and interfere with drill-bit efficiency. Thus the liquid is discarded and the solid mixed with an equivalent amount of water (plus perhaps some more bentonite and barite) to provide replacement clean mud at lower cost.

Where an oil-based mud is used, then a centrifuge can be used to remove most of the oil from solids waste generated by other solids control devices. This has the double benefit of salvaging an expensive liquid and making the waste more environmentally acceptable.

Of all solids-control equipment, centrifuges are the most efficient separators and are said to be the simplest to operate (Ormsby 1973a). However, they are very expensive to operate and to rent or buy. Furthermore their capacity is generally much less than the mud flow-rates used, so they can only process part of the mud. The throughput of a given centrifuge may be limited either by its solid or its liquid discharge rate, depending on the solids concentration in the feed. However, a typical processing rate is 2 $dm^3\ s^{-1}$ (25 g.p.m.) which is rarely more than 10% of the drilling circulation rate.

Mud centrifuges are said to be most effective if the feed is diluted to reduce its viscosity. However, this must not be so much as to allow turbulent flow to commence, which would reduce the separation. Ormsby (1983) recommends that the liquid outflow should have a Marsh Funnel

time of 35 to 37 seconds per quart. In the case of oil muds, the viscosity may be reduced by heating up to 32°C (Ibid.).

Where solids discharge rate is the limiting factor, the liquid throughput can be increased by running at a lower speed (thus making a coarser cut on a greater volume). For this reason, two-stage centrifuging can be used. Patel & Steinhauser (1979) give a solids control diagram for an Alaskan well in which it is clear that two moderate-speed centrifuges draw from an active tank of (desanded and desilted) mud in parallel. A higher-speed centrifuge draws from the outflow tank of the pair, removing further solids and in part feeding back to provide dilution for the lower-speed units.

1.6 Industrial Practice in Solids Control of Muds

Table 1.2 (below) is abstracted from a much larger list of practical aspects of drilling fluid use (ranging from blow-out preventers to ecological considerations) given by Hutchinson & Anderson (1974). It should be noted that the mud system is often changed during a drilling programme, and this implies that the solids control system should also be changed. For example, when barite weighting is added, then the desilting hydrocyclones should not be used, or should be replaced by a mud cleaner and/or centrifuge so as to conserve the weighting agent.

Table 1.2 Equipment required for Different Muds

Equipment	Water/light treated clay	Dispersed weighted	Non-dispersed		Oil muds
			Unweighted	Weighted	
Solids removal Shaker screen	Dual w/med. screens	Dual w/med. to fine screens	Double deck w/ med. & fine screens	Double deck med. & fine screens	Dual w/med. to fine. Double deck w/fine
Sand trap	20-30 bbl. w/45° bottom-large diam. dump	Be careful not to dump liquid mud	Important to settle coarse material ahead of desander-desilter units		Important to settle sand. Be careful of mud loss
Desander	Important-run ahead of desilters	May be used to remove coarse material ahead of desilting equipment	Important to prevent overloading desilters or centrifuge		Can be used by dumping into tank of solvent
Desilter	Important to remove fine silts for low weight	Not used	Essential for low solids muds	Not recommended	Not used
Mud cleaner	Important to remove fine silts for low weight	Excludes lt. solids on medium weight mud	Essential for drilled solids control	Useful on Medium weight muds	Not used
Centrifuge	Not used	Essential for economic control of high wt. muds	May be used to reclaim liquids and dump drilled solids	Essential for high wt. mud control	Can be used to reduce wt.
Degasser	May be used ahead of treatment if gas encountered	Essential in kick control for true wts.	Essential for good kick control practice		Can be used if gas cutting a problem

Of course, the possession of the correct items of equipment is no guarantee of success. They must also be correctly sized, rigged, operated and maintained. Furthermore, the requirements are likely to change during drilling, so the mud system must be updated to cope with the current situation.

Oddly enough, the mud engineer's 'bible' - Gray, Darley & Rogers (1980) has essentially no practical information on solids control, though its importance is mentioned in chapters 1 and 2. This perhaps suggests that solids control has not received sufficient priority in the past. The papers of Ormsby (1973a, 1973b, 1977, 1981) do give practical advice from an obviously knowledgeable source, and are evidently written because of the faults he has found to be common in the field. It is salutary to note that some authors (White 1982c; Williams 198-2b; Young & Robinson 1982a, 1982b, 1982c) have recently warned of incorrect rigging arrangements very similar to those described by Ormsby (1973a, 1973b) nearly ten years earlier.

Leblanc (1978) and Williams (1982a) gave advice on sizing screens, cyclones, centrifuges and pumps. They stressed the economic advantages of a well-designed system, and made recommendations which implied that incorrect practices were not uncommon. Much the same can be said of a paper by Marshall & Brandt (1978) which concentrated on principles rather than sizing, as does a later paper by Williams & Hoberock (1982)

The selection and use of solids control equipment is usually the responsibility of the site drilling superintendent except on some sites (and commonly offshore) where it is provided as a complete package (Wilson, Callender & Mosher 1977; Moore 1978). However, Ormsby (1973a) has pointed out that location and even selection of apparatus on an offshore rig may be determined by the decisions of marine engineers at an early stage, making alterations difficult and expensive. It was reported in 1977 that in North Sea drilling some contractors were making extensive commitments to mechanical solids control while others were mainly relying on dilution (Moore 1977).

In 1975-6 Wells (1975, 1976a, 1976b) showed the great economic advantage of mechanical methods of solids control (as opposed to chemical treatment or dilution), especially for 'high performance' or expensive muds. At about the same time there were attempts to achieve near 'total solids control' in the field (on admittedly favourable sites) by scrupulous attention to the control system (Anon 1976; Dawson & Annis 1977; Wilson, Callender & Mosher 1977). Considerable economical, and ecological benefits resulted.

The 'total solids control' system was developed by Exxon into a packaged unit (Kalil, Speers & Robinson 1982) and marketed by Baroid as 'Unitized Solids Control' (Anon 1983). A major advantage seems to be that it is more difficult to rig incorrectly.

So far as field operation is concerned, the principal failing (most authors cited) appears to be the bypassing of solids control equipment. This may be deliberate - e.g. around a shale shaker which is blocked or otherwise needs attention - or inadvertent - e.g. not realizing that intercompartmental flows will allow some of the mud to pass through untreated while other portions are given the same treatment twice.

The second error most often reported is the failure to make full use of the equipment available. For example, the solids removal process need not be stopped when drilling is halted: by recirculating the mud through the control system it may be possible to clean it more thoroughly than is done during drilling. This is particularly important where there are items which can only treat part of the flow (allowing them to 'catch up' with the drilled solids). Another example is the use of solids control equipment only when accumulated solids causes a problem. In many cases it would have been better to start earlier and thus prevent or delay the problem.

2 BASIS OF THE RESEARCH

2.1 The Need for Solids Control

Drilled solids brought up to the surface by the mud can be discarded with whole mud, separated out, or returned to the hole. There is ample evidence that return to the hole should be avoided as far as is practicable because of the interference with the drilling process and consequently greatly increased costs. Chemical treatment can mitigate some of the effects of accumulated solids, but it is a palliative which is often temporary and always costly.

The use of mud on a once-through basis is not economically viable, though some discarding is necessary in replacement and dilution methods of reducing the level of accumulated solids. Essentially, these methods are required insofar as separation has not been totally successful.

Effective mechanical removal of drilled solids would therefore have the benefits of reducing the loss of mud (which is often expensive to replace) and mud treatment chemicals, plus permitting the drilling process to be as efficient and economic as possible (in terms of days and drill-bits required).

To better understand the problem, it is instructive to compare the mud system with a chemical process operation. In effect, drilled solids are generated within the mud, and are then separated from it. However, unlike (say) a crystallization of a chemical product, the aim is not to optimize the yield and purity of the solid, but that of the recycle liquid. Moreover, it is more difficult to specify what the yield and purity should be. On a practical basis, the designer is faced with a varying quality and type of solid (size distribution, shape factors, grindability etc) in a fluid which is viscous, Non-Newtonian and which may be substantially changed during operation.

Considering the process operation, rather than the design, the mud system differs in two key ways from a typical chemical plant. Firstly, the effects of incorrect process conditions may not be seen for a very long time. In fact, they may just appear as increased drilling costs which might never be specifically associated with a particular poor practice.

Secondly, it is not easy to determine if items of equipment are working well. Methods of assessment have been published (Field & Anderson 1972; API 1974; Wells 1976b; Patel & Steinhauser 1979; Planck 1981) but they demand a commitment of time and effort which may not be welcome - particularly if the results suggest that changes should be made. Furthermore, the assessment would need to be repeated many times to deal with the varying condition of the fluid, its solid content, and flow-rate

In examination of the literature, field visits and discussion with experienced drilling workers, it was found that fundamental features of equipment such as capacity and efficiency were given in a variety of different ways, often ill-defined and difficult to relate to actual operation.

This study therefore set out to define the concept of efficiency of solids control in an effective and useful way, and to provide design information on the efficiency and capacity of a shale shaker as a function of operational variables.

2.2 A Mass Balance Analysis

2.2.1 Introduction

To optimize solids control it is necessary to have some kind of measure of its effectiveness. The view was taken that published definitions of efficiency of screening were generally inadequate, and often misleading, particularly where mixed definitions are used in calculations. This problem is not specific to oil-well drilling, but is more generally in solids screening - see for example the critical comments of Leonard (1974).

Fundamentally, what is required is the separation of drilled solids from original drilling mud. As has previously been discussed, an imperfect separation produces impurities in the liquid mud and impurities in the solid (waste) product. Both of these have economic penalties and must be considered. (Trivially it would be possible to get 100% removal of solids by discarding whole mud, or it might be possible to get a very dry product with a very low yield: neither situation is desirable.)

It is proposed that the best single number definition of efficiency would be an extension of that of Leonard (1974) for solids screening. Instead of a solid being divided into two size ranges (oversize and undersize) the mud is divided into two phases, solid and liquid. Then the following definitions apply:

Efficiency of solid separation =

fraction of total drilled solids delivered to solid phase

Efficiency of liquid separation =

fraction of original whole mud delivered to liquid phase

Overall Separation Efficiency =

solid separation efficiency x liquid separation efficiency.

For example, if a shale shaker removed 80% of drilled solids, and in so doing lost 25% of the mud, the solids separation efficiency would be 0.8, the liquid separation efficiency (1 - 0.25) = 0.75, and the overall efficiency 0.8 x 0.75 = 0.6.

It was considered that such a definition would be useful as a standard means of evaluating the performance of solids control equipment. However, it gives equal weight to losses of either phase, which may not be the case. A fuller description has therefore been developed using the technique of mass balance. This description is the basis for understanding the needs of solids control for the experimental work which follows.

Examination of the literature showed that the technique had been applied to the drilling process in only a very limited fashion, and its use for solids control strategies had been based on inadequate theory. Gray, Darley & Rogers (1980) do not include the concept, and Chilingarian & Vorabutr (1983) only give examples of the calculation of mud volume (from losses, additions and displacement by drill string and casing).

Mass balance has been proposed by Field & Anderson (1972) for the analysis of the performance of solids control equipment. They gave a complete and straightforward method for checking apparatus, which was taken up by the API in their 1974 recommendations on testing of centrifuges, hydrocyclones and shale shakers (API 1974). The impact (or lack of it) of these publications is perhaps indicated by subsequent papers.

Leblanc (1978) cited Field & Anderson (1972) but not the API (1974) in recommending that equipment should be checked by sieving mud before and after processing. Furthermore, he found it necessary to give a formula and graph for the somewhat trivial calculation of the amount of drilled solids produced by a given hole size and penetration rate. Patel & Steinhauser (1979) presented a sampling procedure and calculations for solids removal, but cited none of the above. They did, however, mention that true hole size (from caliper log) was preferable to nominal size for calculation of solids generated.

Planck (1981) presented a method of dealing with the calculations using a programmable calculator, citing the API (1974) and Patel & Steinhauser (1979). He gave a test on a desilter hydrocyclone as an example. Wells (1976b) [no references] explained a mass balance measurement on a centrifuge. (Most manufacturer's literature on centrifuge operation also suggests this.)

In recent years, mass balances have been published on total drilling operations, as part of the quest for 'total solids control' (Anon 1976; Dawson & Annis 1977; Wilson, Callender & Mosher 1977; Kalil, Speers & Robinson 1982).

The above relate to analysis of equipment performance (and calculations of mud make-up requirements), rather than a study of the process. However, Ormsby (1977) and others (White 1982c; Young & Robinson 1982a, 1982b, 1982c) have made some observations on material flows and balances within a system. Overall, it may be stated that mud engineers have the concepts and procedures to make use of a mass balance model of solids control, but to date this has not been successfully applied.

Wells (1976a) used mass balance theory to compare the costs of different solids control strategies. Unfortunately, this contained a major error which has apparently never been corrected. Wells claimed that low gravity (i.e. the drilled) solids content would come to an equilibrium value. For example: "Assuming that the influx rate is 4% low gravity solids per cycle, removal of 50% low gravity solids reaches equilibrium at the influx rate, or 4% low solids per cycle. If each cycle removes only 20% low gravity solids, however, equilibrium is reached at four times the influx rate, or 16% low gravity solids."

The calculation is correct, but the error is in supposing that the solids control system removes particles on a chance basis irrespective of size. That is, a screen which passes 50% of the drilled solids would be expected to remove half of its undersize if it was recycled. In fact, the recycle involves pumping and passage through the drill-bit so it is inevitable that the material will be reduced to a finer particle size.

A new mass balance model is therefore proposed, in a form which is of ready application, and which does not support the dangerous fiction that low efficiency solids control can maintain satisfactory mud condition.

2.2.2 Basis for the Model

The mud system is viewed as two phases, the drilled solids and the rest. These are designated 'solid' and 'liquid'. The solids control system provides a partial separation, providing two streams, a solid contaminated with liquid, and a liquid contaminated by solid. Note that in this sense the liquid phase includes desirable solids (hydrated bentonite and silt-sized barite). The separated liquid is fed to the drilling process where further solid is added and returned to the solids control equipment. The following assumptions are made (though they could be modified for any real situation in which the difference is significant).

[1] There are no losses to formation or by evaporation.

[2] The only input is drilled solids, where one volume of drilled hole gives one volume of solids.

[3] The solids control system discharges drilled solids wet with whole mud.

[4] The solids control system removes a certain size fraction of the drilled solids on one pass only. It does not matter if the cut is sharp or not, only that a certain fraction of the size distribution is removed.

[5] Further passage through the drilling process causes size reduction such that removal is thereafter of zero efficiency. That is, the mass passing through the solids system into the mud becomes permanent and accumulates.

It was found most effective to take quantities on a volume basis, although all the principles of mass balance apply. For discussion purposes, the industry unit of the barrel (bbl) was taken. As is standard for mass balance calculations, concentration ratios were taken. For example, a concentration of 5% is 5 in 95, or a ratio of 0.0526.

2.2.3 Definitions

Total solids in system	S
Total liquid (original mud)	V
Total hole volume	B
Liquid flow-rate (solids-free)	M
Solids input rate (dB/dt)	C
Solids rate in drill-pipe	F
Solids rate in annulus (C + F)	H
Solids removal fractional efficiency	K
Liquid carry-over (ratio liquid/solid)	L
Ratio of S/V	q
Ratio of C/M	r
Ratio of H/M (solids concentration)	x
Time	t

The zero subscript indicates an arbitrary start time t_o.

2.2.4 Derivations

By definition:

$$H = C + F \tag{6}$$

$$F = M\,(S/V) \tag{7}$$

$$B = \int C\,dt \tag{8}$$

hence:

$$B - B_o = \int_{t_o}^{t} C\,dt \tag{9}$$

Solids Mass Balance:

as hole increases from B_o to B, then

$$\text{solids discarded} = K (B - B_o) \quad (10)$$

$$\text{solids accumulated} = S - S_o = (1-K)(B-B_o) \quad (11)$$

$$\text{therefore} \quad S = S_o + (1-K)(B-B_o) \quad (12)$$

Liquid Mass Balance:

as solid is discarded, liquid is discarded in the ratio L to the solids discard, and volume decreases from V_o to V. Hence from equation (10):

$$V_o - V = L K (B - B_o) \quad (13)$$

$$\text{therefore:} \quad V = V_o - L K (B - B_o) \quad (14)$$

Mud Composition in Drill-Pipe:

from equations (12) and (14):

$$q = \frac{S}{V} = \frac{S_o + (1 - K)(B - B_o)}{V_o - L K (B - B_o)} \quad (15)$$

Mud Composition in Annulus:

from equations (6) and (7) plus the definition of x :

$$x = \frac{H}{M} = \frac{C}{M} + \frac{S}{V} \quad (16)$$

therefore:

$$x = r + q \quad (17),$$

To Relate Hole Volume to Mud Composition in Drill-Pipe:

rearrange equation (10) and collect terms:

$$B - B_o = \frac{q V_o - S_o}{1 - K + q L K} \qquad (18)$$

by definition:

$$q_o = S_o / V_o \qquad (19)$$

therefore:

$$S_o = q_o V_o \qquad (20)$$

substitute in equation (18) and collect terms:

$$B - B_o = \frac{V_o (q - q_o)}{1 - K + K L q} \qquad (21)$$

which may be arranged to give:

$$q = \frac{q_o V_o + (1 - K)(B - B_o)}{V_o - L K (B - B_o)} \qquad (22)$$

These are the two equations which relate volume of hole drilled and accumulated solids to the amount of solids removed and the wetness of solids discharge.

2.2.5 Applications

Suppose that drilling is in progress and the solids control system is functioning reasonably well. The tests recommended by the API (1974) can be carried out to determine the rate of removal of drilled solids and the rate of loss of mud associated with it. On the basis of down-hole data and the operator's experience, the rate of drilled solids production can be

estimated (from the penetration rate and gauge hole plus allowance). Thus the fractional efficiency of solids removal K is known, as is the liquid loss ratio L. The current circulating volume V_o and solids concentration ratio q_o will be known.

Hence the equations (21) and (22) allow the operator to predict the additional volume of hole ($B - B_o$) which can be drilled by the time the solids content reaches a given value q. Figure 2.1 shows the curves which result for an initial volume of 1000 bbl (V_o) of clean mud ($q_o = 0$), accumulating solids to a volume ratio (q) of 0.05 (= 4.76%). The solids removal efficiency has been expressed as a percentage (100 K). The dashed line represents those combinations of removal efficiency and wetness of solids discharged which result in the loss of 1 barrel of original mud per barrel of hole excavated. The shaded areas are impossible or unlikely values of L and K.

The operator may be more concerned with the drilled solids in the annulus (because of the risk of a stuck pipe), which can be got from equation (17) if required. [According to Hopkin (1967), "experience shows that more than 5% by volume of cuttings causes tight hole or stuck pipe when circulation is stopped for any reason."]

The operator may use this information in several ways. The following are some examples.

[1] If previous experience suggests that stuck pipe or pumping problems will occur at a particular concentration of drilled solids, equation (21) will predict how much hole can be drilled before this occurs. A suitable safety margin may be allowed, and the mud treated or replaced before the critical point. Such action could be scheduled to fit conveniently in the drilling programme.

[2] If part of the solids control system fails, then a similar calculation will show how long drilling can be continued in safety, or if it would be better to stop and put the matter right.

[3] If it is suggested that the solids control system can be improved, then the effect of that improvement can be calculated in terms of extra hole. For example, a system which is achieving 70% solids removal may not be much benefited by the addition of a centrifuge to remove another 5%. However, the same improvement on system with 90% removal might give almost 50% more hole volume.

[4] As the prediction is as accurate as its input data, any deviations can be used to correct field estimates of hole gauge, loss to formation etc.

[5] Short-term changes can be made to the solids control equipment (e.g. changing screen angle or cyclone flow-rate). The net effect of greater solids removal with wetter discharge can then be estimated to decide on an optimum. This will vary with the cost of mud and its disposal.

[6] Similarly, changes in mud flow-rate or penetration rate can be evaluated for the long-term effect.

Figure 2.1 Mass Balance Prediction of Hole Volume
for solids control efficiency and liquid loss ratio

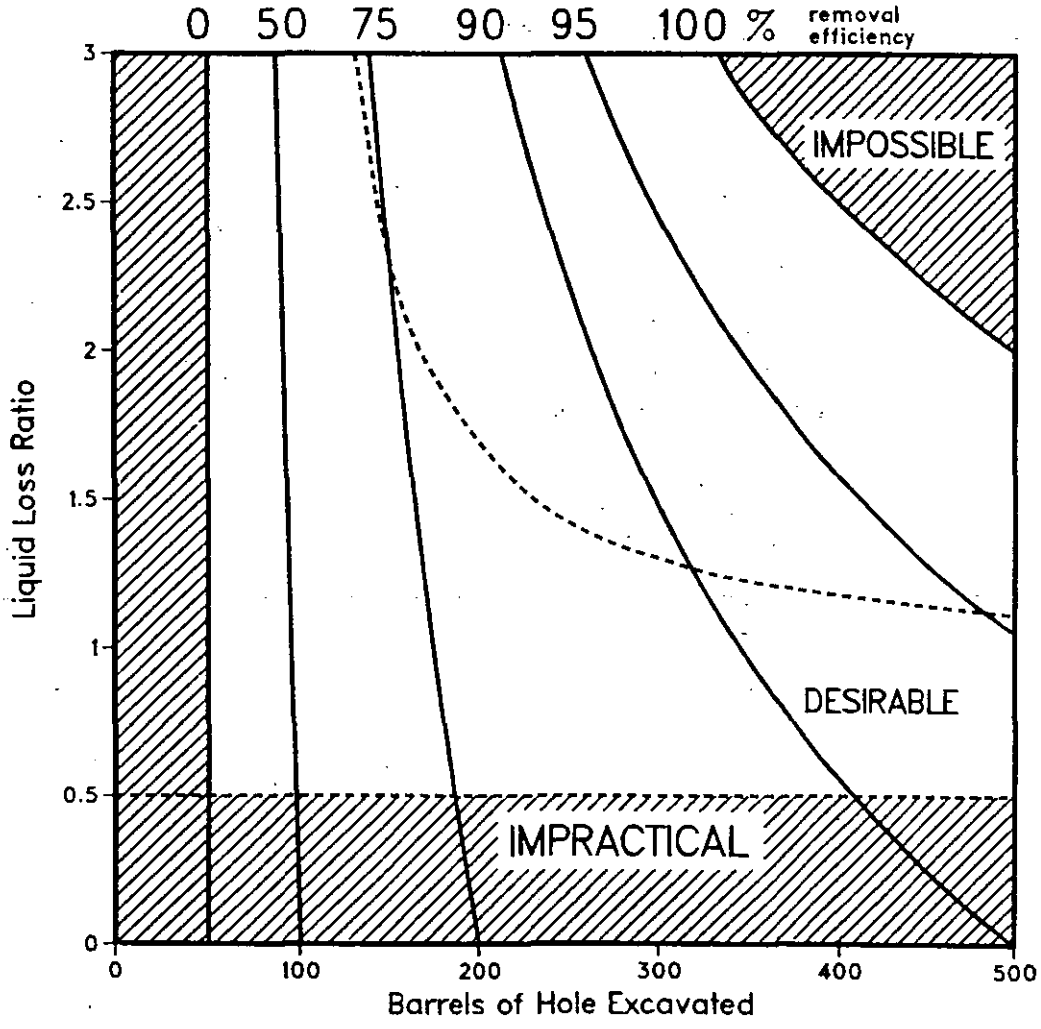

2.3 Operation of a Vibrating Screen Unit

Vibrating screens were originally devices for solid/solid separation, later adapted for dewatering of slurries. Their use for solid/liquid separation of drilling fluids is quite different because solids are a minor component (5% by volume or less). Thus what is satisfactory for solids is not necessarily so for liquids. The fact that the mesh moves is vital because drilling muds are so viscous that they will flow over all but the coarsest static screens. However, mud engineers reasoned that screen movement would "cut into" the mud and effectively thin it, which was empirically the case.

Screen motion is either near-circular or reciprocating, these being the two which are mechanically easiest to achieve. Circular motion can be either be tending to throw the oversize solids uphill or downhill. Reciprocating motion can be normal to the screen or at some angle to it, again uphill or downhill. For steep downward slopes, an uphill motion has been used in solids screening with the intention of retarding particles to give longer residence time. For slight downward slopes a downhill motion may be used to aid conveying in the desired direction.

For horizontal or upward tilted screens, it is clear that screen motion will be the major cause of particle transport from the feed to the discharge end, either by the direction of reciprocating motion being tilted, or the circular motion being towards the discharge in the upper portion of the circle. More complex motions such as tilted ellipses are possible, deliberately or fortuitously. Moreover, a circular motion can be considered as two reciprocating motions of the same frequency and amplitude, phased at 90^{o}. Tilted linear motion results if the two are in phase. Variations in amplitude and phase produce all possible ellipses. This was considered the most general description of screen motion. Mixed frequencies multiply the range of possibilities, which could be the subject of future research.

The main factors to be considered in optimizing a shale shaker or similar device are as follows: fluid flow rate through the screen (preferably large); cut size and grade efficiency for solids separation (preferably small); transport of solids from the surface of the screen (at least as fast as solids are delivered); dryness of solids discharged; mesh

blockages; screen working life. These are not necessarily separate terms: improvement in one aspect of performance may involve the sacrifice of another. However, before any overall optimization can be attempted it is first necessary to know the relationship between performance and operating conditions for the individual criteria. This thesis represents a study of a full-scale unit in the light of these requirements, aimed at a fundamental appraisal of design and operational needs.

The operation of the screen was therefore considered for two purposes: firstly to pass viscous non-Newtonian fluid, secondly to transport separated particles. The effects of circular motion and its two components were examined independently.

2.4 Fluid Effects

2.4.1 Previous Work

Despite the widespread use of shale shakers, there was virtually no information on the fluid capacity of the screens prior to 1978, when Cagle & Wilder (1978a, 1978b) published results of tests comparing a new design with a traditional one. The purpose of the work was to prove the new machine and also a patented screen mesh. However, data was given for work at full scale with 10 muds, and the authors concluded that plastic viscosity was the key factor, proposing a straight line fit for a graph of log(flow-rate) versus plastic viscosity. Work was carried out on a downward-sloped mesh with a linear vibration of 0.68 mm stroke at 60 Hz.

A major research programme was reported by Hoberock (1980, 1982d) and Williams & Hoberock (1982) on the influence of fluid properties, screen motion and screen tilt. Some of the results were also utilized in a more general series of papers on solids control in drilling fluids by Hoberock (1981a, 1981b, 1981c, 1982a, 1982b, 1982c). The results of a computer simulation of flow through a screen were presented as graphs relating fluid properties and other parameters to flow capacity. However, the experimental work only used a single fluid(1980, 1982d). Furthermore, though graphs were given for an upward sloped screen (1982d), the experimental results relate only to downward slopes.

Hoberock presented his model in the form of curves of flow-rate (ordinate) versus length of screen for specified conditions (mesh, tilt,frequency, acceleration, plastic viscosity, yield point). More than 200 of these curves are given in sequential papers (1982a, 1982b). However, his experimental data amounts to 5 curves with one fluid (1.8 % v/v bentonite in water) with conditions as follows: 40 mesh, -10°; 60 mesh, -10°; 60 mesh, -30°; 100 mesh, -10°; 100 mesh, -30°. All were at 60 Hz using a linear vibrator titled "slightly downscreen". The normal accelerations were 5.57 to 8.33 gravities. The rig was quarter scale, and the method was to set the liquid front to a given mark on the mesh, then measure the flow-rate.

This thesis may be considered an extension of the work of Hoberock, using upward slopes and different fluids.

2.4.2 Basis for Investigation

Hoberock's model, being a computer program rather than an equation, was not directly accessible for critical study, and it was not considered worthwhile attempting to generate an equivalent program. However, if proven, it was thought the model would be more useful in the form of an empirical correlation (i.e. an equation rather than graphs). By taking measurements from the graphs, it appeared that a power equation of the form:

$$\textbf{flow-rate} = (\text{width}) \times (\text{length})^2 \times (\text{conductance}) \times (\text{mud weight}) \times (\text{rheology})^{-1} \times (\text{acceleration})^{0.9} \times f(\text{angle})$$

was possible, where "conductance" is a screen property as defined by Hoberock, and where "rheology" is a liquid property analogous to viscosity, probably from a linear combination of plastic viscosity and yield point [this author's hypothesis]. f is some as yet unknown function of the angle.

It would be possible to question some of Hoberock's assumptions (as will later be discussed) but it was felt that this could most properly be done in the light of experimental data. As Hoberock's data was insufficient to validate all the points, further work was required. In addition, the behaviour of near-horizontal screens was important because of their increasing use.

In the above equation, **conductance** was precisely defined (following Armour & Cannon [1968]) as a function of screen geometry, for flow normal to the mesh. It should therefore be the same (or better) predictor for near-horizontal mesh as for downward-sloped mesh. To elucidate the **rheology** term, it was necessary to have (at least) two fluids with different rheologies though (say) similar Marsh Funnel viscosities. Hoberock's use of bentonite was somewhat unsatisfactory because of its thixotropy, that is the flow properties within the screen

would not depend uniquely on conditions in that unit but would also be expected to vary with the time and intensity of pumping in the external circuit. Without a very detailed characterization of the response of the fluid to all these influences any results obtained would be expected to contain uncertainties. For this reason work was carried out with two polymer solutions, providing rheology close to Power Law, and to Bingham Plastic models.

Hoberock's model indicated that flow-rate was nearly proportional to screen **acceleration**, suggesting that in practice this should be maximized (i.e. limited only by the effect of stress on screen life). However, his data did not cover a sufficient range to validate this important point, so it was obvious that this should be tested. Similarly, as **screen angle** only had two values, its functional relationship to flow-rate could not be proven (and in any case was not explicitly stated). Hoberock assumed that only motion normal to the screen was effective, and his computed results showed that **frequency** as such had no significant effect. These were both plausible, but worth confirming.

Possibly the major consequence for fluid capacity actually came from Hoberock's work on solids conveyance. In essence, he demonstrated that solids could be positively conveyed by suitable vibration (as is done in other fields) so that a downward slope was not necessary to carry screened particles off the mesh. This confirmed the move towards near-horizontal shakers (by some manufacturers) which would be expected to have greater fluid capacity. Hence the later papers (1982a, 1982b, 1982d) gave theoretical curves for horizontal meshes although his experimental work was entirely on the more traditional downward slope (as also was that of Cagle & Wilder). There was thus a particular need for experimental data on horizontal and adverse slopes, which is given in the present thesis.

2.5 Particle Effects

Particle effects may be considered under three headings: firstly the effectiveness of the screen at size separation, secondly the tendency of particles to jam into screen openings and therefore obstruct flow, and thirdly the manner in which particles travel on the screen. Some observations were made on the first two, but experiments were particularly carried out on the third. This is because solids conveying is crucial for near horizontal screens. In principle, the capacity of a shale shaker could be limited either by its ability to pass fluid through the screen or by its ability to carry solids off it. It is clear that the motion will affect the residence time of particles on the screen, which is likely to affect solid/solid and solid/liquid separation - i.e. the effective cut point and the wetness of solids discharge.

Hoberock presumed that the analysis of Redford & Boothroyd (1967) applied for particle motion on the mesh. This analysis has been generally accepted for vibratory conveying. However, the author had some doubt of its validity in the present context, because it essentially treats single objects in free flight or sliding motion. It was considered unlikely that such a model could apply to a concentrated bed of particles in the presence of a viscous fluid. However, it was empirically true that (as Hoberock contended) solids could be conveyed by a suitable motion, because two manufacturers produced near-horizontal shale shakers.

The two obvious complications are particle-particle interactions, and particle-fluid interactions. Tests were therefore made with concentrated beds of particles on a dry mesh and then in the presence of fluids. By covering the frequency range of the equipment it was shown that distinct flow regimes could be observed. These do not appear to have been remarked upon in the literature, but the author has noted them on dewatering screens, on shale shakers in the field, and in the photographs of Hoberock. For this purpose, it was necessary to obtain bulk quantities of solid particles in a size range slightly above that of the screens under test.

Practical experience suggested a further complication, in that the ability of the screen to pass fluid might be significant, and a test was carried out to check this.

3 APPARATUS AND METHODS

3.1 Main Rig

3.1.1 General Description

Figure 3.1 shows a general view. Figure 3.2 shows the industrial vibrating screen unit (described in more detail in section 3.1.2) which was the item under study. Figure 3.3 is a diagram of the key features of the apparatus.

The vibrating screen unit was mounted about 2 m above floor level on a specially-built framework. This rested on two vibration-isolating pads set into the concrete floor of the pilot laboratory. A nearby gantry was adapted to provide a catwalk along one side of the vibrating screen unit, and a further access platform was built in front of the unit using proprietry scaffolding and grid flooring. Care was taken that these structures were not in mechanical contact with the screen unit or its support. A wooden bench was located by the other side of the screen unit, to provide sufficient access to the bolts and jacking mechanism to allow routine adjustments.

Beneath the catwalk was located the main tank. This was of mastic-coated steel, rectangular and of nominal capacity 9 m^3 (2000 gallons). The vibrating screen unit was mounted above an integral pan. A chute was constructed on one side so that liquid going into the pan was directed into the main tank. Pipe connections were made to the tank via 6" flanges of centres 0.3 m above the floor. The main pipework was of 6" (0.15 m) diameter mild steel. However, two short sections were of reinforced rubber hose, again to provide a degree of vibration isolation.

A 'Mission' 5x6R centrifugal mud pump (belt driven by a 22 kW electric motor) was located on the same vibration isolating pad as the front legs of the girder framework. The inlet was connected (via rubber hose) to a 6" butterfly valve on a flange on the main tank. The outlet led to a small tank (known as the "possum tank")integral with the vibrating screen unit, giving submerged discharge. The possum tank was constructed so as to overflow via a weir and distributor plate and feed liquid to the screens.

Figure 3.1 [overleaf]

Main Rig - General View

Showing pump, front access platform and solids collection chute. The gutters for alternative solids collection are under the bench. The main tank (black) is on the far side of the rig.

Figure 3.2 [second overleaf]

Main Rig - Vibrating Screen Unit

Showing inlet pipe with orifice plate, discharging into 'possum' tank. The solids input hopper is slung over the distributor plate. The mounting plate for a circular test sieve is on the front of the machine (right of the picture).

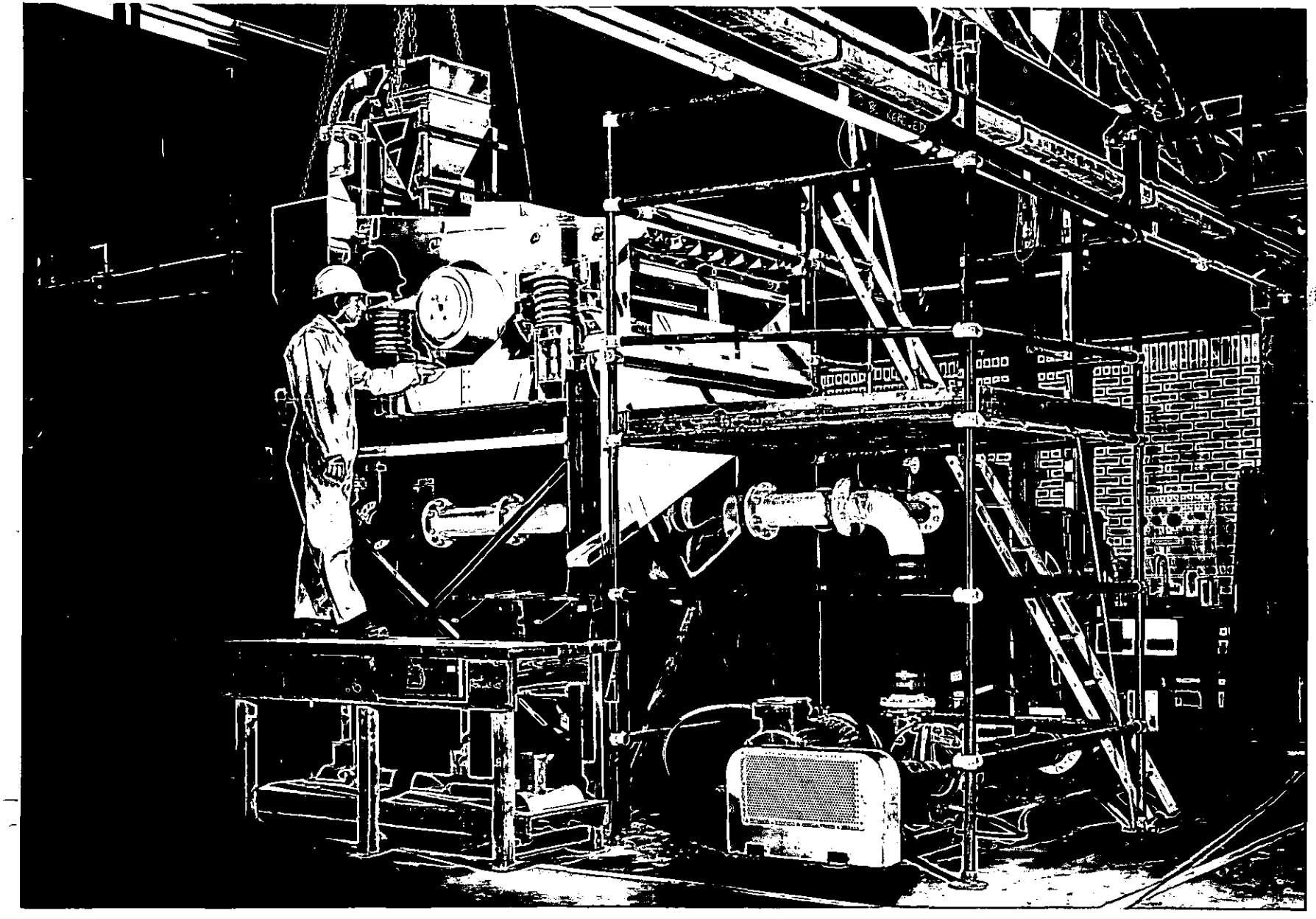

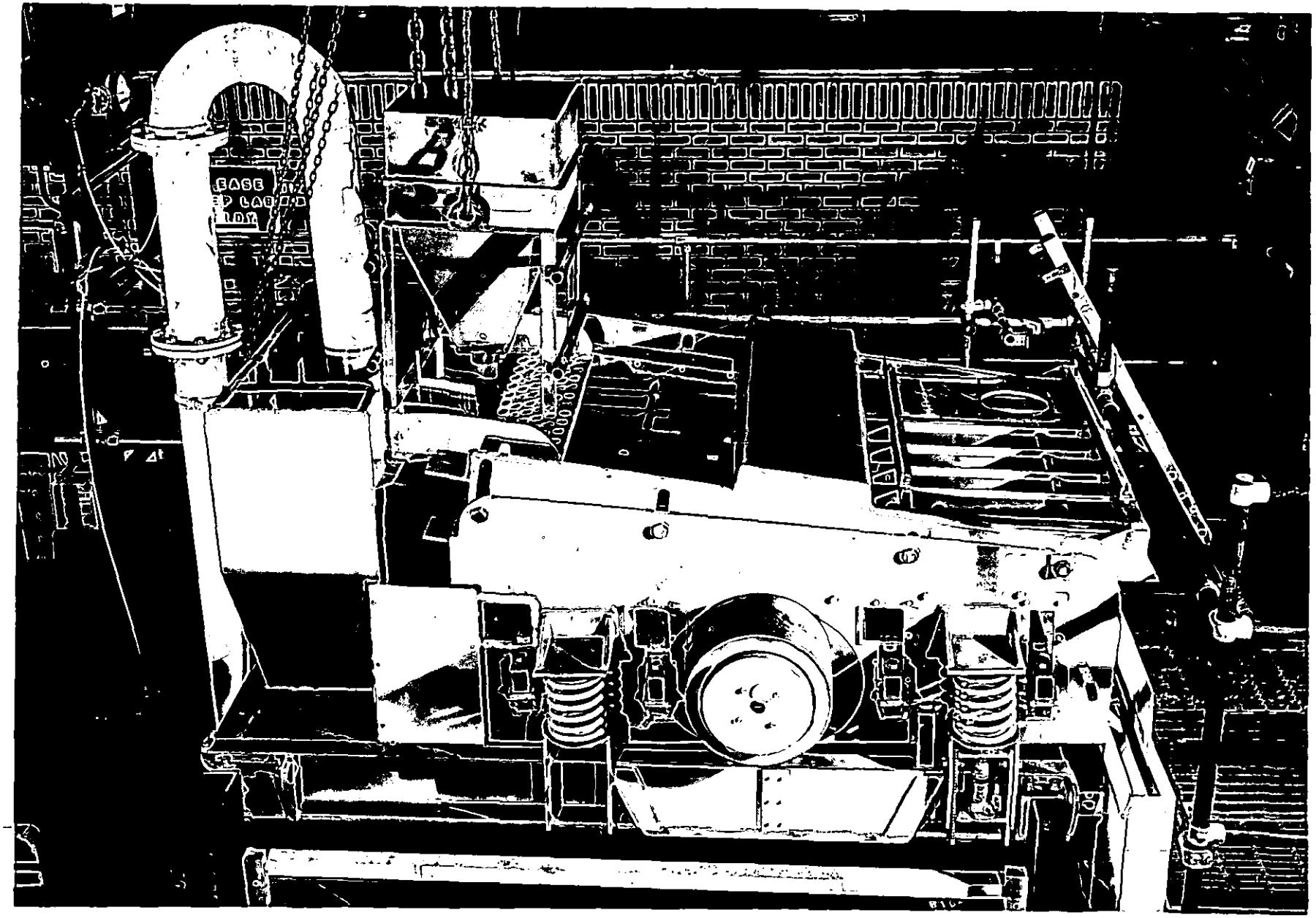

Figure 3.3 Diagram of Main Rig

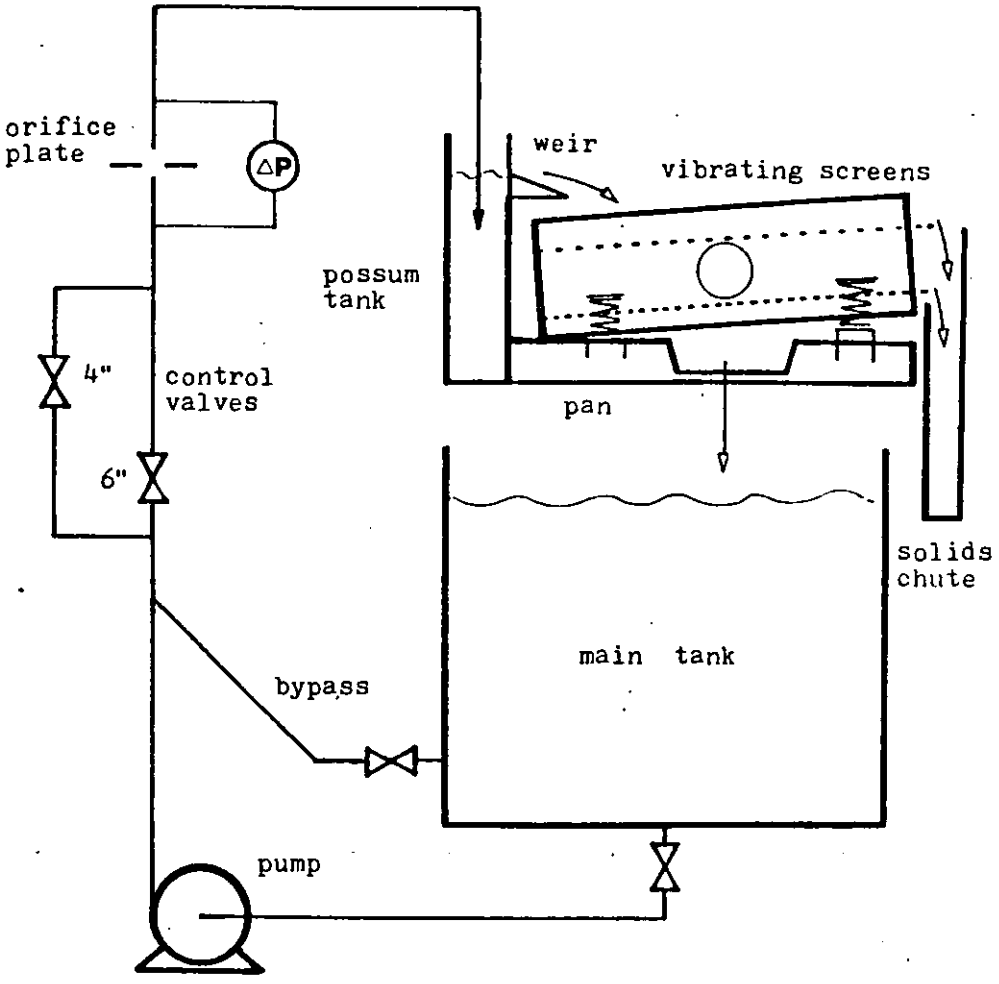

The outlet of the pump was throttled by a 6" Sanders diaphragm valve. To achieve better control, a 4" (0.1 m) pipe was fixed in parallel with a 4" Sanders valve. It was found in fact that all the fluids used gave sufficient flow through the 4" line, but this was not known at the outset. In addition, a side-arm led back (via rubber hose) to a 6" Sanders diaphragm valve on a flange on the main tank. This bypass allowed further control of flow, and was necessary for mixing fluids in the tank.

It was found that the pump could deliver 55 dm^3 s^{-1} (720 g.p.m.) to the possum tank, and exerted a pressure of 2.4 bar (35 psig) at an operating speed of about 22Hz (1300 rpm). (Provision was made for an increase in speed up to 27 Hz, but this was not found to be necessary).

A pressure gauge was fitted on the discharge side of the pump, and an orifice plate with differential pressure gauge was later installed (see section 4.1.9). There were drain valves at appropriate points and a direct connection to the cold water mains to aid flushing of the pipework. A small flow of water was maintained to the drip pan under the pump seal to flush away leakages of rig fluid. The main tank was fitted with a small drain valve and an overflow pipe. The solids collection chutes are described in section 3.1.13.

3.1.2 Vibrating Screen Unit

This was a double deck near-horizontal screen shale shaker, on loan from the manufacturers, Thule United. It is shown in Figure 3.2. It was in fact a prototype unit, differing in some details from the production versions, but of identical size, capacity and general behaviour. This unit was considered to be generally representative of fine screen shale shakers, not just a particular design. However, the Thule unit was particularly suitable for experimentation because the speed could be continuously varied over a wide range, the slopes of both decks could be independently varied, and it could be fitted with both post-tensioned and pre-tensioned screens (see section 3.1.3).

The unit was mounted on a skid, the base of which was made into a pan to receive liquid passing through the screens. An opening was provided on each side of the pan. One was closed off and a chute fitted to the

other to carry liquid into the main tank.

The skid was 1.87 m wide and 2.6 m long, of which 1.9 m was the pan. On the rear portion was mounted a rectangular tank (the "possum tank") of height 0.97 m, width 1.445 m, length 0.435 m. As can be seen from Figure 3.2, the lower portions of the sides were sloped inwards.

A 1.0 m wide opening at the front of the possum tank allowed liquid to flow into the working area over a perforated rectangular plate distributor. The mounting of this distributor was altered and the joints were specially caulked to minimize fluid flows bypassing the screens. At the bottom front of the possum tank was an 8" butterfly valve. This was used to bypass the entire screening section when necessary, and also when measuring flow rates (see section 3.1.8).

The moving portion of the apparatus (the "basket") was oblong and mounted on four large coil springs. In the centre of the basket was a horizontal tube running across the machine. Within this tube was a rotating shaft with weights on one side. The shaft was rotated by a hydraulic motor at one end, the power being transmitted via flexible hose from a floor-mounted hydraulic pump. By conservation of momentum, the effect of the unbalanced shaft was to cause the basket to rotate in the opposite direction. Because of its much greater mass, the circle of rotation was smaller than that of the weights. In fact, the basket was found to describe a approximately circular motion of about 1 mm radius such that the top of the circle was from the rear to the front of the machine - i.e. the direction of flow of fluid.

The basket itself was basically solid steel plate at the rear and two sides, with open front, top and bottom with a number of cross-members. On the top portion were two rails running lengthways. One was fixed, and the other could be moved by adjusting several bolts. The upper screens consisted of rectangles of mesh attached to steel channels which could be slid onto the rails in the basket. Adjustment of the moving rail was used to tension the screen. To provide intermediate support for the upper screen, stretchers were provided in the form of vertical steel strips running lengthways above the mesh. U-channel rubber was fitted on the bottom of these stretchers to prevent damage to the screen. The centre stretchers were lower than the outer ones, so the tensioned screen assumed a curved shape, lowest at the centre. Effectively, the stretchers also

divided the working screen into a set of strips about 0.15 m wide.

In the lower portion of the basket, a rectangular box member ran from the centre of the rear to the front, and there was a smaller box member at the same level on each side. These provided the clamping rails for the lower screens, which could be slid into place from the front. A rear cross-rail was provided, but this did not mate with the screens adequately and required caulking to prevent excessive fluid loss. To fix the lower screens in position, a frame was brought down and bolted at 8 points. There was a spring at the bolting points to lift the frame up when the bolts were loosened, allowing the screens to be removed. The lower screens were provided already tensioned and fixed on angle-iron frames. A strip of rubber was stuck on the top of the angle-iron, and it was on this that the clamping frame actually bore.

The top deck was completely covered by a single piece of mesh, but the bottom deck required 4 sections to be fitted in place. However, both had a nominal superficial area 1.8 m long by 1.2 m wide. The lower deck was completely flat.

The bottom supports of the front suspension springs could be jacked up and bolted in various positions along a vertical slide. This fixed the tilt of the basket, and the lower deck. The upper deck could be tilted relative to the basket, because the stretchers and rails were all attached to an inner framework which was bolted to the basket sides via a series of slots.

The hydraulic power unit had a specified power input of 5.5 kW, and the output was controlled by a variable flow valve. With the manufacturer's agreement, the stops were removed and it was found that the maximum speed of rotation of the basket was 33.3 Hz. (It was calculated that for the estimated mass, the measured motion would require about 3.3 kW, or 60% efficiency, which seems reasonable.)

Figure 3.4 Upper and Lower Screens

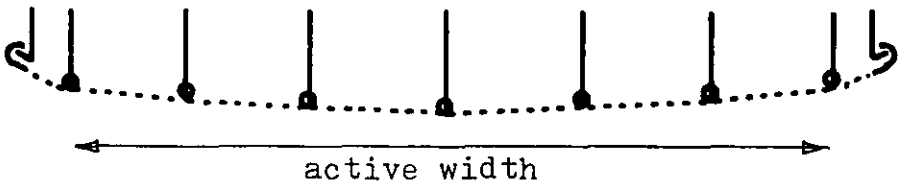

(a) upper screen - cross-section
showing mounting rails, stretchers and rubbers

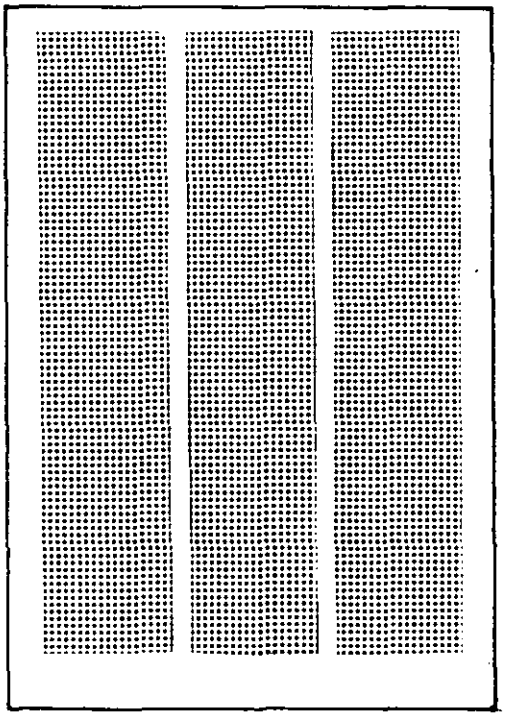

(b) lower screen - plan of one unit
there are 4 of these per deck
only part of the mesh is available because of underlying supports dividing it into 3 strips

3.1.3 Screen Meshes

The method of mounting was described in the previous section. A representation of the mesh units is given in Figure 3.4. The working width of the top screen was 0.99 m and the length 1.82 m, giving a surface of 1.8 m^2. The lower deck consisted of 4 separate units, each of which effectively had 3 strips of width 0.167 m and length 0.81 m, giving a total available area of mesh of 1.6 m^2.

All meshes were of stainless steel, plain square weave. The lower deck units had supporting coarser mesh (18 mesh for the 100 mesh, 30 mesh for the 150 mesh, where the mesh size refers to the number of wires per linear inch). Wire and aperture dimensions are given in table 3.1 (below) obtained from examination under a microscope.

Mesh of sizes 50 and 80 were used on the upper deck. A mesh of size 100 was originally supplied for the lower deck. This was already part-blocked from previous use, and soon developed small holes. However, later on brand-new screens of mesh size 100 and 150 were obtained. Thus except where stated, or where "original 100 mesh" is quoted, the screens can be assumed to be perfect.

Table 3.1 Screens Used on Main Rig

mesh count per inch	50	80	100	150
support mesh count	-	-	20	18
mesh aperture um	315	185	142	98
wire diameter um	200	132	112	71
per cent open area	38	34	31	34
conductance	4.4	2.9	2.2	2.1

3.1.4 Screen Angles

The tilt of the moving portion of the rig could be adjusted by jacking up the front pair of suspension mountings, which were then bolted up to give firm support. The distance between centres of the front and rear mountings was measured as 1.12 m. By simple trignometry, raising the front mountings by 19.5 mm would produce a tilt of 1^{o} of arc. For the small angles involved, this ratio can be taken as constant.

Initially, the mountings were adjusted until the top screen was level in all directions (by 1 m spirit level, effectively to 5' of arc). A mark was made on the sliding portions of the front mountings and a millimetre scale fixed to the stationary portion, so that the displacement relative to horizontal could be directly read. Later on, spacers were made in units of 19.5 mm. These gave a more secure and reproducible set of positions of the front mountings and hence screen angles.

The vertical distance between the upper and lower screens was measured at the front and back, and found to correspond to a relative angle of 3^{o} 10'. Later, the upper screen frame was unbolted and adjusted so that the difference was 4^{o}. It was not possible to bring the lower screen down to horizontal. Even with the front mountings in the lowest position, the screen had an upward tilt of 40'. For practical purposes, the lower screen tilts ranged from +1 to $+8^{o}$, and the upper screen from -3 to $+1^{o}$.

No allowance was made for spring bending, nor the probability that under load the rear springs may be more highly compressed, slightly increasing the upward tilt.

3.1.5 Frequency Measurement

In the commissioning of the rig, the frequency of motion was measured by a hand-held tachometer applied to the end of the central rotating shaft. However, this was not convenient for experimental purposes, so an electronic system was devised.

This comprised a linear motion transducer (Penny & Giles Ltd, type PGS model LP.2 serial 0040377) fixed parallel to one of the suspension springs between the moving basket and the fixed pan frame. This was fed with 10 volts d.c. from a Farnell stabilized power supply type L30AT. The output from the transducer should be proportional to the displacement of the moving head. This output was fed to a Racal Computing Counter, no 9525. This instrument counts the number of cycles of the input signal over a set time period. With the sample time set at 10 seconds, the digital display indicated the rig frequency to the nearest 0.1 Hz.

The frequency measured in this way agreed with the tachometer readings to the precision of the latter. As a further check, a Philips PR 9113/00 stroboscope was used. With the rig running normally, the stroboscope illuminated a target on the side and the flash rate was adjusted until the target appeared stationary. The stroboscope meter and the Computing Counter gave identical readings (14.0, 21.7, 28.3 Hz) and it was therefore concluded that the frequency measurement was correct.

3.1.6 Acceleration Measurement

The front cross member was a square tube. This was drilled and tapped on the top and front so that an accelerometer could be screwed into either position. A Bruel & Kjaer accelerometer type 4334 (serial 358998) was used with the output taken to a valve amplifier and meter, a Derritron Ultrasonics 'g Meter' type A1 (serial 150).

To check the calibration, a metal ring was taped to the cross member with a coin trapped inside. The rig was operated at increasing frequency until the coin could just be seen and heard to move. At this point the g meter was reading 1.00 gravity on the scale 0 to 5 g, 0.997 g on the scale 0 to 1 g. It was therefore assumed that the meter was

correctly calibrated.

Meter readings were recorded versus frequency for the accelerometer in both vertical and horizontal positions. A good straight line resulted from a plot of acceleration versus $(\text{frequency})^2$, with a correlation of better than 0.999. The lines for vertical and horizontal motion were indistinguishable. The simply pooled data gave one standard gravity equivalent to 16.34 Hz in the vertical case, 16.40 Hz in the horizontal. Experimentally, it was found that a frequency of 16.3 Hz gave one gravity to the precision of the instruments.

This agrees reasonably well with a circular motion of 1 mm radius

3.1.7 Displacement Measurement

The motion of the rig was recorded by a direct optical method. Essentially, a point source of light was attached to the rig, and a fixed camera focussed on the light. The camera shutter was opened for a time similar to one cycle of the rig, giving an image in which the rig motion was traced out by the spot of light.

The light source was a pinhole of about 80 μm pierced in brass shim sheet. This was stuck onto the face of a brass cylinder which had been threaded to accept a standard optical fibre coupling. The cylinder was itself fitted onto one face of a 50 mm length of 1 " angle iron. This unit was bolted using 2 bolts onto similar pieces of angle iron, welded to the top of the side panel of the moving portion of the rig. The other end of the optical fibre was mounted to receive focussed light from a lamp on an optical bench, placed on the gantry.

The camera was a 35 mm Nikon, fitted with a 2x converter and extension tubes to get a close-up field of suitable dimensions. For calibration, the rig was stopped and the pinhole mounting removed. It was replaced by a microscope stage micrometer (i.e. an accurately made grid) on a similar holder, illuminated by a spotlight onto a rear translucent screen.

3.1.8 Flow Measurement by Weir

The possum tank distributor was calibrated as a rectangular weir. That is, the height of liquid at the rear of the tank (in excess of that required for the first drops of liquid to pass the distributor) was used to estimate the flow-rate. For a well-behaved fluid and a correctly constructed weir with a smoothing tank ahead of it, the flow-rate should be proportional to $(\text{height})^{1.5}$. In view of the fact that none of these conditions applied, the experimental correlation to this formula was surprisingly good.

Initially, the height was measured on three scales fixed to the inlet pipe, the rear of the possum tank, and the side near the access platform. The average of the three was taken, unless surface swirl was obviously causing a local variation around one.

Once the principle was found to work, a sight glass was constructed (from 1" QVF pipe) at the rear of the possum tank, with a transparent millimetre scale. A rubber diaphragm was fitted to the joint, with a 5 mm hole in it. This greatly inhibited oscillations in the sight glass, but did not affect the steady-state condition.

To calibrate the weir, the possum tank itself was used as the receptacle for the "bucket and stopwatch" method. In this the flow was allowed to stabilize and the weir height noted. The possum bypass valve was opened wide so that the level dropped substantially below the overflow, and was then closed again. The time taken for the liquid surface to rise past two marks was recorded. The possum tank was rectangular in cross-section with a superficial area of $0.629\ m^2$, so a rise of 0.2 m corresponds to a volume of $0.126\ m^3$. At half maximum flow this required a time of about 5.5 s.

From an initial 37 points for water, the flow-rate **Q** ($dm^3\ s^{-1}$) was correlated to the height **h** (mm) according to the expression

$$Q = 0.0414\ h^{1.5},$$

the correlation having a coefficient of 0.997 (>99.9%).

As Figure 3.5 shows, this curve is closely followed by 30 measurements made for polymer rig fluids. The 95% confidence limits (t = 0.975, 2-tailed) are for the total data set. For a flow-rate of the order of 10 $dm^3\ s^{-1}$, these limits correspond to a range of ± 13%.

Figure 3.5 Calibration of Weir with Various Fluids

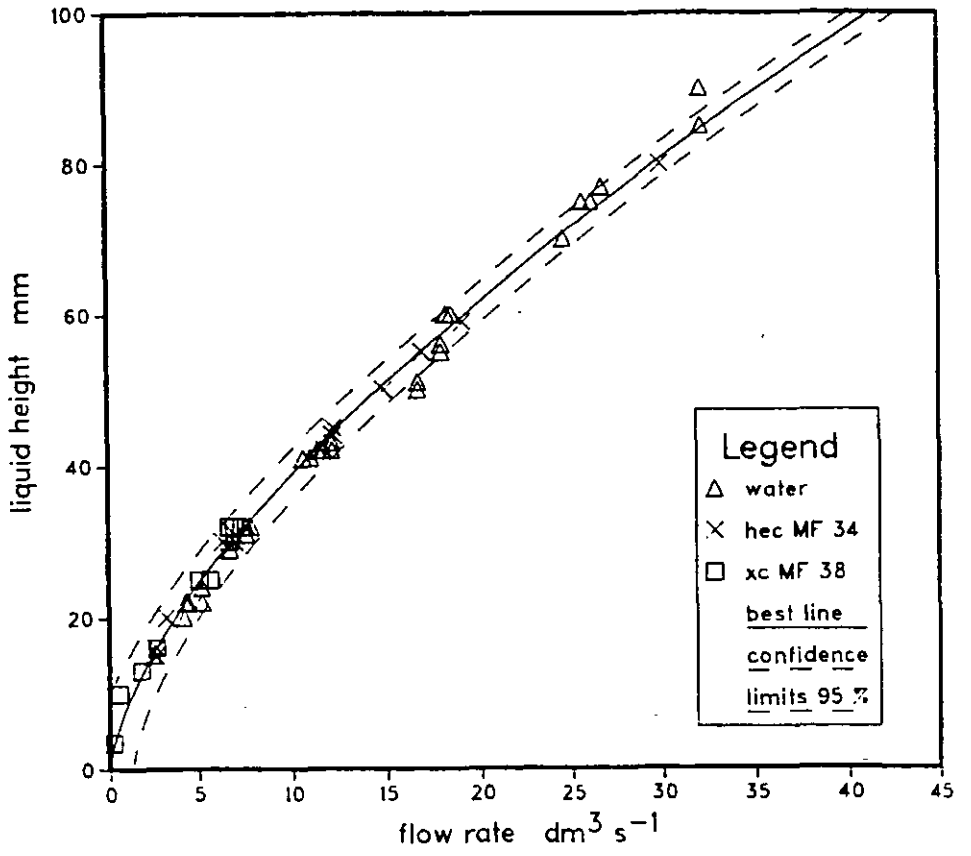

3.1.9 Flow Measurement by Orifice Plate

After commissioning and some experimental work, the vertical pipe leading to the possum tank was lengthened so as to give 10 pipe diameters of straight section, and pressure tappings were fitted on either side of a flange, 1 pipe diameter upstream and 0.5 diameter downstream. An orifice plate was made of 8 mm stainless steel, according to BS 1402, with an orifice of 70 mm.

The pressure difference across the orifice was measured by means of a dial differential diaphragm gauge, a Bourdon 'Microvar' gauge, 0 to 3 psi, in steps of 0.1 psi, which could reasonably be interpolated to 0.02 psi. The orifice was calibrated using an XCD rig fluid of Marsh Funnel time 40.5 s, by the same technique as described in section 3.1.8.

As Figure 3.6 shows, the flow rate could be reasonably fitted to the square root of pressure drop (the standard relationship). On this basis, the regression line through the origin fitted the expression

$$Q = 8.25\ (\Delta P)^{0.5},$$

where the flow-rate Q is in $dm^3\ s^{-1}$, and the pressure drop ΔP is the gauge reading in psi. The standard deviation was 0.53. The full-scale reading corresponds to $14.3 \pm 1.0\ dm^3\ s^{-1}$ [compared with a predicted value of 14.8]. At a flow rate around 10 $dm^3\ s^{-1}$, the 95% confidence limits correspond to a range of $\pm$ 11%.

As a general practice, the orifice plate was used for flow-rates up to 14 $dm^3\ s^{-1}$. Above this, the pressure gauge was isolated and flow readings taken from weir measurements (see section 3.1.8). An occasional check was made with the possum tank and stopwatch. For very low flow-rates (0.04 to 5 $dm^3\ s^{-1}$), it was possible to collect the rig outflow from the discharge chute and record the time for collection of 20 dm^3.

Figure 3.6 Calibration of 70 mm Orifice Plate with XCD fluid of Marsh Funnel 40 s

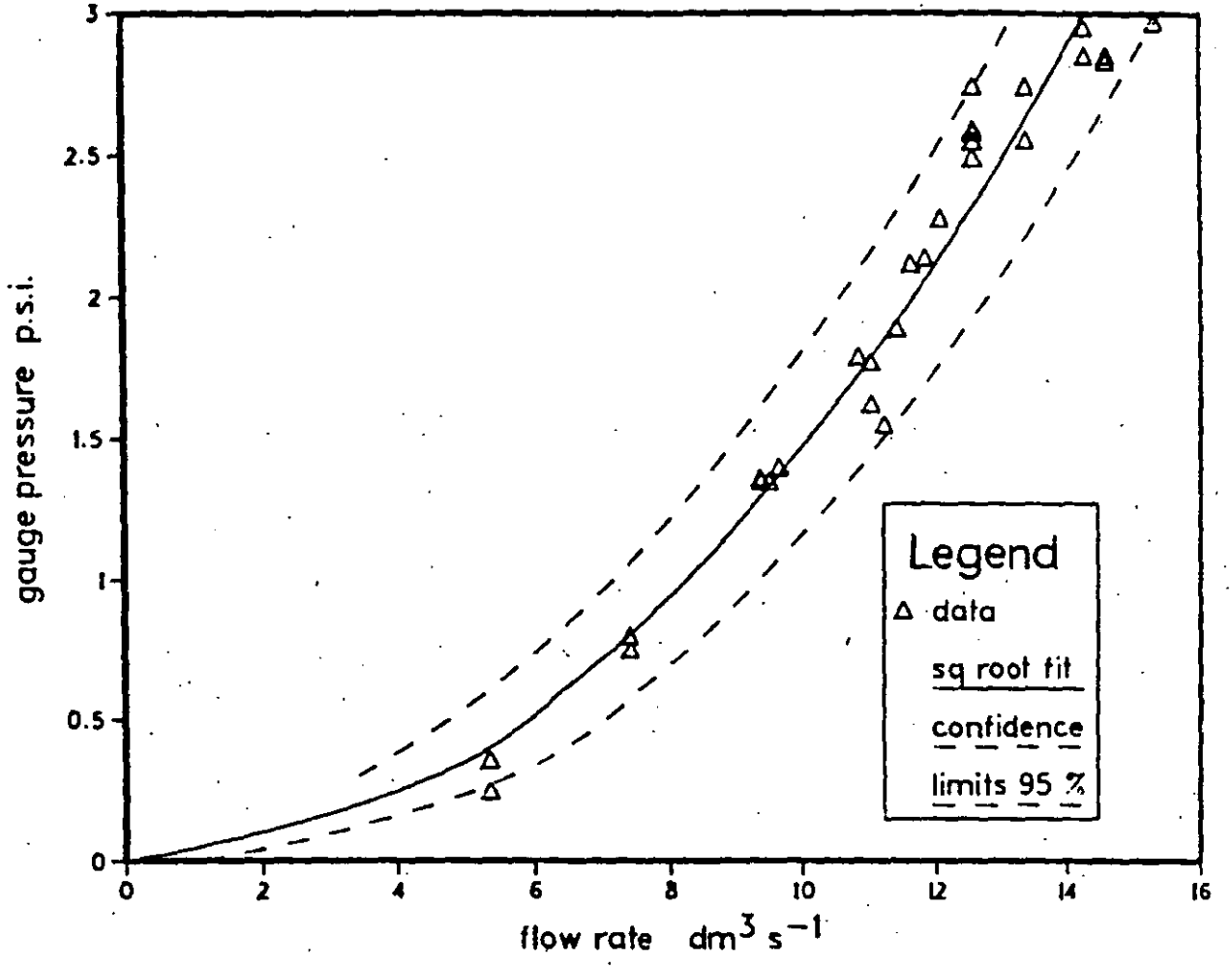

3.1.10 Screen Capacity Measurement

This was solely carried out with the flat pre-tensioned screens. The rig was set up with no upper screen and only the rear lower screens in position. Care was taken to get as good a seal at the rear as possible (see section 3.1.2.).

Generally, the apparatus was operated at a chosen angle and frequency, and the flow to the screens was altered by means of the throttle and by-pass valves on the pipe from the main pump. The limit of screen capacity was taken to be the flow-rate at which the liquid (not foam) started to overflow from the front of the screens. The onset of this condition was usually quite definite for a change of one quarter turn of the valve wheel or the minimum discernible change in flow-rate.

The procedure was somewhat tedious, because it was necessary to allow some time (5 - 10 minutes) for the fluid conditions on the screen to stabilize after making a change in flow. However, the results thereby obtained could be replicated the next day to the practical limits of measurement.

Unfortunately the screens themselves changed with use. Even with clean fluids, the new 100 mesh and 150 mesh screens accumulated solids (rig debris & rust), with noticeable changes in conductance. The old 100 mesh screens supplied with the rig were partially blocked (even after pressure washing) and later developed small holes. The new screens only became available in time for the XCD tests, so it was not possible to make exact comparisons between fluids for truly identical screens.

3.1.11 Conveying Speed Measurement

A fluorescent poster paint was used to mark lines at 0.1 m intervals on the upper and lower screens, parallel to the rear of the machine. These marks gradually wore off, but were sufficiently permanent for use in both wet and dry conditions.

For the tests on dry conveying speed, a quantity of about 50 g was added to a specific point to form a patch which tended to travel together. The time taken for its leading edge to pass 2 marks (200 mm) was measured

with a stopwatch. This quantity was selected because it formed a reasonable spread over one strip of mesh (i.e. between the stretchers) which appeared representative of working conditions.

For the tests on solids concentration, batches from 10 g to 500 g were deposited on a specific point, about 0.5 m from the front of the mesh.

For the tests on particle segregation, batches of 500 g were deposited on the top deck at a point 1.25 m from the front. The particles were collected at the front of the screen in rectangular boxes, the time being noted. The velocity was calculated from the residence time on the screen and a distance of 1.25 m.

3.1.12 Hopper

A steel hopper was used for the delivery of larger amounts of sand to the rig. It also served for the controlled addition of polymer powders when making up the rig fluids in the main tank. It was 0.45 m square and 0.75 m tall, with an exterior frame and stand, plus eyes to enable it to be slung by chains from the overhead crane, as can be seem in Figure 3.1.

The discharge valve consisted of two 76 mm brass discs, the lower of which could be rotated by a lever. Each disc had three holes of 12.5 mm, and when the two sets of hole were brought into line, the contents of the hopper discharged.

Calibration tests showed a virtually constant delivery rate for dry sand with the valve full open (0.28 kg s^{-1}) and quarter open (0.07 kg s^{-1}). This was utilised in tests of continuous operation of the screen.

The polymers were not free-flowing, but a steady discharge rate of about one kilogramme per minute was achieved by manual agitation of the solid in the hopper using a piece of steel strip.

3.1.13 Particle Collection

For tests involving modest amounts of particles, the rig was fitted with two lengths of uPVC rainwater gutter, with end closures. Both were sloped towards the main tank. They were positioned so that material from the upper screen fell into the upper gutter, and material from the lower screen fell into the lower gutter. Any liquid overflow from the upper gutter was directed via a small chute into the lower gutter. Any overflow from the lower gutter was directed by a small chute into the tank. Each gutter was fitted with a short length of down-pipe at the higher end, round which was fitted a plastic bag. This enabled solid material to be swept up with a small brush and collected in the bag.

For larger amounts of solids, a collection chute was constructed from 6 mm polypropylene sheet. This was mounted on the access platform framework (in place of the gutters) and could be raised or lowered to the most suitable height. The chute was of 100 mm width, with a sloping floor (approximately 30^{o} to the horizontal) and solid sides. It discharged on the side away from the tank via a small extension chute into a series of buckets on a bench. The chute wall furthest away from the rig had removable extension boards. These permitted easy access to the screens when necessary, while ensuring that all material discharged from the rig went into the chute.

Except for very liquid discharges, the solid which remained in the chute was quickly cleared with a scraper into the bucket when taking samples.

3.2 Static Mesh Apparatus

3.2.1 General Description

Some 3 mm duralumin plates were milled out to give two approximately equal open areas, as shown in Figure 3.7. These were then covered with stainless steel plain square weave mesh by United Wire Ltd, using their standard bonding and tensioning. To hold these samples of mesh, an open-topped uPVC box was constructed with inner dimensions equivalent to the free mesh, and an outer flange. The bonded mesh was sandwiched between this flange and a backing flange in the form of a duralumin plate with a rectangular open area slightly larger than the free mesh. A seal was made with a soft rubber gasket and the whole was held together by 12 brass bolts in holes drilled through all the components.

This assembly was located on top of a 20 litre plastic bin, and the whole adjusted until the mesh was found to be horizontal in both directions. See Figure 3.9.

The most satisfactory flow arrangement was found to be as shown in Figure 3.8. In this, half of the mesh was blanked off by a piece of heavy rubber, and the fluid was introduced to the centre of this portion via a slightly submerged flexible tubing. This eliminated the possibility of jetting through the mesh and gave a more stable surface over the flow area.

The fluid was pumped from the bin to the mesh using a 3/4 inch Mono pump with a continuously variable gearbox, capable of delivering between 0.1 and 0.5 dm^3, or less by the use of a bypass valve.

Figure 3.7 Support Plate for Static Mesh

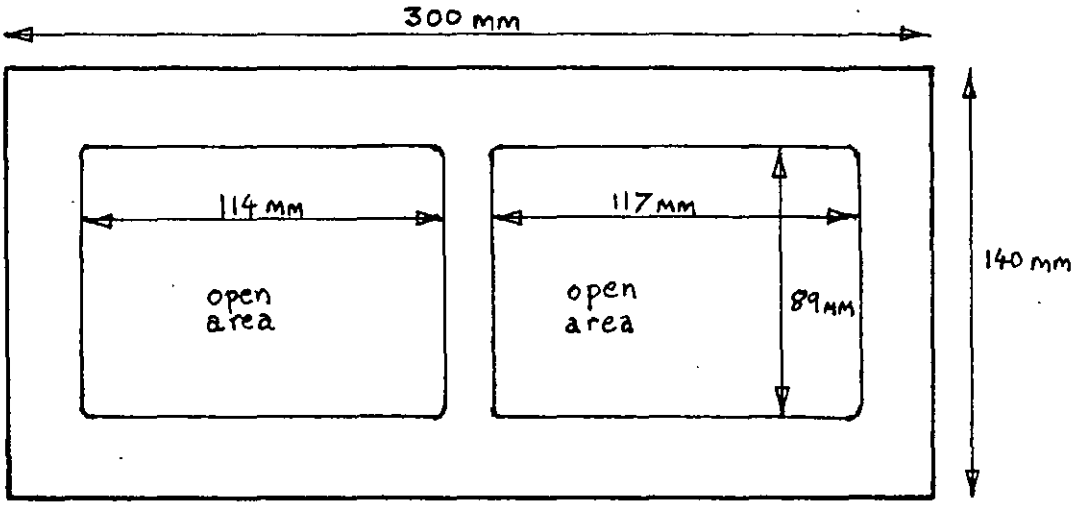

Figure 3.8 Flow Arrangement for Static Mesh

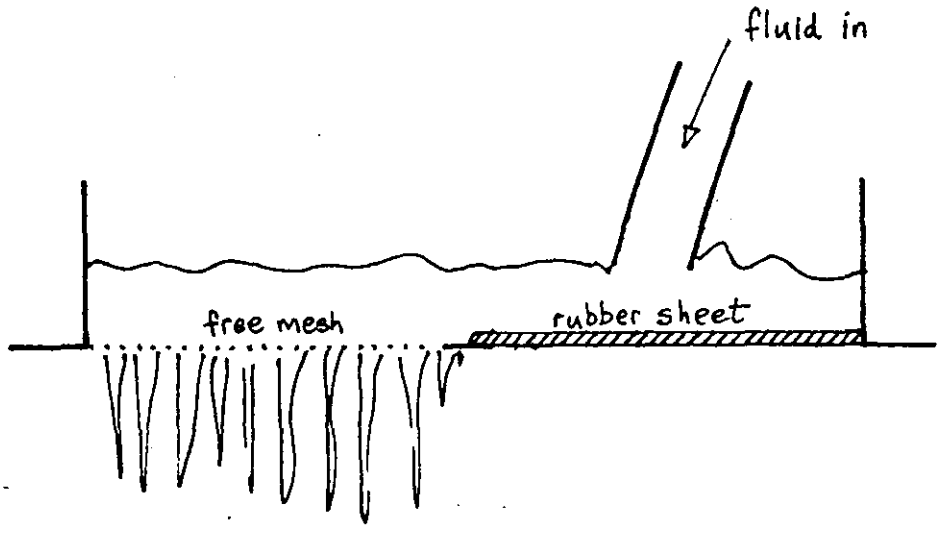

Figure 3.9 [overleaf]

General View of Static Mesh Apparatus

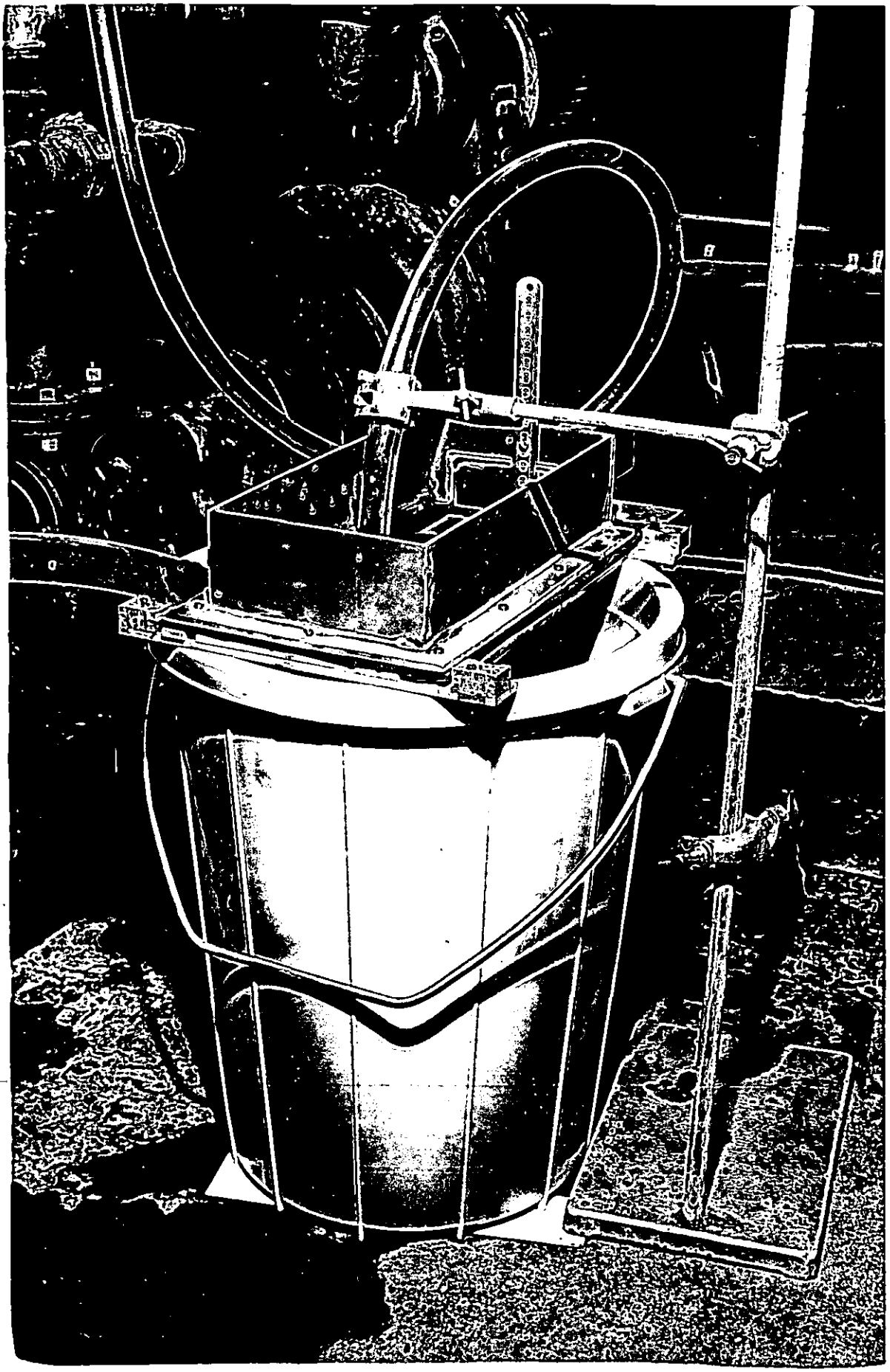

3.2.2 Method of Use

About 16 litres of the chosen fluid was put into the plastic bin, and the mesh assembly located on top and levelled. The pump gear was set at a low value, and fluid circulated through the apparatus. After a few minutes, the temperature was measured. For each experimental value, the pump was adjusted to a particular gear setting, and the liquid height on the mesh allowed to stabilize.

It was noted that air bubbles tended to accumulate on the mesh, reducing its effective area. If these were not removed, then the depth of liquid would steadily increase. It was therefore necessary to remove the bubbles every half minute or so by gentle action with a small soft brush.

The position of the feed pipe was adjusted if necessary to give an acceptably smooth surface over the working area. The height of the liquid above the mesh was measured by means of two precision stainless steel rules. One was bolted to the end of the PVC box farthest from the feed pipe. The second was hand-held, and was usually placed at the other end of the working area. However, if an obvious swirl pattern suggested this to be invalid, another position was chosen. For the same reason, it was sometimes obvious that the fixed rule was in an atypical position, so only the other was used. For very low liquid depths there was an definite slope to the liquid surface, and the average of the two measurements was taken as a single point datum.

The Mono pump gave a flow-rate very closely proportional to the gear setting, but this was not used as the actual flow measurement. For each stabilized liquid condition, the feed pipe was removed and transferred to a measuring cylinder. The time of collection of a suitable amount (250 to 2000 cm^3) was used to establish the flow-rate. All measurements were replicated.

3.2.3 Screen Meshes

The same meshes were used on the static and the vibrating rig (see section 3.3). They were of stainless steel from the same manufacturers and reportedly of the same type and tension as is used for pre-tensioned screens on the Main Rig. It should be noted that although the mesh count was progressive, the difference in wire diameter and the effect of partial obstruction by support mesh meant that they all had about the same number of available holes per unit area, and the apertures of the 100 and the 120 mesh screens were about the same.

TABLE 3.2 Screens Used on the Small Rigs

mesh count per inch	100	120	150
support mesh count	-	18	30
mesh aperture μm	142	141	98
wire diameter μm	112	71	71
holes per sq in x 10^4	1.00	1.44	2.25
% open area of support	100	69.4	44.7
∴available holes per sq in x 10^4	1.00	0.998	1.008

3.3 Small Vibrating Mesh Rig

When most of the main rig work had been carried out, a small experimental vibrating screen was constructed. This has since been further developed by another worker, and the results reported in this thesis have been replicated and extended.

3.3.1 General Description

The apparatus used two linear vibrators manufactured by Derritron Ltd, mounted so that one drove the working box vertically, the other horizontally. The amplitude and frequency of vibration was controlled by input signals from a "Feedback" VPG608 low frequency signal generator. The displacement was measured by two transducers (horizontal and vertical) as described in section 3.1.5 (main rig). The acceleration was likewise measured by the same device as on the main rig (described in section 3.1.6).

The device is shown diagrammatically in Figure 3.10.

The vertical vibrator directly moved a frame of 1/2" square tube. This was suspended by leaf springs from an outer support frame, such that in the null position there was no weight borne by the vibrator (though power was required to move the mass). The outer frame also supported a vibrator mounted horizontally. This pulled the inner frame by a wire, and was opposed by coil springs at the other end. The tension was adjusted so that the position when the vibrator was in mid-range was the same as the freely suspended position. Over the ranges of frequency and displacement used, this gave virtually independent vertical and horizontal motion, with very little normal motion resulting from the operation of a single vibrator.

The working box was of clear acrylic plastic, allowing one of the meshes described in section 3.2.1 to be mounted horizontally between flanges. Liquid was fed to the top section via a distributor plate, and drained by gravity from the lower portion back to the storage vessel. The liquid was fed by the Mono pump described in section 3.2.1.

Figure 3.10 Small Vibrating Mesh Rig

(a) general elevation

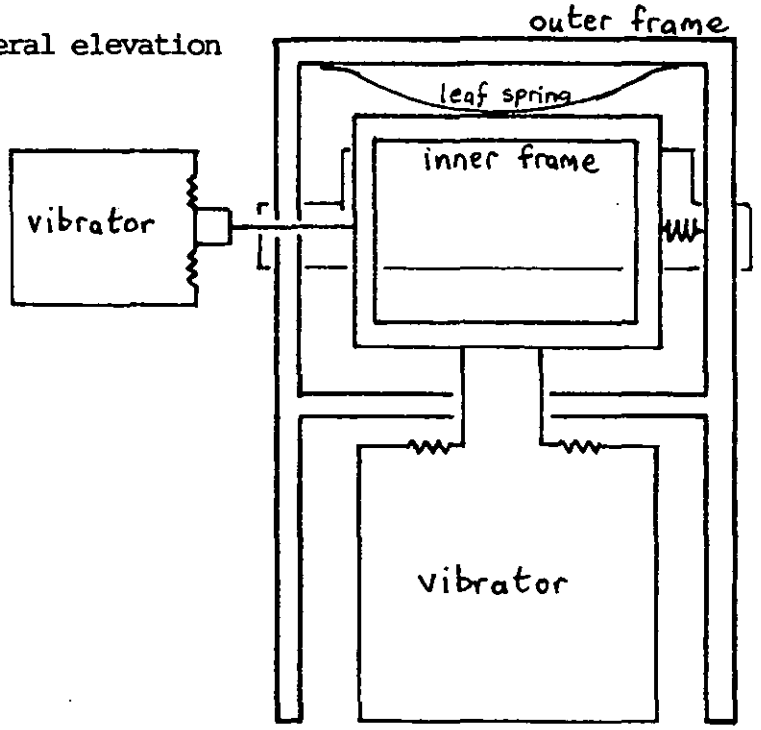

(b) working box

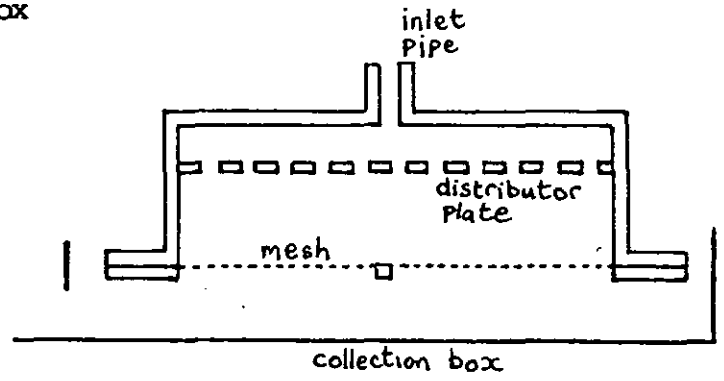

The height of the liquid inside the box could be observed relative to millimetre scales fixed vertically to the walls at three points. A stroboscope made viewing easier.

3.3.2 Method of Use

The most general procedure was to set the unit in motion, then commence the flow of liquid. A pump speed was then found which gave an equilibrium head of liquid above the mesh within the measurable range. The frequency or amplitude of motion was changed and a new equilibrium head measured. Care was taken to step back and forth through the working ranges, to minimize the effect of any experimental drift.

3.4 Weissenberg Rheogoniometer

3.4.1 General Description

This rheometer is well-known (see e.g. Walters 1975; Whorlow 1980) and will only be briefly described here. The instrument was model R16, supplied by Sangamo Controls Ltd

Although other working heads may be fitted, it was used in its usual configuration of a cone and plate. The lower member is mechanically driven. The upper member is supported on a near frictionless air bearing, but as it rotates to follow the lower member, its motion is resisted by a torsion bar in the form of a flat strip of metal. The amount of displacement of the upper member is measured by a non-contact electrical transducer, in which a fixed coil detects the position of a rod moving in and out, the rod being attached to an arm from the upper member.

The output from the displacement transducer was usually read from a panel meter, although a chart recorder was also used. The torsion bar is supplied accurately calibrated, which means that displacement readings can be converted to torque. From the geometry of the cone, the effective shear stress on the fluid sample is then found from the formula:

$$\text{shear stress} = \frac{3\,\delta\,\kappa}{2\,\pi\,r^3} \qquad (24)$$

where κ is the torsion bar constant, δ is the measured deflection, and r is the radius of the cone (25 mm).

The drive mechanism is the special feature of this instrument. Two 1 h.p. synchronous electric motors are fitted, each with its own gearbox. One provides rotary motion, the other oscillating. Because of the coupling used these can be operated simultaneously if desired. However, almost all the work was carried out with rotary motion. Each gearbox covers nearly 6 decades in logarithmic steps (from gear 0.0, the fastest, to 5.9, the slowest). For gear 0.0 the rotary speed is 12.5 Hz, the oscillation frequency 50 Hz. Gear 1.0 is a tenth of this, and so on. For rotary motion, the shear rate can be calculated from the cone angle θ and the frequency of rotation ν , thus:

$$\text{shear rate} = \frac{2\pi v}{\theta} \qquad (25)$$

The vast majority of work was done with a cone angle of 0^{o} 58' 02" and with torsion bars 7 (calibration factor 10.8×10^{-6} N m / μm) and 6 (factor 1.048×10^{-6} N m / μm). A simple computer program was written to convert gear settings to shear rates, and panel meter readings to shear stresses from the selected torsion bar.

The working head region is enclosed in a water jacket which was kept at 25^{o}C. In addition, the jacket held some wet cotton wool, and was fed with a small air stream which had been passed through water at 40^{o}C so as to maintain conditions of high humidity and thus reduce evaporation from the working sample, which was generally aqueous.

3.4.2 Calibration Checks

In principle, the Rheogoniometer is an absolute method of measurement, providing it is accurately set up. The most important regular adjustment is the setting of the gap between the cone and the plate (to the amount by which the cone is truncated). This was checked by a 2 mm precision test block, giving one complete revolution of the adjusting screw and 200% deflection on the least sensitive displacement transducer scale.

The meter output was checked by digital voltmeter and found to be asymmetric to the extent of 1.5%. Results are therefore reported as the average of readings taken with opposite rotations. The time of rotation was checked with a stopwatch for gear 3, and found to be as specified to the precision of the watch.

The natural frequency (rotary pendulum) of the cone assembly on torsion bar 7 was found to be 15.3 Hz, sufficiently high so as not to affect the results. However, noises of uncertain origin were noticeable in the system at frequencies of 1.25, 10 and 360 Hz. The whole assembly rocked on the isolation platform with a frequency of 0.63 Hz, similar to gear 1.3.

Measurements were made on supposedly Newtonian liquids, namely glycerol solutions and silicone fluids. the machine response was (to the accuracy of measurement) linear up to gear 0.3, and within ± 4% of the specified viscosity. The loss of sample from the edge of the cone-plate gap was a common problem for all fluids at the highest speeds.

3.4.3 Method of Use

The machine was checked and if necessary adjusted for level on its vibration isolating platform. The thermostat was allowed to operate for half an hour before checking the zero on the gap-set transducer. The meter was then trimmed so that the correct setting was centre zero on the scale. Gap set measurements were in every case carried out with the torsion bar unclamped. This required care so as not to buckle the bar. However, it seemed to me that the clamping mechanism caused a slight displacement from the free position. In fact, MacSporran & Spiers (1982), in a footnote to their study of the performance of this instrument ascribe the supposed errors in the gap measurement system as being principally due to the clamping head.

With the upper platen raised about 25 mm, and the torsion bar clamped for safety, a small excess of the required amount of sample was placed on the centre of the lower platen. Any obvious bubbles were removed. The upper platen was then brought slowly down to contact the liquid and force it out towards the perimeter. It was lowered further to about 50 um above the desired point, and the excess liquid removed from the periphery with a spatula. It was lowered a little further and the excess again removed. The thermostat housing was closed over the platens and the torsion bar unclamped. The gap was adjusted to about 5 μm above the desired value. About half an hour was allowed for temperature equilibration, and the final gap setting made. This normally left a positive meniscus around the peripheral gap between the platens.

For most fluids, measurements could be made immediately. However, for clay samples it was necessary to leave them static for a couple of hours, or shear them for some time, according to the experiment being carried out.

3.5 Marsh Funnel

3.5.1 General Description

The funnel devised by H. N. Marsh in the late 1920's is now the classical field method of defining the viscosity of a drilling mud. As shown in Figure 3.11, it consists of a long cone, with a handle, terminating in a short pipe which has a brass orifice in it. Essentially, the cone is filled with fluid, which is allowed to discharge under gravity through the orifice. The time taken for a fixed volume (a quart or a litre) to be discharged is than reported as the "Marsh funnel viscosity". Half of the top is covered with a coarse (10 mesh) brass screen to remove lumps and large particles from the sample.

The funnel used was a plastic one, with the brass orifice moulded in, supplied by NL Baroid (Aberdeen) according to API Specification 13B (1980). The brass orifice was a straight tube of length 2 inches (50.8 mm) and bore 3/16 inch (4.76 mm). The cone has a height: base aspect ratio of 2. At the level of the mesh, the distance to the orifice was 11 inches (279 mm), the internal diameter of the cone 5.5 inches (140 mm). For water at 21^{o}C, the API specifies an efflux time of 26.0 $\pm$ 0.5 s for a quart. This funnel had a time of 25.9 s (std devn 0.18) for a quart, 27.7 s (std devn 0.12) for a litre.

Figure 3.11 The Marsh Funnel

[overleaf]

3.5.2 Method of Use

American practice is to collect a quart (946 cm^3) of funnel efflux, but some European companies use a litre, and it was this latter practice which was adopted. In the field, a jug is generally used, but in this project it was found convenient to use a 2-litre conical flask. It was found (by weighing with water) that the top of the 1000 ml mark on the flask was the correct calibration, and this was used.

To make a reading the funnel was held vertically with the orifice closed by a finger. The funnel was carefully filled with liquid until the level was just in contact with the mesh. (About half the mesh was wetted, the line of contact being clearly visible as the funnel was slightly tilted.) With the funnel over the receiver, the finger was removed from the orifice and the stopwatch started. Timing was stopped when the liquid in the receiver rose to the calibration mark.

Readings were generally reproducible to 0.2 seconds, and other users were able to replicate, once practised in the technique.

3.5.3 Application

The Marsh Funnel was used as a routine quality check on the rig fluid. The fluid was mixed so as to give a funnel time similar to those likely to be found in real drilling fluids. Regular checks confirmed that the fluid was maintaining its viscosity.

In addition, the funnel time was investigated to see if this simple and robust device could give any useful guide to flow through vibrating screens. The discharge of the funnel was modelled (see Appendix 1) and the results used to interpret experimental measurements with different fluids and funnel viscosities (see section 7.3.6).

3.6 Sieve Analysis

Stainless steel wire-woven test sieves of nominal diameter 200 mm were used. These were manufactured by Endecotts Ltd according to BS 410:1976, with apertures of 45, 75, 105, 125, 152, 185, 210, 250., 300, 355, 420, 500 & 720 μm. Not all sieves were used for every analysis, and a coarser sieve was sometimes used (see below). Each analysis was duplicated.

Trials showed that a charge of about 100 grams gave a satisfactory result without overloading any sieve for the range of solids used. Experimental samples were therefore divided down to approximately this quantity (85 to 120 g). Samples up to 3 kg were divided by a 6-way rotary divider (with re-division and/or combination as necessary). Larger samples were first of all split by a simple 2-way riffle. For commercial solids, an entire sack was divided in this way to give samples for analysis. At the same time, suitable quantities were packaged for use as test samples.

The stack of sieves was vibrated on a Fritsch 'analysette' type 03502 sieve shaker, at an energy setting of 80%, intermittent at 50%, for 35 minutes. Each sieve containing a substantial amount of solid was then given further hand treatment (shake and tap) for a minute or so before the solid was removed for analysis. The amounts collected were weighed to a precision of 0.01 gram on a top-load balance. Some tailings were weighed to 0.001 gram on a single-pan analytical balance.

Because the main rig tended to shed quantities of rust and paint, a 1 mm pre-sieve was used for rig samples, and it was generally necessary to ignore the fraction greater than 500 μm or 710 μm, which contained significant rig debris.

3.7 Other Analytical Techniques

3.7.1 pH

The pH of experimental fluids was measured using an EIL 7050 pH meter with a combination glass electrode, and using manual temperature compensation. The calibration was checked at the start of every major experimental programme, using freshly made-up standard buffers (from BDH tablets) of pH 4.2 and pH 9.0.

As a quick check on rig fluid condition, a sample was often tested with phenolphthalein indicator, a pink colour (pH 8.3+) being considered satisfactory.

3.7.2 Specific Gravity

The specific gravity of solids and small samples of liquids was tested by standard technique using a 50 cm^3 (nominal) specific gravity bottle.

The density of rig fluid under working conditions was checked by weighing a measuring cylinder filled with 500 cm^3 of sample (including bubbles, solid particles). The entrainment of air into rig fluid was monitored during experiments by means of a spirit hydrometer, directly immersed in the possum tank. This covered a specific gravity range from 0.789 to 1.00, a lower value being indicative of increased air content. The runs were terminated when the entrained air exceeded 2% by volume.

3.7.3 Surface Tension

This was measured with a du Nouy tensiometer manufactured by Cambridge Instruments Ltd, serial number C636845. The wire was checked with a precision weight according to the manufacturer's instructions. A 10 mm diameter platinum ring was used. This was cleaned in a 5% solution of RBS35 (commercial cleaner), and rinsed with dilute hydrochloric acid and distilled water before use.

The standard technique was adopted, except for very viscous samples. In the latter case, the tension was increased stepwise, allowing 60 seconds each time for the ring to pull off. The lowest reading to cause pull off within this time was taken.

3.7.4 Ostwald Viscometer

Two Ostwald U-tube viscometers were used. One was size C with a stated calibration constant of 0.02795 cS s^{-1}. The other was size D (serial number 6588) uncalibrated. Size C was used to measure the viscosity of ethanediol, and this was then used to find the calibration factor for the size D viscometer. The viscometers were used in a thermostatted water bath,with a precision mercury-in-glass thermometer. For measurements below room temperature the bath was cooled with additions of ice then allowed to rise to the desired temperature.

3.7.5 Microscopy

The majority of examinations of mesh and particles were carried out with a Leitz Orthoplan binocular microscope. For photography, a Leitz Orthomat unit was fitted. Both incident and transmitted light observations were made, using the appropriate sets of lenses. The built-in illumination was sometimes supplemented with portable external lights. This was particularly necessary when examining the screens from the main rig, because the microscope stage and condenser had to be removed to allow the screen frame in.

3.7.6 Photography

The examination of particle motion on the mesh was assisted by taking cine film using a 16 mm Bolex camera at 64 frames per second. A Nikon 35 mm still camera was used to provide records of effects observed, and for study of rig motion (see 3.1.7).

4 MATERIALS

The following is brief record of substances used for the experimental work.

4.1 Solid Particles

To test the behaviour of solids on the screen, it was necessary to obtain material which was inert and not easily degraded (i.e. not significantly altered by usage in the experiments) of suitable size range and in sufficient quantities. It is common in experimental work with particle beds to use spheres, because they are simple to describe mathematically. However, it was felt that the freedom to roll would give movement quite different from the industrial situation. A more appropriate set of particles would result from the crushing of amorphous material.

Sand was an obvious mineral, because it is actually fairly common and is thus suitably representative of inert drilling solids. Alumina was also used because it was available for grit-blasting in prepared size ranges. It is much denser, which allowed tests to include the possibility of particle inertia being a factor. The alumina was selected from the manufacturer's technical specifications. The sands were selected by sampling and sizing a range of industrial sands. Figure 4.1 shows the shapes of the particles used.

Figure 4.1 Micrographs of Particles Used

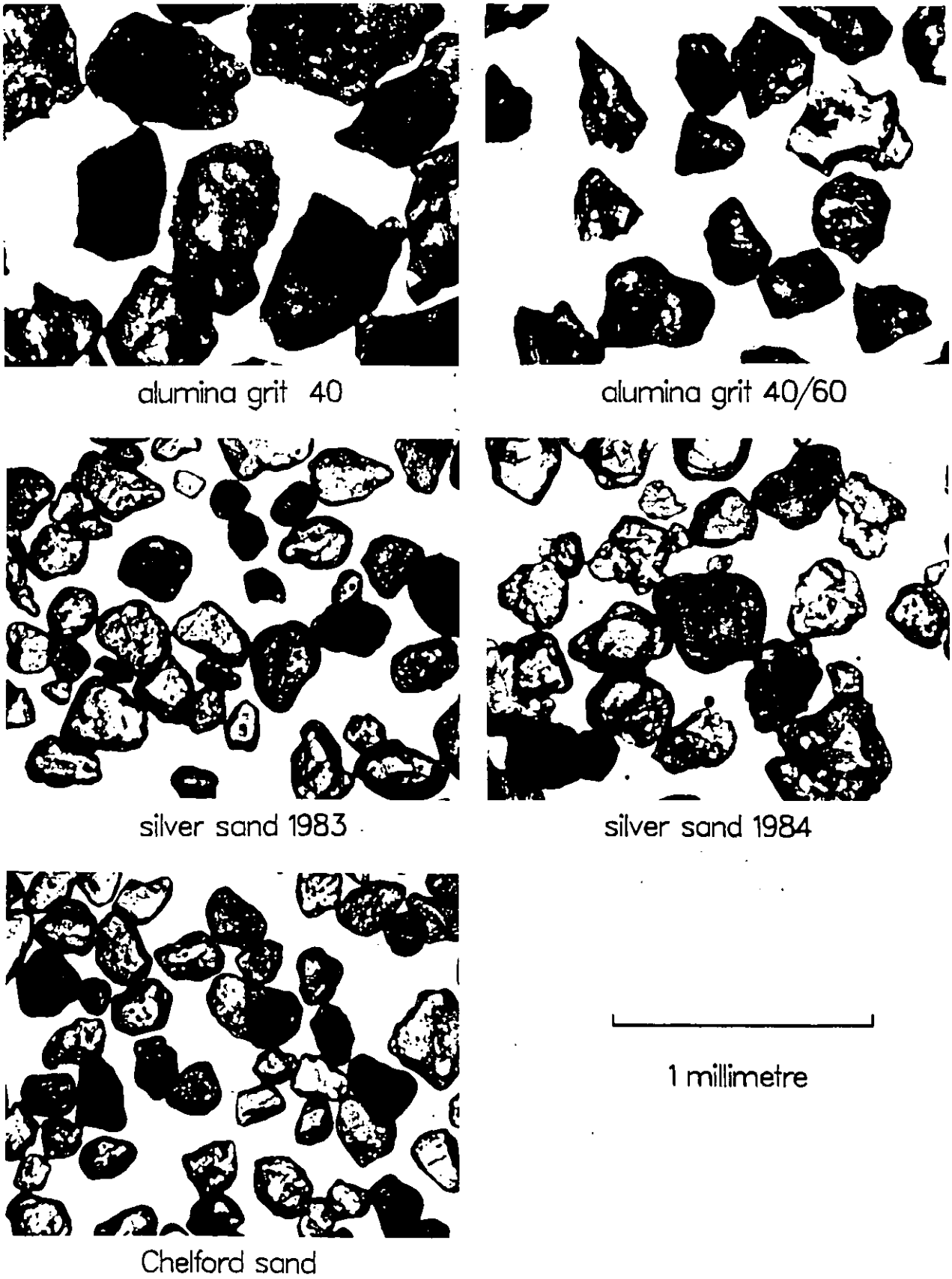

4.1.1 Alumina Grits

These were supplied by Abrasive Developments Ltd, and are sold for grit-blasting purposes. The particular grade is a brown amorphous alumina, relatively tough, and not very sharp. The specific gravity was 3.95.

Two sacks were obtained of sizes denoted by the supplier as "40 grain" and "40/60 grain". These were sized, and it was found that the 40/60 was mainly (78%) below, whereas the 40 was mainly (93%) above the anticipated cut point of the 50 mesh top screen (aperture 325 μm, expected cut around 300 μm). Hence an equal mixture was prepared for use in measuring the actual cut point. Conveniently, less than 1% of the smaller alumina was smaller than the aperture of a 100 mesh screen (142 μm), so the undersize could be collected. Size distributions of the two grits and the mixture are shown below.

Figure 4.2 Size Distribution of Alumina Grits by sieve analysis

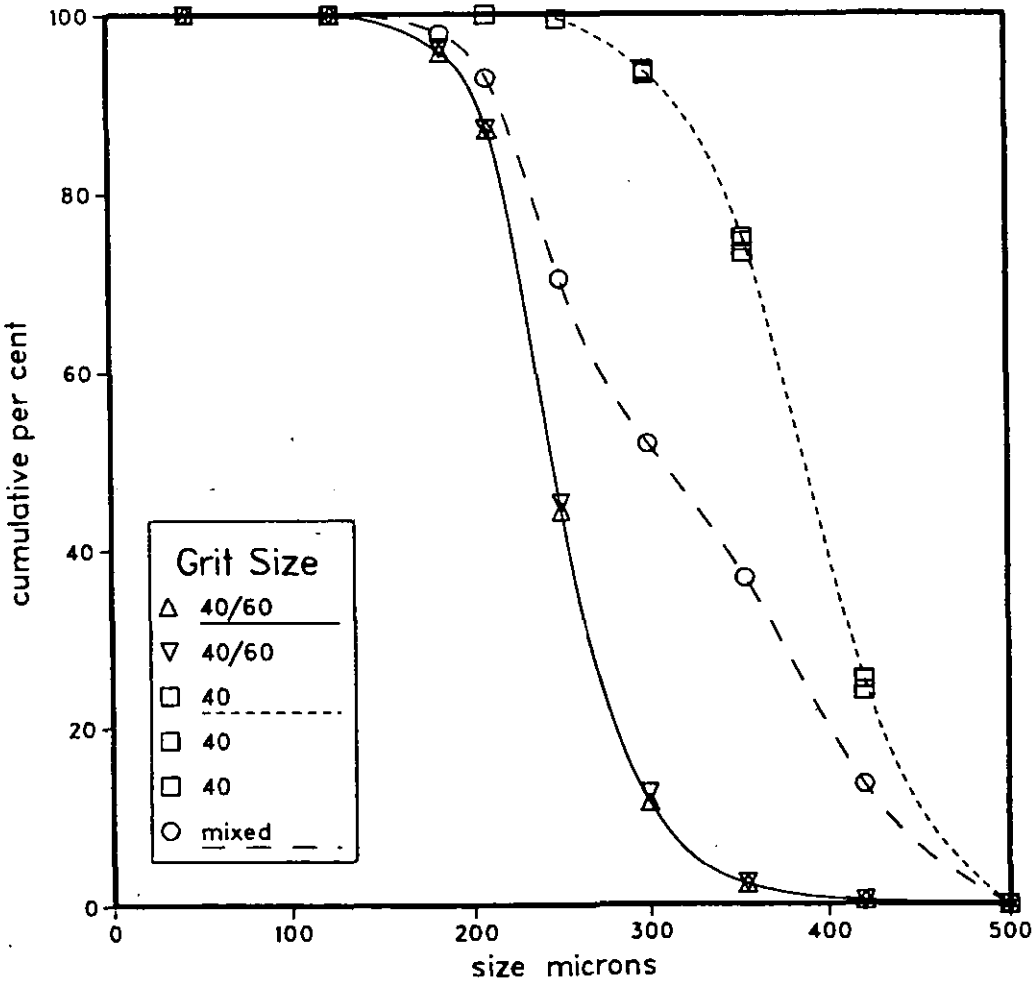

4.1.2 Silver Sand [1983]

This was a washed non-sharp sand sold by Black Diamond Ltd of Coventry as "Silver Sand". It was found that its D_{50} diameter was 281 μm, virtually identical to the cut point of the upper (50 mesh) screen as determined by tests with alumina. It was therefore also used for cut point determination.

Figure 4.3 Size Distribution of Silver Sand [1983] by sieve analysis

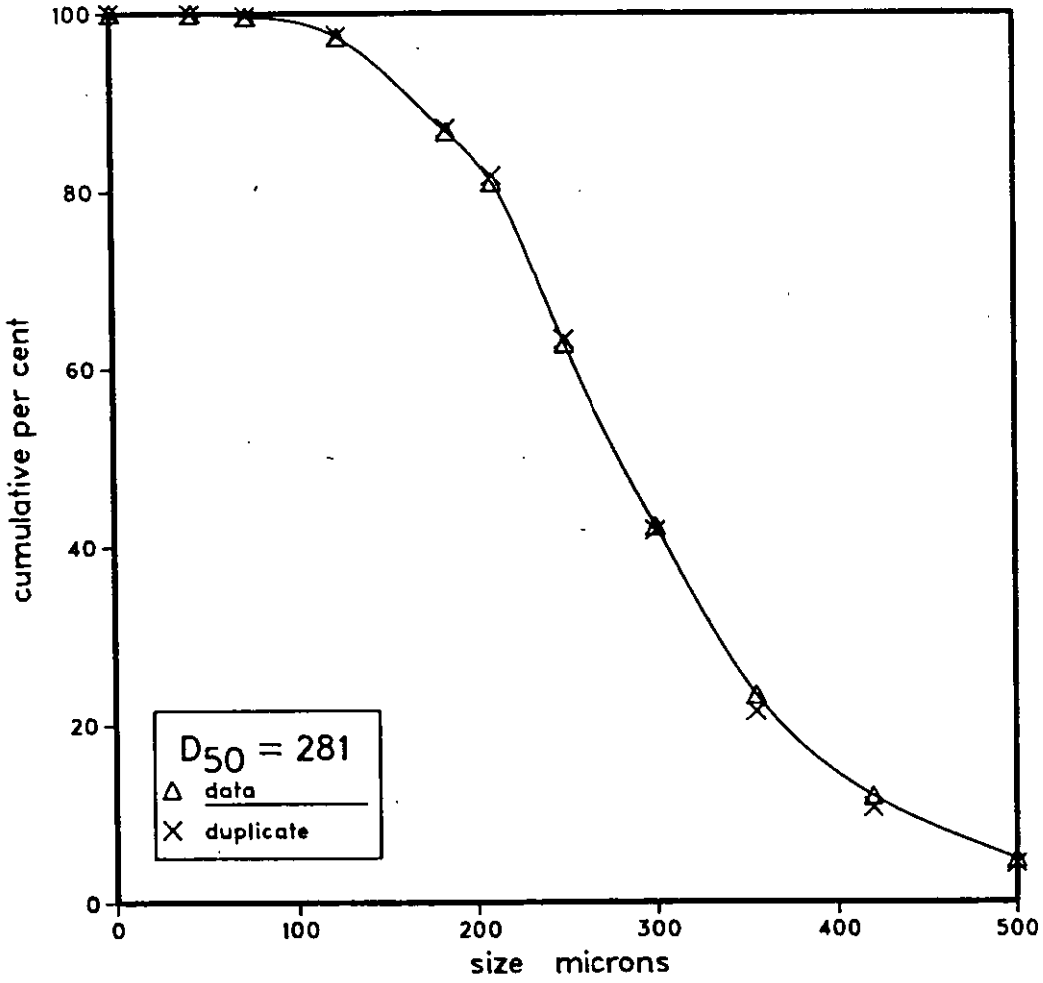

4.1.3 Silver Sand [1984]

This was a washed non-sharp sand sold by PCP builders of Shepshed as "Silver Sand". The entire 50 kg batch was passed through a 1.2 mm sieve to remove grit and foreign particles. The resulting size distribution is shown in Figure 4.4. It was found to have a D_{50} of 339 μm, with the majority (97%) being greater than the nominal aperture (142 μm) of the lower deck (100 mesh) screen. It was therefore used to represent the sort of size range which such a screen might carry in practice. The specific gravity was measured as 2.65.

Figure 4.4 Size Distribution of Silver Sand [1984] by sieve analysis

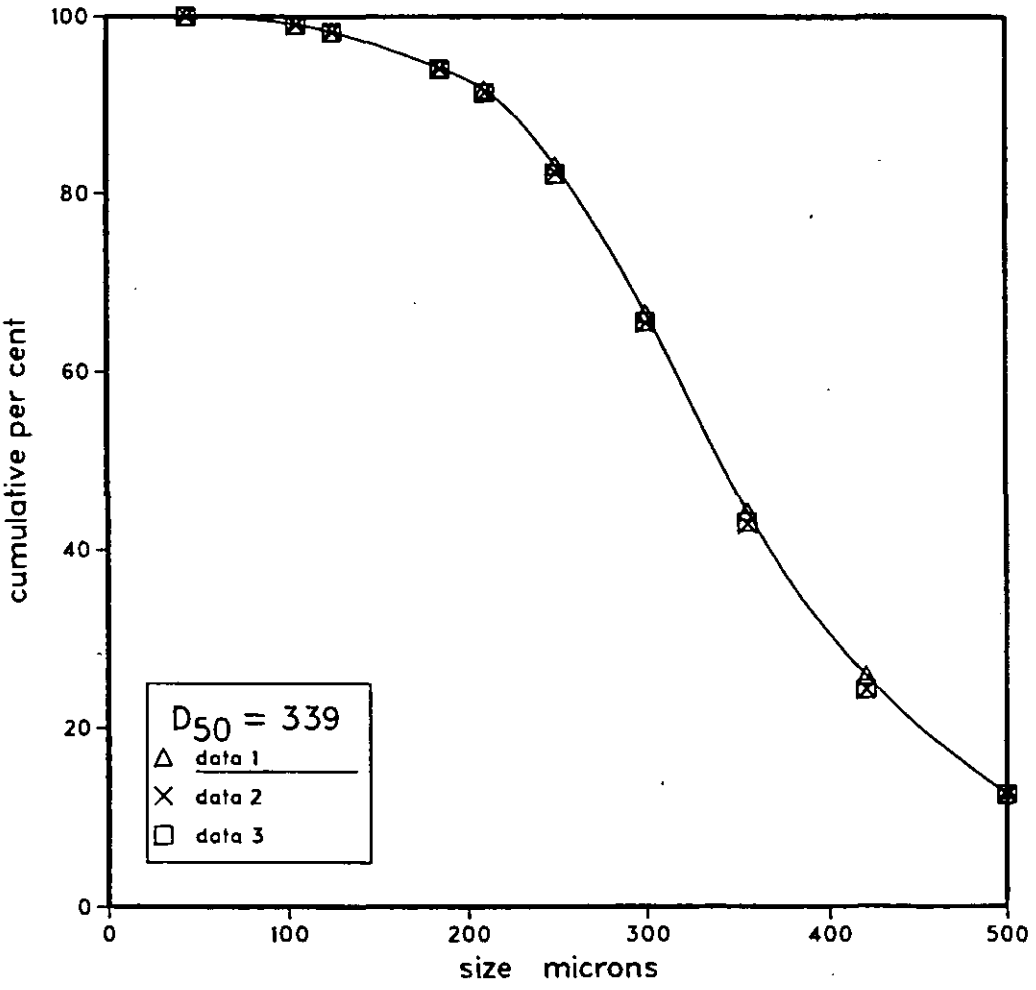

4.1.4 Chelford Sand

This was a clean sand of narrow size distribution, being the by-product of an industrial screening process, supplied by Powder Products Ltd. The size analysis above shows good replication between different sacks. It was used for solids conveyance tests on the main rig, under conditions of heavy solids loading and typical fluid and vibration conditions. It roughly represents the solid which might be found on the lower deck of a double-deck shaker with 60 and 100 mesh in place.

Figure 4.5 Size Distribution of Chelford Sand by sieve analysis

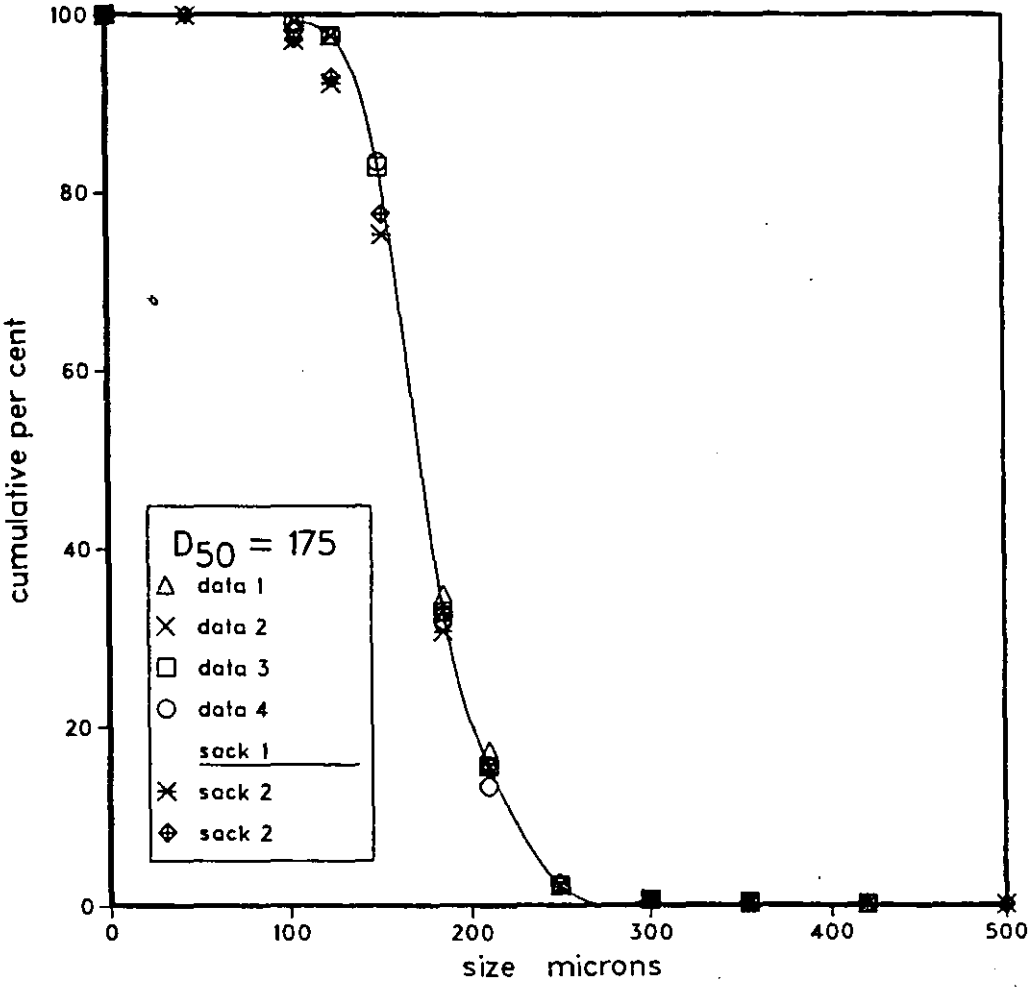

4.2 Liquid Components

The base fluid for experimental work was water, adjusted to a suitable rheology by the addition of the following components. Non-potable mains water was generally used. This had a total hardness of 280 mg dm^{-3}, and when tested for viable micro-organisms gave a count of 10^3 - 10^4 per cubic centimetre. The glycerol solutions were made up in distilled water.

4.2.1 Hydroxy Ethyl Cellulose (HEC)

This was used in the commercial form as sold for drilling fluids, under the trade name 'WO 21', by Milchem Drilling Fluids Ltd. The supplier recommended an in-use concentration of 1 to 3 lb/bbl (0.28 to 0.86%) giving Marsh Funnel times from 40 to 100 s.

According to Lauzon (1982), it is manufactured by the action of ethylene oxide on alkaline cellulose. It is non-ionic, stable to salts, and tolerates pH from 4 to 12. Another supplier claims that HEC is more resistant to biological degradation than many other polymers. The solutions are highly shear-thinning, and it was found experimentally (see section 5.2) that they approximate Power Law behaviour. This was therefore used as one type of rheology.

4.2.2 Xanthan Gums (XC, XCD)

These are bacterially-produced polysaccharide gums, first described by Jeanes, Pittsley and Senti in 1961. The rheology of the commercial form was described by Whitcomb and Macosko (1978), who reported its exceptionally pseudoplastic nature (see sections 5.3 - 5.4 for rheograms). It was therefore used to provide shear-thinning liquids of distinctly different rheology to HEC.

Two commercial forms were utilised, the one referred to as 'XC' being 'Milpolymer 350' from Milchem Drilling Fluids; the one referred to as 'XCD' was a dispersible form from Kelco Oil Field Products under the trade name 'Kelzan XCD'. They had very similar rheologies. The first-named

supplier recommended a concentration of 1 lb/bbl (0.28%) with a resulting Marsh Funnel time of 35 to 38 s.

Lauzon (1982) states that the solutions are stable to a wide pH range, but liable to biodegradation. This was a considerable practical problem on the main rig experiments.

4.2.3 Bentonite Clay

The clay used was supplied by International Drilling Fluids as 'Wyoming Bentonite'. At least 5% was above the clay size, the largest particle observed under the microscope being 170 um. It was therefore not possible to measure the rheology of rig fluid directly on the Weissenberg Rheogoniometer, because the particles larger than 10 um could damage the working head. A technique was developed to prepare grit-free samples for rheological measurements: tests showed that the particle size distribution below 5 um was similar to that in unseparated clay suspensions, so it is fair to assume that the rheology was not markedly affected by the grit removal process.

Apart from this difficulty, bentonite muds are opaque, which was some disadvantage. However, their principal drawback in performing experiments under controlled conditions is that they are thixotropic: that is the rheology will vary with shear history. Thus it would not have been possible to compare like with like on the main rig. For this reason, the main tests were carried out on the main rig with polymer solutions, but a limited number of runs were carried out with bentonite suspensions to confirm that the behaviour was similar.

4.2.4 Glycerol

This was supplied by Fisons Ltd as 'SLR Glycerol'. It was used in simple mixtures with distilled water to provide a viscous but essentially Newtonian fluid for small-scale tests. Solutions were made up at nominal concentrations and the viscosities found experimentally. Cost precluded its use on the main rig.

4.2.5 Calibration Fluids

Dow-Corning silicone oils of viscosities 10 and 100 cS (+ 5%) were used to check the Weissenberg Rheogoniometer. Glycerol mixtures (see above) and Fisons 'SLR Ethandiol' were used as secondary standards, on the assumption that a calibrated Ostwald viscometer was correct.

4.2.6 Preservatives

All rig fluids were kept in the pH range 9 to 11 by the addition of Fisons 'SLR Sodium Hydroxide (pearl)' as often as necessary. Small laboratory samples were usually adjusted by 1.0 mol dm^{-3} NaOH volumetric reagent.

After the dumping of rig fluid, the tank was cleaned out with a boiling-water pressure washer, and treated with hypochlorite bleach overnight.

BDH 'Panacide' had been recommended as a suitable preservative, but did not prove totally successful. It is believed that it may function by deposition onto clay particles and onto the oil surface of oil-based fluids, but due to its low water solubility was less effective in a polymer solution. Instead, BDH 'Phylatol' was found to be satisfactory, at an initial level of 1000 p.p.m..

4.3 Method of Mixing Fluids

Preparation of the non-Newtonian fluids required the dispersion and hydration of a solid in water. It was found that the best technique was to control addition and mixing so that the powder was well dispersed initially, without lumps. It was then permitted to hydrate overnight. Thereafter, quite moderate levels of agitation were sufficient to break down any gels and produce a homogeneous liquid.

4.3.1 Small Scale

A 'Silverson' high-shear laboratory mixer (no. 15198) was usually employed (though with care other stirrers could be used). This was found to give adequate mixing of a volume of 1.5 litres in a 2 litre beaker. Accordingly, the ingredients for a fluid were weighed out in amounts for batches of this size. (Up to 40 litres were in fact prepared by combining these portions.) Minor components such as preservatives and NaOH were first dissolved in water and the appropriate volume used (this being subtracted from the water in the beaker). The order of addition varied with the fluid. For example, NaOH was added first for the bentonite, last for the polymers, due to the different speeds of hydration in its presence.

The powder was added over several minutes. For those fluids which showed a marked increase in viscosity during the addition, it was necessary to increase the mixer power to maintain the flow conditions in the beaker. Once all the powder had been dispersed to a smooth liquid, the beaker was emptied into the working receptacle, and the next batch prepared. The combined batches of fluid were left overnight, then mixed with an ordinary stirrer of appropriate size for at least an hour.

4.3.2 Large Scale

The main rig tank was filled to about 60% with mains water and a suitable preservative added. In the case of bentonite, NaOH was added first, but for polymers it was added last. The necessary amount of solid was weighed out and loaded into the hopper described in section 4.1.12. As many hopper loads as necessary were used.

The main pump was operated so as to circulate back into the tank, initially throttled well down. This gave a jet of water travelling across the tank, being deflected by the opposite wall. The resulting flow pattern gave a linear region across the tank in which the surface layer was being drawn down into the body of the liquid. The hopper was suspended so as to discharge into this region.

Solid was discharged from the hopper at a rate of about 1 kg per minute, with manual agitation. As the viscosity of the fluid in the tank increased, the throttle valve was progressively opened in order to maintain the same degree of tank circulation without splashing.

Once all the powder and any other chemicals had been added, the pump was permitted to run for the rest of the working day, the valve being opened up only as much as was required to give good circulation within the tank. By this means the liquid experienced the maximum possible shear in the pump and in passing through the throttle valve.

The mixture was left to stand overnight to permit hydration, then circulated back to the tank for some hours in order to give a homogeneous mixture. All fluids were kept for a week with daily mixing before they were deemed to be fully conditioned and in a stable state for experimental use. During this period, the pH was measured and if necessary adjusted with NaOH.

4.4 Maintenance of Rig Fluid

One of the major experimental difficulties was preventing the degradation of the rig fluid by biological action. It was found that once serious microbiological attack had occurred then the situation could not be retrieved. (This was probably due to the presence of enzymes even when the organism had been killed.) The only successful procedure was to dump the fluid, clean out the apparatus and prepare new fluid. Unfortunately, this was a rather costly as well as time-consuming process.

All polymer fluids showed a slow decline in viscosity with time. Part of this was probably due to mechanical breakdown of the polymer molecules by repeated passage through the pump. A further contribution may have come from local base-catalysed hydrolysis during the dissolution of the solid NaOH which was added to maintain the pH.

Biological breakdown was indicated by the fluid becoming more acid, by a sulphurous odour and by the presence of black sludge (sulphide) on metal surfaces. The latter two symptoms indicate anaerobic sulphate-reducing bacteria. Support of this is given by the observation that over the weekend the fluid on occasion went a clear pale green (suggesting reduced ferrous iron). Mixing gradually converted it to a rust colour (deposition of hydrated ferric oxide due to absorption of oxygen from the air).

Three methods were tried unsuccessfully.

[1] The use of a commercial preservative, BDH 'Panacide' did not stop catastrophic degradation, even at the maximum recommended concentration.

[2] Scrupulous control of pH did not itself prevent a sudden overnight conversion.

[3] Continuous mixing (to keep the fluid aerated) proved impractical because the pump discharge was too great unless heavily throttled, and other pumps available were too small.

Finally, a procedure was evolved which enabled a tank of XCD to be kept for 4 months before needing to be dumped. This involved the use of 1000 p.p.m. of the preservative BDH 'Phylatol', being topped up by a further 200 p.p.m. each month. In addition, the pH was monitored daily and kept between pH 9 and 11 by the addition of NaOH. Further, the fluid was mixed for at least an hour each day (except weekends) to maintain its equilibrium with the oxygen of the air. Daily Marsh Funnel measurements were used to confirm that the condition was stable. (In the case of XCD, readings fell from 41.2 s to 39.7 s in the period March to June, then suddenly dropped in July, when the fluid was promptly discarded.)

5 PROPERTIES OF EXPERIMENTAL FLUIDS

The following is a record of experimentally determined properties which were relevant in interpretation of fluid flow studies reported in the next chapter.

5.1 Rheology of Aqueous HEC

Figure 5.1 shows (on both linear and logarithmic plots) the rheograms of HEC rig fluid, corresponding to a concentration of about 0.2% and 0.3%. The curvature of the linear plot shows that these solutions are strongly shear-thinning, and the relative straightness of the log plot suggests that they can be reasonably well represented by the Power Law.

Rheograms were made for laboratory solutions from 0.1 to 2.0%. The Power Law was found to be less valid for concentrations of 0.5% and above. The highest concentration used in any mesh experiment was about 0.4% (Marsh Funnel 50 s).

5.2 Rheology of Aqueous XC

Figure 5.2 shows rheograms of XC rig fluid corresponding to about 0.15% (MF 32), 0.3% (MF 35) and 0.4% (MF 38). Comparison with the curves for HEC demonstrates that XC is more nearly Bingham Plastic than Power Law, with a relatively low flat curve almost coming to an intercept on the stress axis. Taking the Marsh Funnel 32 seconds as an example, the XC and HEC have much the same viscosity at around 1600 s^{-1} but at 46 s^{-1} the XC has 5 times the viscosity. The increased low-shear viscosity was of particular significance in the static mesh experiments.

5.3 Rheology of Aqueous XCD

This was a readily dispersible form of XC, of very similar rheology, as shown by Figure 5.3. In fact, it was slightly more shear thinning. That is, 0.4% solutions had the same apparent viscosity at around 300 s^{-1}, but XCD showed about 13% greater viscosity at 30 s^{-1}, about 9% less at 3000 s^{-1}.

Figure 5.1 Rheograms of Rig Fluid - HEC

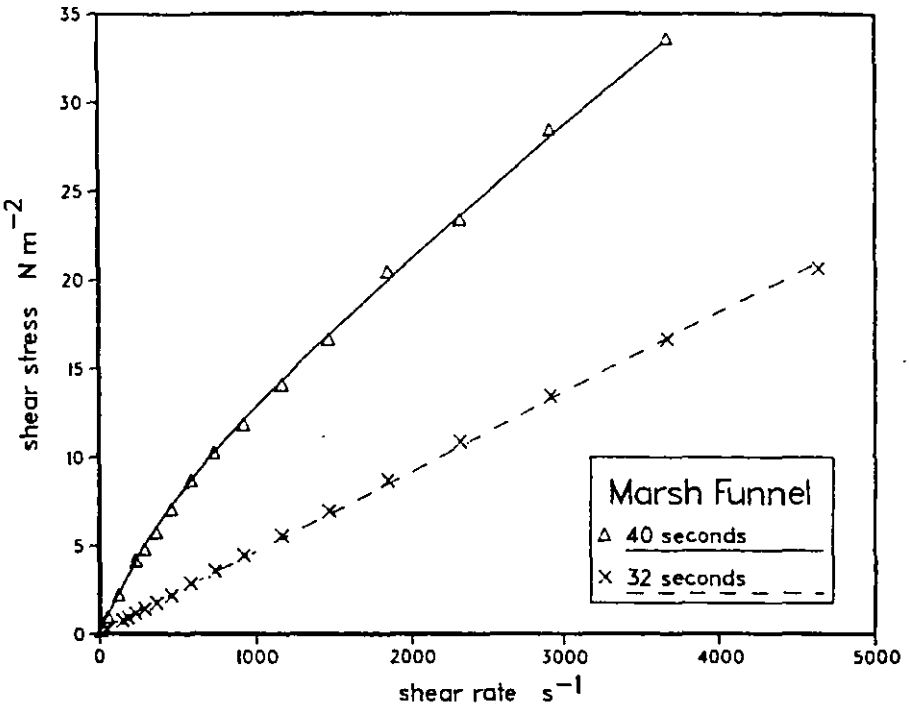

Logarithmic Plot of Above

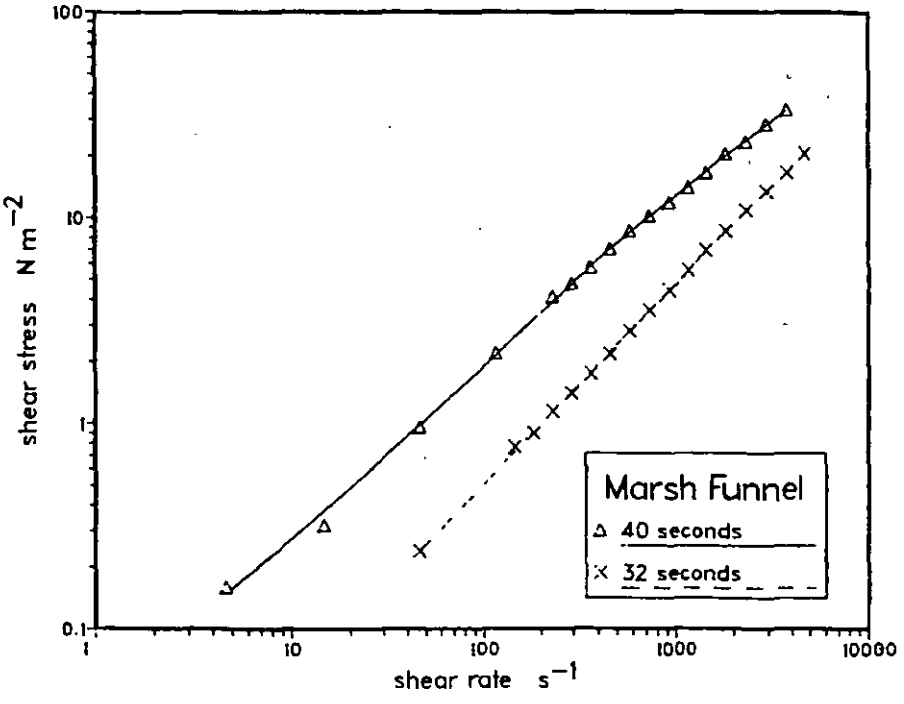

Figure 5.2 Rheograms of Rig Fluid - XC

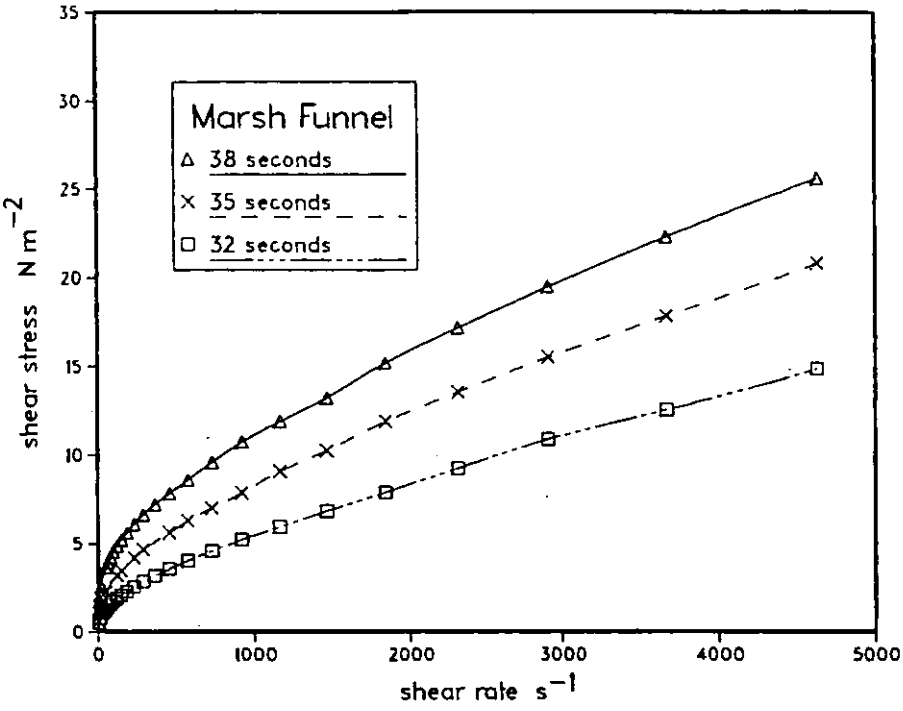

Logarithmic Plot of Above

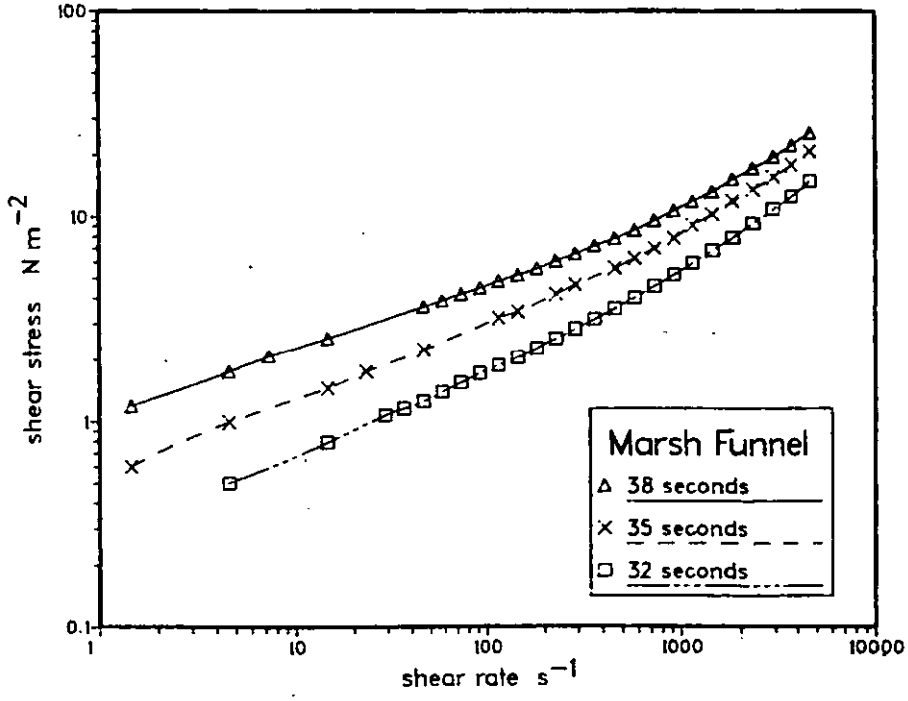

Figure 5.3 Rheograms of Rig Fluid - XCD

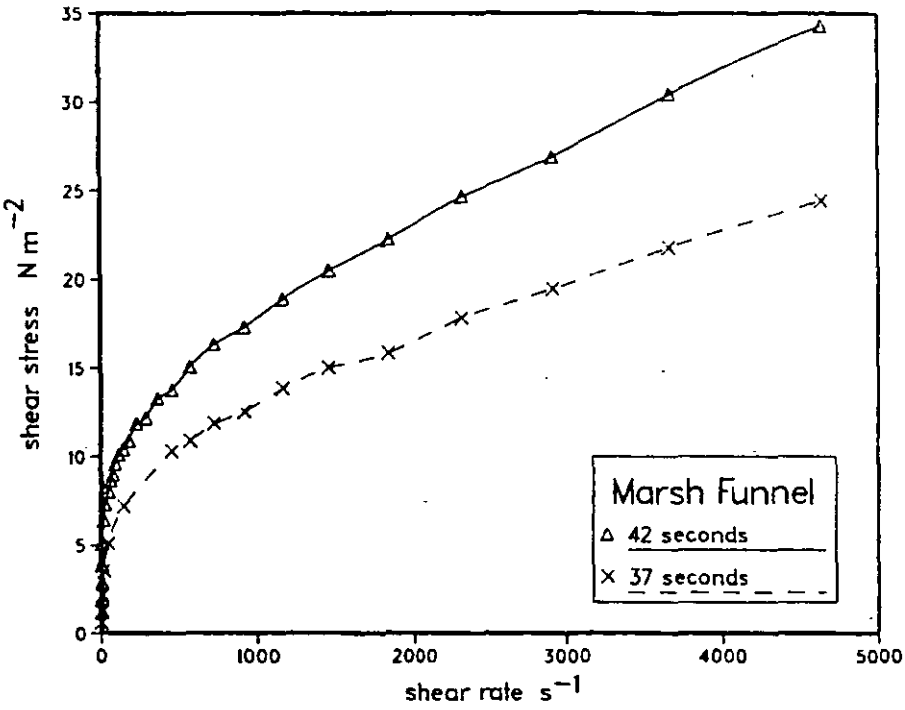

Logarithmic Plot of Above

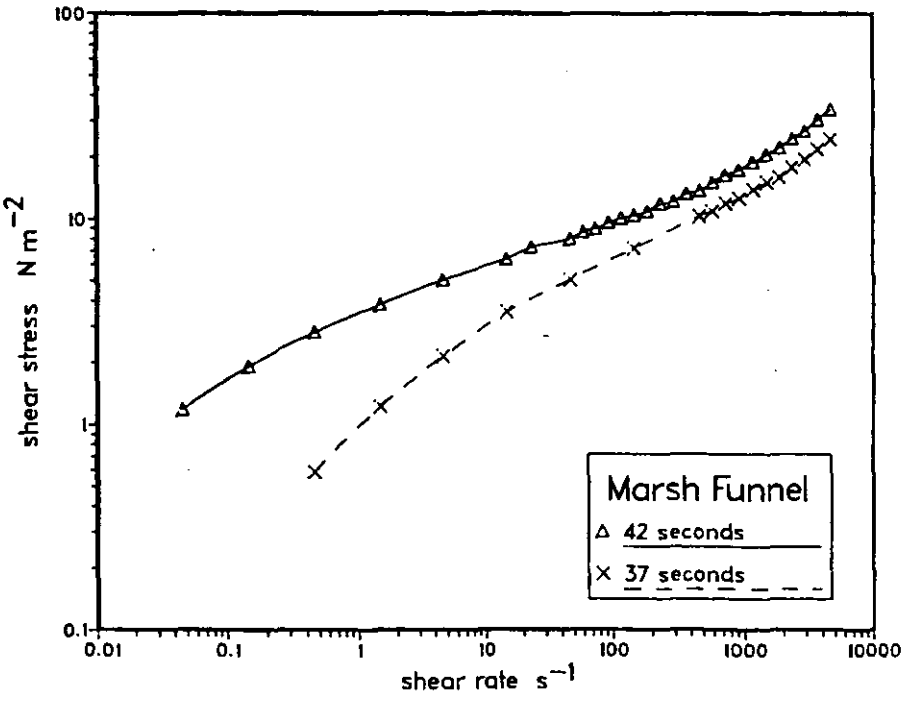

5.4 Rheology of Aqueous Bentonite

As explained in section 1.4.2, the apparent viscosity of a bentonite dispersion changes with time of shear, hence it cannot be described by a single rheogram. Some joint work by the author (Roberts & Pitt 1982) suggested that the change in structure with shear-rate could be represented by a surface on a three-dimensional plot, but the rate of change of structure would also involve time. While it is conceivable that a full description might be developed for a single composition under ideal conditions, there was no practical way to specify the rheology at any moment on the main rig. (Marsh Funnel time varied from 67 to 47 s during one day.) Figure 1.4 gives specimen rheograms.

5.5 Surface Tension Measurements

Table 5.1 (below) shows the effect of principal fluid components on the surface tension of distilled water. As the ambient temperature varied, these have all been normalized so that the distilled water surface tension was taken as 100%.

The clay had no significant effect, the XC and XCD had a negligible effect, and the HEC had a small effect. However, the BW Defoamer was clearly a surfactant, and after prolonged use (to temporarily clear the mesh for observations) caused a major reduction in the surface tension of the HEC rig fluid.

It was concluded that surface tension changes resulting from HEC, XC, and XCD were insignificant compared with viscosity changes.

One problem experienced when using HEC solutions was their tendency to foam. Foaming is commonly associated with low surface tension, but the measurements below do not support this for HEC. The problem with foaming in these liquids is that their rheology precludes easy bubble disentrainment.

TABLE 5.1 Surface Tension of Aqueous Solutions

Material	Normalized Surface Tension
distilled water	100.0 ± 0.3 %
+ 0.25% XCD	100.0 ± 0.8
+ 0.25% XC	97.9 ± 0.2
+ 5.0 % clay	99.9 ± 0.2
+ 0.25% HEC	92.2 ± 0.2
+ 0.5 % HEC	92.4 ± 0.2
+ 1.0 % HEC	91.3 ± 0.5
+ 200 ppm defoamer	54.7 ± 0.5
+1000 ppm defoamer	50.3 ± 0.1
rig HEC + defoamer	69.8 ± 1.4

6 FLUID FLOW THROUGH SCREENS: EXPERIMENTAL RESULTS

6.1 Introduction

Tests were actually carried out on the Main Rig first, and the small-scale tests followed to test some ideas which this experience had suggested. However, it is convenient to present the results as follows: firstly static mesh, secondly independent horizontal and vertical motion, thirdly these combined to a basically circular motion on the Main Rig.

The small scale tests may be considered as pieces of the mesh on the main rig in isolation. On the Main Rig, tilts of up to 8° were used. The small-scale tests were entirely on horizontal mesh, but it may be asserted that for these low angles the tilted mesh can be represented by a series of horizontal strips (as Hoberock did). Furthermore, on the small scale it was possible to vary frequency and acceleration independently, whereas they were interrelated on the Main Rig.

The tests show that mesh movement does not affect its resistance to flow for a Newtonian fluid; that for a shear-thinning fluid the flow resistance of a horizontal screen can be reduced by vertical oscillations, but there is probably little effective reduction in viscosity by motion in the horizontal plane.

For non-Newtonian fluids there was found to be a distinct difference in flow capacity of screens at low and high frequency. The small-scale tests indicate that this was a function of acceleration rather than frequency itself. The relatively sharp transition contradicts the Hoberock model where flow increases with acceleration. A more dramatic change was shown by the more plastic (higher viscosity at low shear) fluids. However, at frequencies in the upper region, the relationship between screen flow capacity and screen tilt was similar for fluids of different rheologies but the same Marsh Funnel time.

6.2 Static Screen Tests

The relationship between flow rate and static head is shown in the following graphs. It should be noted that the meshes used had different wire thicknesses, and the 120 mesh and 150 mesh had backing support screens. Thus flow resistance would not be expected to be simply related to mesh count.

Figure 6.1 shows the spread of data from different runs with glycerol. Part of the scatter is due to temperature fluctuations affecting the viscosity. However, the data suggest a straight-line relationship, going through the origin. Figure 6.2 shows a similar conclusion for the other two meshes. Thus for a Newtonian fluid, flow-rate is proportional to head (in this range) - i.e. Darcy's Law.

Figures 6.3 and 6.4 show equivalent experiments with HEC of the same Marsh Funnel viscosity. Clearly the effective viscosity of the HEC is much higher at the (low) shear rates obtaining on passage through the screen, because the flow-rates are lower.

Figures 6.5 and 6.6 show equivalent experiments with XCD of Marsh Funnel viscosity 41 s. (XCD of Marsh Funnel viscosity 50 seconds gave too low a flow rate for the experimental range.) The graphs give indications of curvature and of intercept - i.e. a certain head of liquid can be supported with virtually no flow. This is clearly due to the virtual Yield Point on the rheogram - i.e. a small amount of stress can be applied with almost negligible resulting shear. As a general observation, the plots of flow-rate versus height resemble the rheograms: this is obviously because the height determines the shear stress applied and the flow-rate the resulting shear rate.

As previously noted, the meshes were not progressive in dimensions, so the effective resistance does not follow an obvious pattern. For each fluid, the data gave very similar lines for the 100 and the 120 mesh, and about half the flow-rate for the 150 mesh.

It may also be observed that for these conditions the Marsh Funnel time is not a good predictor of flow-rate: e.g. for 100 mesh, HEC of MF 50 s gave similar flows for XCD of MF 41 s, whereas glycerol of MF 50 s gave about half the flow-rate.

Figure 6.1 Flow Rate of Glycerol versus Liquid Height for a static screen of 100 mesh

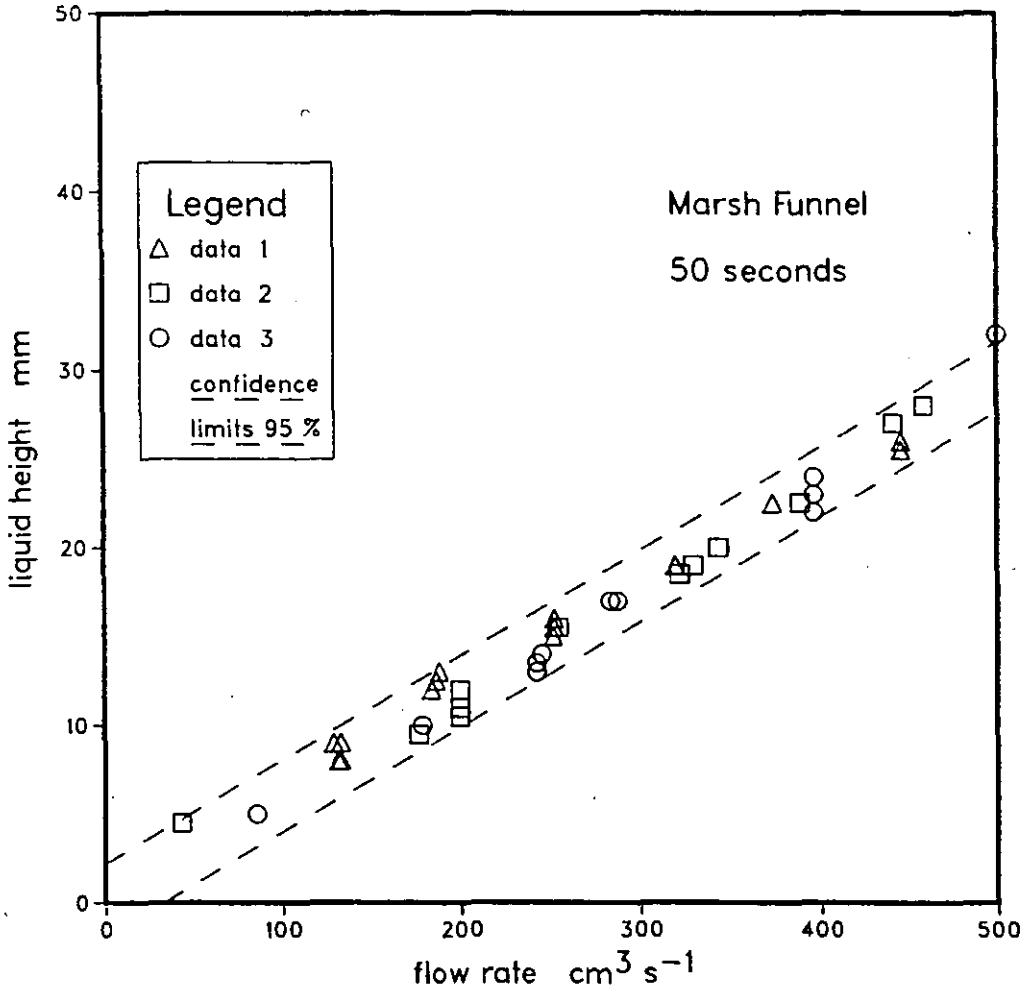

Figure 6.2 Flow Rate of Glycerol versus Liquid Height for static screens of 120 & 150 mesh

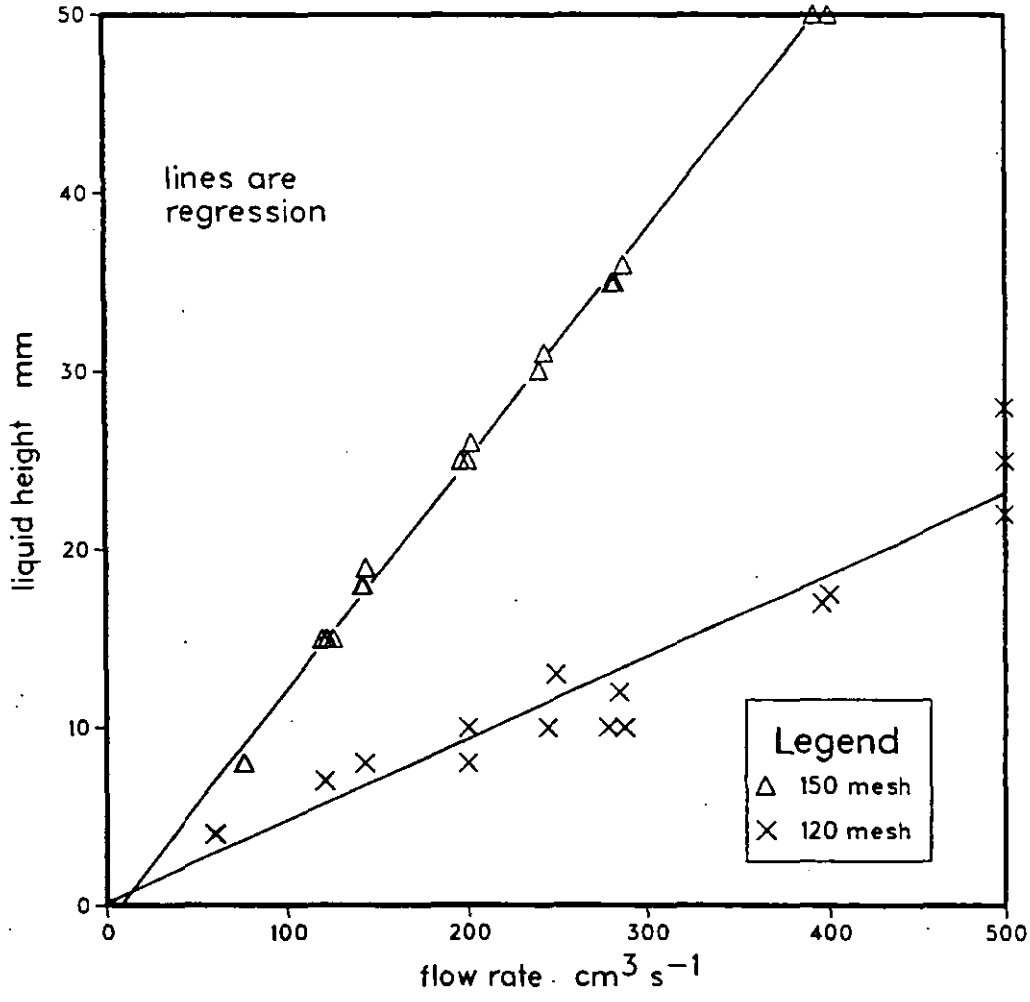

Figure 6.3 Flow Rate of HEC versus Liquid Height for a static screen of 100 mesh

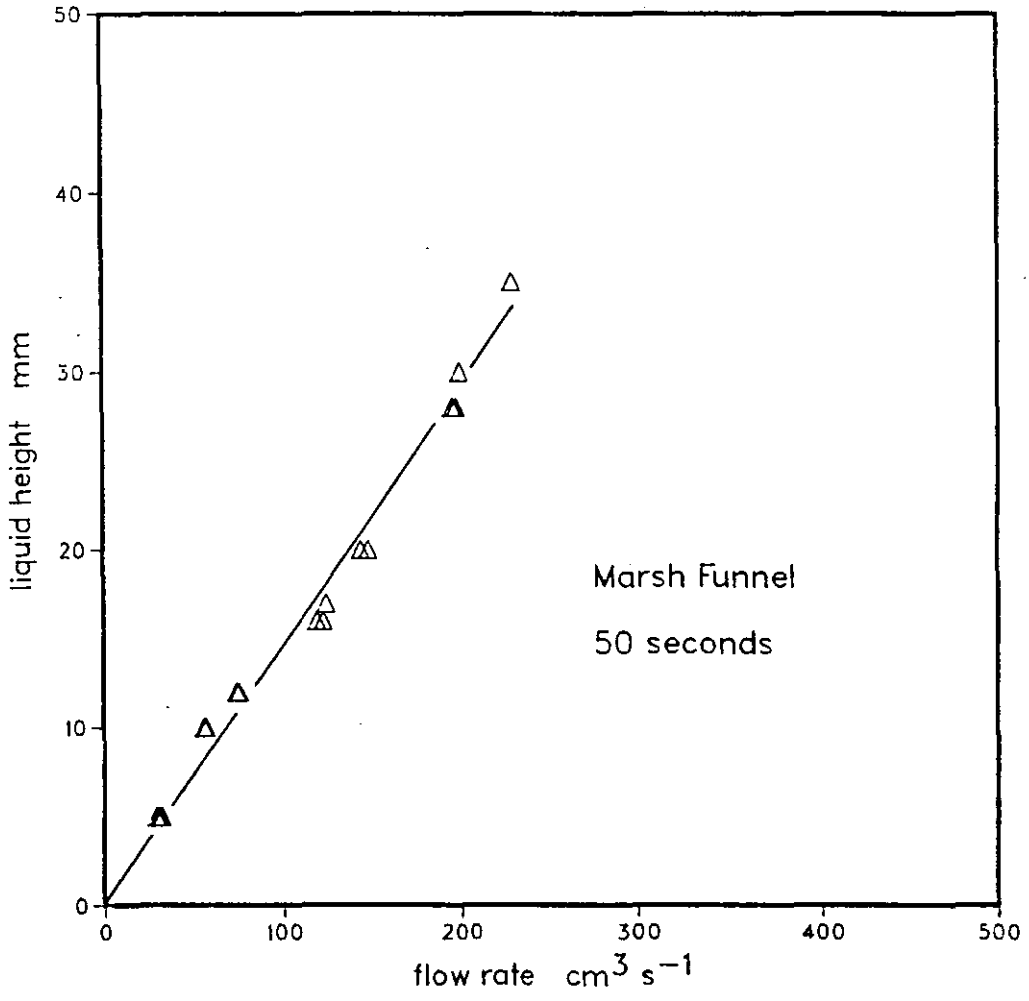

Figure 6.4 Flow Rate of HEC versus Liquid Height for static screens of 120 & 150 mesh

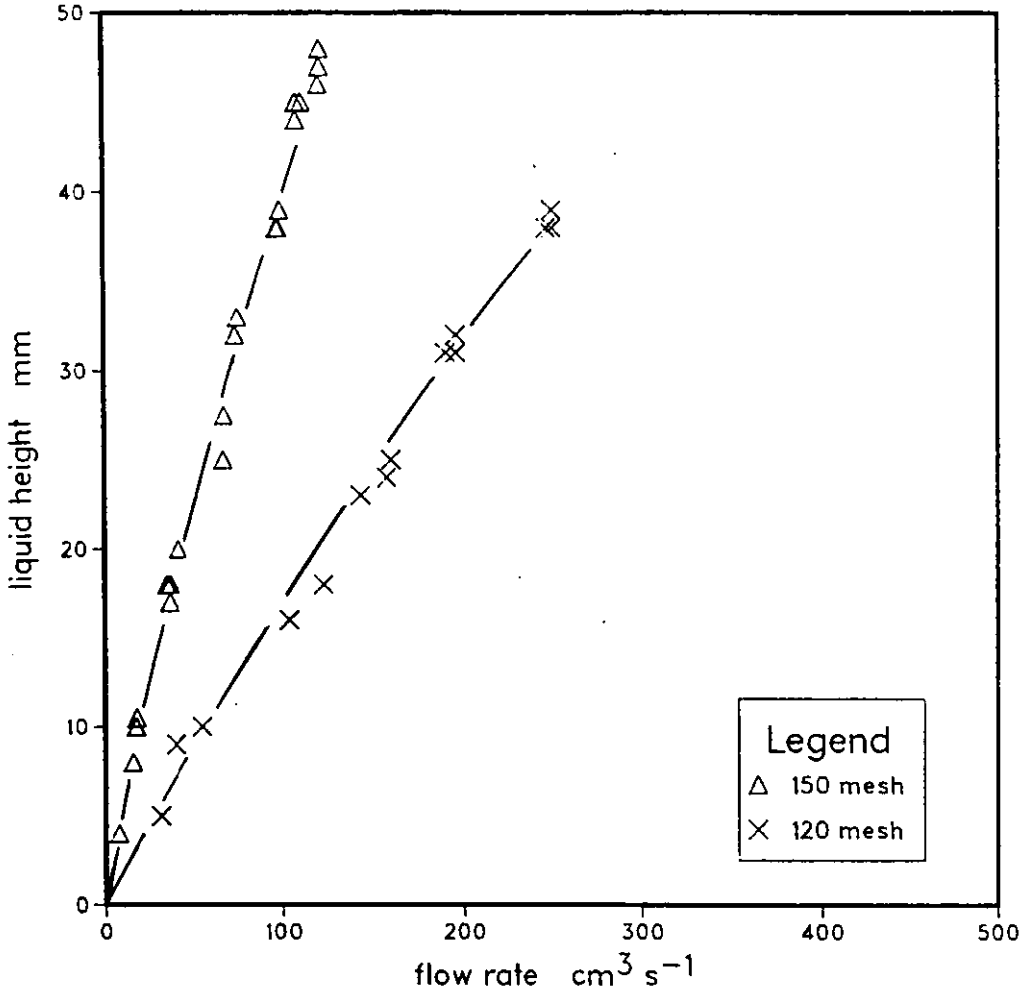

Figure 6.5 Flow Rate of XCD versus Liquid Height for a static screen of 100 mesh

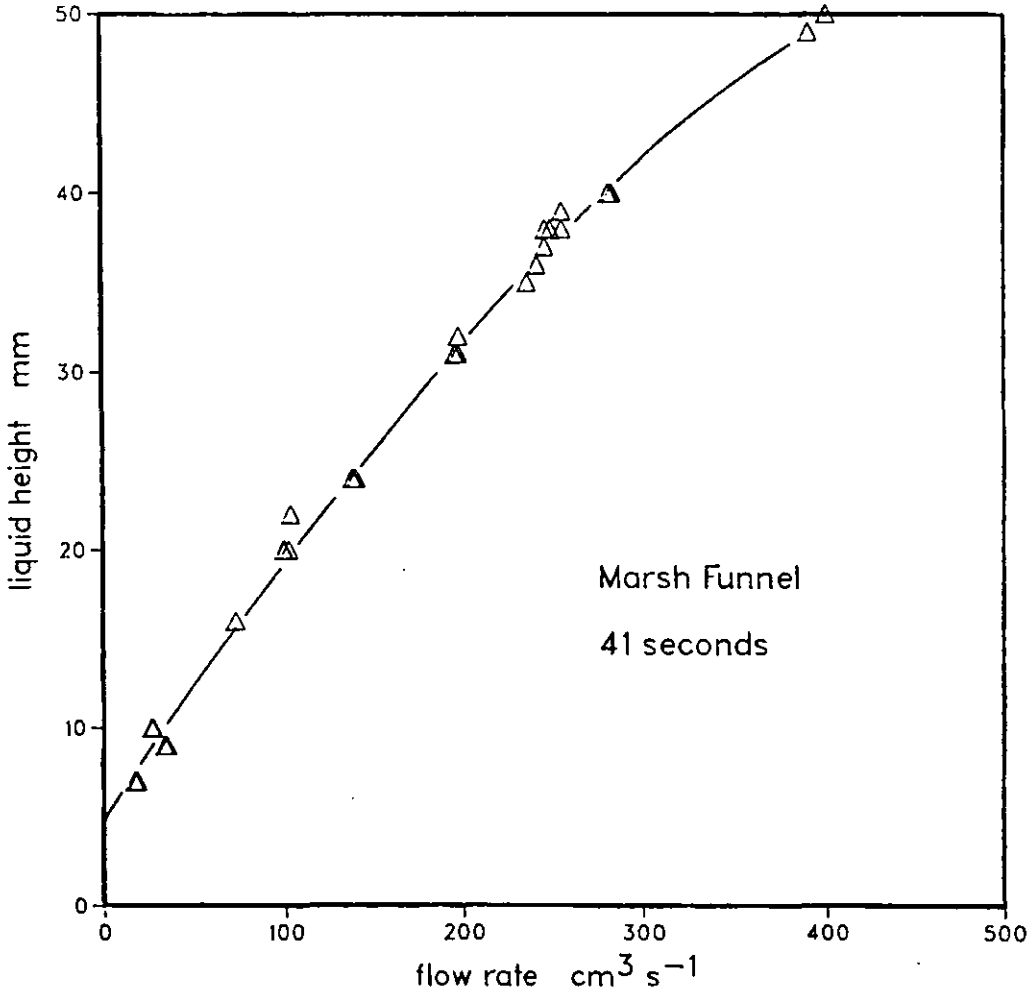

Figure 6.6 Flow Rate of XCD versus Liquid Height for static screens of 120 & 150 mesh

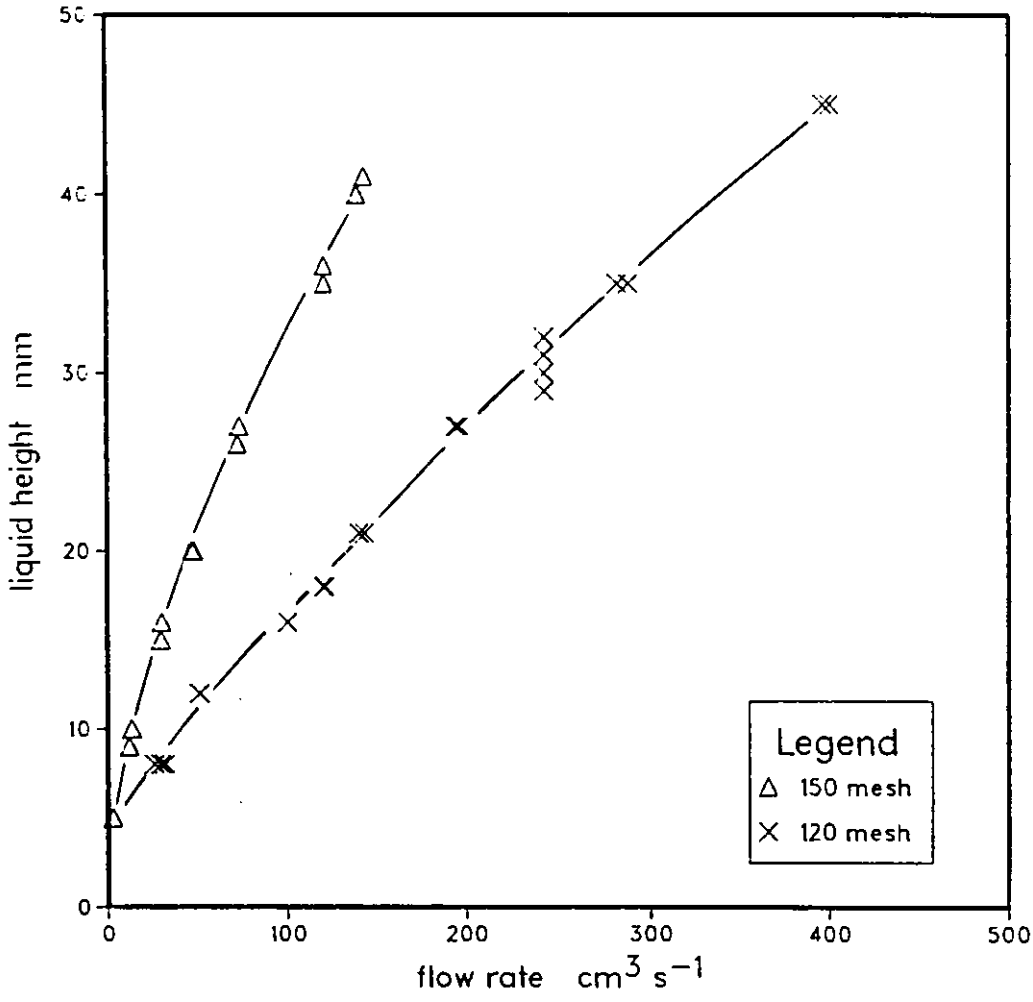

6.3 Small Vibrating Screen Tests

These were limited in scope due to the various constraints of commissioning the small rig. However, they were the basis for modifications to the rig and a more complete experimental programme which has since been commenced by another worker. The following are results of experiments to find the effect of either horizontal or vertical vibration alone on a piece of horizontal mesh supporting a head of liquid, glycerol and XCD. Tests with HEC were unsuccessful due to the formation of stable froth.

6.3.1 Aqueous Glycerol

For vigorous vertical vibration only, Figure 6.7 demonstrates that the flow-rate of glycerol solution is directly proportional to the head. A more viscous solution was found necessary than that used in the static tests, because the latter utilised only half the screen and had lower measurable liquid heads (1 to 50 mm, compared with 15 to 100 mm).

Tables 6.1 and 6.2 show that frequency and acceleration had only a small effect on the liquid head supported by a set flow-rate of 0.126 $dm^3 s^{-1}$. Both horizontal and vertical vibration gave similar results, but zero vibration gave a steady build-up of liquid height, along with obvious build-up of bubbles on the mesh. It was concluded that the principal benefit was in dislodging bubbles, but that for the Newtonian fluid there was probably little actual aid to flow through the mesh

Figure 6.7 Flow Rate of Glycerol versus Liquid Height on a vertically vibrating screen

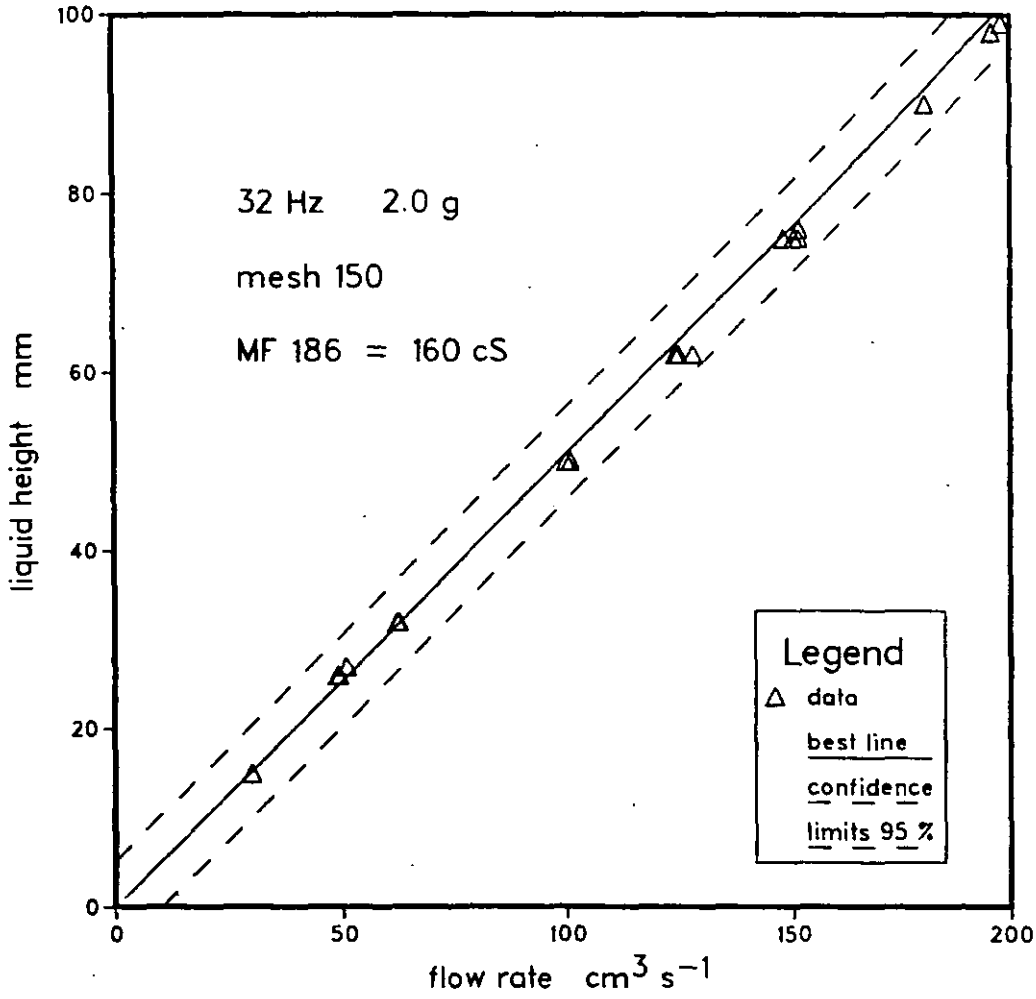

Table 6.1 Glycerol Heights for Horizontal Vibration				
frequency **Hz**	**16**	**24**	**32**	**56**
acceleration **'g'**	liquid height **mm**			
1	72	70	72	70
2	72	68	68	67
3	67	64	64	66
4	65	63	62	65

Table 6.2 Glycerol Heights for Vertical Vibration				
frequency **Hz**	16	24	32	56
acceleration **'g'**	liquid height **mm**			
0.5	81	67	70	68
0.75	77	66	69	68
1.0	71	66	66	68
1.5	67	67	65	67
2.0	62	67	65	66
3.0	--	64	65	65
4.0	--	60	65	63

N.B. It was not possible to measure at > 2 g at 16 Hz because the apparatus was too disturbed by the violence of the motion.

6.3.2 Aqueous XCD

Figure 6.8 shows a relationship between liquid head and flow-rate for vertical vibration which is quite different from the Newtonian case. The solid line represents the data already given in Figure 6.6 for the same mesh and similar fluid. Tentatively, this suggests that there is a difference between liquid heights above and below 38 mm. With lesser heads one may suppose that the main effect of vibration is to dislodge bubbles, so the relationship between flow-rate and head is similar to the static case. With greater heads there is a different relationship, which can be fitted to a straight line which would extrapolate to an intercept on the vertical axis at 20 mm.

The work on the main rig provides some support for this notion, as will be discussed. However, it is clear that more results with a range of fluids and meshes are required.

As for the glycerol, the effect of horizontal and vertical vibration were compared for a range of frequencies and accelerations. The flow-rate was 0.2 $dm^3\ s^{-1}$, and the equilibrium head was noted. (N.B. to obviate drift in the results, readings were not taken in order, hence the trends shown cannot be interpreted as changes with time.)

Figure 6.9 shows the relationship between head and acceleration for horizontal motion at a range of frequencies similar to those used on the main rig. Figure 6.10 shows similar results for vertical motion. A more detailed discussion will follow, but it is clear that vertical acceleration is more effective in reducing screen resistance, particularly above 1 **g**. These figures do not show any clear dependence on frequency. This aspect was tested for the same liquid and screen over a wider range, as shown in Figure 6.11. It is surmised that the obvious dips at around 25 and 50 Hz are due to mesh resonance effectively increasing the screen motion (and acceleration) in excess of that applied to the frame. This should be tested with screens of different dimensions. The difference between 0.5 **g** and the 1.0+ g accelerations is striking.

Figure 6.8 Flow Rate of XCD versus Liquid Height on a vertically vibrating screen

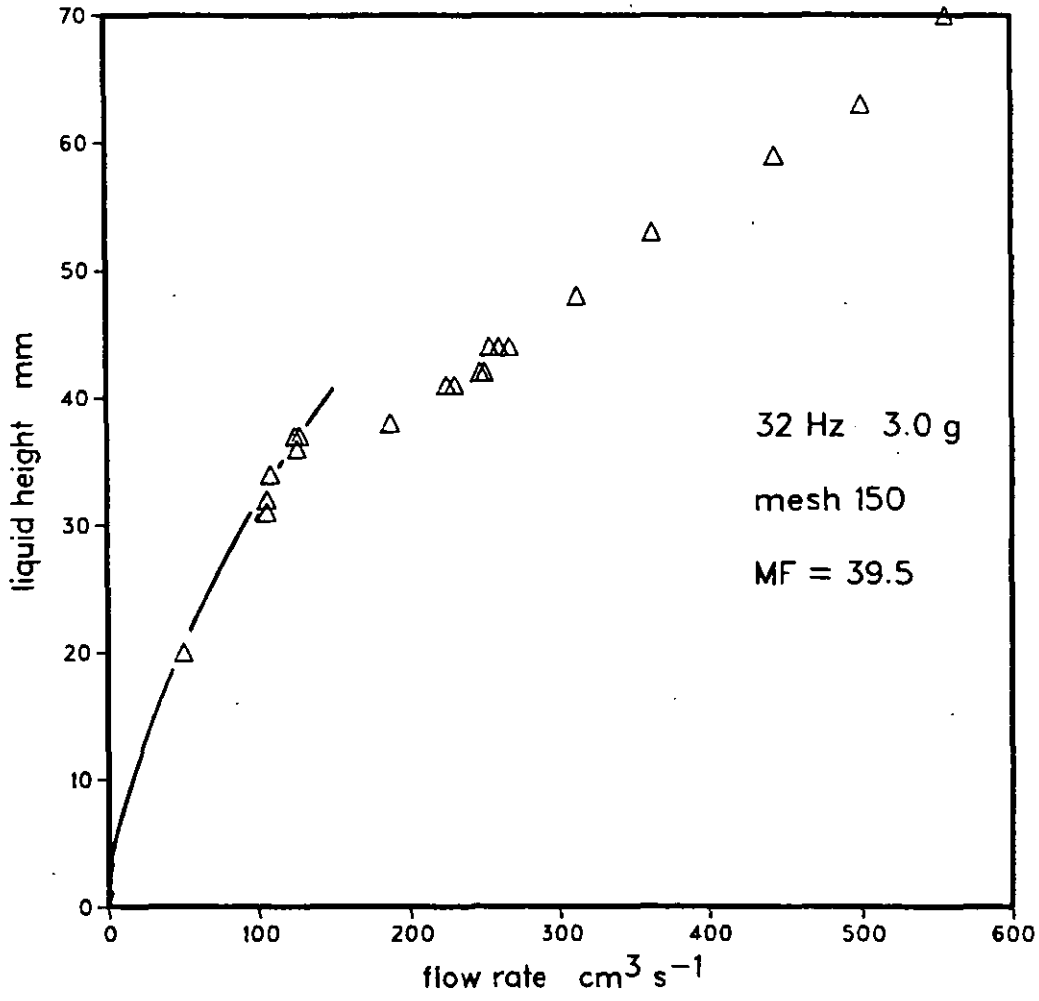

Figure 6.9 Flow Rate of XCD versus Acceleration on a horizontally vibrating screen

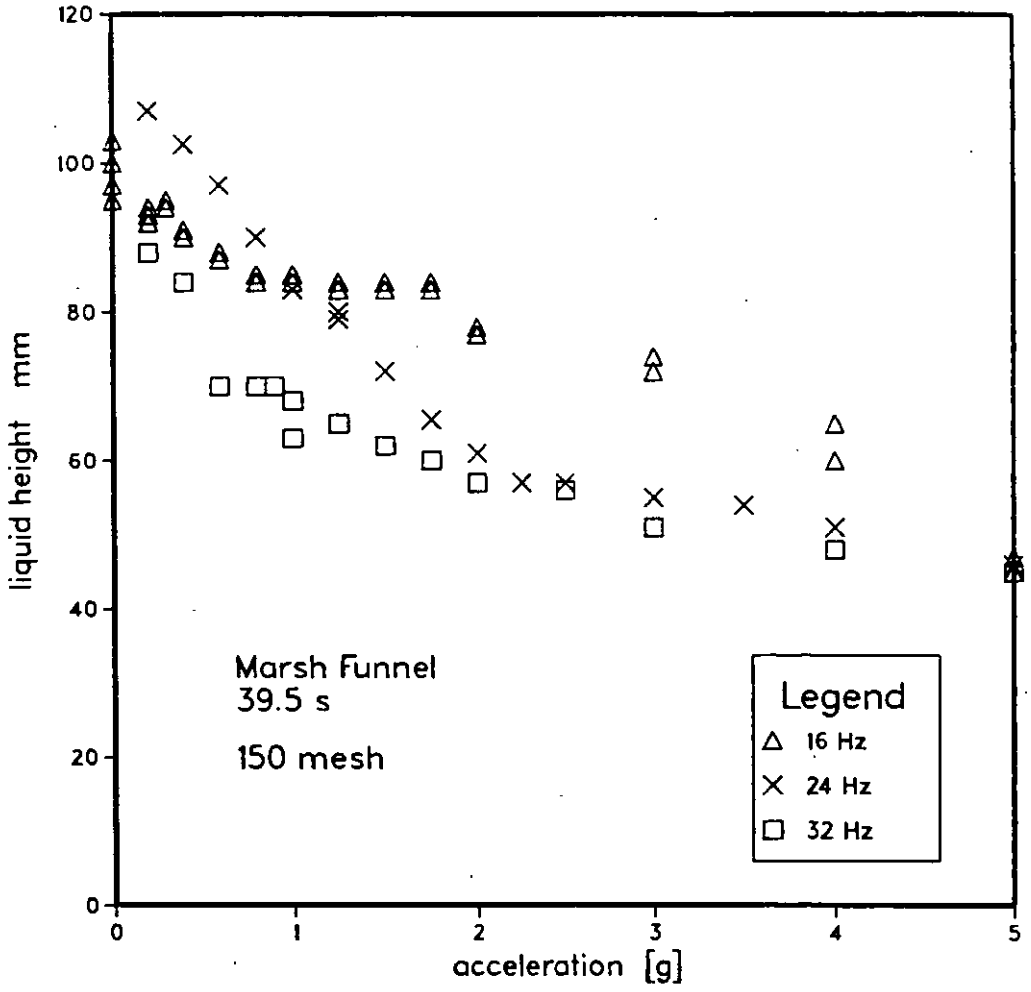

Figure 6.10 Flow Rate of XCD versus Acceleration on a vertically vibrating screen

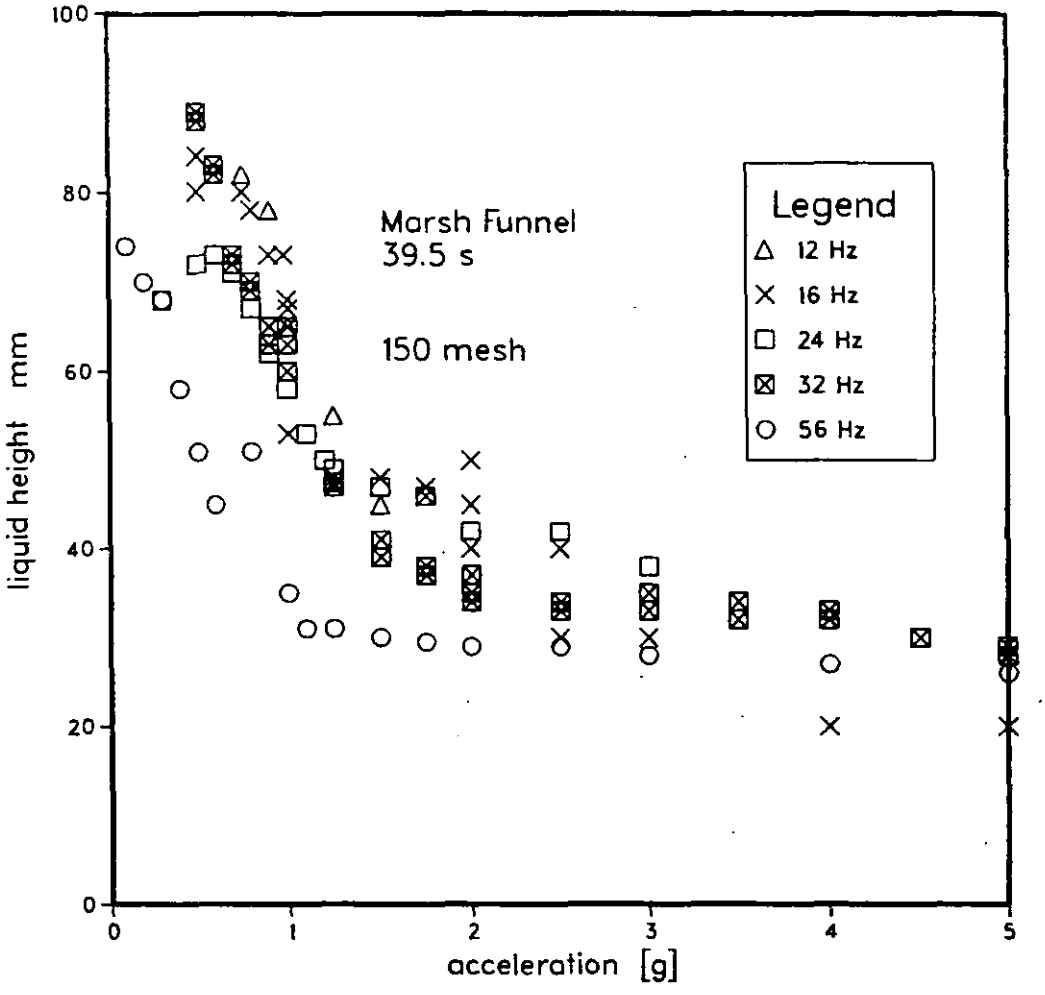

Figure 6.11 Flow Rate of XCD versus Frequency on a vertically vibrating screen

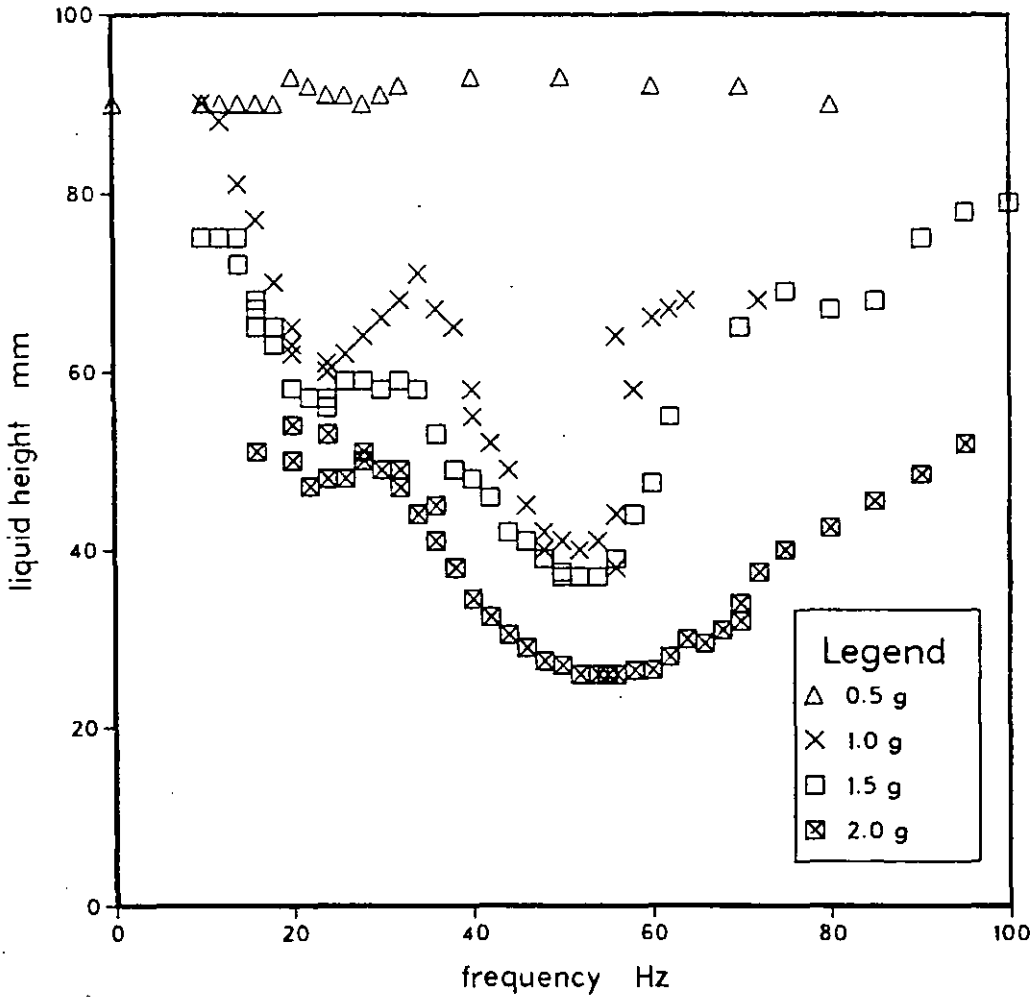

6.4 Main Rig Tests

These were mainly carried out on screens with a slight upward tilt, and mostly using the flat screens on the lower deck. As a standard criterion, the flow which would just fill the lower rear screens was used, being both convenient experimentally and representative of typical field conditions.

6.4.1 Effect of Screen Angle for HEC, XC, XCD

Figure 6.12 gives data for two concentrations of HEC on the same mesh, and the lines are parabolas fitted by least squares regression. These suggest that the screen is given additional flow capacity by an upward tilt, and that this additional capacity is proportional to the square of the angle. However, for this fluid there is (by extrapolation) significant flow capacity for the horizontal screen.

Figure 6.13 shows similar data for XC solutions. However the lower parabola shown is not a best fit, but that taken from the HEC data for similar Marsh Funnel viscosity. Furthermore, the XC curve for MF 38 s is a little to the right of the HEC curve for MF 40 s. This suggests a family of curves defined by Marsh Funnel times which can equally be applied to the two types of fluid, despite their very different rheologies.

Figure 6.14 shows another parabolic fit for XCD on a finer mesh, where it appears that the horizontal screen would have virtually zero flow capacity. The dotted lines are the 95% confidence limits. 30 Hz was chosen in preference to 20 Hz as the selected frequency because of accumulated experience and observations of a phenomenon which will now be described.

Figure 6.12 Flow Rate of HEC versus Screen Angle
(20 Hz original 100 mesh MF 32 & 40 s)

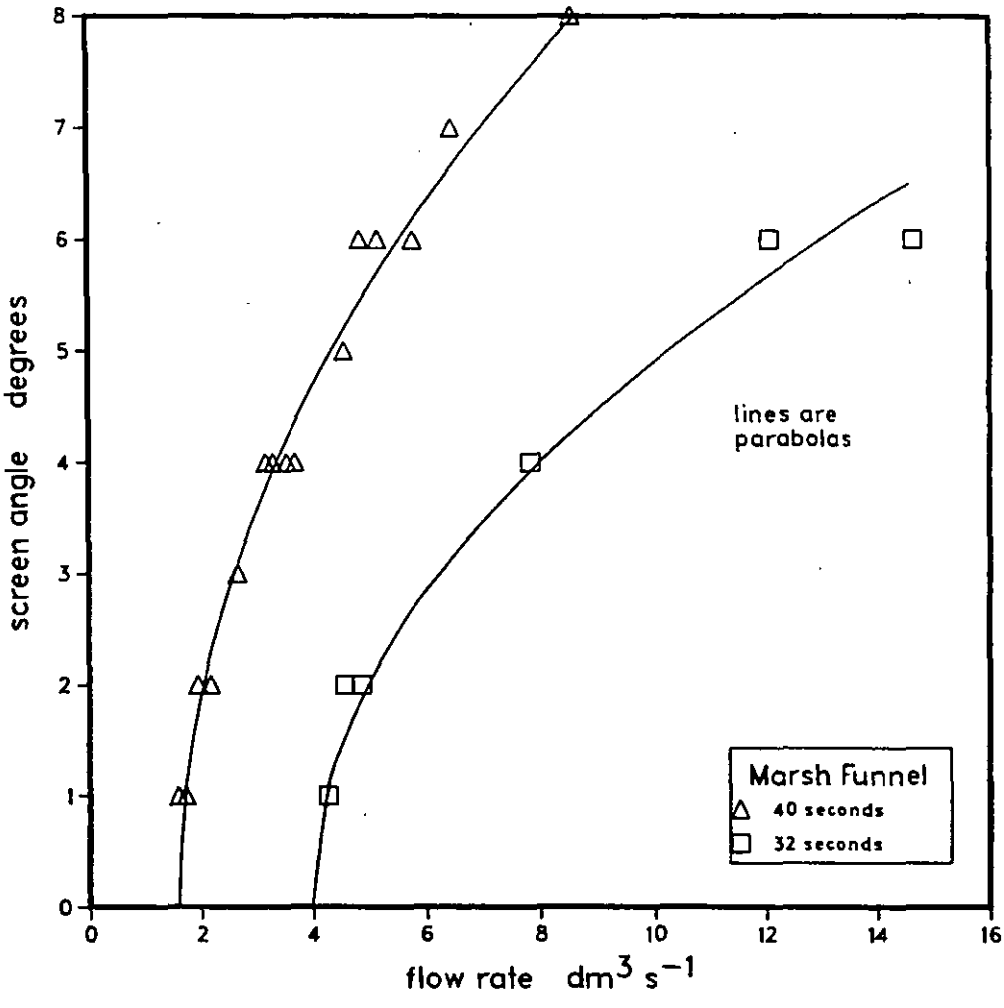

Figure 6.13 Flow Rate of XC versus Screen Angle
(20 Hz original 100 mesh MF 32 & 38 s)

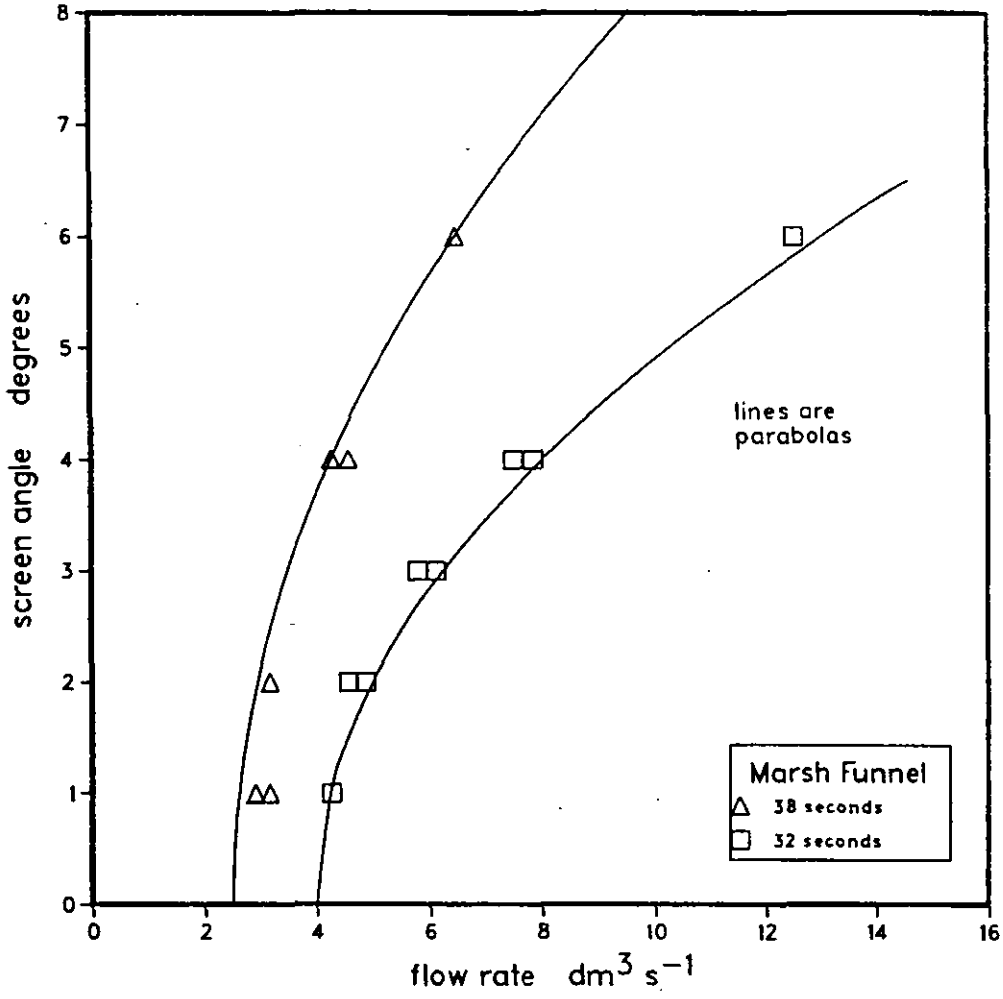

Note: parabola for 32 seconds is not best fit, but is from Figure 6.12 for comparison.

Figure 6.14 Flow Rate of XCD versus Screen Angle
(30 Hz 150 mesh MF 40 s)

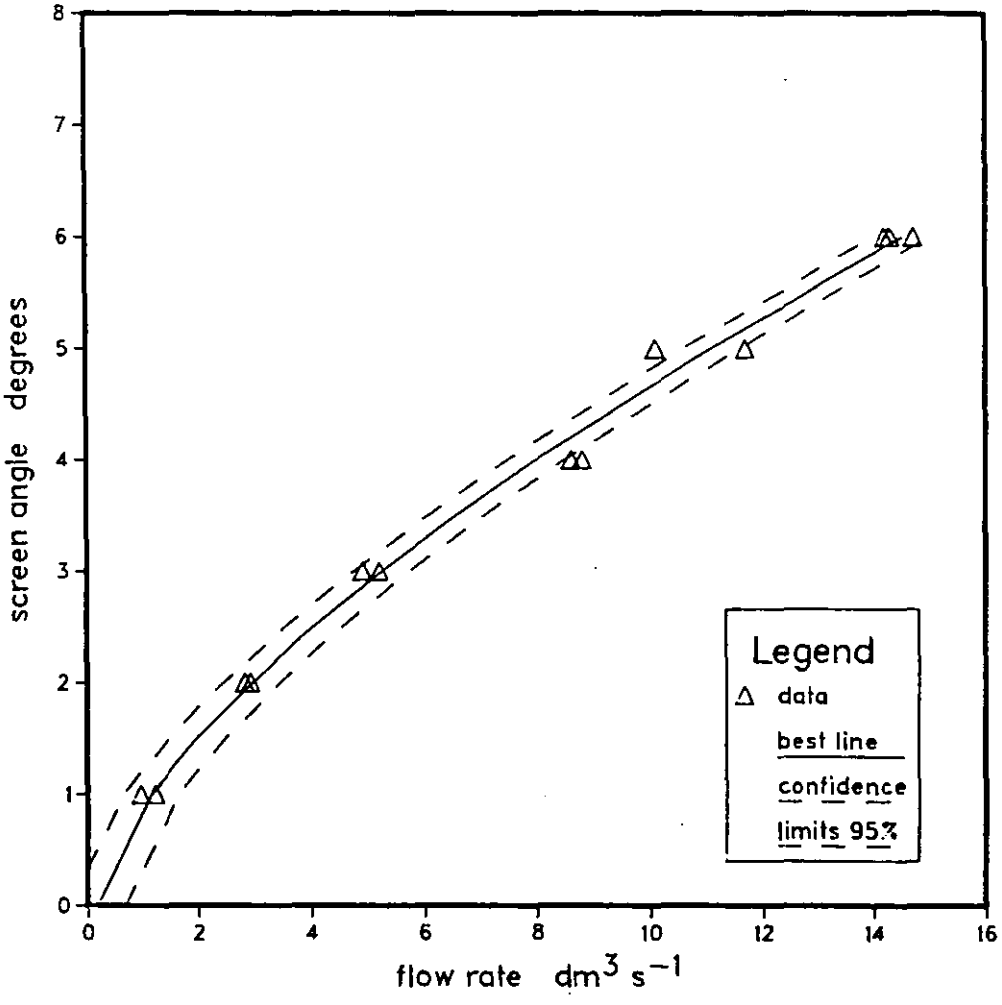

6.4.2 Effect of Vibration Frequency for HEC, XC, XCD

Figure 6.15 contains data for the most concentrated HEC used (Marsh Funnel 40 s). Fewer measurements were taken for angles of an odd number of degrees. For this reason, and also for clarity, they are presented separately.

It can be seen that the effect of frequency is small but beneficial. Essentially the flow capacity is the same for frequencies between 0 and 10 Hz, increases and then becomes frequency independent between 20 and 30 Hz. The effect is most marked at high angles. It was less readily discernible with lower concentrations of HEC.

For XC of similar Marsh Funnel time, the effect was much greater, as shown in Figure 6.16. Although frequency was the experimental variable, this was directly related to the screen acceleration. The frequency corresponding to 1 gravity is indicated on this graph, and it is noteworthy that it goes through the transition.

This phenomenon was investigated in more detail using fresh rig fluid (XCD) and new screens (100 and 150 mesh). The Marsh Funnel time was 41 s.

Figure 6.17 demonstrates that the XCD solution would not pass through the screen (other than by weeping) when the driving force was limited to the hydrostatic head on the mesh. For the lowest hydrostatic head (1° tilt, about 1 - 2 mm) screen vibration did not have any effect until the peak acceleration exceeded 1 gravity. Furthermore, accelerations beyond 2 gravities (23 Hz) did not give any additional benefit. A similar pattern was observed for other screen tilts, but the onset of measurable flow occurred at a lower frequency (hence acceleration) for greater angles of tilt (hence greater hydrostatic heads).

Figure 6.18 shows the same pattern for a finer mesh. However the smaller holes permitted negligible flow for accelerations below 1 gravity for tilts of up to 4°. As might be expected, the limiting flow-rates (accelerations > 2 g) were less than for the coarser mesh.

Figure 6.15 Flow Rate of HEC versus Frequency for angles 1 to 8° (100 mesh MF 40 s)

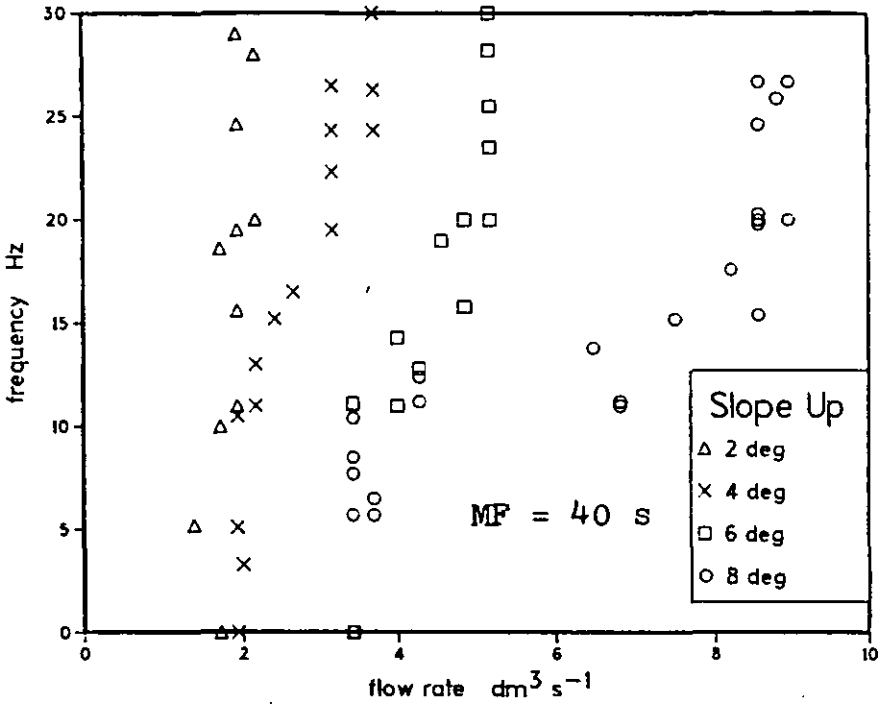

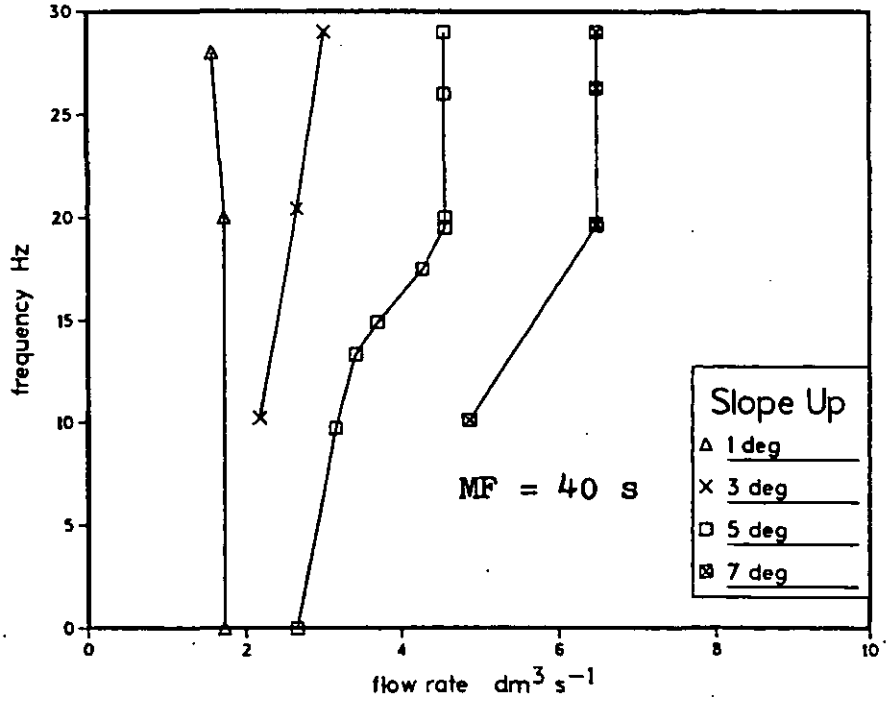

Figure 6.16 Flow Rate of XC versus Frequency for angles 4 to 6^{o} (100 mesh MF 39 s)

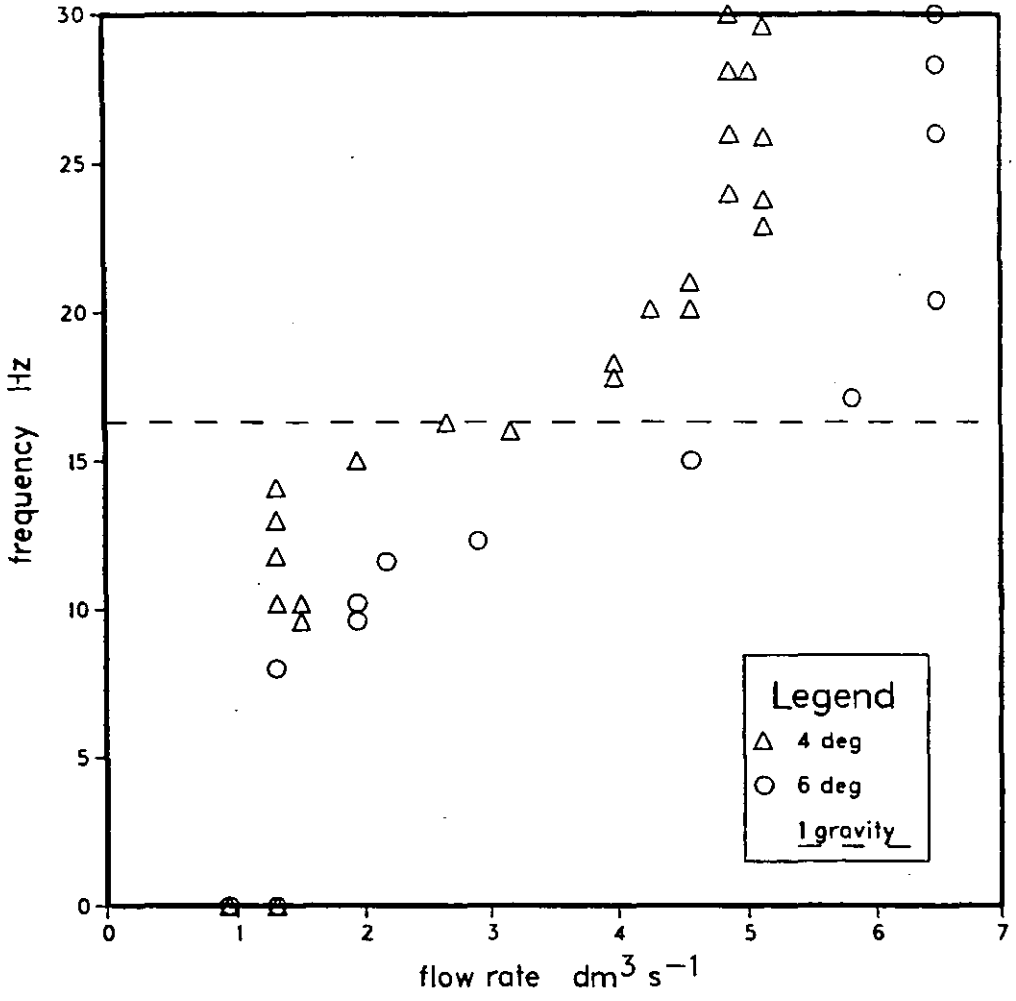

Figure 6.17 Flow Rate of XCD versus Frequency for angles 1 to 6° (100 mesh MF 41 s)

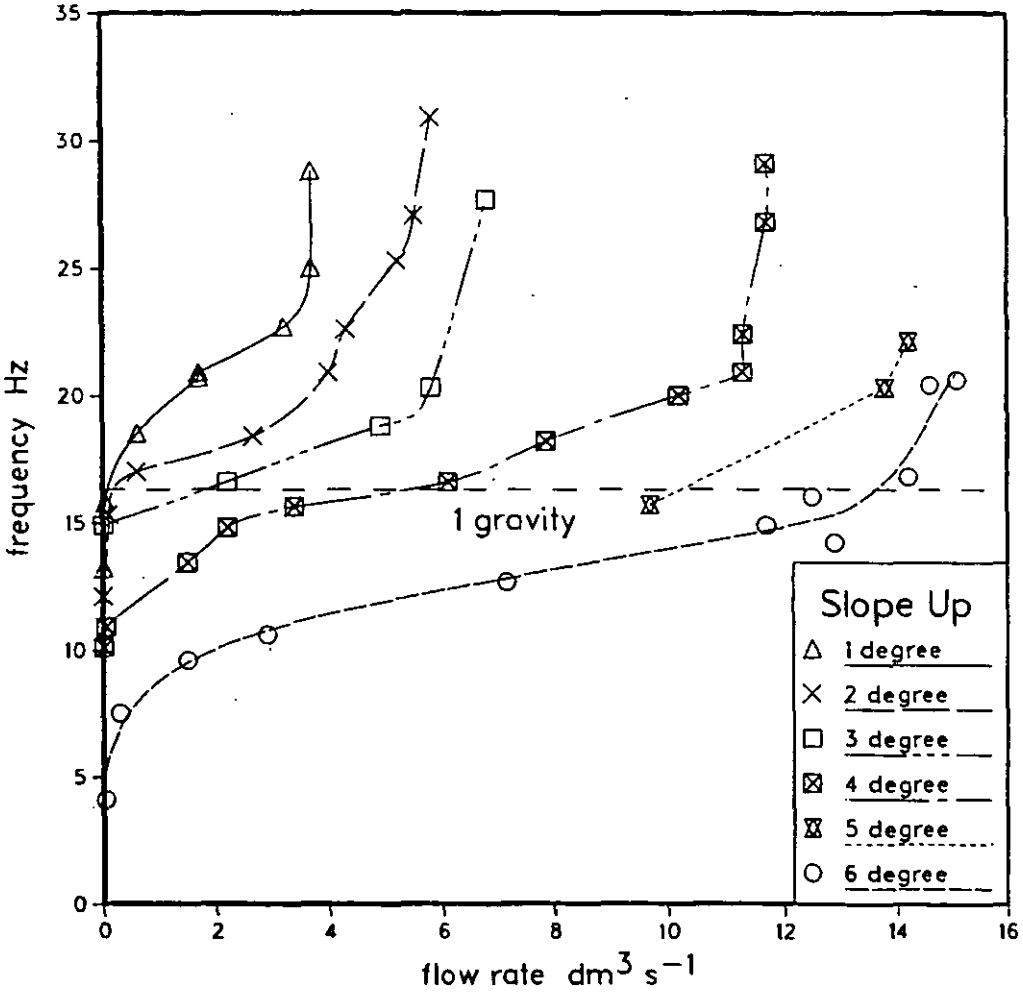

Figure 6.18 Flow Rate of XCD versus Frequency for angles 1 to 6° (150 mesh MF 41 s)

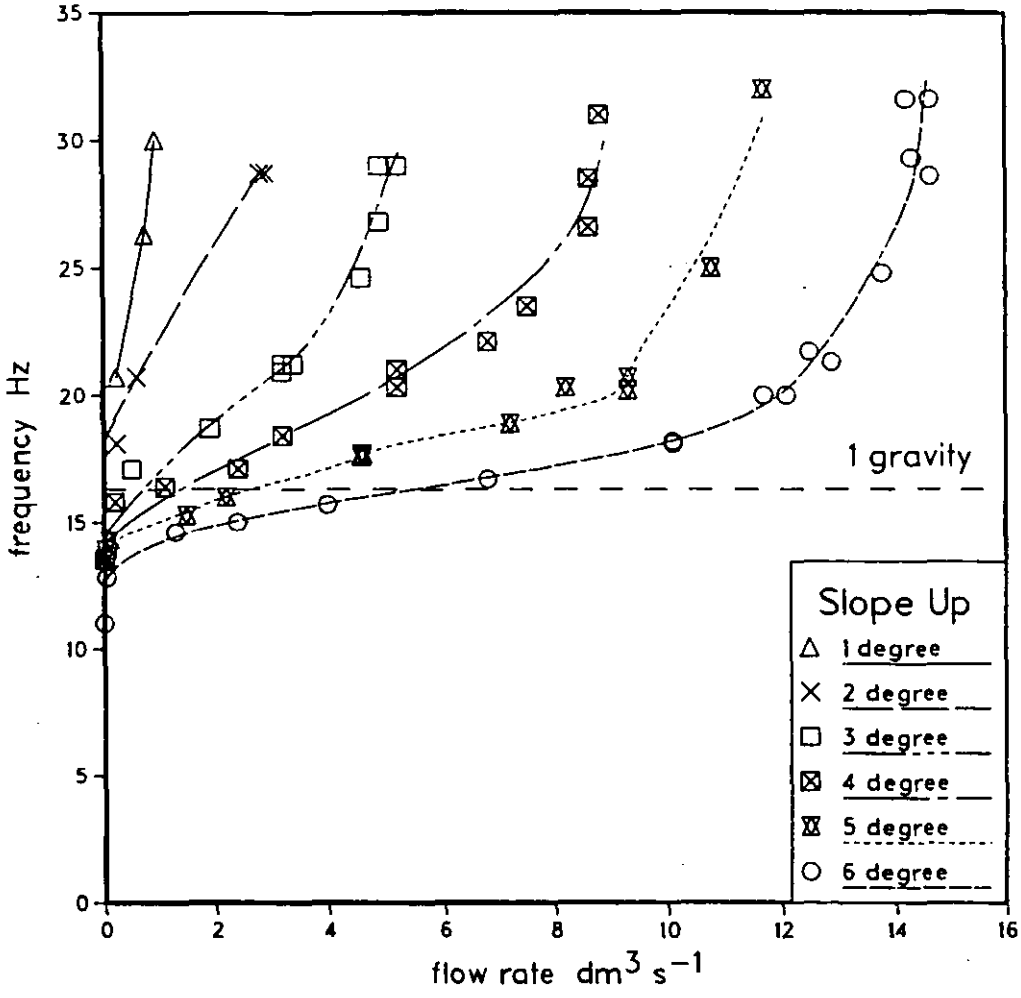

6.4.3 Effect of Solids on Screen Capacity

Figure 6.19 shows a comparison of the fluid capacity of a screen tilted upwards at 4^{o} in the presence and absence of screenable solids. In the former case there was sufficient solids in the system to maintain a thin film on the mesh when the motion was stopped. In both cases the screens were freshly power washed, and the Marsh Funnel time was 38 s.

For no vibration the solids-covered screen was essentially impermeable, whereas the empty one passed a significant amount of fluid. However, under vigorous vibration the solids-covered passed almost the same amount of fluid as the empty screen.

This was verified on the small vibrating screen rig, where a small amount (12 g) of oversize sand was found to form an obstruction to flow such that the fluid capacity (for the same head) was about half that of an empty screen for vibrations significantly below 1 g, and virtually identical for vibrations of 2 g at the same frequency. The fluid was aqueous XCD of Marsh Funnel time 39 s. The tests covered frequencies from 16 to 64 Hz. A similar result was obtained from a more limited test carried out with HEC rig fluid, passed through a circular analytical mesh bolted to the main rig. With a layer of alumina particles the sieve passed only a small flow-rate at low frequencies, but the flow-rate was greatly increased by vibrations above 1 g.

This can reasonably be interpreted as particles being thrown off the screen by the motion and thus spending less time covering holes. This has great importance because any practical usage of a vibrating screen will be in the presence of particles. It has been suggested (Hoberock 1980, 1982a) that the solids-free fluid capacity can be used as a basis for screen selection, on the grounds that in the presence of solids the true capacity will be some fraction of this value. However, the above results suggest that this should be the capacity at 2 g or above. In the case of fluids such as dilute HEC vibration only gives a little improvement of flow-rate, so a low acceleration might be selected, giving no solids levitation.

The effect of vibration in moving particles on the mesh was investigated in more detail, as described in Chapter 8.

Figure 6.19 Effect of Solids on Flow Rate of XC versus Frequency (original 100 mesh 4^{o} MF 38 s)

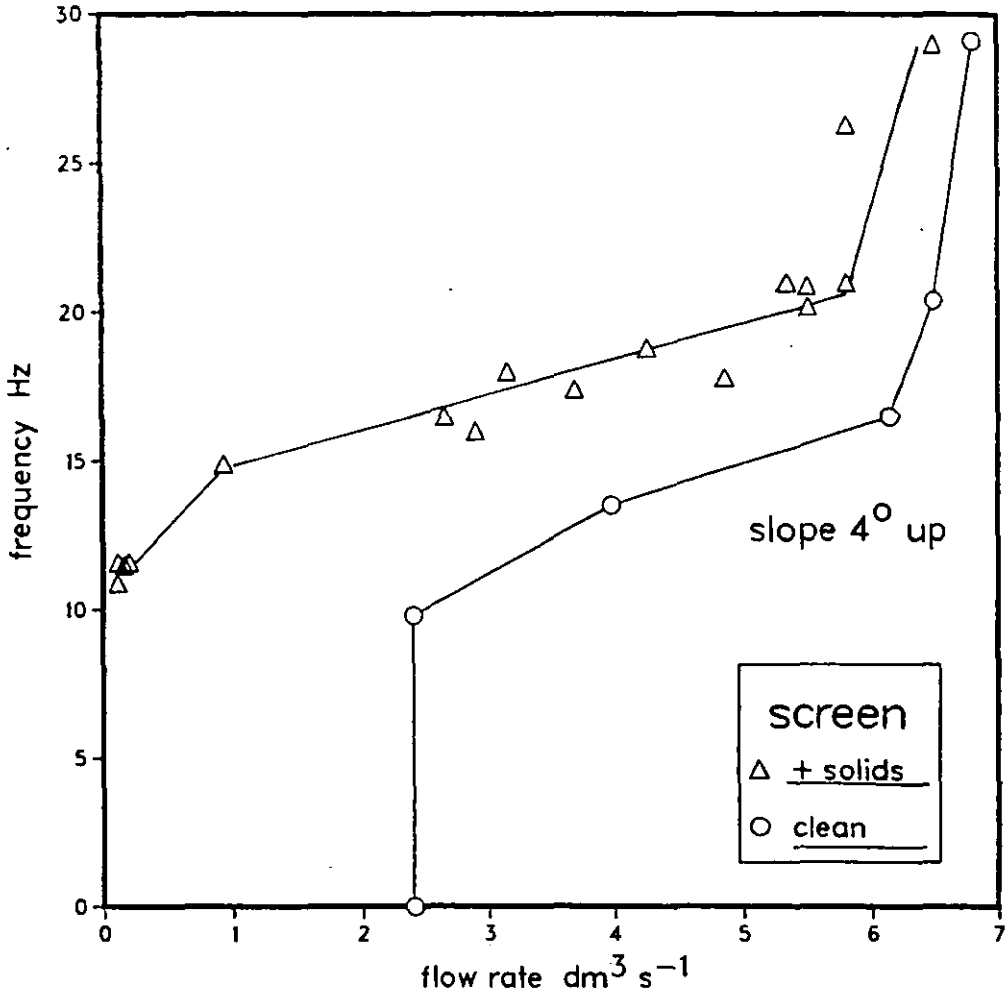

6.4.4 Active Screen Length

The fluid capacity tests (above) were carried out on a screen of fixed length. Some limited experiments were carried out to measure the length of screen in use for a given flow-rate and other specified conditions.

6.4.4.1 Effect of Flow Rate on Active Screen Length

Figure 6.20 shows the relationship between flow-rate and screen bearing liquid for water and HEC (Marsh Funnel 32 s) on a horizontal screen, with and without vibration. It will be noted that the effect of vibration on water was to increase the active length. This was presumably by the motion throwing liquid forward and/or an upward flow of air through the screen forming bubbles which inhibited the flow.

By contrast, with all other rig fluids (HEC, XC, XCD, clay) the effect of vibration was to reduce the active length. This was observed on many occasions as a drawing back of the liquid front when the vibration frequency was increased from a low to a high value. For this fluid, the effect of vibration was to increase by a factor of 3.7 the capacity of a given area of mesh.

Figure 6.21 shows data for the same fluid under vibration on the lower deck, which had an upward tilt and a finer mesh. These measurements were complicated by the fact that the support framework provided a small area of impermeable mesh. For fluid edges forward of this region, the impermeable length has been subtracted, leaving a length of free mesh only. (Note that there is a discontinuity in the effective head due to this omission.)

Some data of Hoberock for a similar mesh and comparable though different fluid have been added for comparison. These show a downturn towards the origin for lengths less than 0.8 m, which were not accessible on this rig.

Figure 6.20 Flow Rate of Water and of HEC versus Active Length of Horizontal 50 Mesh Screen

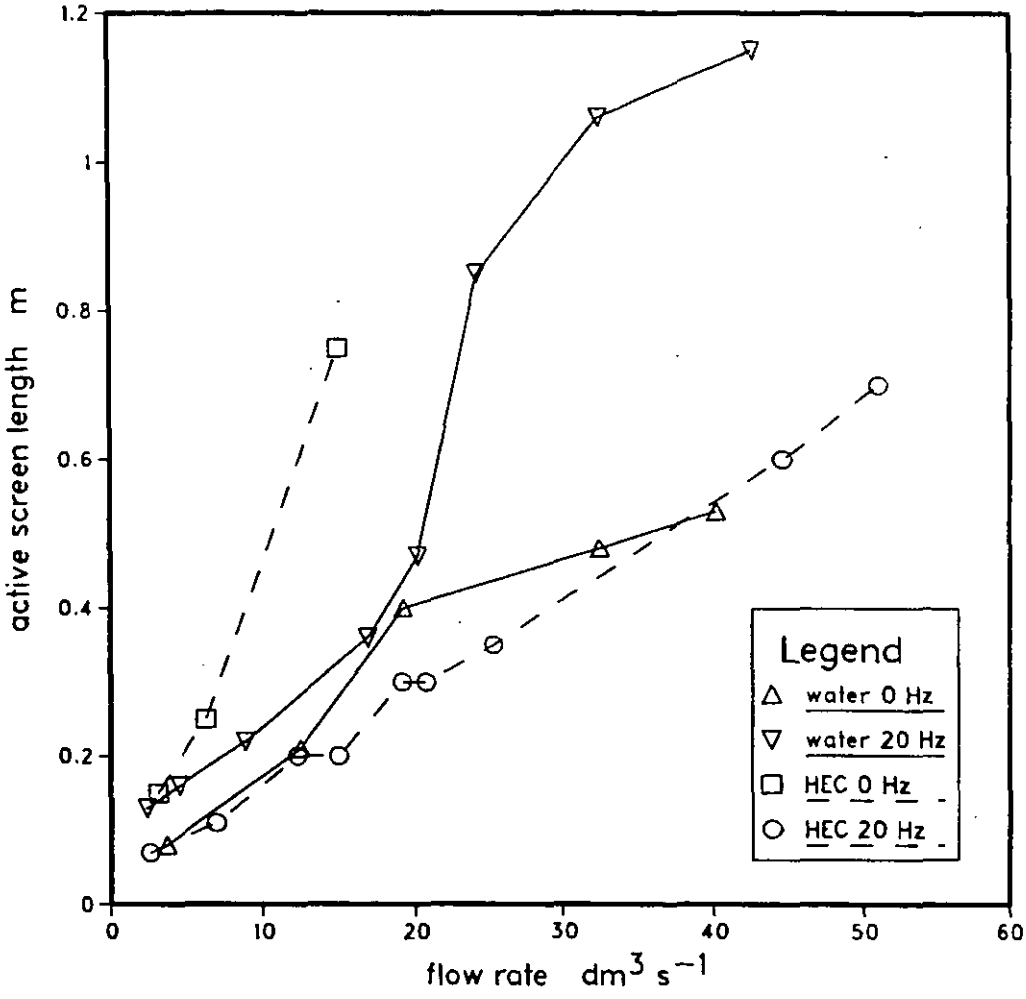

Figure 6.21 Flow Rate of HEC versus Active Length of 100 Mesh Screen at 4^{o} and 22 Hz

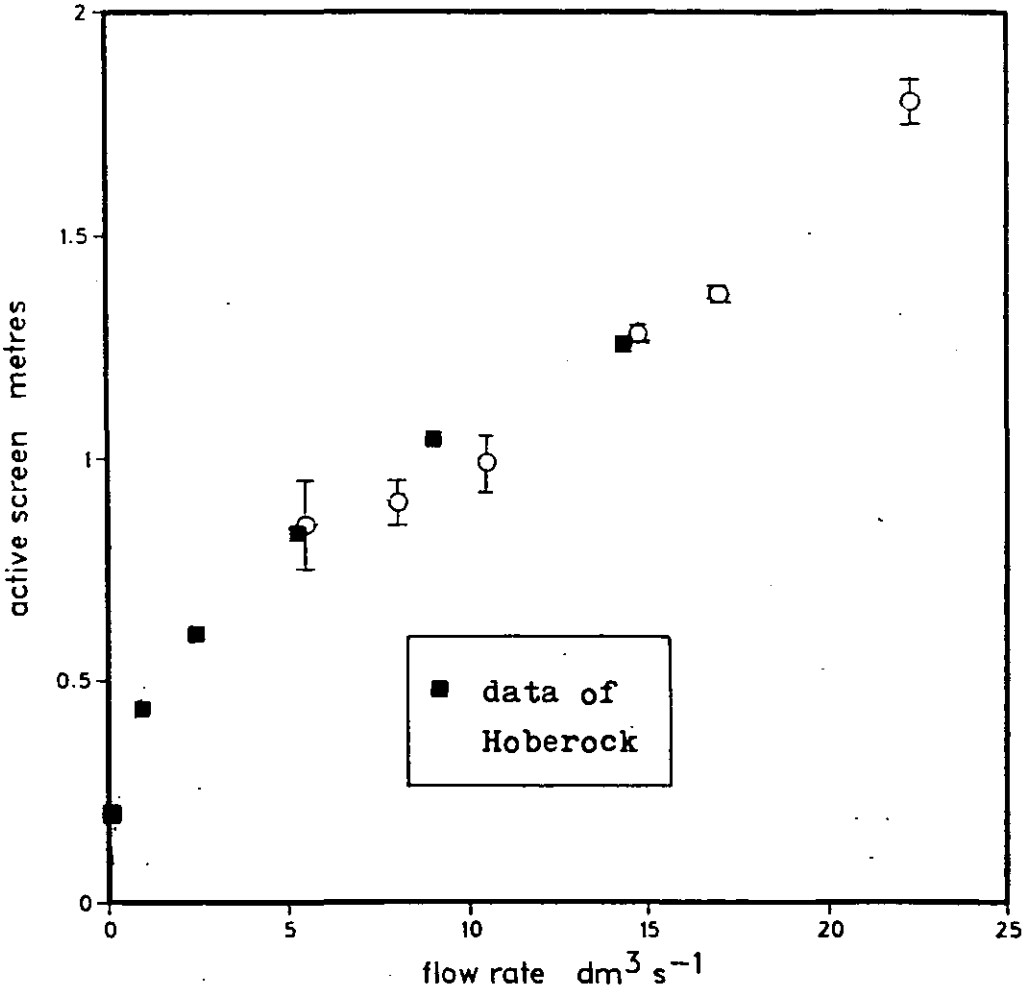

Note: Hoberock data included for comparison of data pattern only. Mesh was 100, tilt was -10^{o}, frequency was 60 Hz, fluid was bentonite in water, and rig was different. See section 5.3.4.

6.4.4.2 Effect of Vibration Frequency on Active Screen Length

Two different criteria were considered to determine the position of the forward limit of the active mesh. The simplest is the position of the liquid front on top of the mesh. However, this was difficult to determine with HEC rig fluid because of the formation of froth, which was transported forward and obscured the mesh. A second criterion was therefore developed, namely the foremost point at which there was significant liquid detachment from the underside of the mesh.

Figure 6.22 shows that the active length appears to be progressively reduced by increasing frequency (by up to a quarter). A similar reduction was observed for other polymer fluids.

Figure 6.23 shows the liquid front for a clay fluid, utilizing both criteria. It appears that the leading edge is at virtually the same position by both criteria for screen accelerations in excess of one gravity, whereas at lower accelerations [frequencies] there is a significant forward region of the mesh which is supporting fluid, but not passing it.

This may be interpreted as the region in which the head and screen acceleration combined are insufficient to overcome the plastic resistance to flow of the fluid through the mesh holes. Greater heads of liquid cause flow even with minimal screen vibration, and conversely screen accelerations greater than one gravity cause flow even with minimal heads.

Figure 6.22 Active Screen Length versus Frequency (HEC MF 34 s, 100 mesh 4^{o} 5 dm^3 s^{-1})

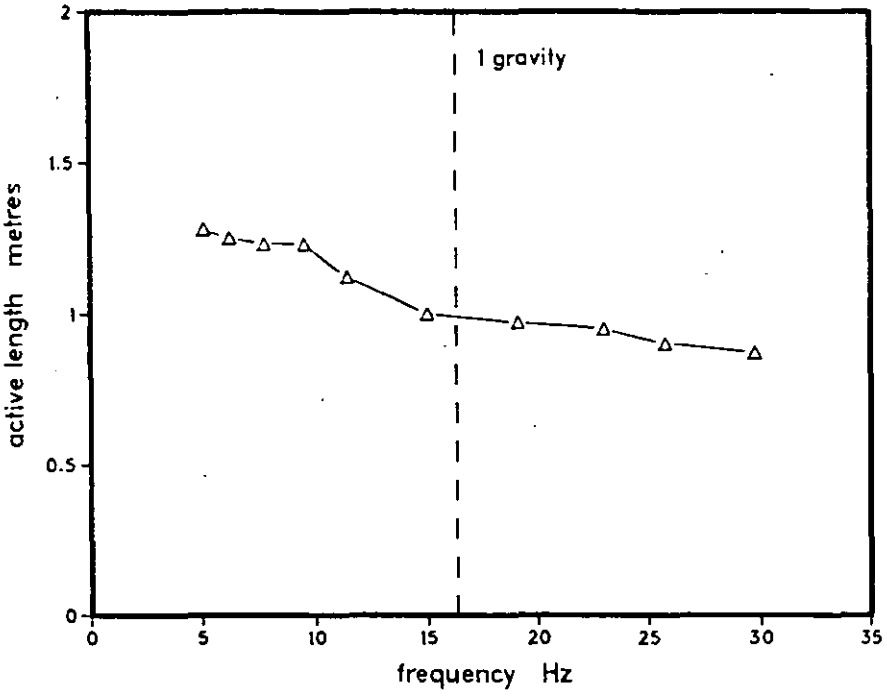

Figure 6.23 Active Screen Length versus Frequency (Clay MF 55 s, 80 mesh 2^{o} 4.5 dm^3 s^{-1})

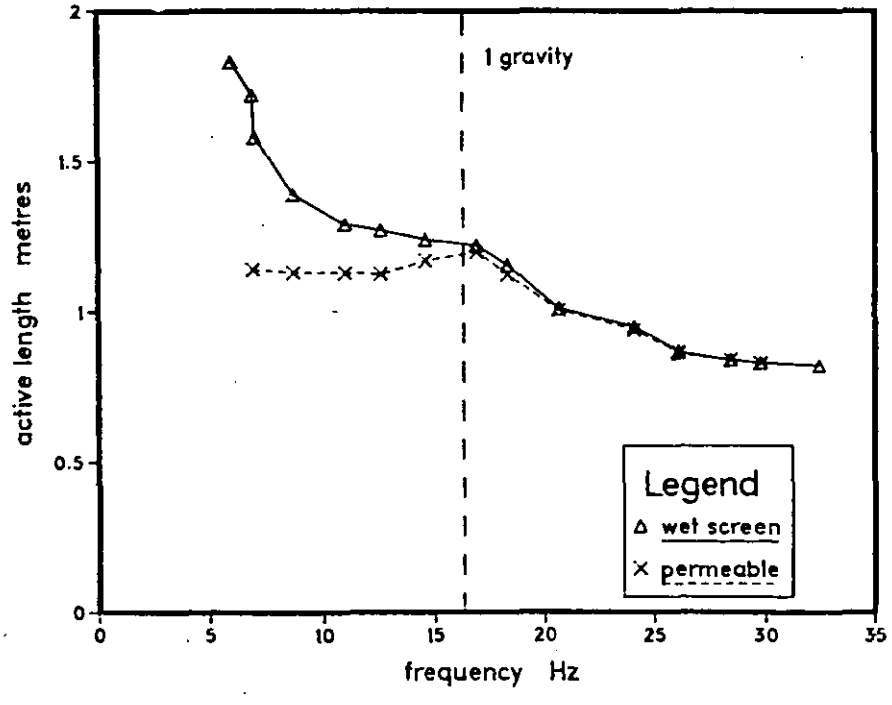

6.4.5 Liquid Surface on Tilted Vibrating Screens

The liquid surfaces were observed in order to find the character of the flow and the height profile along the length. With all fluids except water, the surface above the lower rear screen showed a pattern of standing waves at low frequencies. As the frequency (and acceleration) was increased, the peaks became more pronounced and closer together, until (around 16 to 18 Hz) the peaks began to break off and splashing occurred.

In addition, a calm patch was sometimes visible towards the rear, but this was affected by the feed disturbance, and in any case was not readily accessible on the lower screens. The phenomenon was better demonstrated on the upper screen, using a more viscous liquid (because the mesh was coarser) as shown in Figure 6.24. This was taken from the front of the apparatus, looking slightly down. It can be seen that despite the considerable agitation and splashing of the forward portion, the rearward portion of the liquid is calm. The transition region was relatively small, about 10 cm, showed a perceptible slope, and was characterized by rollers.

The profile of this fluid (height versus length from rear) is shown in Figure 6.25. Measurements were made of depth on the mesh, but these have been corrected to a horizontal datum, and the position of the screen indicated. It is obvious that the liquid head is not simply related to the length of active screen, but that two distinct regimes exist.

Figure 6.24 [overleaf]

Appearance of Clay Liquid on Upward Tilted Vibrating Screen (80 mesh 26 Hz 2^{o})

Appearance of Clay Liquid on Upward Tilted
Vibrating Screen [80 mesh 26 Hz +2°]

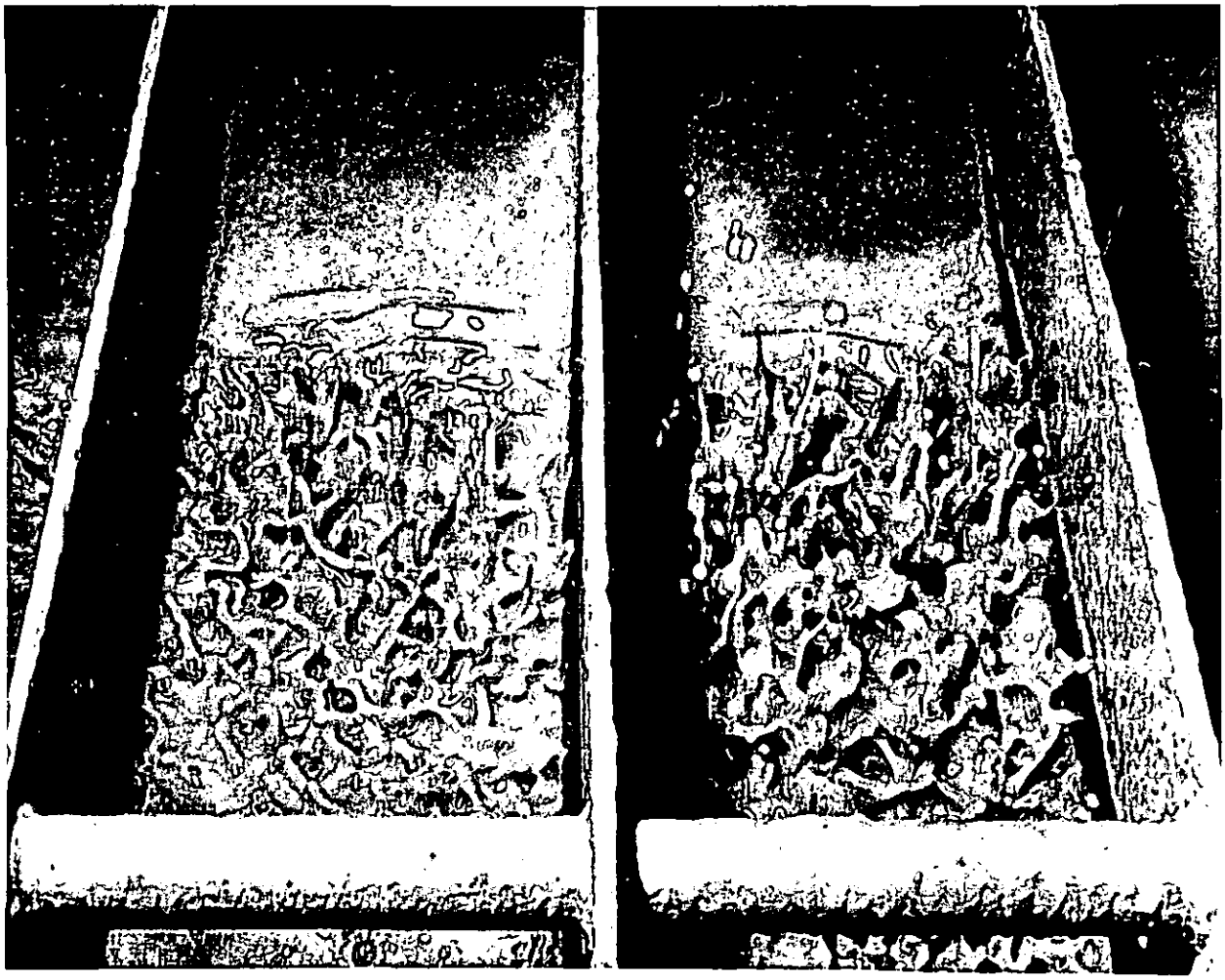

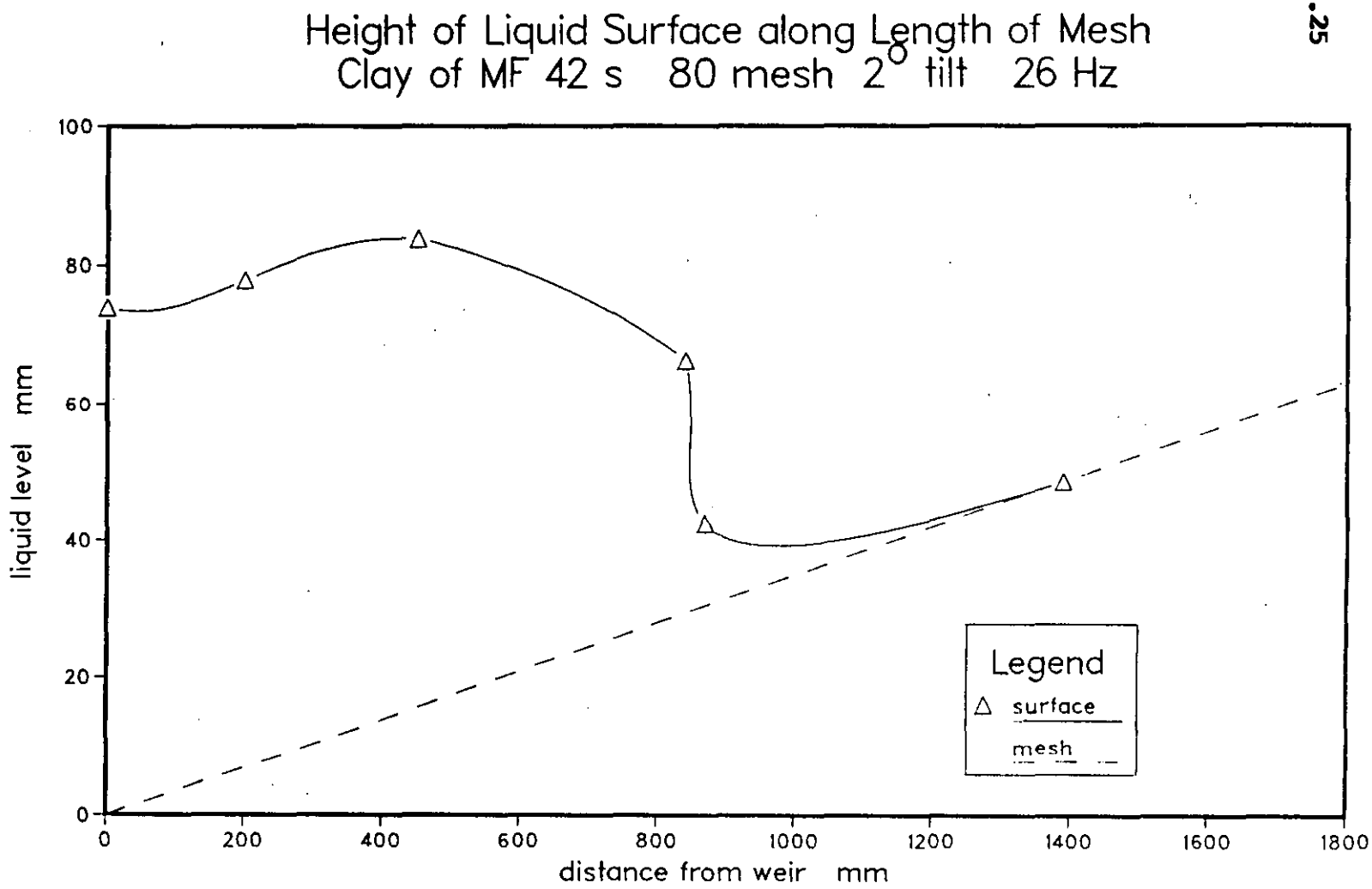
Height of Liquid Surface along Length of Mesh
Clay of MF 42 s 80 mesh 2° tilt 26 Hz
liquid level mm
distance from weir mm
0
20
40
60
80
100
0
200
400
600
800
1000
1200
1400
1600
1800
Legend
surface
mesh

Figure 6.25

7 FLUID FLOW THROUGH SCREENS: DISCUSSION

7.1 The Work of Hoberock

Hoberock (1980) created a computer model of fluid flow through a near-horizontal downward-sloping screen, oscillating (simple harmonic motion) normal to the plane of the screen. The fluid flow along the screen was taken from Chow (1959) for flow down a channel with a gridded base. The flow through the screen was considered as through a thin filter, using the formulae of Armour and Cannon (1968) to convert mesh dimensions to a conductance. Values of conductances for common oilfield screens were tabulated (Hoberock 1981b). This formula envisaged the flow as equivalent to creeping flow through an array of regular spheres. Hoberock took the drilling mud to be a Bingham Plastic and added a drag force due to the yield value of the fluid to the resistance specified by Armour and Cannon.

The driving force was considered to be a hydrostatic head, being the product of the fluid depth, the fluid density and the effective gravitational field. This field was the algebraic sum of gravity and the screen acceleration at any moment in time. The flow was therefore summed over one cycle of the screen motion, with the proviso that during any period when the gravitational field was less than zero, then there was no flow - i.e. reverse flow did not occur.

The screen was considered in narrow strips, starting at the feed end, with the greatest depth of fluid. An incremental procedure (Runge-Kutta Marching technique) was then used to calculate flow for each strip in turn. This terminated when the liquid height was 5 times the screen thickness. A simple extrapolation was then used to bring both film thickness and fluid flow to zero, giving the total length of screen in use.

It may be noted that to calculate flow through the screen, the mesh was considered to be horizontal. However, the tilt of the screen was used to calculate fluid flow along it. This was modified for screen motion by finding the net velocity of the fluid relative to the screen throughout the cycle to calculate the momentary Reynolds number. This then gave the momentary friction factor for flow along the screen, after Chow (1959). The average value over the cycle was used.

The model as originally presented (1980) only dealt with significant downward slopes. However, the majority of flow-rate curves presented for user guidance were for a horizontal screen with a circular motion of frequency 20 Hz and 6 **g** acceleration. The final paper (1982d) gave curves for a 100 mesh screen with an adverse slope of 1^{o}, 2^{o} and 4^{o} to show that this required a shorter screen length than a downward tilt of 15^{o} for the same flow capacity. There was no comment as to how the channel flow portion of the model was altered to deal with an upward slope, but the author said "the results....represent only suggestions as to what may be possible." (1982d).

The model curves of flow-rate versus screen length were paraboloid: that is, they suggest that flow-rate is proportional to screen length to the power 2. (Samples from the graphs gave values from 1.99 to 2.2.) The model curves all go through the origin, but the experimental curve for the finest mesh and flattest deck (given in Figure 6.21 of this thesis) showed no measurable flow for the first measured mesh length, 8 inches (0.2 m). In this respect, Hoberock's own data include a result at odds with his model, but in agreement with the present author's observations.

In explaining how to use the curves, Hoberock (1982a) gave an example where for a given width of shaker, screen mesh and mud properties the nearest curve was used to estimate the length of screen required. He then said this should be doubled to allow for 50 % blockage of the mesh. He then added 25% to allow a dewatering area (arbitrary but as good a guess as any) and suggested that a sufficient number of screens should be specified to give at least that total length. These suggestions do not, however, accord with the second-order dependence. Thus, for example, the equivalent of a single length of 100 inches would be met by 4 units of 50 inches, not 2 as he suggests (1982a). Similarly, with an even distribution of blockages, a screen with 50% blockage would require 1.414 times the length of an unblocked one, not twice.

The present author's opinion is that a better technique would be to work backwards from a commercial unit (supposing that, say, only 2/3 of the width and 3/4 of the length were actually available) and calculate its capacity, then multiply to the total flow-rate required.

Model curves were given (1982a) on the effect of mud weight, plastic viscosity and yield point on the flow versus length curve (horizontal 100 mesh screen, 20 Hz). By taking measurements from these curves, the present author concluded that volumetric flow-rate was virtually proportional to mud weight (density), and that a unit change in plastic viscosity was equivalent to about 4 units change in yield point. The effect of increased mud weight is to increase the driving force, so this result is reasonable. The rheological effect will be discussed in the light of other work in the following section.

It was implicit in the model that frequency would have only a small effect, but that increased acceleration would always mean increased flow. Hoberock's model curves showed such effects, and his limited experimental results did not contradict them. The present thesis supports the first contention, but not the second. That is, frequency has been shown to be of minor effect, but acceleration produces a non-linear response, with rapidly-diminishing returns. This can be accounted for by modifying his description of flow during oscillation, as will shortly be shown.

The concept of conductance was crucial to Hoberock's model, and his tabulated values have since been quoted by manufacturers. He stopped short of saying that flow was exactly proportional to conductance, but strongly implied that it was nearly so (1982d). However, his experimental results only give the same fluid on two different screens (at two different tilts). Measurements from his graphs indicate that a 66% increase in conductance gave between 115 and 130% increase in flow-rate. The present author's work with screens of similar conductance but different hole size found a 4% increase in conductance associated with a 33% increase in flow-rate. Therefore conductance has not been shown to be a simple predictor of relative flow capacity for different screens. An alternative approach is proposed in section 7.3.

7.2 The Work of Cagle and Wilder

In 1978, Cagle & Wilder presented a paper at the Drilling Technology Conference, Houston. This was adapted and published simultaneously in almost identical form in the 'Oil and Gas Journal' and 'World Oil' (1978a; 1978b).

The work reported was an empirical comparison of the fluid flow capacities of two different designs of shale shaker, and of a new style of screen. It was carried out on full-scale apparatus, using a total of 10 muds. In addition test were made in the field at two sites. (Some measurements on solids separation were added by Cagle in 1981.)

The muds were described in the normal industry way as Bingham Plastics, defined by a plastic viscosity **PV** and yield point **YP** from a Fann viscometer. No model was produced, but the authors observed that flow capacity was strongly dependent on plastic viscosity, and proposed a straight line fit for a graph of log(flow-rate) versus plastic viscosity. They also asserted that there was a great increase in flow capacity of screens for plastic viscosities below 10 cP. For example, for **PV** 6.5 cP the straight line would predict of the order of 800 US gallons per minute, whereas the experimental value was 1580 US g.p.m..

The present author's analysis of the results in the light of those of Hoberock (see previous section) found a simpler fit to the data by plotting on a linear scale flow-rate versus $(PV + 0.25YP)^{-1}$, where **PV** and **YP** are the plastic viscosity and yield point respectively, in the usual industry units of cP and lb/100 ft^2. This is shown in Figure 7.1, below. Further, by supposing that flow-rate was proportional to mud density (assuming unweighted muds to be 9 lb/US gallon) then the weighted muds approached the same correlation. This relationship is not only more plausible than the log-linear fit, it is also more practical, since it has the quantity to be predicted on a linear scale. There was no difference between dispersed and non-dispersed muds. However, the two polymer muds detailed showed exceptional behaviour: the one with both low **PV** and **YP** gave a flow similar to an enormously viscous clay, whereas the more viscous polymer gave a very high flow rate. If the data are correct, this illustrates the importance of the shape of the rheogram as well as its value at two arbitrary points.

The correlation does not extend to the low viscosity datum (where the predicted value would be 850 US g.p.m.), but is no worse than the log plot. It is contended that this anomalous behaviour is likely to be due to the combination of fluid rheology and screen dimension (not just the former as Cagle & Wilder suggest) - i.e. it indicates a different character of flow, as will now be discussed.

Figure 7.1 Data of Cagle & Wilder for Flow of Various Muds Through a Shale Shaker with a 100 Mesh Screen.

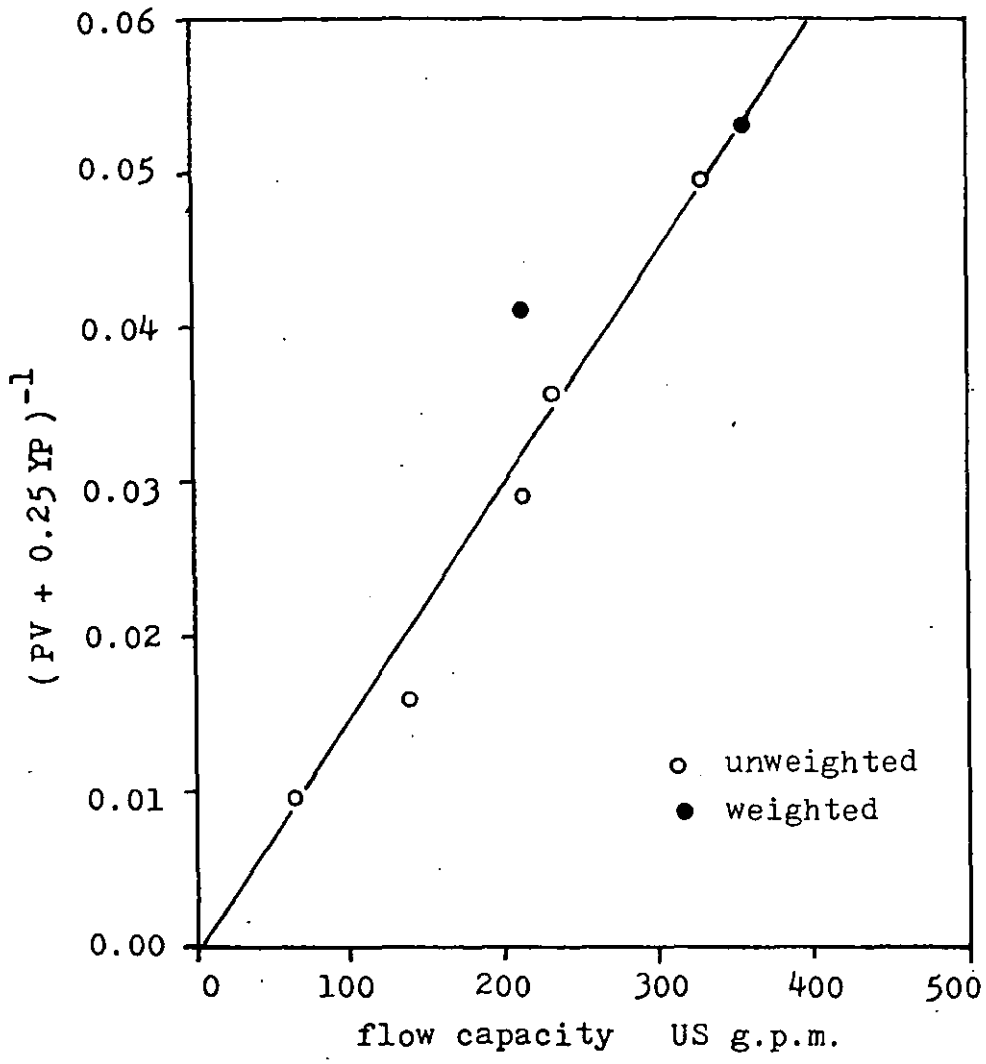

7.3 Factors Determining the Rate of Flow Through Screens

7.3.1 Character of Flow

To arrive at an appropriate model for the resistance to flow due to the screen mesh, it is necessary to determine the probable flow regime. For this purpose, the mesh will first be considered stationary in an infinite fluid passing through the mesh at a rate as was found experimentally. The mesh will then be supposed to move at a rate and motion similar to the main rig, without affecting the fluid and its velocity relative to the fluid determined.

The definition of Reynolds Number requires a velocity, a characteristic dimension and a viscosity (or its equivalent in the generalized form). For flow normal to and through a mesh, Weighardt (1953) made the reasonable suggestion that the velocity to be taken is the average one through the open area, and this has been generally adopted. He treated the mesh as a set of independent cylinders. However, Armour and Cannon (1968) took this velocity and visualized the mesh as an array of spheres for laminar flow, and an array of tubes for turbulent flow. They defined the Reynolds Number on the basis of a tube, which for plain square mesh had a dimension equal to the mesh aperture.

Taking this approach for the experimental work reported in this thesis, then for XCD on an upward tilted 100 mesh screen, the maximum flow rate for 4^{o} tilt was 11.7 $dm^3\ s^{-1}$. The working mesh was 0.8 m^2, with an open area of 31%. Hence the mean velocity was:

$$v = 11.7 \times 10^{-3} / (0.8 \times 0.31) = 0.047\ m\ s^{-1}.$$

The generalized Reynolds number for flow through a tube can be expressed as (Metzner & Reed 1955):

$$Re_g = \frac{d^n\, v^{2-n}\, \rho}{\left(\frac{k}{8}\right)\left(\frac{6n+2}{n}\right)^n} \qquad (26)$$

Insofar as this fluid can be roughly approximated to a Power Law, values of n the Power Law index and k the Power Law factor are 0.3 and 2.0 respectively. For d the mesh aperture of 0.142 mm is taken. For ρ the density of water 1000 kg m^{-3} is taken. This gives Re_g equal to 0.72.

Chhabra & Richardson (1985) considered non-Newtonian flow through a static mesh in terms of the drag around the wires. In this case the wire diameter was the critical dimension, and the velocity was as before. They defined a Reynolds number as:

$$Re_{NN} = \frac{d^n v^{2-n} \rho}{k} \qquad (27)$$

The use of this Reynolds number definition based on wire diameter of 0.112 mm gives a lower value still, of 0.19. An assumed effective viscosity of 15 cP gives a value of 0.44 for the ordinary Reynolds number.

Now consider the motion of the mesh wires. For the maximum 32 Hz, and a circular motion of 1 mm radius, the wire velocity is 0.20 m s^{-1}. The Reynolds number according to Chhabra and Richardson would be 2.25. At a more usual frequency it would be proportionately less.

Since these calculations were based on high values, it can be taken that the work reported in this thesis generally represents Reynolds numbers of the order of 1 or less. Hence the character of the flow was creeping, and resistance to flow was predominantly due to the drag surface, not shape (Becker 1959). Moreover, inertial effects may be neglected compared with viscous ones (Happel & Brenner 1965). (However, a calculation for water flow through the coarsest screen gave a Reynolds number of 66. Hence it is possible with less viscous fluids and/or coarser mesh to move to a different flow regime. This is presumably the effect observed by Cagle & Wilder for low-viscosity mud - see previous section.)

Some idea of the shear-rate can be got from the well-known expression (e.g. Skelland):

$$\dot{\gamma} = 8 v / d \qquad (28)$$

For the fluid and mesh as before, this gives a shear rate of 2648 s^{-1}. For the same fluid through 150 mesh, the flow-rate under the same conditions was 8.8 dm^3 s^{-1}. Hence the velocity was 0.032 m s^{-1} and the wall shear rate was 2614 s^{-1}.

These values are comparable with those found for the Marsh Funnel, which supports the idea that Marsh Funnel time has some validity as a measure of viscous properties on the screen. Moreover, since the values are very similar, it may be asserted that the effective viscosity was virtually the same in both cases.

7.3.2 Screen Resistance

The usual representation of resistance to fluid flow caused by solid bodies is in terms of a drag coefficient or friction factor, which is somehow related to the Reynolds number. This coefficient generally indicates that the applied force is proportional to the square of the fluid velocity.

In the previous section, two Reynolds numbers have been defined. The first case was the flow of fluid through a static mesh, where the applied force comes from a pressure drop. In the second case, the drag comes from regular motion of the mesh through the fluid, and the drag coefficient would define the force required to sustain such motion - i.e. the power output of the vibrator. What is in fact wanted is a measure of the resistance to flow of the moving screen, which cannot truly be equated to either description.

At low Reynolds numbers, drag is inversely proportional to Reynolds number: Chhabra & Richards (1985) have shown this to be the case for Reynolds numbers up to 5 for Power Law fluids passing through woven metal meshes. It may therefore be taken to apply to the present study. The Reynolds number for screen motion is several times that for fluid passage, so it might be argued that the effect of oscillation is to reduce the effective drag and thus the flow resistance. However, the evidence of this thesis is that any such reduction is negligible for a viscous Newtonian fluid. Thus it cannot provide a sufficient explanation for changes in flow-rate of 10 or more times observed with shear-thinning fluids.

Hoberock (1980) claimed that increasing acceleration always increased flow capacity (i.e. reduced screen resistance), which in the limit would give zero resistance. This is not plausible, and in the present work it was instead found that flow capacity and hence screen resistance tended to a constant value at 2 to 3 gravities. It is therefore proposed that for the range of properties and meshes used in screening of drilling fluids, each screen has a finite minimum resistance to the passage of fluid. Screen oscillation may be said to overcome the reluctance of fluids with high viscosities at low shear rate to pass through small holes (as will shortly be discussed) but does not remove this minimum drag.

Present evidence is that well-managed shale shakers probably operate fairly close to minimum screen resistance. Hence a definition of this resistance would be of practical value (to predict the flow capacity of different meshes) even without a complete model for how the increased flow is achieved.

There are currently two definitions of screen resistance (or rather its reciprocal) in use. A third will now be proposed.

[1] The most widely quoted measure of a screen is its open area. It is traditionally assumed (Hoberock 1982d) that flow capacity is proportional to open area, and this is in fact explicitly stated in a machine patent (Krynock & Ruhe 1973) and manufacturer's literature (Swaco 1975). Frankly, this is a mis-application of a formula appropriate to dry screening (e.g. Gluck 1965). By any hydrodynamic reasoning it cannot be so, and field experience is that finer screens give lower flow rates. Nevertheless, manufacturers invariably quote percentage open area.

[2] Williams & Hoberock (1982) introduced to mud screening the concept of 'conductance' originated by Armour & Cannon (1968). This essentially views a screen as a thin filter obeying Darcy's Law. The conductance is the permeability divided by the screen thickness. Armour & Cannon produced formulae for calculating values from the geometric properties of the mesh, and Williams & Hoberock produced tabulated values for common styles and sizes of shale shaker screens. Under the same conditions, flow rate should be proportional to conductance. The data is thus easy to use, and evidently more sensible than open area.

[3] Going back to Weighardt (1953), the present author proposes that the surface area of the wires making up the mesh should be taken as the criterion. For a square mesh of N_m wires per inch (mesh count) of diameter d_w microns, the surface area of the wires per unit area of mesh is proportional to $N_m^2 d_w$. As these are the ordinary basic specifications, this quantity, the **screen resistance coefficient**, can be readily calculated. The flow capacity of different screens under the same conditions is then taken to be proportional to the reciprocal of this coefficient, which may be named the **specific conductivity**. For the common case of a screen with a support mesh, the resistances are added, and the overall reciprocal taken. This would apply to ordinary layered screens, but for special designs there may need to be a correction for the way in which one layer may 'shadow' another.

7.3.3 Fluid Properties

For a fluid upon a near-horizontal mesh, increased **density** will give a greater pressure on the mesh, thereby increasing the driving force and hence the volumetric flow-rate through. **Surface tension** is important insofar as it is necessary for the liquid to wet the mesh, but a low surface tension is liable to give rise to problems with foam formation. However, the key property must be **viscosity**, here considered to be non-Newtonian.

Take the case of a fluid with a yield stress, static above an aperture in a horizontal sheet, where the aperture is approximately equivalent to a vertical tube. A force balance shows that equilibrium the hydrostatic pressure is balanced by the shear stress at the wall of the aperture. If this value is less than the yield stress of the fluid, then no flow will occur. If it is greater then plug flow will occur. Thus there is a minimum head (corresponding to the yield stress) required for flow to be initiated.

For higher pressures then the flow rate will increase as the head above this minimum value. The relationship between excess head and volumetric flow-rate is difficult to determine exactly even for the simplest fluid models (Wilkinson 1960). However for shear-thinning fluids (such as the Bingham Plastic, or Herschel-Bulkley fluid) of properties such as might be found in drilling muds, then an approximate relationship would be expected of the form:

$$\text{flow-rate} = x\,(\Delta P - \Delta P_{min})^{y} \qquad (29)$$

where ΔP is the differential pressure; ΔP_{min} is that required to initiate flow; **x** is a constant for a given tube and fluid; and **y** is an index something less than unity.

If the aperture is not an ideal tube, then this relationship will be further modified. Moreover, it is generally accepted that a true yield stress does not exist in actual fluids commonly represented by Bingham behaviour. In practice, a small amount of flow will occur even where the notional yield stress is not exceeded.

However, for the qualitative description which follows it is convenient to accept equation (29) with the power **y** being unity. In the conceptual model it is easy to see how the results would need to be corrected for a degree of curvature, but the important point is that it provides an explanation in accord with observed behaviour. Exact values may be found empirically.

7.3.4 The Effect of Oscillation

It has been demonstrated in section 6.3.2 that the vertical component of motion is the controlling one. Therefore consider a horizontal screen with liquid passing through due to a head of liquid h_o upon it. For fluid in Poiseuille flow passing through holes the wall shear stress is proportional to h_o. Now suppose the screen is oscillated vertically in a sinusoidal fashion. Alternatively it might be moved in a circular path which is the equivalent of phased sinusoidal motion in both the vertical and horizontal planes.

Figure 7.2 Variation of Stress During One Cycle of a Vertically Oscillating Horizontal Screen

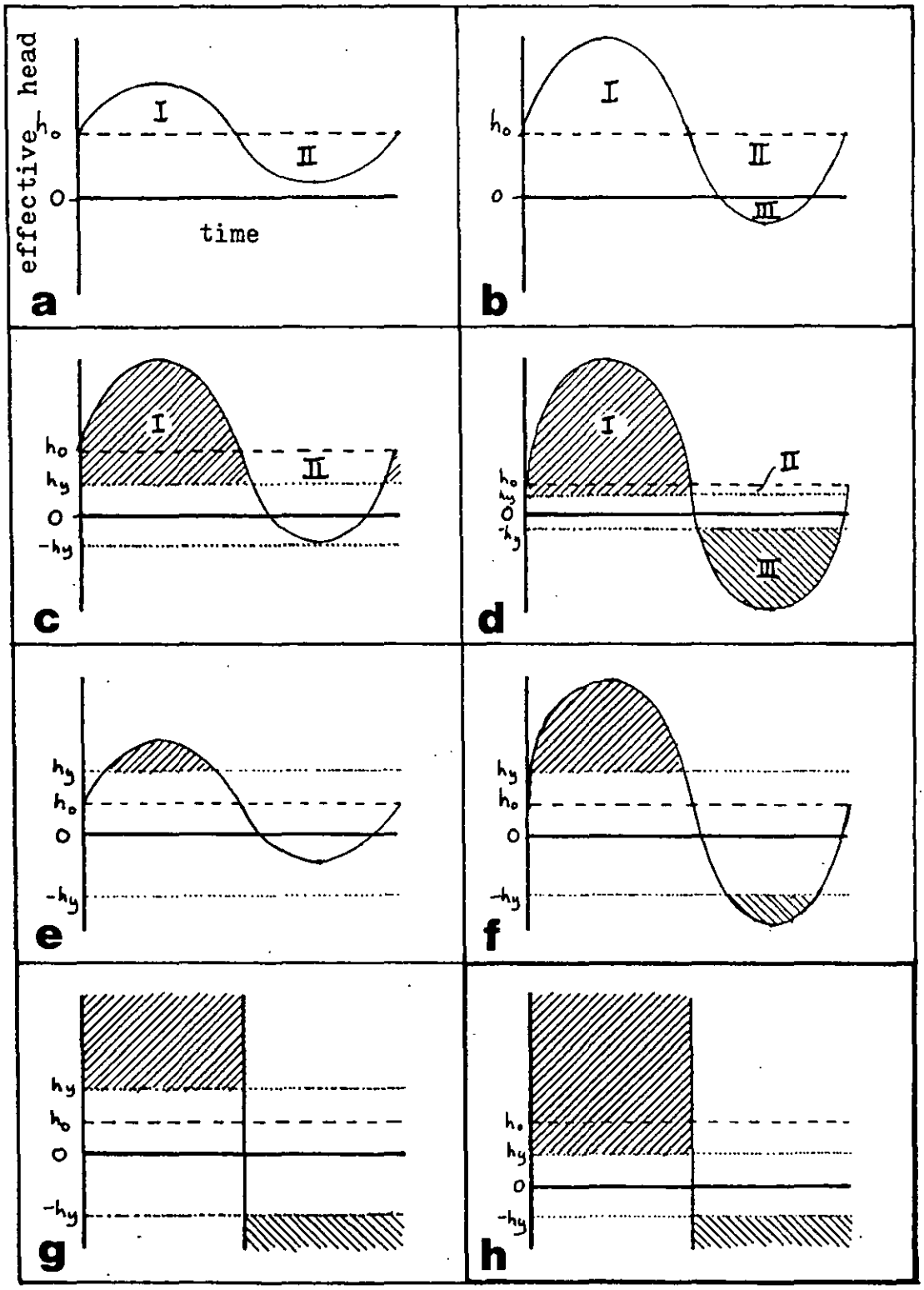

see text for legend

For such motion the screen is subject to a cyclic acceleration, which may be considered to vary the relative gravity field, which is the equivalent of varying the effective head, as shown in Figure 7.2(a). For half the cycle the head is increased, and for half it is reduced. The areas I and II are equal. For laminar flow of a Newtonian liquid through a pipe, the flow-rate is proportional to the wall stress. Taking this to be approximately true for flow through a mesh, then the effects of I and II cancel out, and flow is not markedly affected by oscillation, as was found experimentally.

[**Note:** from the correlation of Grootenhuis (1954) for air flow through wire gauzes, the present author calculated that the product of the resistance group (friction factor) and Reynolds number was approximately constant ($\pm$ 30%) over the range Re = 0.05 to 5. Recently Chhabra & Richardson (1985) have shown for the flow of liquids through square meshes that the product of a similar resistance group (drag coefficient) and the Reynolds number is approximately constant over the range Re = 10^{-5} to 5. These results indicate a flow rate proportional to stress for Newtonian fluids through meshes.]

Figure 7.2(b) illustrates the case where the applied acceleration exceeds 1 gravity. For the portion marked III there is effectively negative head on the screen. Hoberock (1980) assumed that under such circumstances the flow would be zero, but it is also possible to suppose that liquid flows upwards from beneath the screen. In the former case, total flow during the cycle would be increased, and would continue to increase with higher peak accelerations. For Newtonian fluids this means that flow through the mesh would not be increased by oscillation of less than 1 g peak acceleration, but would increase thereafter. Experimentally this did not occur to any appreciable extent (see section 6.3.1). Thus the evidence is that during the negative head part of the cycle, fluid from a layer beneath the mesh moves back upwards. This is reasonable if the frequency of oscillation is such that the layer underneath does not have time to detach. Excessive negative flow would be expected to draw in air, accounting for the bubbles which were actually observed.

Figure 7.2(c) illustrates the condition when the fluid has a yield stress. It is supposed that there is a minimum head h_y required for the wall shear stress to match this, so no flow occurs for any lesser effective head. In this case the static head $h_o > h_y$, so there is flow. Under oscillation the flow is represented by area I, but the net improvement must take account of the area II (above the h_y line) which is lost flow. In order to get negative flow, the applied acceleration must also overcome a yield stress in the opposite direction. That is, for effective heads between h_y and $-h_y$ the flow is zero.

Figure 7.2(d) shows a cycle with a peak acceleration of several gravities. If negative flow is permitted, then it is clear that the net positive flow is represented by the difference between the two shaded areas. It is further obvious that increasing the amplitude will affect both positive and negative flows, and will thus only marginally alter the net flow-rate. this is in agreement with the results reported in this thesis, but contrary to Hoberock's model.

Figures 7.2(e) and 7.2(f) illustrate the case where $h_y > h_o$ giving zero flow under static conditions, as was essentially observed for XCD on 150 mesh (see section 6.4.2). No flow occurs until the effective head is in excess of h_y for part of the cycle. The flowrate then increases with acceleration until a head of $-h_y$ is reached during the negative part. Thereafter negative flow occurs for part of the cycle, so there are diminishing returns on net flow for higher accelerations. These limits correspond to accelerations of $(h_y/h_o - 1)$ gravity and $(h_y/h_o + 1)$ gravity. Thus an optimum acceleration might be proposed as about 2 gravities more than that required to get observable flow.

As an example, take XCD through 150 mesh at 4^o tilt. Measured flows were: at 13.8 Hz, zero; at 15.3 Hz, 0.2 $dm^3\ s^{-1}$. (This corresponds to 0.94 **g**.) An increase of one gravity gave 22.7 Hz and a flow of 7.1 $dm^3\ s^{-1}$. An increase of a further gravity gave 28.0 Hz and 8.6 $dm^3\ s^{-1}$. Only a tiny increase to 8.8 $dm^3\ s^{-1}$ was observed for higher accelerations.

Figures 7.2(g) and 7.2(h) illustrate the limiting situation of very high accelerations for $h_y > h_o$ and the reverse. Each shows an infinite sine curve symmetrically truncated about its median, the h_o line. By symmetry, the excluded areas cancel out. In both diagrams the net positive flow area is identical to the area under the h_o line. Thus in a simplistic fashion, the effect of large accelerations can be said to obviate the fluid yield stress. Furthermore, this represents a limit to the flow which can be achieved. Once a substantial fraction of this value has been obtained there is little advantage in further acceleration.

It is interesting to take the special case where $h_y = h_o$ since this permits some simplified calculations. Taking the approximation that flow is directly proportional to the stress in excess of the yield stress, then the areas under the sine curves can be calculated. For zero applied acceleration, flow is incipient. It increases linearly with acceleration up to 2 **g**, when it is 64% of the limit. Thereafter the flowrate increases at a lesser and lesser rate, tending towards the limit. It is 78% at 3 **g**, 84% at 4 **g**, 88% at 5 **g** and 94% at 10 **g**.

7.3.5 Prediction of Flow Capacity

A complete model of mud screening would permit the prediction of the liquid capacity of any specified screen and operational conditions for any mud of measured properties. A lesser but more practical target would be to predict the effect of varying mud properties or screen tilt or screen mesh, where the other two remain constant and where the vibration is near optimum. This would have great benefit in the field. For example, if a shale shaker is performing at less than full capacity then it would be often be advantageous to change to a finer screen (to remove more solids) if this did not risk overflowing. Similarly, where mud properties and/or flow-rate are to be changed for down-hole needs, it would be helpful to know what change if any is required for the screen to continue to process full flow. The present thesis offers the following guidelines.

Mud Properties. It is proposed that **density** increases volumetric flow-rate. Further evidence is required, but for the present a simple proportionality is suggested - e.g. 10% increase in weight gives 10% greater flow. Note that this is the density of the mud plus cuttings above the screen giving a flow of mud minus cuttings (different density, different flow-rate) below the screen.

For muds of a similar class it is proposed that a single value for the **viscosity** can be taken, using one of 3 criteria. The **Marsh Funnel time** can be used as a guide, providing it is the excess time over 26 s for a litre (see section 7.3.7). The **Fann viscometer** readings can be used, taking the formula **(PV + 0.25YP)**. Alternatively, the **apparent viscosity** at around 2500 s^{-1} may be used. In each case flow is inversely proportional to this value. It has been shown that different rheologies give a similar relationship between screen tilt and screen capacity where the Marsh Funnel times are similar. The two examples given by Cagle & Wilder suggest that clear polymer fluids may be significantly different from clay fluids of the same measured properties, but this might reflect a problem of measurement.

(These definitions of viscosity would give different numbers, so they should not be mixed. Reliable data is not currently available to determine how they could be interconverted, but in principle it should not be difficult to accumulate in the field.)

Screen Tilt. For a given fluid and screen there is a certain flow capacity for the horizontal case. (For fine screens and fluids of high yield stress this may be virtually zero.) Upward tilts increase this capacity according to the square of the angle, thus the maximum angle should be used. (A 10% increase in tilt would give 20% increase in capacity.) However, the practical limit is the need to convey solids, which is the controlling factor. (This is discussed in chapters 8 and 9.)

The relationship between tilt and increased capacity may be expressed as a parabolic equation of the form:

$$Q = Q_o + c_a \theta^2 \qquad (30)$$

where Q is flow capacity, Q_o the capacity at zero tilt, θ the angle of adverse tilt, and c_a a constant dependent on both mud and mesh. More data would be required to get a complete expression for c_a, but it may be observed that it is small for combinations of high viscosity and coarse mesh, larger for either low viscosity or fine mesh. For combinations of high viscosity and fine mesh, Q_o can be virtually zero.

Screen Mesh. For the situation where there is a useful flow and machine conditions are near optimum, it is proposed that the flow is inversely proportional to the exposed area of the wires, which is itself proportional to $N_m^2 d_w$, where N_m is the number of wires per inch and d_w is the wire diameter.

For other circumstances particularly where flow is minimal, the relationship between screen and fluid properties and flow rate is clearly complex. However, it appears likely that certain minima may be established for the horizontal screen. For example, given a certain fluid and fixed screen length, there is a certain minimum hole size below which flow is negligible. Conversely, a certain minimum screen length may be required to build sufficient head for significant flow for a specified mesh and fluid. Thereafter the parabolic rule applies.

7.3.6 Test of Predictions

The work of Hoberock and of Cagle & Wilder was drawn upon to test the predictive power of the proposals given in the preceding section.

Hoberock (1980) provides experimental data (flow-rate versus length) for the same fluid through two different screens, namely 60 mesh and 100 mesh, at -10° and -30°. By measurements on his graphs, the 100 mesh screen was found to permit a flow-rate between 0.445 and 0.50 of that of the 60 mesh screen. The 100 mesh actually had a greater percentage open area, so using this as a basis would predict 1.09 times the flow. His quoted values for conductance predict 0.60 times the flow. The expression $N_m^2 d_w$ also predicts 0.60 times the flow. In this case, both conductance and wire surface give an over-estimate of about 25%, which is much better than the open area criterion.

In the present thesis, the same fluid (XCD) was passed under the same conditions through fresh clean 100 and 150 mesh screens. The prediction on the basis of open area would give the 150 mesh as 0.90 of the flow-rate of the 100 mesh. The prediction on the basis of conductance would be 0.96. The prediction on the basis of $N_m^2 d_w$ would be 0.75. The values found were as follows:

Table 7.1 Relative Flow Capacity of 150 and 100 Mesh Screens for XCD MF 40 s at 25 Hz

angle degrees	1	2	3	4	5	6
ratio	0.25	0.53	0.72	0.74	0.66	0.80

Note that the parabolic curve suggests virtually zero flow for the 150 mesh when horizontal. However, for tilts greater than 2° the ratio is reasonably fitted by the $N_m^2 d_w$ prediction.

Cagle & Wilder (1978b) gave results for actual drilling operations where the screen and the mud were varied. This is the only set of field data known to the author to be complete enough to allow testing in the following manner. It was supposed that each screen specified was reasonably well loaded. The flow-rate given for the first (coarsest) screen was then used to predict a flow-rate for subsequent screens, using $N_m^2 d_w$ for the screen resistance, **(PV + 0.25YP)** for the mud viscosity, and supposing flow proportional to density to correct for mud weight. The results were as follows.

Table 7.2 Comparison of Predicted and Actual Flow-Rates in the Field (Cagle & Wilder 1978b)

mud properties			mesh specifications		flow-rate USgpm	
PV	YP	MW	N_m	d_w um	pred.	actual
8	14	9.3	50	285	410	410
10	10	9.3	38	376	495	420
12	6	9.4	50	285	353	367
14	6	10.3	70	206	**237**	314
12	7	10.6	50	285	391	380
42	5	16.5	100	114	**121**	152
42	6	17.0	100	114	**124**	152
44	7	17.6	70	206	138	145
38	8	17.9	70	206	160	163

The results are sufficiently close to support the model, remembering that this was an actual drilling operation, not a test of screen capacity. Thus the actual flow-rates were set for the down-hole needs, and screens were fitted according to site judgment. The most serious discrepancies (shown in **bold**) are underestimates, but these are immediately followed by the fitting of a coarser screen. It is surmised that they coincide with a screen close to overloading, and may actually represent practical limits.

7.3.7 Use of the Marsh Funnel Viscosity

In section 6.4.1 it was noted that the relationship between screen tilt and flow rate seemed to be represented by a set of curves dependent upon Marsh Funnel time. Remarkably, the evidence suggested that very similar curves would apply for fluids of different rheology but the same Marsh Funnel time. The experiments did not cover a wide enough range to establish this as a definite general principle, but it is worth considering, since even an approximate match would be of great practical benefit. In fact, it would enable the creation of a standard set of curves for each mesh which predict fluid capacity for any combination of tilt and funnel viscosity - i.e. graphs such as 6.12 and 6.13 at intervals of (say) 2 seconds for times from 32 to 64 seconds.

It was shown above (section 7.3.1) that an estimated wall shear stress for XCD passing through 100 mesh was of the order of 2600 s^{-1}. It is shown in Appendix 1 that the mean wall shear stress for the same fluid in a Marsh Funnel was about 94000/40, where 40 is the efflux time in seconds. This gives about 2400 s^{-1}. In view of the different geometries and uncertainties, this is a reasonably good match. Furthermore, the screen shear rate is virtually the same for the 100 and 150 mesh screens. In fact, using the screen resistance model above, a predicted flow capacity for a coarse 40 mesh screen under the same conditions was 2676 s^{-1}. Thus for a given fluid the screen shear rate is approximately constant over the range of meshes in commercial use.

This suggests that for a set of meshes from one manufacturer, in a series of dimensions which progress in a conventional way (mainly based on mechanical requirements) then there is an important element of similarity in the flow of a given liquid, and the Marsh Funnel time is an approximate measure of this factor.

It is shown in Appendix 1 that the time taken for liquid to flow out of the Marsh Funnel may be considered as the sum of two times, one of 26 s for the inertial requirements, and the remaining time for the viscous element. The second portion, which may be described as the **excess time** (i.e. in excess of 26 seconds) is for Newtonian fluids proportional to the $(\text{viscosity})^{0.87}$. As inertial effects are negligible in the flow of fluid through the screens considered (as shown in section 7.3.1) then this excess time may be approximately taken as a measure of the reluctance of the fluid to pass through the mesh. The calculations given in Appendix 1 suggest that this would allow changes in Marsh Funnel time to be matched to changes in flow capacity, where a given mud was deteriorating or being modified. However, the same Marsh Funnel time would not guarantee the same flow capacity if a mud was replaced with another of a different type.

It is therefore proposed that the Marsh Funnel excess time can be used to quantify the relationship between mud properties and screen capacity as a useful field approximation during drilling. It should be possible to predict the effect of changes of screen mesh, screen tilt, and mud rheology, providing the type of mesh and of mud are not altered. The prediction cannot be expected to be exact, but gives a quantitative result where there presently is none, using the simplest possible measurement.

7.4 Flow Across The Mesh

Flow along an upward-tilted screen may be considered as an open channel with steady but non-uniform, spatially-varied flow. So far as can be ascertained, this has not been mathematically described, even for solids-free Newtonian liquids in the absence of vibration, though Chow (1959) derived expressions for downward-sloped gridded channels, and French (1985) has given some attention to flow up adverse slopes.

Experimentation has shown that the liquid surface cannot in general be approximated to a horizontal plane, and in some circumstances may not even be close to a tilted plane. In particular, the liquid depth may vary considerably over a short distance, which may tentatively be ascribed to a **hydraulic drop**, being the reverse of the more commonly known hydraulic jump in open-channel flow.

To determine if this explanation is tenable, it is necessary to make an estimate of the Froude Number for the flow. This dimensionless group is defined as:

$$Fr = v\, d_h^{-0.5}\, g^{-0.5} \qquad (31)$$

where v is the linear velocity, d_h is the hydraulic depth, which for a wide flat channel is the mean depth, and g is the acceleration due to gravity. A Froude Number of less than one is associated with so-called **tranquil flow**, a value greater than one indicates so-called **rapid flow.** In the former case gravitational forces predominate over inertial ones, whereas the reverse is true for rapid flow. A hydraulic jump is obtained by placing some kind of restriction in a channel with rapid flow such that kinetic energy is lost and the Froude Number falls below unity. This results in the same flow-rate being carried at a lower velocity but with a greater depth, so that the liquid level actually rises in the direction of flow.

It is here proposed that the situation shown in Figure 6.24 and the section given in Figure 6.25 depict a hydraulic drop: i.e. a tranquil flow at the rear, changing in a short distance to rapid flow at the front. (The surface rollers visible in the transition are also observed in hydraulic jumps.)

It is supposed that fluid moving along the screen has forward momentum. Mass is lost by passage through the screen, but little or no momentum, because the direction is normal to the flow. Therefore the velocity of the fluid would increase (less an allowance for frictional losses). At the same time, the liquid level falls and the base of the channel (the screen) rises, so the hydraulic depth decreases until the Froude Number approaches the critical value, at which point there is a switch to rapid flow with a consequent further increase in velocity and reduction in depth.

In the case given it is estimated that the velocity of the fluid at the rear was 0.375 m s^{-1}. For a depth of 73 mm, as measured, this gives a Froude Number of 0.44. For the same velocity at the depth of 37 mm just before the transition, the Froude Number would be 0.66. However, if there had been any increase in velocity due to conservation of momentum, the Froude Number could approach unity.

The profile given in Figure 6.25 would be expected to assist fluid flow because it permits a greater head of fluid on the mesh at the rear. However, in the presence of solid such advantage might be outweighed by the tendency of tranquil flow to stratify. That is, solids can partially settle to the floor of the channel, in this case forming an obstruction. It seems that rapid flow, in which the flow tends to be homogeneous, would be preferred for the flooded portion of the mesh.

The difference in appearance of the liquid surface at the front and rear is believed to be due to the depth rather than the flow regime. Nicoll, Strong & Woolner (1968) showed that for a porous plane oscillating in an infinite fluid, then the disturbance of the fluid was limited to a definite distance from the plane. This distance was increased as the square root of liquid viscosity. The distance was reduced by mass transfer through the plane, away from the side under consideration.

The hypothesis is therefore made that an agitated surface results when the disturbance due to the screen propagates a greater distance than the liquid height above the screen.

It was observed that a smooth surface could be changed to an agitated one by the addition of a heavy load of solid. This might effectively increase the liquid viscosity, but it is even more likely to reduce flow through the screen and thereby increase the envelope of disturbance. The transition shown in Figure 6.8 at about 35 mm is also associated with a change in surface from a smooth one at higher levels to an agitated one at lower levels. It may be concluded that flow enhancement is maximum when the mesh disturbance is absorbed within the fluid, and less effective when it is dissipated by ejecting material from the upper surface.

7.5 Further Work

The results reported above may be extended both theoretically and practically. So far as the practical work is concerned, it would be beneficial to have field data to confirm if the prediction in section 7.3.5 is generally applicable.

On the theoretical side, more experimental data are required from the small rig (a programme is under way) to fully substantiate the physical model proposed in section 7.3.4. In particular it would be valuable to eliminate the bubble problem, and to relate flow to acceleration and rheology for several fluids. This should enable a more precise mathematical model to be produced for non-Newtonian fluid passing vertically through an oscillating horizontal mesh.

It would then be necessary to extend this to the tilted mesh situation where the fluid must also have a horizontal component of motion. In the light of section 7.4 it is suggested that tranquil and rapid flow should be separately considered. The hydraulic drop is an interesting phenomenon but will probably not prove desirable on working screens.

It is envisaged that more information on solids transport is required before a theoretical model of fluid flow can be extended to include the prediction of flow in the presence of solids, but this does not preclude the empirical development of predictions such as that in 7.3.5 for field usage.

8 SOLIDS TRANSPORT ON SCREENS: RESULTS

8.1 Introduction

The ability of the screens to act as a vibratory conveyor was tested for the range of angles and frequencies available. Three conditions were considered. Firstly, concentrated particles moving within a liquid, which was envisaged as the general case aside from the special situation at the liquid front. Secondly, a slurry in which particle interactions have a major effect, being the condition expected around the leading edge of the liquid. Thirdly, a cake from which much of the drainable rig fluid has been lost, representing solids transport from the liquid to the front of the screen.

The latter two situations could be more or less directly observed, but it proved impossible to get quantitative results on the main rig for solids within the body of any non-Newtonian liquid used. The process was therefore represented by dry free-flowing solids. This may be justified by common experience in sieving, where it is known that particle adherence can be overcome either by having very dry material, or by working in the flooded liquid state. That is, the total absence or the total presence of fluid avoids the particle-particle adhesions which can result from limited amounts of fluid. Of course, the viscous effects are very different in liquid and in air. These could be studied by a substantially modified version of the small vibrating rig.

8.2 Dry Solids Conveyance on the Main Rig

In conveying experiments with both dry particles and particles in the presence of liquid, it was found (as is discussed in more detail in sections 8.2.3 and 8.3.2) that under the conditions used on the full-scale rig significant conveying did not occur until a considerable depth of particles had been built up, this bed corresponding to a layer tens or hundreds of particles thick. Hence any consideration of particle motion must regard the particles as an interacting bed rather than as individual objects. In the case of particles moving in the presence of liquid it was noted that there was a moving bed under the liquid on the flooded mesh. For the dry experiments the particles were sieved to be of the same order as the mesh opening, with very few being sub-size and blinding was not a problem.

8.2.1 Motion of the Main Rig

The actual movement of the Main Rig was examined as described in section 3.1.7, to see how much it deviated from circular. Figure 8.1 gives prints from the actual film taken. These show that the motion is close to circular just above the drive shaft, but becomes elliptical at the front and rear of the unit. This may be readily understood in terms of the unit rocking fore and aft on the mounting springs as the centre of gravity shifts each cycle. The amplitude of this motion was about 0.5 mm at the measuring points.

The forward ellipse is tilted at nearly 45° from the vertical, which accounts for the vertical and horizontal accelerations being the same. For a unit rocking as described, one would expect the tilt of the ellipse to deviate more from the vertical with greater displacement from the axis of oscillation.

Figure 8.1 Motion of the Main Rig as Shown by Photography of a Point Light Source

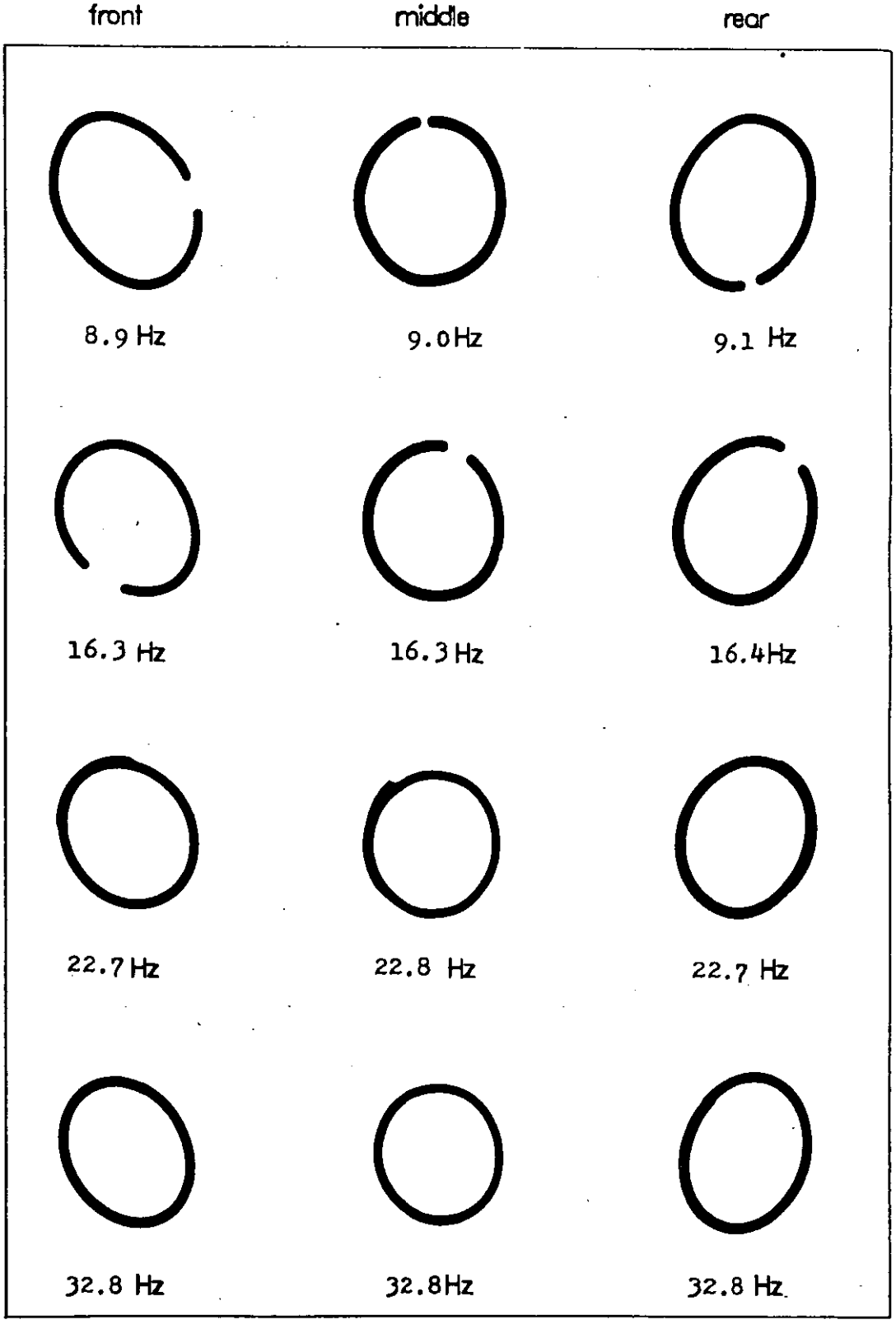

The size of the ellipse changed with frequency (i.e. acceleration) but the ellipsicity did not. This was 1.07 $\pm$ 0.03 at the centre, 1.24 $\pm$ 0.06 at the front, and 1.23 $\pm$ 0.02 at the rear. As acceleration is proportional to displacement (for constant angular speed) this means that the acceleration varied by up to 24% during the cycle.

These tests represent virtually the whole practical range of frequencies of the unit. The amplitude of the ellipse varied by about 8% at the rear and about 16% at the middle and front between these extremes.

8.2.2 **Effect of Frequency and Tilt**

Figure 8.2 shows the velocity of a bed on a horizontal 50 mesh screen, for 3 different types (shape and density) of particles. There seems to be little difference between them, but the frequency of vibration has a major and complex influence. Figure 8.3 shows the velocity of a bed on a downward sloping screen (i.e. in the direction aided by gravity). Figure 8.4 shows the velocity on an upward tilted screen (i.e. up an adverse slope).

Several flow regimes are apparent. They can most easily be observed on figure 8.4, but can be matched on the others. This general pattern was observed on both pre-tensioned and post-tensioned screens of different meshes, and also on test sieves mounted on the rig. It is thus not a screen resonance phenomenon. It has also been observed by another worker in preliminary experiments on the small vibrating rig, using circular motion. It is therefore not a peculiarity of this particular unit, but is probably general to screens for this class of applied motion. (It might not apply to other motions, such as from linear vibrators.)

Figure 8.2 Conveying Speed of Particles on a Dry Mesh of 0^{o} Slope

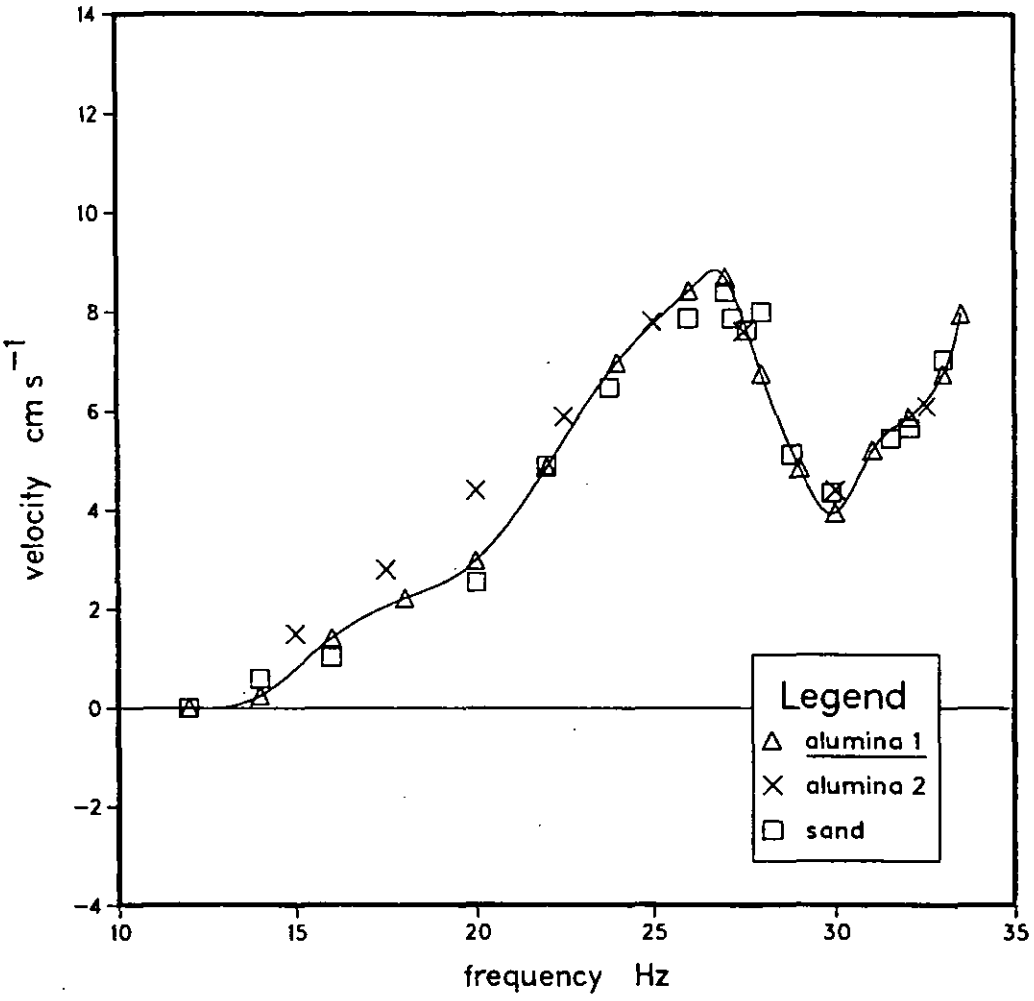

Figure 8.3 Conveying Speed of Particles on a Dry Mesh of -3^{o} Slope

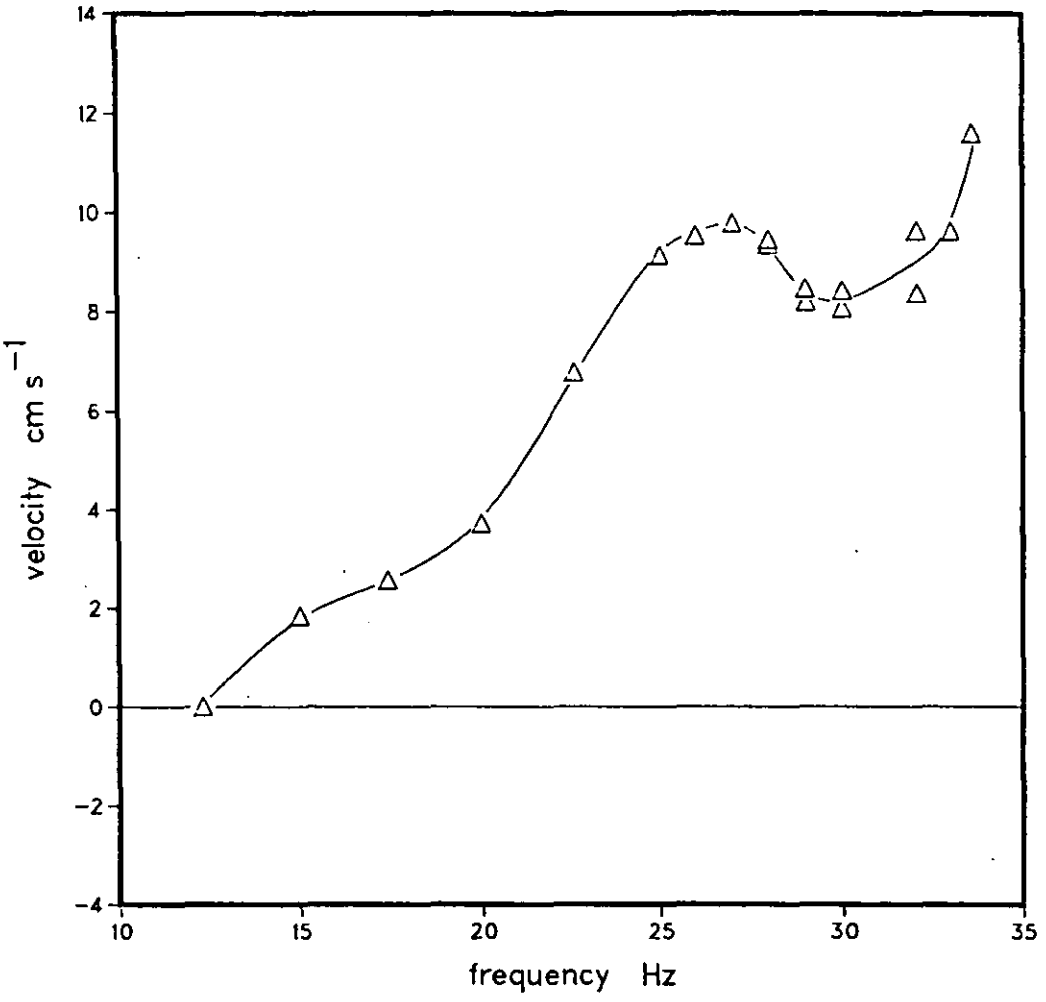

Figure 8.4 Conveying Speed of Particles on a Dry Mesh of +2° Slope

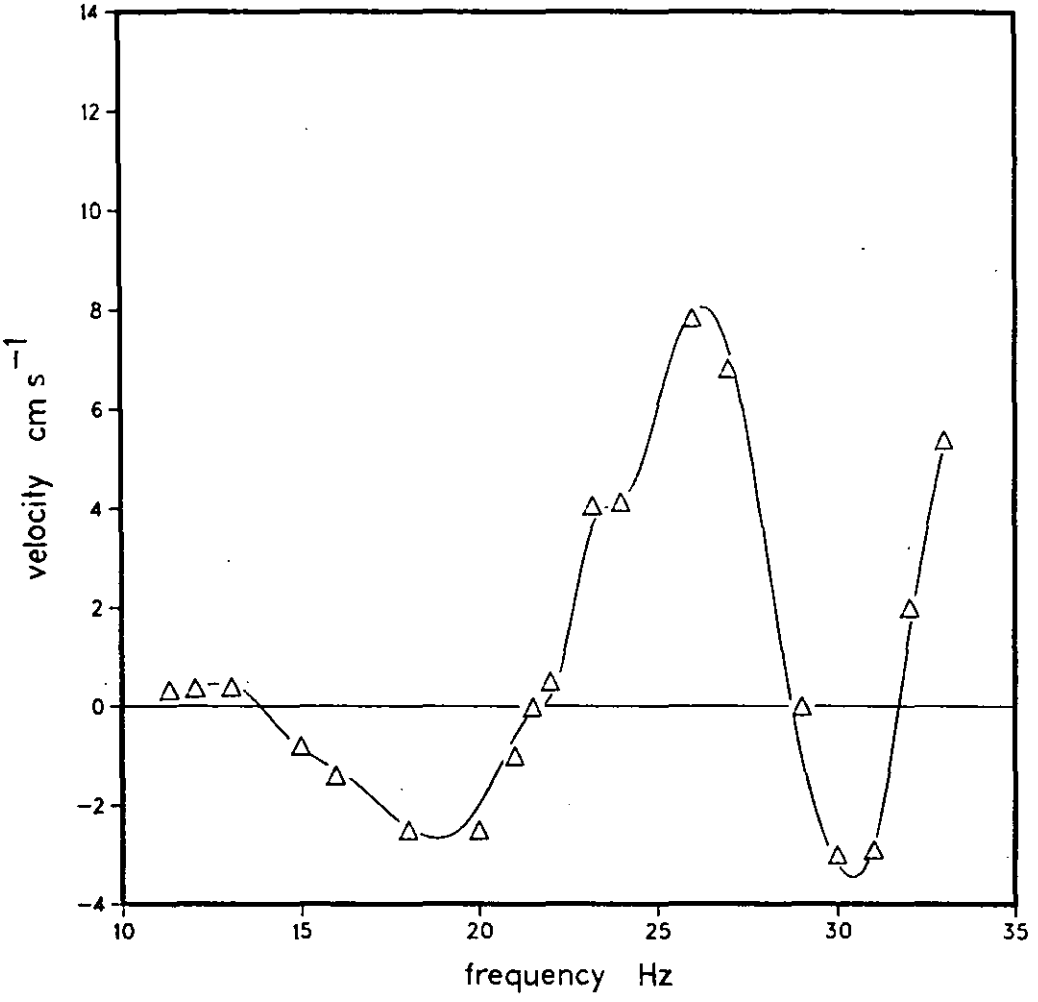

To fully interpret this behaviour it would be necessary to separate the effects of frequency and acceleration. This was not possible on the main rig, but is an obvious line of study for development of the small vibrating rig. The following description gives equivalences in terms of a standard gravity **g** (9.81 m s^{-2}).

Up to about 12 Hz / 0.5 **g** there is no motion. Greater vibration gives a creeping motion, presumably due to jostling and particles rolling. As the motion approaches and exceeds about 16 Hz / 1.0 **g**, then the bed tends to slide in the direction of slope, presumably due to the mesh momentarily detaching from the bed with a loss of friction (the principle of the vibratory chute). For a horizontal mesh the motion tends forward.

Above about 21 Hz / 1.7 **g**, there is positive forward conveyance, even up an adverse slope. This vibratory conveying starts to fail at about 27 Hz / 2.8 **g**. Particles going uphill tend to slide back, and even downhill conveying is less fast.

Finally, above 31 Hz / 3.6 **g** there is again evidence of a strong positive conveyance, even up an adverse slope.

. Figure 8.5 shows the relationship between screen slope (where positive means adverse, and negative means downward) for fixed frequencies. It covers the regime in which there is positive conveying, since this is of greatest practical significance. Here 26 Hz may be taken as optimum. (27 Hz gave similar or lower velocities, 28 Hz gave much lower on adverse slopes.)

Taking the case of a screen nominally set horizontal, these figures indicate that solids conveying is not significantly affected by a downward tilt of a couple of degrees. However, the conveying is severely curtailed by an adverse slope of the same order, unless the frequency is close to optimum. When this is the case, particle conveyance is clearly due to screen motion and only marginally affected by gravity - i.e. screen tilt in either direction. This implies a very precise tuning of both frequency and tilt.

Figure 8.5 Particle Conveyance as a Function of Screen Angle for a Fixed Frequency of Vibration

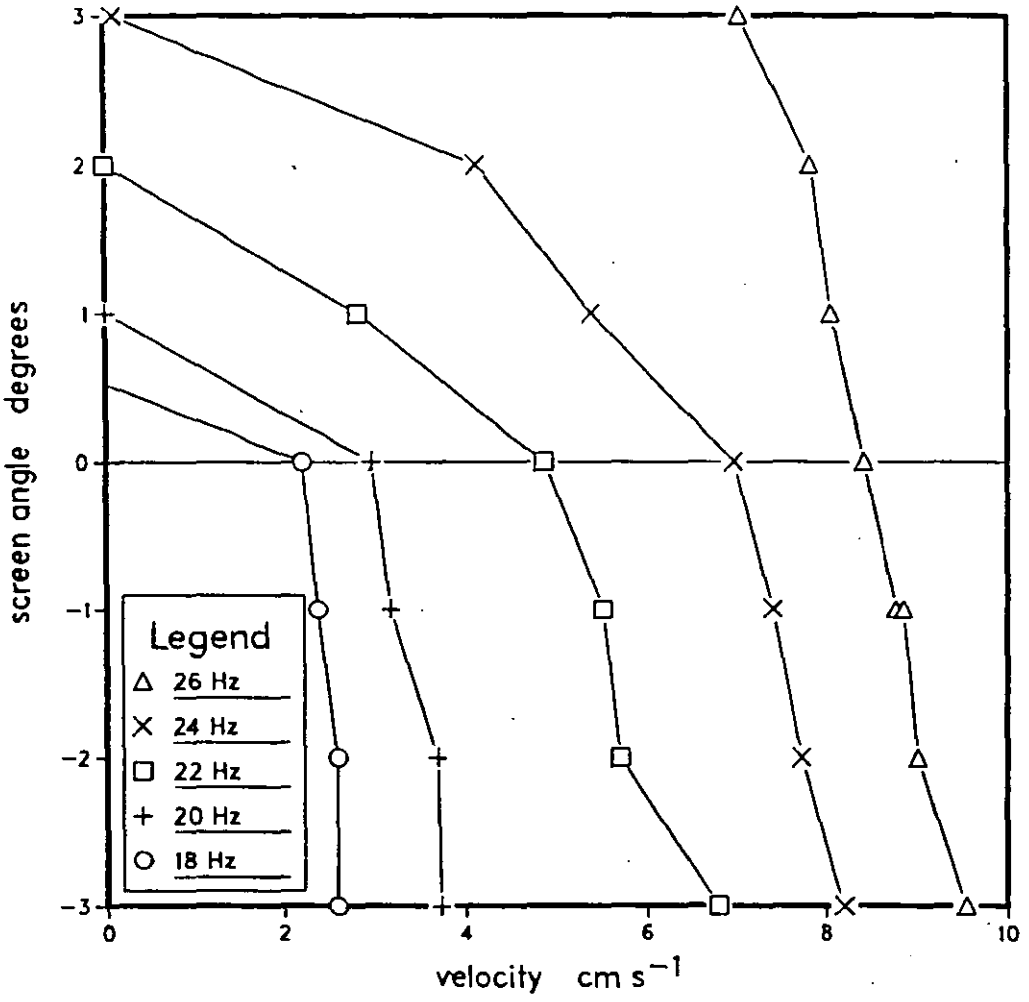

8.2.3 Effect of Surface Loading

It was observed that at an adverse slope of 4^{o} and a frequency of 26 Hz the particle bed tended to distribute both forwards and backwards in roughly equal amounts (a more extreme form of the bed spreading usually observed at all slopes). The influence of surface loading was tested as follows.

A weighed portion of alumina '40' grit was deposited at a point 0.5 m from the front of a vibrating screen (pretensioned 100 mesh at 26 Hz). The manner of application resulted in the sample being spread over an area roughly 0.2 m square (observed with the aid of a calibration grid painted on the mesh). This gave a nominal surface loading. The particles transported off the front of the mesh were collected, weighed and expressed as a percentage of the original amount.

Figure 8.6 shows the results obtained. It was thought that there was some probabilistic mechanism, so the results were plotted on log-probability graph paper. This gave good straight lines at high and low loadings with a discontinuity around 1 kg m^{-2}. These straight lines are shown as curves on a linear plot, giving a good fit to the data.

These results strongly suggest that active forward transport (upper curve) requires sufficient loading for a high degree of particle interaction. A much less efficient process is evident for diffuse (low interaction) beds, the critical loading being of the order of 1 kg m^{-2} for these sets of particles.

On a continuously-fed screen, such behaviour would result in the build-up of surface loading until the rate of forward transport was equivalent to the feed rate. The presence of a liquid would be certain to alter the situation, but a qualitatively similar distinction between interactive and diffuse beds might still be expected.

Figure 8.6 Particle Conveyance on a $+4^{o}$ Tilted Screen as a Function of Surface Loading

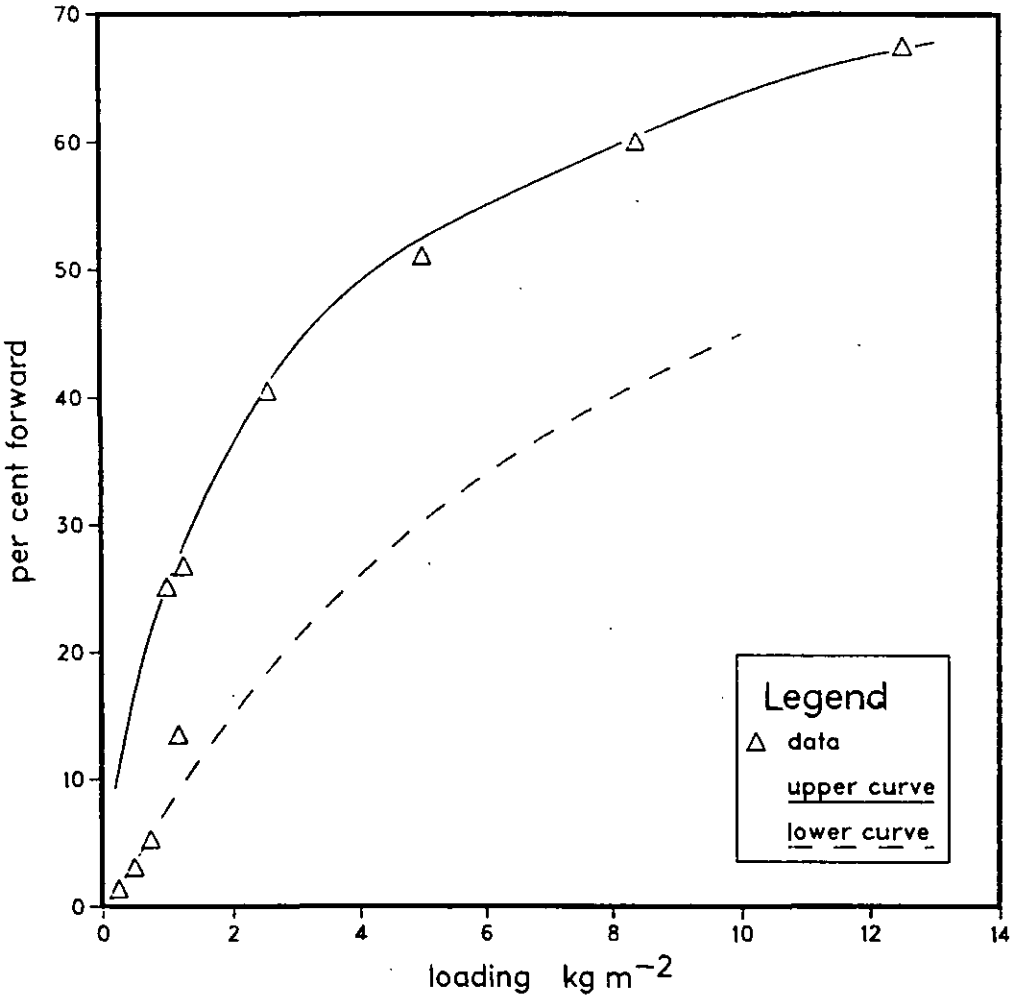

8.3 Slurry Conveyance on the Main Rig

Tests were carried out with the rig running under stable conditions when batches of 5 to 15 kg of sand or alumina (pre-wetted with rig fluid) were added to the upper or lower deck. The behaviour was observed qualitatively, and compared with field observations. The appearance was sufficiently similar to that of wellsite screens for the laboratory tests to be considered representative of field conditions, so a more thorough programme was carried out.

8.3.1 The Effect of Mesh Permeability

With the lower deck running three-quarters full and substantial solids loading, it was noticed that the solid tended to accumulate in a ridge half-way up the total screen length. Three possible explanations were: [1] a fortuitous balance of mechanisms, [2] minimum conveyance near the axis of rotation, or [3] poor conveyance over the join between the two mesh units. Taking the last possibility, the hypothesis was made that this was due to the mesh being impermeable at this point (i.e. fixed with resin onto support frames).

To test this idea, two blank plates were made from 6 mm steel, and arranged as shown in Figure 8.7(a). This gave half the rig with the usual configuration, and half with a screen unit straddling the centre-line. The components on both sides were bolted together so as to give a flush top not dependent on location. The joints were sealed with silicone rubber to give an impermeable surface with a good grip.

The rig was run as usual (fluid XC, 2° upward tilt, 21.2 Hz) with the screens almost completely covered with liquid, and 20 kg of silver sand [1984] was added over 20 minutes to the rear. A further 10 minutes later the rig was suddenly stopped (both flow and motion) and the screen allowed to drain. Solid was found to have accumulated as shown in Figure 8.7(b). A similar pattern was found at 25.5 Hz, i.e. accumulation on the impermeable parts of the deck.

Figure 8.7 Effect of Mesh Permeability on Slurry Transport
(a) Layout of Lower Screen Deck

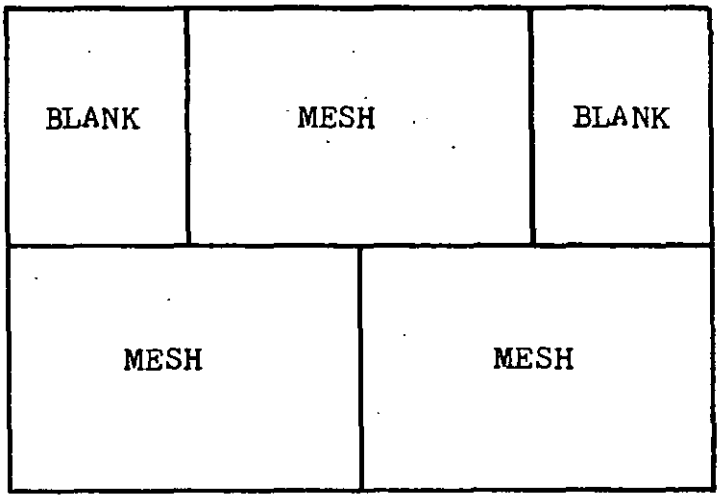

(b) Location of Accumulated Solids

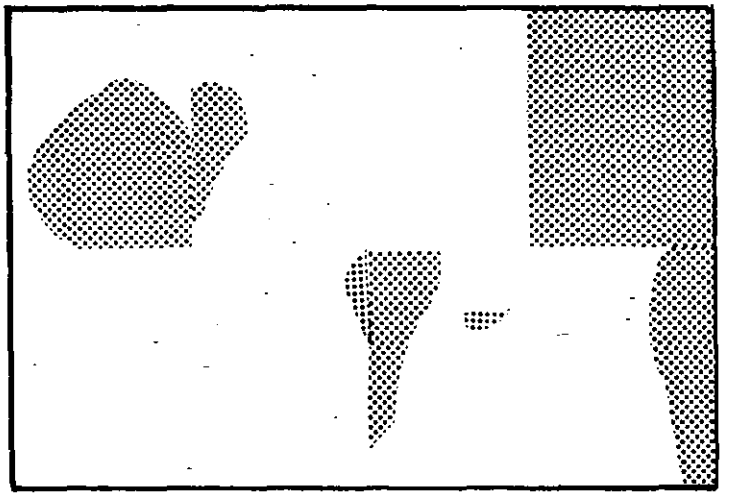

This confirms the third explanation, and demonstrates the importance of mesh permeability, which has not been remarked upon before, so far as can be determined. An interpretation is as follows. For the particle bed to lift off the mesh surface requires air or rig liquid to fill the space underneath. This would normally come through the mesh. If the mesh were obstructed it is possible that for dry particles air could come around and through the bed, but for a viscous fluid this would not be quick enough. Hence the particle bed is stuck to the mesh: it cannot leap forward, though it may slide on a viscous layer of fluid.

8.3.2 **Observed Flow Regimes**

For effective forward conveyance of concentrated slurries, two distinct sorts of motion were observed for all solids and fluids examined. These are illustrated in Figure 8.8. At lower frequencies (Figure 8.8a) the solid moved forward as a sheet, which wrinkled presumably due to the velocity at the front being less than that at the rear. (Materials were Chelford sand in water.)

At higher frequencies (Figure 8.8b) the sheet tended to break up to form balls. The use of coloured tracer particles and cine photography indicated that such balls had internal motion rather like a fluidized bed. Individual particles travelled up through the centre and down the outside of the ball in a roughly symmetrical fashion, taking of the order of 30 seconds to complete a trip.

The transition from one regime to the other typically occurred over a couple of Hz around 24 Hz. Identical effects were observed for different rig meshes (both decks, pre- and post-tensioned, different mesh counts) and for circular analytical sieves mounted on top of the rig.

The behaviour was observed for the rig fluids water, HEC, XC, XCD and clay, and for the particles alumina grit 40, alumina grit 40/60, silver sand 1983, silver sand 1984, and Chelford sand. The author saw similar behaviour with clay mud and drill cuttings in the field. Hoberock (1980, Fig 11E) gives a picture with little explanation for a sand in clay slurry.

Figure 8.8 Slurry Motion on a Tilted Vibrating Mesh
[a] Sheet Flow 21.6 Hz

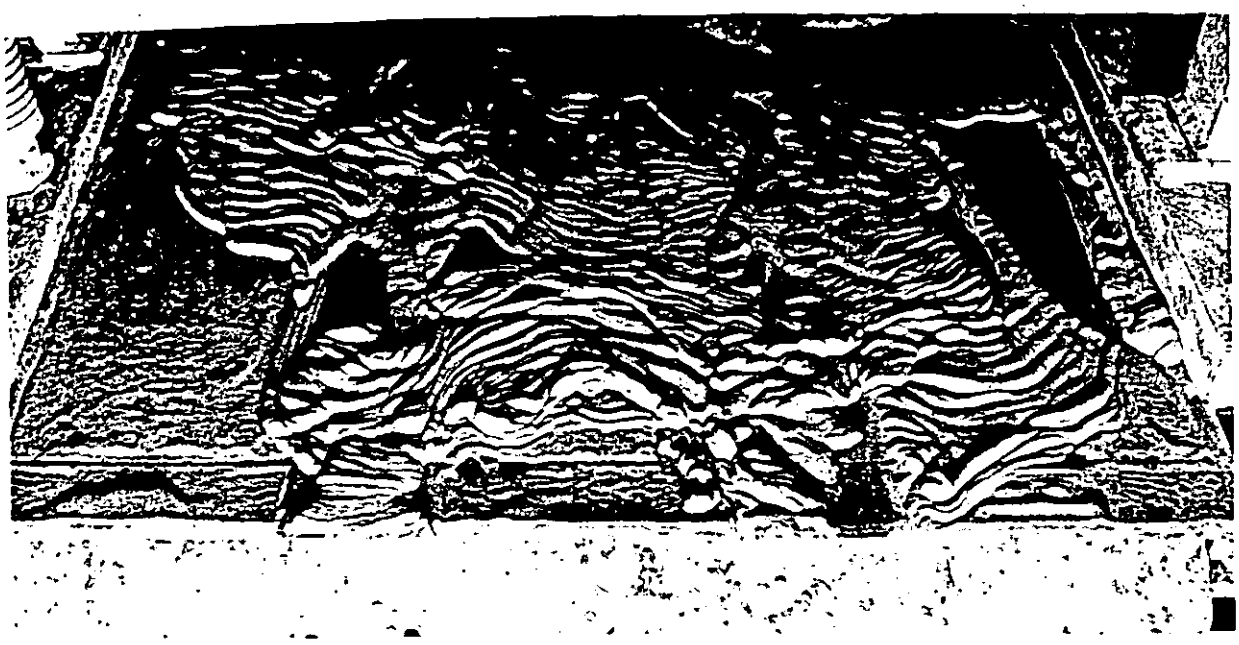

Slurry Motion on a Tilted Vibrating Mesh
[b] Ball Formation 26 Hz

The formation of apparently fluidized balls was not only controlled by frequency. It was favoured by slurries of high liquid content, of less angular particles and of lower viscosity. However, a well-formed ball with internal circulation did not always show the best forwards conveyance. It seems there is a requirement for sufficient adhesion between particles for the ball to survive, and for sufficient freedom of motion for the particles to circulate. The adhesion between slurry and mesh is obviously complex and important in determining transport.

This behaviour was readily observed forward of the liquid front, and in the region just before it. It was more difficult to view the more flooded region at the rear, but as far as could be ascertained the same pattern prevailed. That is, at lower frequencies the solids formed a bed the full width of the channel, moving together as one mass. At higher frequencies domes would rise (often above the surface of the liquid) giving rise to balls (of the order of 80 mm diameter)at the liquid leading edge. Movement forward was then typically by balls of the order of 30 mm diameter breaking away. At the front of the screen, the balls did not easily pass the impermeable strip, so tended to accumulate into a larger ball, defined by the mesh channel. This then came into equilibrium with pieces breaking and falling off the front, the mass being replaced by slurry joining at the rear. It is supposed that a similar process was at work at the liquid leading edge.

8.3.3 **Measured Velocities**

The following results come from tests with batches of 50 grams of Chelford sand (as a slurry in excess water) deposited onto a vibrating screen about 0.5 m from the front. Each batch moved as a sheet or ball according to the frequency.

The mesh was run either 'dry' or 'wet'. In the 'dry' state it was fully wetted with water just before the experiment, but the ball was allowed to dewater. This was intended to represent conditions forward of the liquid front. In the 'wet' experiments a liquid film was kept on the mesh by means of a spray, so the slurry was less prone to dewater. This was intended to mimic conditions for solids approaching the liquid front.

Figure 8.9 Conveying Speed of a Sand Slurry on a Dry Mesh of -3^{o} Slope

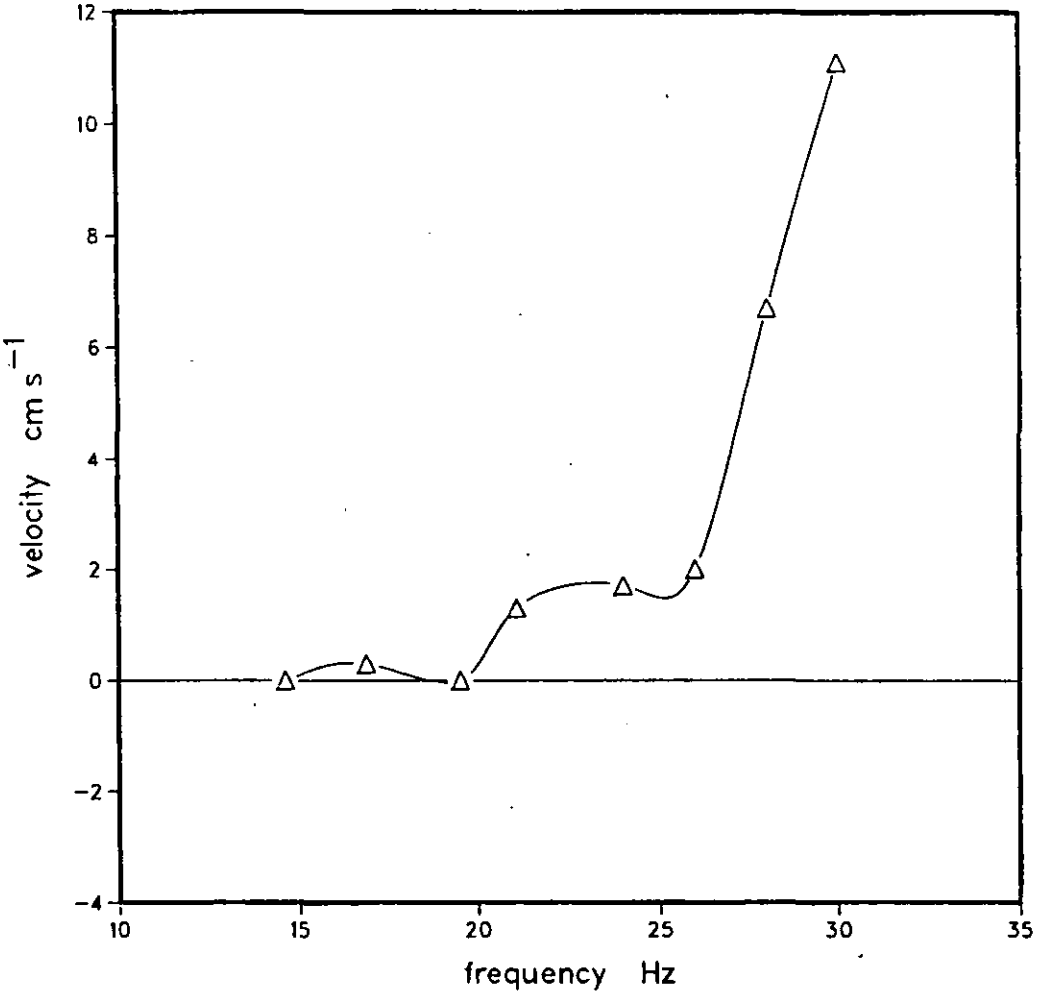

Figure 8.10 Conveying Speed of a Sand Slurry on a Dry Mesh of $+1^{o}$ Slope

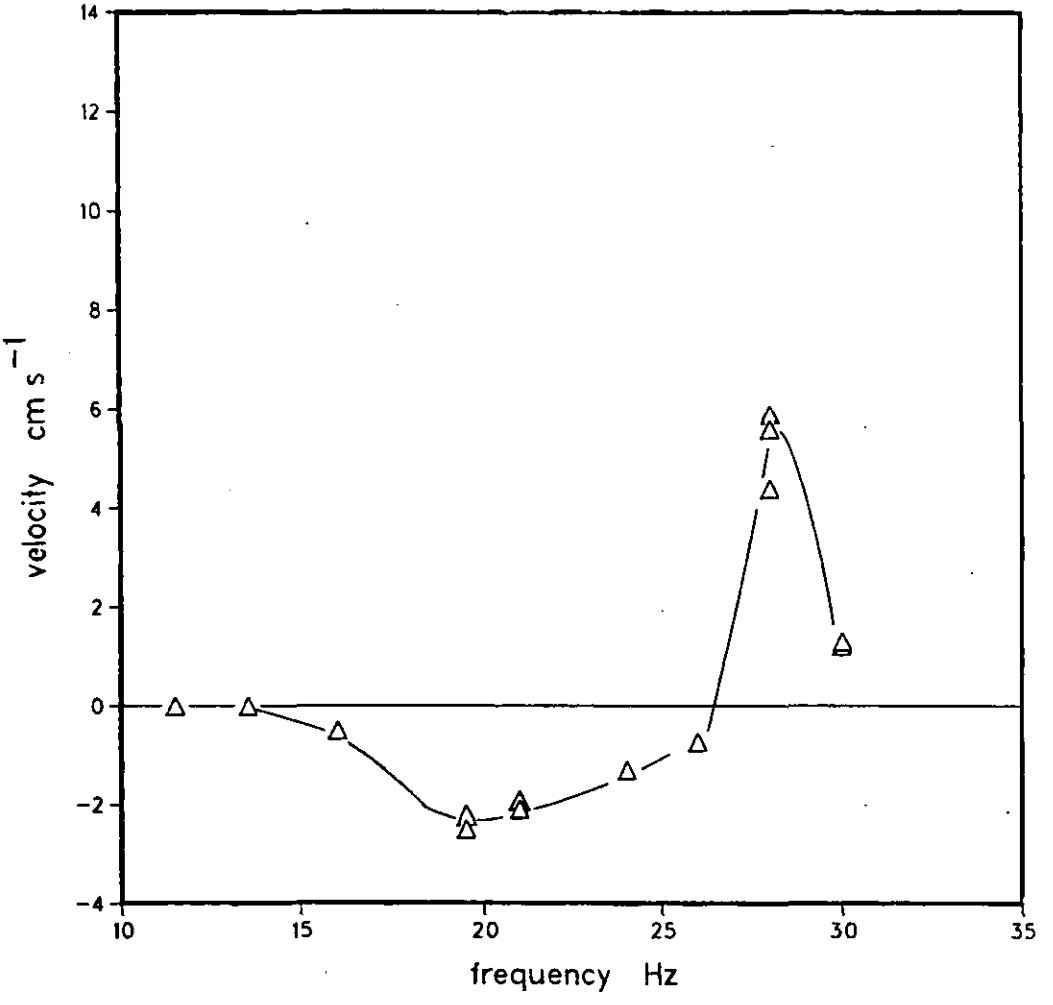

Figure 8.11 Conveying Speed of a Sand Slurry on a Wet Mesh of +2° Slope

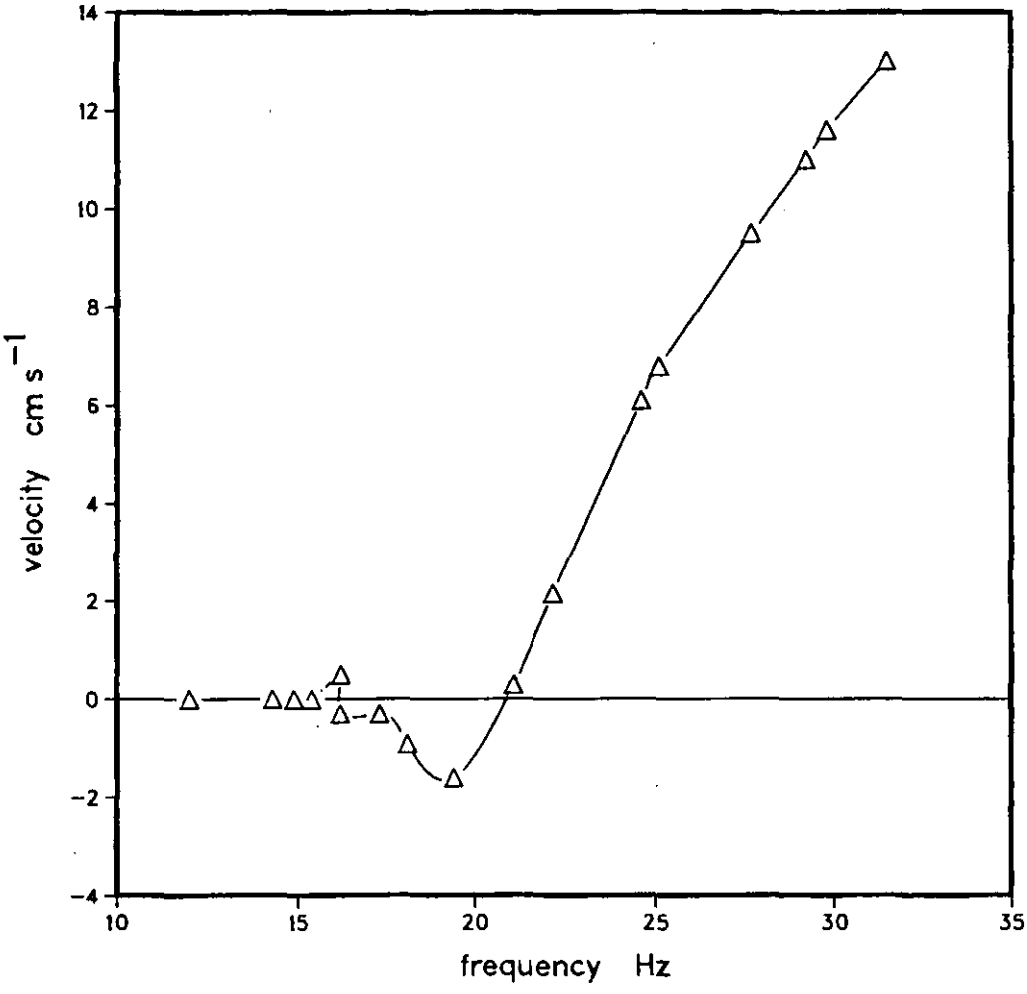

Figure 8.9 shows the effect of frequency on speed for slurry on a downward-sloping 'dry' mesh, and should be compared with figure 8.3. Only forward motion was apparent, but the effect of the liquid was to cause the mass to adhere to the mesh and thus move more slowly forward. However, at higher frequencies the dewatered lumps (rather than fluidized balls) skipped down the mesh almost as freely as the dry particles.

By contrast, Figure 8.10 shows motion for a slight adverse tilt, giving only backwards sliding except for a very narrow region of frequencies around 27 Hz. Thus it might be averred that horizontal or downward slopes are required to convey separated solids on the 'dry' portion of the screen.

However, Figure 8.11 shows that slightly wetter solids can be made to convey very well, even up adverse slopes. The general behaviour is similar to that observed for dry particles (figure 8.4) but without the loss of efficiency above 27 Hz. The similarity may be explained by both systems allowing relative motion of particles (unlike the more dewatered case where particles are adherent). The difference at higher frequencies [accelerations] suggests that the loss of conveyance arises from the bed becoming detached from the mesh, which is inhibited by the presence of a viscous liquid.

The difference between figures 8.10 and 8.11 is primarily due to the amounts of liquid present. Taken together, they suggest that forwards conveying (say at 26 Hz) of a ball could be converted to backwards travel by a dewatering process. In fact, this was frequently observed, though the cause had not been appreciated prior to these tests. In a number of combinations of fluids, particles and meshes, wet slurry balls had been seen to travel forward, and to reverse their direction as they dried out.

These tests on single batches of slurry did not take into account an effect which can be seen in figure 8.8(a). That is, slurry at the front of the screen was pushed forward by additional material arriving from the back. This is obviously a major factor in practical use of these units, ensuring some solids discharge even if the conditions are not optimum.

8.4 Mesh Blockages

The causes and practical treatment of mesh blockages are not well understood. While not a prime aim of this research, some observations were made which it is worth recording here, for the benefit of further experimenters.

8.4.1 Field Test

A unit similar to the Main Rig was operated at the premises of Thule United, Aberdeen. It was loaded with used clay-based drilling fluid containing unspecified sandy drill cuttings. It had a 30 mesh screen on the upper deck, and 80 mesh on the lower deck.

A test was run in which the flow rate was set so that liquid just covered the rear lower screens. The rig was then run continuously until liquid also filled the front lower screens - i.e. the rear screens were blocked. The screens were then removed, gently hosed to remove mud and examined under a low-power microscope. A count was made over samples of 80 screen apertures to determine the fraction which had particles lodged in them. This was then repeated at different point on the screen. (In the figure given overleaf, each number represents 6 of these counts, i.e. 480 screen holes.)

This test was carried out with the lower screen at two angles. The screens were pressure-washed before use, and examined with the microscope to ensure that the initial particle count was insignificant. Both runs were done at a frequency of 27.3 Hz, which had been found to give good solids conveyance.

Figure 8.11 Mesh Holes Blocked on Field Rig (per cent)

(a) 0^{o} tilt

front

60.1	42.2
76.1	84.6
97.5	87.7
92.3	87.3

rear

overall = 77.3 %

(b) 3^{o} tilt

front

83.8	60.5
94.4	89.0
87.8	80.5
78.2	71.8

rear

overall = 80.7 %

To some extent the results above illustrate the fact that distribution from the possum tank was rather uneven. There was not any great difference between the two angles, except that it took longer for the 3^{o} tilt to reach the overflow condition.

It was noted that mesh holes with two particles were extremely rare where the percentage was below 75%, but common above 90%.

8.4.2 Chelford Sand on the Main Rig

The application of 94 kg of Chelford sand completely blocked a set of 100 mesh screens on the lower deck. That is, more than 90% of the holes examined had particles lodged in when the screen had been gently hosed and dried. The rig fluid was XCD and the frequency 21.4 Hz. The sand was fed at the rate of about 4 kg per minute.

One screen unit (a quarter of the deck, about 0.4 m^2) was rigorously cleaned and the solids collected. These amounted to 27.4 g, of which only 0.9 g was retained on a 210 um sieve. (It appeared to contain the majority of flakes removed from the frame by the washing procedure.)

From the hole count, this gave a mean particle diameter of 153 μm, compared with the screen nominal aperture of 142 μm. This is reasonable if one considers non-spherical slightly oversized particles becoming wedged in place. Interpolation of the the size distribution for the sand revealed that about 10% was between 142 and 153 μm.

By contrast, 150 mesh screens conveyed a similar quantity of sand without difficulty, since the sand had less than 1% near mesh size.

8.4.3 General Observations

With water as the working fluid, screen holes could become blocked only by solid particles lodging in them. However, with all other fluids it was possible for the fluid to bridge holes upon drying out. Drying out could occur forward of the liquid front on hot days, or overnight if the rig mesh was left without hosing down.

The XC and XCD polymers were particularly insidious because they dried clear. It was thus possible to have a lower deck which seemed unobstructed by normal inspection (including viewing against the light) but which was largely impermeable. Moreover, the solid did not readily dissolve in rig fluid or water, although steam jetting proved satisfactory. To prevent the problem required rigorous hosing while the screens were vibrated. This prevented the formation of window-panes, but did not necessarily remove a thin coating from the wires. It is supposed that this effect could cause unrecognized problems in the field.

Particles on the mesh could be categorized for cleaning purposes as (a) loose (b) removable by hosing (c) removable by pressure washing (d) not removable. As the last category accumulated, there was an inexorable reduction in hole availability, even with regular pressure washing. However, there was a subjective impression that particles left in place tended to become more difficult to remove: e.g. particles in category (b) could lock more firmly into place and thus require pressure washing if neglected.

9 SOLIDS TRANSPORT ON SCREENS: DISCUSSION

9.1 Introduction

For solids sieving on a moving screen, the applied motion has two principal purposes. Firstly, the bed of particles must be agitated so that individual particles are offered to the screen apertures for passage through. Secondly, the bed must move so that oversize particles are carried off and the working area of screen is cleared for further feedstock. If the latter function is too effective, then the former may be impaired. That is, rapid removal of particles means that there is insufficient residence time on the mesh for there to be a chance for most sub-size particles to actually meet an aperture so as to permit passage through. This would give an effective cut point much smaller than the screen aperture, and also a less sharp cut. For this reason, many successful traditional designs of downward-tilted screens actually retard bed movement (by change of slope or by applied motion) at the discharge end of the screen in order to permit greater removal of fines.

The devices considered in this thesis may actually be considered combinations of wet screening (rear flooded mesh) and dewatering (forward of the liquid front). When used with cyclones for barite salvage (see section 1.5.4) then a sharp cut is desirable, but more usually it is the maximum separation between solid and liquid which is important. Generally, the carry-over of fine particles is not at all a disadvantage, providing this does not give a discharge so wet as to lose large amounts of whole mud.

It may therefore be proposed that an ideal motion would give as fast a bed movement as possible, consistent with some agitation and the avoidance of violent acceleration. The bed velocity could then be reduced by tilting the screen up, allowing a greater liquid flow-rate.

9.2 The Effect of Acceleration

Ephithite (1983) said "the theory of screening fine particles shows the high speed to be necessary in order to give an exciting force of some 5 g to the particles", but correspondence with the author has ascertained that this remark is based on company practical experience (of dry screening) rather than any actual theory. A similar basis is probably the origin of Hoberock's assertion of 4 to 6 g as the favourable range (1985c). That is, it has been found by manufacturers that this order of acceleration gives good results for dry screening. It is generally accepted (personal communications) that screen displacement during motion should be of the same order of magnitude as the mesh pitch (i.e. distance between centres of wires). Thus a high speed unit with a small amplitude is preferred for fine mesh, and a lower speed unit with larger amplitude for coarser mesh, both running at a similar peak acceleration.

It is obvious that a peak acceleration of at least 1 gravity is required for particles to actually lift off the screen (and particularly for oversize particles to lift out of apertures). According to Kluge (1953) the motion is one of sliding and rolling up to about 1.5 **g**, causing excessive wear of the mesh. The mesh life also gives an effective upper limit on acceleration of about 6 **g** due to fatigue of the wires (Hoberock 1981c). The manufacturers of the screens used in this thesis recommend a limit of 4 **g** for the fine mesh ones.

The classic paper on vibratory conveying is that of Redford & Boothroyd (1967), which is actually concerned with movement of objects on a solid surface. This is cited by Hoberock (1980) as showing that "particle-conveying speed increases with increasing normal screen acceleration". There exists, however, a much earlier analysis by Kluge (1953) precisely on particle motion on screens, which seems to have been generally overlooked. An almost identical model was independently proposed by Takahashi, Suzuki, and Tanaka (1968) for the behaviour of particle beds on a vibrating plate.

Kluge showed that particle behaviour can be interpreted in terms of the position of the screen when a projected particle or bed of particles actually lands back on it. Hence for a vertical acceleration of about 1.7 g, the screen is at lower dead centre when the particle lands. Interestingly, for an acceleration of 5g the screen position would be the same, but the particle would have remained aloft for one and a half cycles instead of about half a cycle. (It would correspondingly have travelled about three times as far in the horizontal direction.) Kluge suggested that vertical accelerations of greater than 4 g were not worthwhile because a throw of greater than one cycle meant that the energy of one cycle was not fully utilized.

The behaviour of dry particles on a horizontal screen as shown in figure 8.2 can be well correlated to this explanation. This is illustrated in Figure 9.1, and may be described as follows.

Figure 9.1 Trajectories from a Screen with Circular Motion

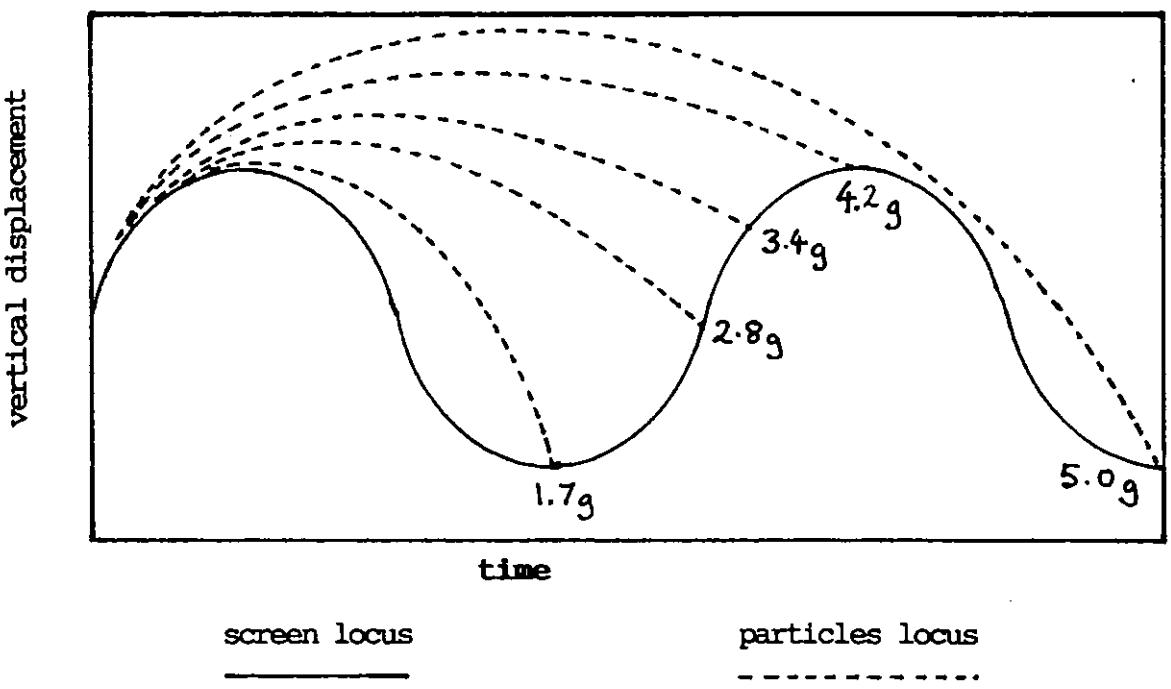

From 0.7 g [13.6 Hz] Kluge asserted that relative motion is possible because there is upward pressure by the mesh during the forward half of its cycle, but reduced pressure on the particles during the backward portion. The reduced friction essentially enables the screen to be slid away from under the particles. This accounts for the small amount of movement below 1 g acceleration. From 1 g [16.3 Hz], there is sliding and rolling motion. Particles which lose contact land again during the downward half of the screen cycle.

For an acceleration of 1.7 g [21.3 Hz] the calculated trajectory means that projected particles will land when the screen is in its lowest position. For higher values of acceleration/frequency the particles will land on a mesh moving upwards, which accounts for an observable transition in behaviour at this point. An acceleration of 2.8 g [27.3 Hz] gives a landing with the mesh in its mid-point and maximum vertical velocity, which would be expected to give maximum impetus. This corresponds to peak velocity on the experimental results.

Higher accelerations mean that contact is made at a lower velocity and the particles are less efficiently 'bounced on'. The next experimental transition at about 30 Hz [3.4 g] corresponds to a point one-eighth of a cycle on, when the mesh is moving (for circular motion) upwards at 45° to the horizontal. Beyond this point it may be argued that loss of vertical impact is more than compensated for by horizontal impact tending to knock particles forward (the mesh velocity is greater than the average solids velocity). Limitations of the Main Rig prevented exploration of higher accelerations, but it may be noted that the highest acceleration possible, 4.2 g [33.5 Hz] corresponds to particles landing on the top dead centre of the screen motion.

It is clear that tilting the screen must affect the exact landing point, as well as the tendency for the particle bed to move under gravity, but the evidence (figures 8.2, 8.3, 8.4) is that a similar pattern obtains for small tilts in either direction. It should be noted that while the theory was based on free trajectory, the effect was found by this author (and presumably agreed with the practical experience of Kluge) for beds of particles with considerable particle-particle interaction. This suggests that it may have some validity on a flooded mesh - i.e. the presence of fluid may affect the exact values, but the relationship between conveyance and acceleration will show the existence of different regimes and optima. Likewise, slurry movement forward of the liquid front might show behaviour which is a compromise between either the bed or the individual particles being in free trajectory. This was observed (see section 8.3.3) but cannot be fully explained without further work, on the developed Small Rig.

9.3 Other Factors

9.3.1 Screen Motion

The evidence is that frequency itself does not exert a major influence, only the acceleration resulting from it. However, changing the type of motion may well have an effect. In particular the use of vertical and horizontal motion of the same frequency but independent amplitude and variable phase can produce elliptical or linear motion in any direction. This is considered to be the most valuable feature of the Small Rig, particularly for determining the best conditions for solids transport forward of the liquid front.

The main rig had a fixed amplitude (slightly increased at higher accelerations), so this could not be used as a variable. There is the convention mentioned above in which the amplitude should at least be comparable with mesh dimensions. It is supposed that this is so that particles are carried over the wires from one aperture to another. However, this could be a fruitful area for investigation on an extended version of the Small Rig.

9.3.2 Screen Tilt

Adverse tilt can only be detrimental to solids conveying. However, the greatest possible adverse tilt is desirable to maximize the liquid flow-rate. The experimental evidence of this thesis supports the limit of 5^{o} tilt suggested by Redford & Boothroyd (1967), which has also been found in commercial practice (Hoberock 1982b). However, it is believed that elliptical or linear motion might be found to permit greater slopes to be used. An important point (see figure 8.5) is that near optimum motion the conveying speed was much less sensitive to small changes in slope. This has practical consequences in that it is easier to adjust the frequency than the slope to the precision needed.

9.3.3 Particle and Mesh Properties

Conveying did not appear to be significantly affected by variations in particle size, shape and density (though it is possible to imagine an artificial situation of, say, spherical particles of narrow size range which might behave differently by rolling). The experiments covered an insufficient range to conclusively determine if there was any important relationship between particle size and mesh dimensions with regard to conveying, as opposed to sieving. However, there was no indication of such behaviour.

Although the theory of Kluge is based on free trajectories, it appeared to fit the experimental situation of particle beds rather than separate particles (i.e. low surface concentration with little particle-particle interaction). This must be due to the fact that the bed acts as an object on a vibrating sheet, whereas the individual particles may strike the wires at various angles and rebound accordingly, thus randomizing the motion. Such rebounds are prevented by the presence of a sufficient concentration of particles, and hence the dimensions of particles and wires are not important.

9.4 Slurry Conveying

9.4.1 Flooded Mesh

Further work is required on a developed version of the Small Rig, but the evidence of the present thesis is as follows. For dilute suspensions, material accumulates until there is a sufficient concentration of particles for a bed to be formed at the liquid front, and ultimately move forward. Two distinct types of bed can be seen to form, and they continue out of the flooded portion onto the front of the screen. The transition between these regimes is not exact, but occurs round about an acceleration of 2 **g** (23 Hz).

The lower-frequency regime is a creeping flow, which may reasonably be taken to be the free-trajectory model described above, severely inhibited by the presence of viscous fluid. However, the high-frequency regime closely resembled a vibrationally fluidized bed. (These are unusual, but the author has direct experience of an experimental one.)

There is very little published on vibrational fluidization. However, the motion observed in this thesis was similar to that described by Kroll (1955) and Ratkai (1976) for a cylindrical bed in which particles travel up the centre and down the outside. A theoretical analysis was given by Takahashi, Suzuki & Tanaka (1968) for circulatory motion in a hopper. They observed fluidized behaviour experimentally over a range from 2 to 3.5 **g**, which is in accord with the present thesis. Their model was for dry particles on a slope of the order of 45°, but it could be the basis for the wet condition on a shallow slope.

A significant feature of this model is the existence of two zones in the bed: a fully fluidized one on top, and closely-packed region adjacent to the slope. The existence of such a lower region on the mesh would be disadvantageous because of its obstruction to flow, but further work would be required to confirm this.

The observed failure of solids to pass impervious mesh (section 8.3.1) in both creeping and vibrational flow is evidence for the requirement that the bed lifts off the mesh. It is unable to do this if fluid cannot flow into the space thereby created. Thus as the mesh becomes blocked at the rear solids would tend to accumulate unless the liquid feed disturbs them. This process is less relevant to downward-sloping screens, where material can slide down in the absence of positive conveying.

9.4.2 Non-Flooded Mesh

On the flooded portion of the mesh, particle beds would have all spaces filled with liquid and also be surrounded by liquid. By contrast, forward of the liquid front dewatering can and does take place. For ball motion, measurements of material collected from the front indicated that the minimum rig fluid content was equivalent to that in loosely packed settled solid - i.e. all the voids were filled with liquid (ratio of solid:liquid 1:0.7 by volume). A slightly lower liquid content could be observed with water, which undoubtably drained more freely than typical drilling fluids. It therefore seems that ball motion of conveyed solid involves particles in close proximity with enough freedom to move relative to one another, but with sufficient adhesion and particle-particle contact to maintain a structure. This is supported by the observations on a variety of fluids and particles on a sieve mounted on the main rig, where fluidized balls were favoured by less angular particles and by combinations of lower viscosity with higher fluid content.

By contrast, creeping flow required a much greater volume of liquid to be present, of the order of 5 times the solid volume, suggesting that the particles move essentially independently, and the main interactions are particle-fluid ones. A lower ratio of liquid to solid produced a pourable slurry, but no motion up until fluidization appeared at higher frequencies. (Note that dewatered material could be pushed off the front of the mesh by the pressure of creeping slurry from behind.) This therefore suggests that the creeping conveyance involved relatively free motion of particles in a fluid.

The observed variations in velocity with frequency suggest a complex balance between motion of the bed as a whole relative to the mesh and motion within the bed of particles. For a downward-sloping mesh there is a plateau region in performance from about 21 to 26 Hz (1.7 to 2.6 g) in which velocity is unaffected by changes in frequency. As the velocity seems adequate to clear the mesh but still permit time for dewatering, this would seem a sensible operating region. It presumably gives sufficient lift to aid the bed in sliding down under the influence of gravity. Greater frequencies/accelerations give increased positive conveyance (which may not always be a advantage).

With upward-sloped meshes, the same plateau occurs, but as it gives motion in the wrong direction, it is not useful. There is a major difference between a 'dry' and a 'wet' mesh (see figures 8.10 and 8.11), the former having a very narrow range of effective conveying frequencies. It therefore seems that liquid on the mesh (from the solids or from streamers of foam) has a valuable part to play, and should not be eliminated from a desire to get a dry discharge. (It is likely that the mesh will be kept wet by the dewatering of solids if there is a sufficient discharge rate.)

9.5 Further Work

The above results have some implications for dry screening, but in the context of drilling fluids it is suggested that the following investigations are required.

(a) Experiments should be carried out on a lengthened version of the small rig, using a transparent fluid to observe particle behaviour when the bed is fully immersed. The transport needs to be studied in respect of the frequency, amplitude, acceleration and relative phase of the vertical and horizontal motions.

(b) A similar study should be made of slurry on a non-flooded but wet mesh to determine the influence of applied motion on the bed velocity and on bed behaviour.

(c) The influence of fluid and particle properties and the ratio of solid to liquid should be determined.

(d) From the above it should be possible to determine the degree of dewatering which gives the best results, and the motion which can transport up the most adverse slope. Any increase in slope with satisfactory transport should have major benefits.

10 CONCLUSIONS

10.1 Analysis of Solids Control

The general nature of solids control in drilling for oil and gas has been examined in terms of the separation of whole mud from drilled solids. A new definition of efficiency of separation has been proposed. A mass balance model has been derived which should enable both proper analysis of individual solids control devices and the forward planning of mud solids control within the drilling programme. Both of these concepts would require field testing for validation and further development.

10.2 Screening of Drilling Mud

It was concluded that the greatest benefit to economic solids control would come from maximizing the efficiency of the shale shaker, so this was the main intent of the work.

10.2.1 Comparison with Hoberock

The work of Hoberock has been extended, and his hypotheses in part contradicted. His model has therefore been modified to take this into account. In particular:

(a) It was confirmed that acceleration rather than frequency is the controlling factor in assisting flow through the mesh.

(b) It was confirmed that it is the vertical and not the horizontal component of motion which has this effect.

(c) However, flow does not increase indefinitely with greater acceleration but tends to a limit.

(d) Furthermore, for fluids with an apparent yield stress, then a finite head can be supported on a mesh with negligible flow through. A minimum acceleration is required to initiate flow.

(e) Above the minimum acceleration, flow increases until there is negative flow during part of the cycle. This gives rapidly diminishing returns.

(f) For the shear-thinning fluids tested, this resulted in effectively two regions of acceleration (frequency) where the flow-rate was relatively insensitive to variations in acceleration, with an intermediate transition zone. Below 0.5 **g** (12 Hz) was a low flow region. Above 1.5 **g** (20 Hz) was a high flow region.

(g) The relationship between tilt and flow-rate agrees with the near-parabolic shape given by Hoberock. This has now been confirmed experimentally for a range of fluids and two different meshes.

(h) For the relationship between flow-rate and screen length, Hoberock's curves going through the origin cannot be entirely supported. Experiment and the developed model both indicate that for many fluid-screen combinations it is possible to have a finite length with negligible flow.

(i) Neither Hoberock's characterization of mud rheology in terms of its plastic viscosity nor his definition of screen conductance have proved entirely successful in predicting flow capacity of screens. Therefore an alternative approach has been used.

10.2.2 **Prediction of Flow Capacity**

A simple method of comparing the fluid capacity of different screens and muds has been developed, which gives a sufficiently good fit to the results in this thesis and available field data.

The fluid rheology is characterized by a single number derived from either:

(a) The Marsh Funnel time in excess of 26 seconds for a litre (25.4 s for a quart),

or (b) A combination of (PV + 0.25 YP) where these have the usual industry units.

(It is possible that the apparent viscosity at about 2500 s^{-1} might also be used.)

The screen is characterized in terms of its wire surface area per unit superficial area, which is proportional to the (wire diameter)x(mesh number)^2 for a square mesh.

Taking the acceleration to be in the upper flow region, then flow-rate is inversely proportional to both these quantities. The flow-rate is proportional to fluid density.

The relationship between flow-rate and tilt has been shown to be parabolic, and there is partial evidence that different fluids with the same Marsh Funnel time give the same curve for a given mesh. Thus it is concluded that a set of design curves may be produced for each screen mesh, which can be simply matched to measured fluid properties.

Further field data is required to check the prediction, and in particular to determine if the definitions of the rheology term need to be modified for best fit and to make them interconvertible.

10.2.3 **Liquid Depth**

It was concluded that a minimum liquid depth is required to get the maximum benefit from screen motion. Shallower liquids dissipate energy from the top surface. The depth depends on fluid properties and screen motion, but is of the order of 35 mm for materials tested. A less permeable screen (intrinsically or due to obstruction by solids) requires a greater depth.

The relationship between liquid depth and distance along the screen can be very complex. A sudden change was experimentally observed, which has been explained in terms of a change from tranquil to rapid flow, giving a hydraulic drop. Further practical and theoretical work would be required to prove this explanation, but it is thought that the hydraulic drop probably has no useful value in this context.

10.3 Solids Transport on a Tilted Vibrating Screen

It was concluded that liquid flow could be aided by vertical oscillation of moderate acceleration, and that the flow capacity could be increased by greater adverse slopes to give a greater head of liquid. However, the slope is limited by the need to transport solids forward, which requires some horizontal component of motion. A preliminary study was made of the processess involved.

10.3.1 Dry Solids

The transport of beds of particles on a dry mesh has been shown to have a complex relationship with the screen acceleration. The maxima and transitions observed can be fitted very well to a model based on the free trajectory of the bed intersecting with the moving mesh at a more or less advantageous point in the cycle. Conveyance up a slope was limited to a narrow region around 2.8 g (27.3 Hz),when the mesh has maximum upward velocity at the point of intersection.

A similar model could be made for motions other than circular, and it is suspected that conveyance up greater slopes might be achievable with angled linear motion.

10.3.2 Solids on the Flooded Mesh

Active forward transport requires a minimum peak acceleration of about 1 g (16 Hz). Up to about 2 g there is a characteristic behaviour which has been called 'creeping flow' when the bed moves forward in waves. Above this value there are formed apparently fluidized lumps with internal circulation.

The creeping bed can proceed forward of the liquid front under pressure from material behind, but with vibrationally fluidized solid there is a process of accumulation and dewatering at the leading edge before the slurry moves forward in discrete lumps.

For both regimes there was poor conveyance over an impervious plate, indicating that upward flow of fluid is required for the bed to leave the mesh and move forward.

Further work is required on the Small Rig to investigate behaviour with different combinations of vertical and horizontal motion.

10.3.3 Solids Forward of the Liquid Front

Solids show similar transport regimes on the forward portion of the screen as on the flooded portion. However, the vibrationally fluidized beds tend to form discrete balls, which may join and break up for reasons which are not yet understood. It appears that a certain amount of adhesion is required for conveyance up adverse slopes in the ball regime. If the mesh becomes dry and the ball dewaters, then the ball can skip and roll backwards rather than sliding forward. The fluidized balls contained much less liquid than the creeping flow solids bed, so it is probably not advantageous to attempt to dewater them.

A much longer version of the Small Rig would be required to investigate this behaviour.

10.3.4 General Conclusion

Work is required on the best combination of horizontal and vertical motion to move a solid slurry out of a liquid and up a slope. The vertical component should have sufficient acceleration to aid the flow of a pseudoplastic fluid through the mesh. The horizontal component need not have the same amplitude. If the two components are phased differently, then the trajectories predicted by the method of Kluge (1953) will need to be re-calculated, as the optima will not occur in the same place as for circular motion.

APPENDIX 1 The Marsh Funnel: A Theoretical Analysis

A1.1 Method

A general description of the Marsh Funnel and its use has been given in section 3.5. So far as could be ascertained (from the literature and writing to the manufacturer) there was no theoretical interpretation or correlation of Marsh Funnel times with physical properties. A method of numerical integration was therefore devised.

It was assumed that (at any moment) an inverted cone of liquid provided a hydrostatic head **h** causing a pressure drop $\triangle P$ through the working orifice, dependent on the density ρ and the acceleration due to gravity **g**, thus:

$$h \rho g = \triangle P \qquad (32)$$

This pressure drop was partially converted to kinetic energy and partially dissipated in fluid friction.

$$\triangle P = \triangle P_{ke} + \triangle P_f \qquad (33)$$

The kinetic energy term can be written as a function of the mean linear velocity **v**:

$$\triangle P_{ke} = 0.5 \rho v^2 \qquad (34)$$

It was assumed that the fluid obeyed the Power Law and that flow was laminar. Considering the orifice as a short tube (and neglecting entrance effects) then Skelland (1967) gives:

$$\triangle P_f = 2 k \left(\frac{3n + 1}{n}\right)^n \left(\frac{v^n L}{R^{n-1}}\right) \qquad (35)$$

where **L** and **R** are the length and radius of the tube, and **k** and **n** are the Power Law constants for the fluid.

Use was made of these three equations in a set of BASIC computer programs as follows. For a given height of fluid above the orifice, the total pressure drop was calculated from equation (32). From an initial guess, an iterative routine was used to converge on a value of the velocity **v** which satisfied equations (33), (34) and (35). This velocity was then applied for a short time period. For this time period, the volume discharged was calculated, and thereby a new value for the height (from the cone geometry). The current value of **v** was used as a first guess in a repetition of the above routine to get a new velocity, and the process continued.

By this method, liquid was discharged from the cone in a series of tiny increments until the total volume discharged reached one litre. The sum of the times taken for the increments was the calculated Marsh Funnel time.

The Reynolds number and the shear rate were calculated at the beginning and end of the discharge, using the formulae of Skelland (1967):

$$Re = \frac{(2R)^n \, v^{2-n} \, \rho}{k \, 8^{n-1}} \qquad (36)$$

$$\dot{\gamma} = 4 \, v \, / \, R \qquad (37)$$

It was found that for efflux times below 30 seconds, then the Reynolds number exceeded 2000 for some of the time, but for times in excess of this, it was less. Thus the assumption of laminar flow was justified, since drilling muds generally have Marsh Funnel times in the region of 35 to 55 s.

From the accumulated results it was observed that if the Marsh Funnel time was **MF** s, then the average wall shear rate during discharge was given approximately by the formula:

$$\dot{\gamma} = 94\,000 \, / \, MF \qquad (38)$$

which means that for typical drilling muds the Marsh Funnel represents a measurement of viscosity at shear rates of the order of 2700 to 1700 s^{-1}.

A1.2 Results

A range of fluids were measured on the Weissenberg Rheogoniometer, and their behaviour fitted to Power Law by regression on the log-log rheogram. The Power Law constants **n** and **k** thereby obtained were used in the programs to compute a Marsh Funnel time. Table A-1 shows how these calculated values compare with experimental ones. The agreement is close enough to support the method.

Having shown the programs to be valid, calculations were then made to determine how the Funnel time varied with **n** and **k**. These are shown in Figure A-1. (Data points are given for one curve.) For highly shear-thinning fluids then a small change in **n** can have a large effect on the Funnel time (and presumably on viscosity-controlled laminar flow through orifices in general).

There is an obvious lower limit, which is 26.05 seconds, which is the inertia-limited time for fluids of negligible viscosity. This applies to all densities because the density term then cancels out in equation (34). It is therefore proposed that the Marsh Funnel time in excess of 26 seconds can be taken as a measure of the fluid viscosity at about the shear rate given by equation (38).

For Newtonian fluids, the viscosity was correlated to the excess time to the power 0.87. Thus for example for two fluids having Marsh Funnel times of 36 and 46 s, the latter has twice the excess time and about 1.8 times the viscosity. This correlation is shown in Figure A-2, along with a similar one where the minimum time is 25.4 s.

Figure A-1 Calculated Marsh Funnel Times for Power Law Fluids

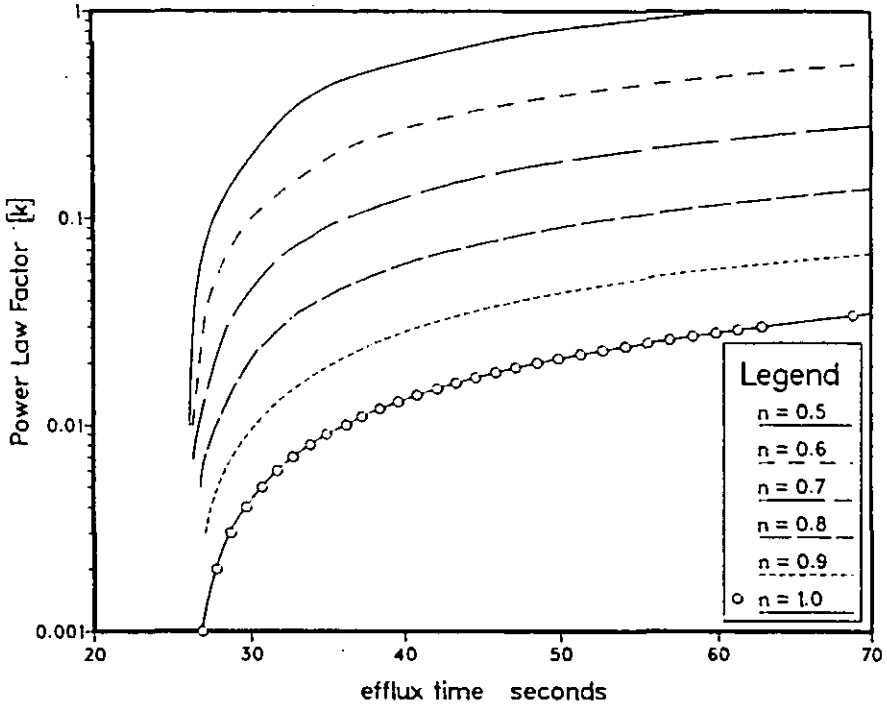

Figure A-2 Calculated Marsh Funnel Times for Newtonian Liquids

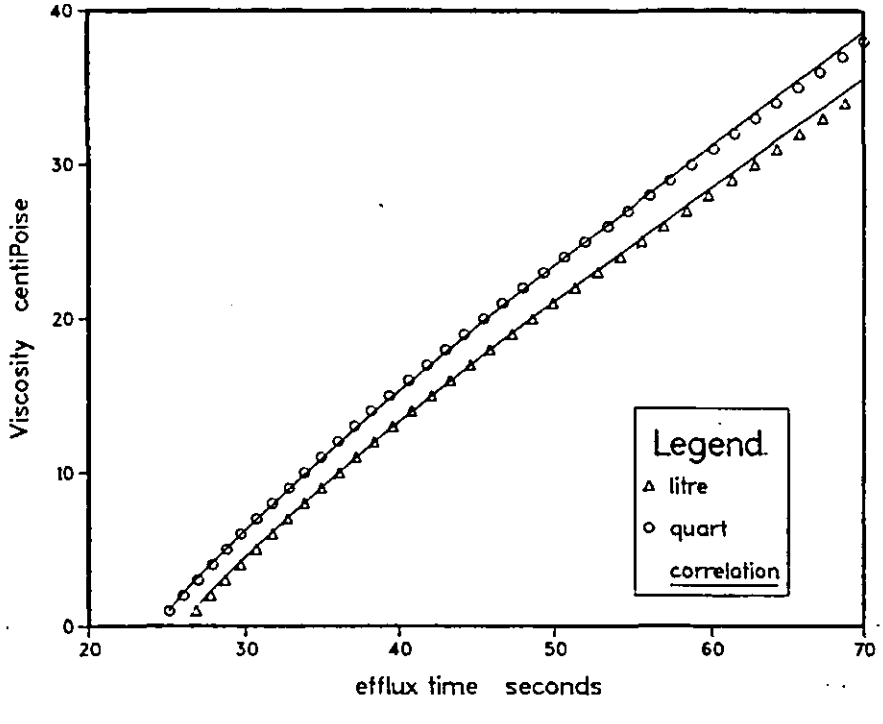

Table A-1 Comparison of Calculated and Measured Marsh Funnel Times

material	time seconds		Power Law	
	measured	calculated	n	k
water	27.7	27.0	1.0	0.001
ethandiol	45.9	45.9	1.0	0.020
aq. glycerol	43.3	43.3	1.0	0.016
	46.5	46.5	1.0	0.0186
	48.7	48.6	1.0	0.020
	51.3	51.8	1.0	0.225
	54.2	54.8	1.0	0.0246
XCD rig	37.0	36.7	0.32	1.90
	42.0	42.3	0.27	2.77
HEC rig	34.0	33.2	0.70	0.074
HEC 0.4%	50.2	50.8	0.577	0.47
HEC 0.5%	77.0	73.9	0.415	2.14
HEC 0.5%	77.0	81.0	0.426	2.11

Notes:

(1) Two calculated values are given for the 0.5% HEC based on regression either way.

(2) The Newtonian fluids are based on Ostwald viscometer measurements, and include allowance for density.

(3) The polymer solutions are calculated from Weissenberg Rheogoniometer measurements, assuming a density equal to water.

From the experimental data on aqueous polymer fluids, a similar correlation can be found, taking the effective viscosity at a shear rate of 1000 to 2000 s^{-1}. However, the constant of proportionality varies from fluid to fluid, so the Marsh Funnel cannot be used as a rheometer. Nevertheless, for any given drilling fluid, this relationship might be useful to quantify changes due to dilution or degradation of the viscosifier, as Table A-2 (below) shows. The ratio of excess times to the power 0.87 is seen to be comparable to the ratio of effective viscosities.

Table A-2 Comparison of Changes in Marsh Funnel Time and in Effective Viscosity at 1460 s^{-1}

material	time seconds		ratio of excess times	$(\text{ratio})^{0.87}$	ratio of effective viscosity
	1	2			
HEC	52.1	36.5	2.48	2.20	2.42
XC	41	32	2.50	2.22	2.27
XCD	42	37	1.45	1.39	1.38
DFVIS	48.5	35.5	2.37	2.12	2.12

APPENDIX 2: Layout of Screens

Shale shaker design has progressed from a steep downward slope to a near horizontal to the upward-sloped screen used in this thesis. From a chemical engineering viewpoint, the most noticeable feature of this separation process is that it is co-current, and an improvement would be expected if it was made counter-current. That is, the liquid feed and the solid product should travel in opposite directions.

On a downward-tilted screen it was of course necessary for the flow to be co-current, but upward tilted screens with positive solids conveyance do offer the possibility of counter-current operation, which is potentially their greatest advantage.

A means is therefore suggested for achieving this with minimum modification. On a double deck unit it is safer at allow the top screen the possibility of a downward slope in order to cope with 'gumbo' (sticky clay balls), but in any case, counter-current operation should give the greatest benefit on the finer screens used on the lower deck, because these are the ones in greatest danger of overflowing.

At the same time, some ideas are given for what seem to the author to be important operational problems. Firstly, if the lower screens overflow (due to blockage or wrong selection) then normal practice is to bypass the entire unit until the problem is rectified. It is fair to say that some screening would be preferable to no screening, so a different bypass is proposed.

Secondly, blockages tend to occur on the lower screens at the rear, where they are relatively inaccessible for inspection or cleaning. Thirdly, consideration has been given to a more complex arrangement of screens with an element of self-adjustment. This would remove some of the difficulty of screen selection, while ensuring that as much of the fluid as possible is screened by as fine a mesh as possible, with the minimum operator intervention, and even allowing for progressive blockage. In order to do this, advantage is taken of the fact that balls of particles will travel across a mesh considerably coarser than their constituents.

Figure A-2 Proposed Alternative Layouts for Double-Deck Shakers

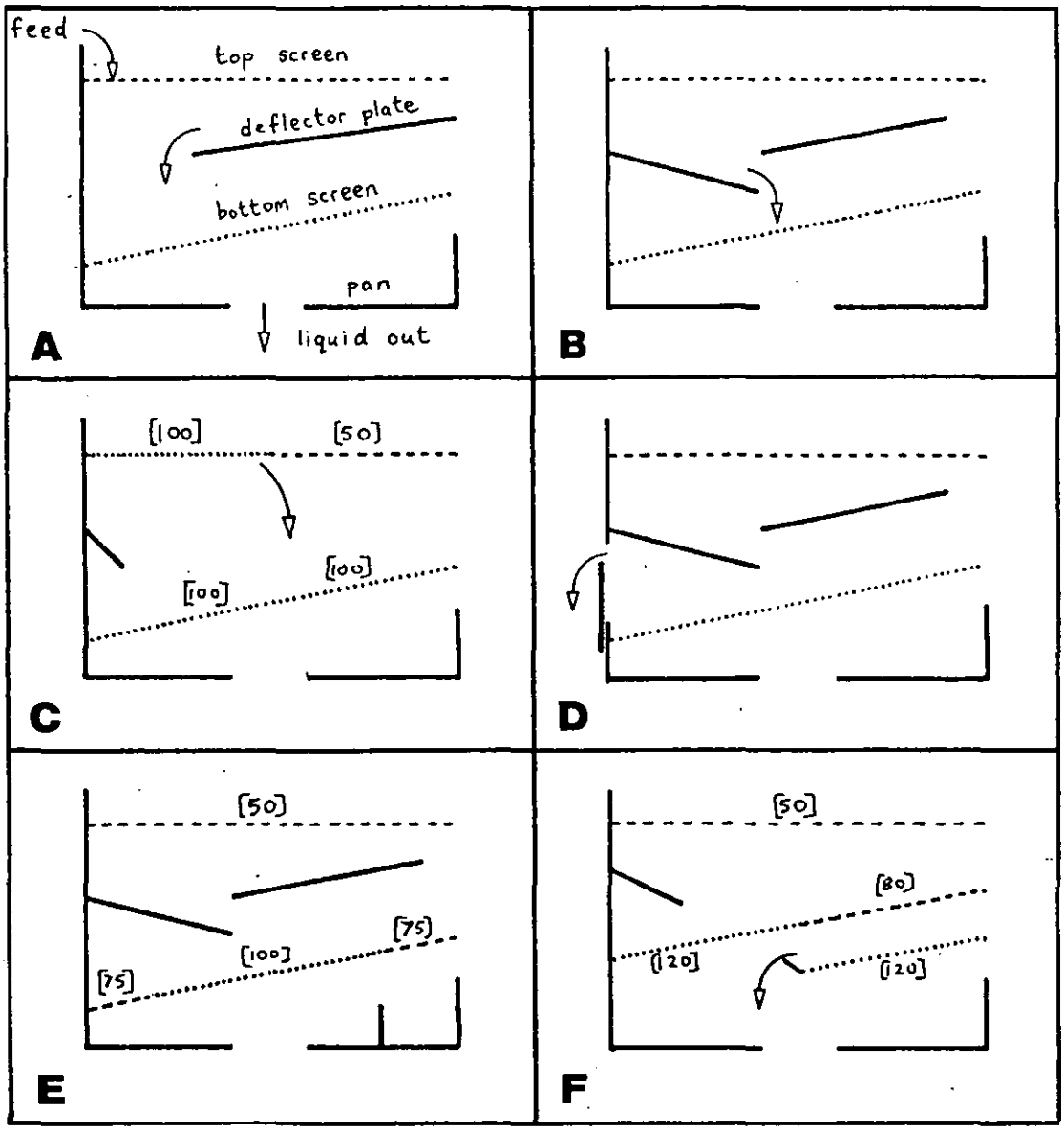

Figure A-2(a) shows a simplified diagram of the present design. There is a top relatively coarse screen, approximately horizontal. The liquid is fed in at one end via a distributor plate which reduces but does not by any means eliminate jetting through the mesh. Thus some particles may be driven with force into the lower screen. The liquid spreads forward and solids separate from the leading edge to be carried off the front. Any liquid passing the mesh forward of the distributor is returned to the rear of the device by a deflector plate. On the Main Rig problems were experienced at low angles because this plate tended to overflow forwards.

The lower screen operates at a slight upward tilt, and is fed from above at the rear. Thus solid has to be conveyed the full length in order to be removed. since the rear of the screen receives particles first, it tend to block first, forming an impermeable strip which grows. Thus the portion of the screen with the greatest head of liquid (which would give the greatest flow for clean fluid) is inactive.

Figure A-2(b) shows a different deflector plate so arranged that fluid is fed to the middle portion of the lower deck. As the solid moves uphill, the liquid flowing to the rear will tend to be relatively free of particles, thus permitting greater flow rates. There is no reason to suppose the solid discharge will be any wetter, because the length of the non-flooded mesh can be the same.

In the figures which follow, mesh sizes are given for illustrative purposes to indicate coarser and finer. Figure A-2(c) shows a two-part upper mesh, finer at the feed end. This will tend to carry liquid further forward because of its lower permeability, giving a broad feed to the middle portion of the lower deck. A small deflector plate prevents jetting through onto the lower deck. By having the first portion of the upper deck the same mesh as the lower deck, it is intended that near-size particles can be (in part) trapped where any blockage will be visible. If this upper mesh blocks quickly, then a different size or rectangular mesh can be tested before replacing the lower deck. For this purpose, it is advisable to have upper and lower decks of the same type (probably pre-tensioned). Under adverse conditions a relatively coarse screen might be used at the front of both decks (e.g. 80 + 30 over 80 + 50) to give complete removal of coarse and some removal of fines (carried over the coarse as balls).

Figure A-2(d) shows a movable plate covering a slot at the rear of the basket. In the event of the liquid coming too far forward on the bottom screen, the plate is lowered to permit some liquid to overflow into the pan. Thus all the fluid is screened by the upper mesh, and a large fraction by the lower, while the dryness of the solids discharge is maintained. this would seem far superior to a conventional bypass.

Figure A-2(e) shows a speculative design in which the lower deck has a fine mesh middle and a slightly coarser front and rear. It is supposed that this will give a cut nearly as good as a 100 mesh while giving a life nearly as good as a 75 mesh. At the rear it is assumed that there will be fewer particles so any solids losses will be reduced. At the front it is assumed that ball transport will lose relatively few sub-mesh particles. However, the coarser mesh at the rear should give an improved flow-rate and is less likely to block. The coarser mesh at the front will give some time between the point when the lower screen ought to be changed (when the leading edge reaches the front of the 100 mesh) and the point when it is convenient to do so.

Figure A-2(f) takes this idea further with a 2 deck unit in which the lowest half-deck is made to overflow to the rear. it will be seen that all the fluid is screened by the top 50 mesh deck. As much as possible is screened by the 120 mesh rear middle deck. If this is all the fluid, then the lowest half-deck has only to trap particles from the solids carried across the front 80 mesh portion of the middle deck. If not, then the remaining fraction is at least screened to 80 mesh and passed to the lowest screen. As much as possible is screened to 120 mesh, and the remainder overflows back to the pan. Thus for example if a full deck of 120 mesh could handle 15 litres per second, but the actual feed rate was 20 litres per second, then this arrangement would ensure that 15 litres per second was screened to 120 mesh and 5 litres per second to 80 mesh. The reduced solids load on the lowest screen might actually improve upon this performance.

REFERENCES

ADAMS,N. (1977) How to control differential pipe sticking.
Petrol Eng (Nov) 44-50

AMERICAN PETROLEUM INSTITUTE (1974) "Bulletin on Drilling Fluids Processing Equipment" **BUL 13C** 1st edn

AMERICAN PETROLEUM INSTITUTE (1978) "Bulletin on Oil and Gas Well Drilling Fluid Chemicals" **BUL 13F** 1st edn

AMERICAN PETROLEUM INSTITUTE (1980) "Bulletin on the Rheology of Oil-Well Drilling Fluids" **BUL 13D** 1st edn

AMERICAN PETROLEUM INSTITUTE (1981) "Specification for Oil Well Drilling Fluid Materials" **SPEC 13A** 8th edn

AMERICAN PETROLEUM INSTITUTE (1982) "Recommended Practice for Standard Procedure for Testing Drilling Fluids" **RP 13B** 9th edn

ANDERSON,D.B., & ESTES,J.C. (1981) Review of low solids mud control gives new insights. **World Oil** 192 (5) 79-85

ANON (1976) Closed mud system passes field tests.
Oil Gas J 74 (39) 24-25

ANON (1983) Closed mud system speeds drilling, clean-up.
Oil Gas J 81 (40) 91

APLING,A.C. (1984) Blinding of screens by sub-sieve sized particles.
Trans Inst Min Metal C 93 (Jun) 92-94

ARMOUR,J.C., & CANNON,J.N. (1968) Fluid flow through woven screens.
Am Inst Chem Eng J 14 (3) 415-420

BECKER,H.A. (1959) The effects of shape and Reynolds Number on drag in the motion of a freely oriented body in an infinite fluid.
Can J Chem Eng 37 85-91

BOBO,R.A. & HOCH,R.S. (1954) The mechanical treatment of weighted drilling muds. **Trans Am Inst Mech Eng** 201 93-96

BOOTH,J.H., & McCALLION,H. (1963) On predicting the mesn conveying velocity of a vibratory conveyor.
Proc Inst Mech Eng 178 pt 1 (20) 521-538

BRADLEY,D. (1965) "The Hydrocyclone"

BRANDT,L.K., & LOVE,W. (1982) "Shale Shakers" IADC Mud Equipment Manual: Handbook 3

BRERETON,T. (1975) Probability screening and the effect of major operating variables. **Filtr Sep** (Nov) 692-696

BROWNING,W.C. (1976) Colloid aspects of drilling fluid rheology. **Proc Colloids Surf Intl Conf**, Puerto Rico, June 1976, 563-581

CAGLE,W.S. (1981) Tests reveal shaker screen efficiencies. **World Oil** 193 (2) 91-94

CAGLE,W.S., & WILDER,L.B. (1978a) Layered screen shaker handles high volumes without plugging. **Oil Gas J** 76 (14) 72-81

CAGLE,W.S., & WILDER,L.B. (1978b) Layered shaker screens improve mud solids control. **World Oil** 186 (4) 89-94

CHAMBERS,K.M. (1966) How drilling fluids affect drilling performance. **API Pacific Coast Conf 1966** Paper 801-421

CHAMBRE SYNDICALE DE LA RECHERCHE ET DE LA PRODUCTION DU PETROLE ET DU GAZ NATUREL: SUBCOMITE DES TECHNICIENS (1982) "Drilling Mud and Cement Slurry Rheology Manual"

CHENG.,D.C-H., & EVANS, F. (1965) Phenomenological characterization of the rheological behaviour of inelastic reversible thixotropic and antithixotropic fluids. **Brit J Appl Phys** 16 1599-1617

CHENG.,D.C-H., RAY,D.J., & VALENTIN,F.H.H. (1965) The flow of thixotropic bentonite suspensions through pipes and pipe fittings. **Trans Inst Chem Eng** 43 T176-T186

CHHABRA,R.P., & RICHARDSON,J.F. (1985) Flow of liquids through screens: relationship between pressure drop and flow rate. **Chem Eng Sci** 40 (20) 313-316

CHILINGARIAN,G.V., & VORABUIR,P. (1983) "Drilling and Drilling Fluids" rev. edn

CHOW,V.T. (1959) "Open-Channel Hydraulics"

DARLEY,H.C.H. (1976) Advantages of polymer muds. **Petrol Eng** (Sep) 46-52

DAWSON,R., & ANNIS,M.R. (1977) Exxon tests validate total mechanical solids control. **Oil Gas J** 75 (22) 90-100

ELSON,T.P., SOLOMON,J., NIENOW,A.W., & PACE,G.W. (1982) The interaction of yield stress and viscoelasticity on the Weissenberg Effect. **J Non-Newton Fluid Mech** 11 1-22

EPHITHITE,H.J. (1983) High frequency screening of fine materials. **Filtr Sep** 20 (2) 148-150

FELLER,R. (1977) Clogging rate of screens affected by particle size. **Trans Am Soc Agr Eng** 1977 758-761

FIELD,L.J., & ANDERSON,D.B. (1972) An analytical approach to removing mud solids. **J Petrol Tech** (Jun) 663-671

FRENCH, R. H. (1985) "Open-Channel Hydraulics"

GRAY,G.R., DARLEY,H.C.H., & ROGERS,W.F. (1980) "The Composition and Properties of Oil Well Drilling Fluids"

GROOTENHUIS,P. (1954) A correlation of the resistance to air flow of wire gauzes. **Proc Inst Mech Eng** A168 837-846

HALL,J.D. (1968) Minimum solids fluid reduces drilling costs. **World Oil** (Dec)

HAPPEL, J., & BRENNER, H. (1965) "Low Reynolds Number Hydrodynamics"

HARRIS,J. (1977) "Rheology and Non-Newtonian Flow"

HEILHECKER,J.K., & ROBINSON,L.H. (1973) "Method and Apparatus for Treating a Drilling Fluid" **U.S. Pat** 3766997

HOBEROCK,L.L. (1980) A study of the vibratory screening of drilling fluids. **J Petrol Tech** (Nov) 1889-1902

HOBEROCK,L.L. (1981a) Modern shale shakers are key to improved drilling. **Oil Gas J** (23 Nov) 107-113

HOBEROCK,L.L. (1981b) Screen selection is key to shale shaker operation. **Oil Gas J** (7 Dec) 130-141

HOBEROCK,L.L. (1981c) Dynamics of shale shakers affect performance. **Oil Gas J** (21 Dec) 80-87

HOBEROCK,L.L. (1982a) Curves are useful guide in finding fluid capacity limits for conventional shaker screens. **Oil Gas J** (18 Jan) 92-101

HOBEROCK,L.L. (1982b) Flow limits for unconventional shaker screens. **Oil Gas J** (18 Jan) 92-101

HOBEROCK,L.L. (1982c) Field operation of shale shakers can extend service life. **Oil Gas J** (1 Feb) 124-126

HOBEROCK,L.L. (1982d) Flow limits in vibrating screen separation of drilling fluids. **Filtr Sep** 19 (2) 109-114

HOPKIN,E.A. (1967) Factors affecting cuttings removal during rotary drilling. **J Petrol Tech** (Jun) 807-814

HUTCHINSON,S.O., & ANDERSON,G.W. (1974) What to consider when selecting drilling fluids. **World Oil** (Oct) 83-94

JEANES,A., PITTSLEY,J.E., & SENTI,F.R. (1961) Polysaccharide B-1459. **J Appl Polymer Sci** 5 (17) 519-526

KALIL,I.A., SPEERS,J.M., & ROBINSON,L.H. (1982) Skid-mounted system for both weighted and unweighted muds developed and field-tested. **Oil Gas J** 80 (15) 132-143

KENNEDY,J.L. (1974) Mud cleaner discards solids, saves barite. **Oil Gas J** 72 (1) 82-92

KING,G.R. (1959) Why rock-bit bearings fail. **Oil Gas J** 57 (46) 166-182

KLUGE, W. [trans Shergold, F.A.] (1953) Modern Vibratory Screens. **Quarry Managers J** (March) 506-526

KROLL, W., (1955) Flisserscheinungen an Haufwerken in schwingenden Gefassen. **Chem Ing -Tech** 27 33-39

KRYNOCK,R.A., & RUHE,R.W. (1973) Vibratory screening apparatus for the fine screening of liquids. **U.S. Pat** 1326133

LAUZON,R.V. (1982) Water soluble polymers for drilling fluids. **Oil Gas J** 80 (16) 93-98

LeBLANC,L. (1978) How to design a money-saving solids control system. **World Oil** (Oct) 61-66

LEONARD,J.W. (1974) Determination of industrial screening efficiency. **Trans Soc Mining Eng (AIME)** 256 185-187

LOTT,W.G. (1973) Treating muds with fine mesh screens. **Oil Gas J** 71 (29) 119-130

LOVE,T. (1983) Stickiness factor: A new way of looking at stuck pipe. **Oil Gas J** 81 (40) 87-90

MacSPORRAN,W.C., & SPIERS,R.P. (1982) The dynamic performance of the Weissenberg Rheogoniometer. 1. Small amplitude oscillatory shearing. **Rheol Acta** 21 184-192

MARSHALL,W.H., & BRANDT,L.K. (1978) Solids control in a drilling fluid. **Proc 3rd Symp Formation Damage Control SPE 7011** 109-112

METZNER,A.B., & REED,J.C. (1955) Flow of non-Newtonian fluids - correlation of laminar, transitional and turbulent flow regimes. **Am Inst Chem Eng J** 1 434-440

MOONEY,M. (1951) The viscosity of a concentrated suspension of spherical particles. **J Colloid Sci** 6 162-170

MOORE,W.D. (III) (1977) North Sea mud chemistry is unique. **Oil Gas J** 75 (6 Jun) 132-150

NICOLL,W.B., STRONG,A.B., & WOOLNER,K.A. (1968) On the laminar motion of a fluid near an oscillating porous infinite plane. **J Appl Mech (Trans ASME)** 35 (1) 164-166

NL BAROID PETROLEUM SERVICES (undated) "Manual of Drilling Fluids Technology. Volume 1. Basic Mud Engineering"

OGDEN,P. (ed) (1983) "Chemicals in the Oil Industry"

ORMSBY,G.S. (1973) Proper rigging boosts efficiency of solids removal equipment. **Oil Gas J** 71 (19 Mar) 120-132

ORMSBY,G.S. (1981) Understanding solids control improves drilling efficiency. **Petrol Eng Intl** (Dec) 120-130

ORMSBY,G.S. (1982) "Hydrocyclones" IADC Mud Circulation Committee Mud Equipment Manual: Handbook 6

OSTWALD,W. (1925) Ueber die Geschwindingkeitsfunktion der Viscosität disperser Systeme. **Kolloid-Z** 36 99-117

OSTWALD,W. (1929) Ueber die rechnerische Darstellung des Strukturgebietes der Viskositt **Kolloid-Z** 47 176-187

PARKER,R.C. (1983) The market for chemicals in the oil industry. in OGDEN,P. (above) 179-217

PATEL,J. & STEINHAUSER,J. (1979) A material balance method to evaluate drill fluid solids removal equipment. **Petrol Eng Intl** (Mar) 86-94

PIERCE,D.M., & ALEXANDER,A.H.D. (1984) High-weight polymer mud stops magnesium/saltwater contamination, saves time. **Oil Gas J** 82 (36) 83-86

PLANCK,J.W. (1981) How to evaluate solids control equipment in the field. **Petrol Eng Intl** (Jan) 54-68

RANNEY,M.W. (1979) "Crude Oil Drilling Fluids"

RATKAI, G. (1976) Particle Flow and Mixing in Vertically Vibrated Beds. **Powder Techn.** 15 187-192

REDFORD,A.H., & BOOTHROYD,G (1967) Vibratory feeding. **Proc Inst Mech Eng** 182 (1,6) 135-146

ROBERTS,G.P., & PITT,M.J. (1982) unpublished results

ROBINSON,L.H. (1982) "Mud Cleaners and Combination Separators" IADC Mud Equipment Manual: Handbook 7

ROBINSON,L.H., & HEILHECKER,J.K. (1975) Solids control in weighted drilling fluids. **J Petrol Tech** 27 1141-1144

ROGERS,W.F. (1963) "Composition and Properties of Oil Well Drilling Fluids" 3rd edn

SIMPSON,J.P. (1985) The drilling mud dilemma - recent examples. **J Petrol Tech** 37 (2) 201-206

SKELLAND,A.H.P. (1967) "Non-Newtonian Flow and Heat Transfer"

SPEERS,A. (1984) Computer aids analysis of drilling fluids. **Oil Gas J** 82 (47) 118-135

SQUIERS, J. C. (1984) Fluid flow resistance models for wire weaves. **Filtr.Sep.** 21 (4) 327-330

STEVENSON,R. (1983) Oil drilling chemistry. **Chem Brit** 19 895

SWACO DRESSER Ltd (1975) "Fine Screening"

SVAROVSKY,L. (1981) Hydrocyclone selection and scale-up. **Filtr Sep** 18 (11) 551-554

TAKAHASHI, H., SUZUKI, A., & TANAKA, T., (1968) Behaviour of a Particle Bed in the Field of Vibration: I. Analysis of particle motion in a vibrating vessel. **Powder Techn.** 2 65-71

THURSTON,G.B. & POPE,G.A. (1981) Shear rate dependence of the viscoelasticity of polymer solutions: II. Xanthan gum. **J Non-Newton Fluid Mech** 9 69-78

TRAWINSKI,H. (1978) Hydrocyclones: applications and practical operation. **Filtr Sep** 15 436-442

WALKER,R.E.(1976) Mud behaviour can be predicted. **Oil Gas J** (13 Sep) 63-68

WALTERS,K. (1975) "Rheometry"

WELLS,P. (1975) Mud solids control - part I: contamination can cost $ 2500 / bbl. **Petrol Eng** (Sept) 26-34

WELLS,P. (1976a) Mud solids control - part II: it's cheaper to throw mud away than to dilute it with water! **Petrol Eng** (Jan) 66-78

WELLS,P. (1976b) Mud solids control - part III: mud maintenance through proper solids control system. **Petrol Eng** (Jun) 62-70

WHITCOMB,P.J., & MACOSKO,C.W. (1978) Rheology of Xanthan gum. **J Rheology** 22 (5) 493-505

WHITE,D.L. (1982a) Hydrocyclone performance predicted by settling rate. **Oil Gas J** 80 (41) 151-156

WHITE,D.L. (1982b) Tests show differences in cyclones. **Oil Gas J** 80 (43) 151-157

WHITE,D.L. (1982c) Good field practice helps cyclones do the job. **Oil Gas J** 80 (45) 211-223

WHORLOW,R.W. (1980) "Rheological Techniques"

WIEGHARDT,K.E.G (1953) On the resistance of screens. **Aeronaut Quart** 4 186-192

WILKINSON, W. L. (1960) "Non-Newtonian Fluids"

WILLIAMS,M.P. (1982a) Solids control for the man on the rig 2. Hydrocyclone and centrifugal pump sizing. **Petrol Eng Intl** 54 (13) 102-110

WILLIAMS,M.P. (1982b) Solids control for the man on the rig 3. Fluid routing, maintenance and troubleshooting. **Petrol Eng Intl** 54 (14) 50-66

WILLIAMS,M.P., & HOBEROCK,L.L. (1982) Solids control for the man on the rig 1. **Petrol Eng Intl** 54 (12) 58-84

WILSON,W.P., CALLENDAR,J.R., & MOSHER,J.R. (1977) Ice-island mud discharge controlled. **Oil Gas J** (14 Nov) 185-193

YOUNG,G.A., & ROBINSON,L.H. (1982a) How to design a mud system for optimum solids removal: Part 1 - principles of equipment arrangement. **World Oil** (Sept) 57-61

YOUNG,G.A., & ROBINSON,L.H. (1982b) How to design a mud system for optimum solids removal: Part 2 - arrangement of hydrocyclones. **World Oil** (Oct) 105-110

YOUNG,G.A., & ROBINSON,L.H. (1982c) How to design a mud system for optimum solids removal: Part 3 - hydrocyclone sizing and centrifuge arrangement. **World Oil** (Nov) 159-174